République Algérienne Démocratique et Populaire

Ministère de l'Enseignement Supérieur et de la Recherche Scientifique

Université du 20 Août 1955 Skikda

Faculté de Technologie

Département De Génie Mécanique

N° of ordre : **D012124017D**

THÈSE

Présenté en vue de l'obtention du diplôme de

DOCTEUR

Filière : Electromécanique

Spécialité : Mécatronique

Par :

Mr. KHADEM Mohammed

Conception et Contrôle d'un robot parallèle à câbles avec l'application à la réhabilitation

Soutenue publiquement le : 27 juin 2024

Devant le Jury compose par :

Nom et prénom	Grade	Qualité	Affiliation
KELAIAIA Ridha	Professeur	Présidant	Université du 20 Août 1955 Skikda
INEL Fouad	Professeur	Encadrant	Université du 20 Août 1955 Skikda
CARBONE Guiseppe	Professeur	Co- Encadrant	Université du Calabria, Italie
KHERIEF Nacer Eddine Mohamed	MCA	Examinateur	ENSET Skikda
BOUACHARI Amel	MCA	Examinateur	Université du 20 Août 1955 Skikda
BABESSE Saad	MCA	Examinateur	Université du Setif1

Année scolaire : 2023/2024

PEOPLE'S DEMOCRATIC REPUBLIC OF ALGERIA
Ministry of Higher Education and Scientific Research

University of 20 August 1955, Skikda

Faculty of Technology

Department of Mechanical Engineering

N° of order: **D012124017D**

THESIS

Presented with a view obtaining the diploma of

DOCTOR

Branch: Electromechanical
Specialty: Mechatronics

By:
Mr. KHADEM Mohammed

Design and Control of a Cable-Driven Parallel Robot with Rehabilitation Application

Defended on: June 27, 2024

Before the jury composed of:

Name	Grad	Quality	Affiliation
KELAIAIA Ridha	Professor	Chairperson	University August, 20th1955 Skikda
INEL Fouad	Professor	Supervisor	University August, 20th 1955 Skikda
CARBONE Guiseppe	Professor	Co-supervisor	University of Calabria, Italy
KHERIEF Nacer Eddine Mohamed	MCA	Examiner	ENSET Skikda
BOUACHARI Amel	MCA	Examiner	University August, 20th 1955 Skikda
BABESSE Saad	MCA	Examiner	University of Setif1

Scholar year: 2023/2024

DEDICATION

I dedicate this humble work:

- *To my dearest parents who have helped and encouraged me throughout my studies.*
- *To my dear brothers and sisters.*
- *To my entire family.*
- *To all my friends, especially Kicha Yahiya*

with whom I have shared my best moments and experiments scientific.

Khadem Mohammed

Message of thanks for my supervision

*I would like to extend my deepest gratitude to **Professor Inel Fouad** and Professor **Giuseppe Carbone.** Your guidance and cooperation at each step of my research trajectory have been invaluable. From the initial stages of formulating my research proposal to the final stages of defending my dissertation, your support has been unwavering. As I navigated this journey, everything was new to me, including the use of advanced technology and research methodologies. Your contributions, particularly by providing clear and practical examples for each assignment, were instrumental in ensuring everything went smoothly. Your willingness to offer detailed feedback and your patience in addressing my questions helped me develop a deeper understanding of my field. Thank you immensely for being our mentors and for being such kind and caring professors.*

Message of thanks for my professors

Additionally, I would like to extend a heartfelt thanks to all the professors for their cognitive and moral support throughout my academic path. The lectures, seminars, and one-on-one discussions have significantly contributed to my academic growth. Your encouragement and expertise have greatly enriched my learning experience, and I have benefited immensely from your knowledge and

wisdom. I wish you all continued success in your endeavors and hope to collaborate with you in the future.

Message of thanks for my university

I also want to express my sincere gratitude to Skikda University and its administrative staff for their unwavering financial and moral support during my research journey. The scholarships, grants, and resources provided were crucial in allowing me to focus on my studies and research without financial worries. The administrative staff's efficiency and willingness to assist with any issues ensured a smooth and productive academic experience. Your assistance has been crucial in helping me achieve this milestone. I wish the university continued prosperity and success in the future and hope to see it rise to new heights of academic excellence.

Thank you all for your support and encouragement.

ملخص

تقدم هذه الأطروحة بحثاً عن روبوت موازي يعمل بالكابل بهدف تأهيل وتدريب الأطفال الصغار والمعاقين في مهام الرسم والكتابة. تم تحديد الطوبولوجيا الهرمية لأنها توفر ثلاث درجات حرية انتقالية (Dofs) بمجموعة متكونة من خمسة كابلات في شكل مدمج. بالإضافة إلى ذلك، تم تصميم هذا الروبوت بميزات جديدة، فهو غير مكلف، وسهل التحكم فيه، وسهل النقل إلى أي مكان في المنزل أو المدرسة لأنه مناسب لمكتب منزلي أو طاولة الفصل الدراسي. في هذا البحث، نقدم الخطوات الرئيسية لتصميم الروبوت الموازي الهرمي المعتمد على الكابلات. يتم توجيه اهتمام خاص لتصميم الهيكل والمؤثر النهائي بالإضافة إلى إنشاء نماذج محاكاة مناسبة. تم اقتراح العديد من عمليات المحاكاة من خلال تنفيذ النماذج الحركية والديناميكية لإثبات جدوى مهام الكتابة/الرسم المتعددة. يتم اقتراح واجهة مستخدم محددة تسمح بالمسارات المستمرة والمتقطعة. يتم تطبيق التحكم في الوضع المنزلق لتحقيق دقة تتبع مناسبة على المسار المطلوب. أخيرًا، تم إجراء التحقق التجريبي بنجاح من خلال النظر في مسارات متعددة لإظهار الجدوى الهندسية وفعالية التصميم المقترح ونماذج المحاكاة.

الكلمات المفتاحية : الروبوت الموازي المتحرك بالكابل، جهاز التمرين، التحكم في وضع الانزلاق، تمارين إعادة التأهيل.

Résumé

Cette thèse présente un robot parallèle novateur à entraînement par câble conçu pour aider les jeunes et les enfants handicapés dans leurs exercices de dessin et d'écriture. Le robot utilise une configuration pyramid, offrant trois Degrés de Liberté de Translation (DOFs) actifs avec un ensemble redondant de cinq câbles, le tout dans une forme compacte et portable. Notamment, ce robot se distingue par son abordabilité, sa facilité de contrôle et sa mobilité, le rendant adapté à une utilisation dans des environnements domestiques ou scolaires, où il peut facilement s'adapter à un bureau ou à une table de classe. Dans ce document, nous exposons les étapes principales de la conception de ce robot parallèle pyramid à entraînement par câble. Notre attention se porte sur la conception structurelle, l'effecteur final et la création de modèles de simulation précis. Nous présentons diverses simulations, englobant à la fois des modèles cinématiques et dynamiques, pour mettre en avant la capacité du robot à effectuer diverses tâches d'écriture et de dessin. Nous proposons également une interface conviviale prenant en charge des trajectoires continues et intermittentes. Afin d'assurer un suivi précis le long des trajectoires souhaitées, nous utilisons une stratégie de contrôle en mode glissant. Enfin, nous validons avec succès notre conception et nos modèles de simulation grâce à des essais expérimentaux, impliquant plusieurs trajectoires, mettant en évidence la faisabilité et l'efficacité de notre approche en ingénierie.

Mots-clés : robot parallèle à câbles, dispositif d'exercice, contrôle en mode glissant, exercices de réhabilitation.

Abstract

This thesis introduces an innovative cable-driven parallel robot designed to aid young and disabled children in drawing and writing exercises. The robot utilizes a pyramid configuration, offering three active translational Degrees of Freedom (DOFs) with a redundant set of five cables, all within a compact and portable form. Notably, this robot is characterized by its affordability, ease of control, and mobility, making it suitable for use in home or school environments, where it can easily fit on a desk or classroom table. Within this paper, we elucidate the primary steps involved in designing this cable-driven pyramid parallel robot. Our focus extends to the structural design, the end-effector, and the establishment of precise simulation models. We present various simulations, encompassing both kinematic and dynamic models, to showcase the robot's ability to perform diverse writing and drawing tasks. We also propose a user-friendly interface that supports both continuous and intermittent trajectories. To ensure accurate tracking along desired paths, we employ a sliding mode control strategy. Finally, we successfully validate our design and simulation models through experimental trials, involving multiple trajectories, highlighting the engineering feasibility and efficacy of our approach.

Keywords: cable-driven parallel robot, exercising device, sliding mode control, rehabilitation exercises.

TABLE OF CONTENTS

LIST OF FIGURES

LIST OF PAINTINGS

ABBREVIATIONS LIST

LIST OF SYMBOLS

CHAPTER III. MODELS OF CABLE-DRIVEN PARALLEL ROBOT

CHAPTER IV. CONTROL STRATEGY OF THE PROPOSED

CHAPTER V. EXPERIMENTAL AND VALIDATION RESULT

LIST OF FIGURES

LIST OF TABLES

ABBREVIATION LISTE

AC: *Adaptive Control*

CDPR: *Cable Driven Parallel Robot*

DOF: *Degrees Of Freedom*

GUI: *Graphical User Interface.*

IDE: Integrated Development Environment.

IMU: Inertial Measurement Unit.

LABVIEW: *Laboratory Virtual Instrument Engineering Workbench*

MATLAB: *Matrix Laboratory,*

MPC: *Model Predictive Control*

NC: *Nonlinear Control*

NIST: *National Institute of Standards and Technology*

OL: *Open-Loop*

PD: Proportional-Derivative

PI: *Proportional-Integral*

PID: *Proportional-Integral-Derivative*

SMC: *Sliding Mode Control.*

USB: *Universal Serial Bus*

LIST OF SYMBOLS

$\overrightarrow{A_i}$: *vector between points* (o, M_i);

c_i: *viscous damping coefficient of the i-th Motor shaft;*

$\overrightarrow{d_i}$: *vector between points* $(\grave{o}, a)$;

H: *height from base to motor axis;*

i: *number of cables.*

J_i: *rotational inertia of the i-th shaft-pulley system;*

k: *side length of the end-effector (the shape of the end-effector is square);*

L_{i0}: *initial length of the i-th cable.*

L_i: *length of the cables;*

M_i: *starting points of the cables on the base frame.*

$\overrightarrow{P_i}$: *vector between points* $(o, \grave{o})$;

R: *workspace side length;*

r_i: *radius of the i-th pulley;*

$\overrightarrow{S_i}$: *vector between points* (M_i, a);

α_i: *is the angel between cable with plane* (X, Y)

β_i: *rotation angle of the i-th pulley;*

θ_i: *is the angle between cable and (Y) or (X)axis*

τ_i: *torque of the i-th motor;*

General Introduction

General Introduction

Cable-driven parallel robots (CDPRs) belong to a category of robots that utilize cables or wires instead of inflexible links for the transmission of forces and movements spanning from the robot's base to its end-effector. These robots have garnered considerable scholarly interest owing to their remarkable capacity for bearing heavy loads, expansive operational workspaces, and proficiency in achieving remarkable speed and precision. The manipulation of the end-effector is facilitated through the coiling of a cable or wire around a drum or winch. Their versatility extends to various applications, including employment in motion simulators, telescope positioning, and camera tracking systems, as exemplified in studies such as (M. Gouttefarde, 2015).

The inaugural cable-driven parallel robot (CDPR), named RoBoCrane, emerged in 1989 through the efforts of the National Institute of Standards and Technology (NIST) (J Albus, 1992) . Since that milestone, diverse variants of CDPRs have emerged to cater to specific applications. These encompass a hybrid design melding a wheeled robot with a cable-driven system (M. Korayem, 2020) , a 6-degree-of-freedom (6DOF) CDPR catering to upper and lower limb mobility (B. Sheng, (2016).) (G. Carbone, 2018), as well as a CDPR dedicated to upper limb rehabilitation (E. Oyman, 2022) (M.A. Laribi, 2019). However, these innovations may not universally accommodate all motion requirements due to heightened complexities in modeling. In response to this challenge, the need for precise models has been underscored, an aspect explored in works such as (M. Zarebidoki, 2022) . Instances of cable-driven robots tailored for extensive workspaces are documented in references (B. Billel, 2014) (G. Boschetti, 2019) (R. Wang, 2021), while the inherent suitability of CDPRs for tasks demanding high dynamics is highlighted in (I.B. Hamida, 2021.) .

The versatile applications of CDPRs span a spectrum of domains, encompassing roles as motion simulators (I. Chawla, 2021), facilitators of large-scale telescope orientation (J.P. Merlet, 2019) , operators of expansive camera systems (I. Chawla P.M. Pathak, 2021), and even participants in construction endeavors (F. Zhang, 2021). These adaptable robots have found utility in industrial contexts, a fact attested by reports in (J.-B. Izard, 2012.) (Y. Wang,

2022) (W. Yuqi, 2022.) . Notably, CDPRs have made impactful inroads in medical scenarios, aiding post-stroke and paraplegia patients, as evidenced in works like (G. Rosati, 2005) (W.M. Nunes, 2011). As for controlling CDPRs, as expounded in (M.A. Khosravi, 2013) , researchers predominantly rely on Proportional-Integral-Derivative (PID) controllers for low-level control strategies. Although researchers have explored an array of control algorithms, the Proportional-Derivative (PD) controller has found application in planar cable-based robots, as elaborated in (F. Inel, 2014) (F. Inel M. N., 2020) . In pursuit of enhanced control precision and responsiveness, the utilization of sliding mode control is detailed in works such as (A. Alikhani, 2012) (A. Zaatri, 2014), offering a means to bolster the efficacy of robotic system control. The adaptive sliding mode controller emerges as a dependable tool to regulate motor torque and speed, thereby holding end-effector trajectories and facilitating seamless interactions with intended payloads.

Children facing disabilities often encounter challenges when embarking on their educational journeys, particularly in tasks involving drawing and writing. Endeavors in research are actively pursued to uncover methods that simplify these skill-building processes, enabling children to engage in writing and drawing activities more effortlessly. Within this context, our these introduces an innovative cable-driven robot shaped like a pyramid, designed with a primary focus on rehabilitation exercises. This robot's core purpose revolves around imparting drawing and writing skills to young children within the primary school spectrum. Nonetheless, the robot's applicability extends to diverse related scenarios, encompassing the instruction of foundational skills like arranging shapes and sorting colors. Beyond this, the robot assumes the role of a valuable aid for individuals grappling with vision impairment or other illnesses necessitating efforts towards reclaiming drawing and writing proficiencies.

This Thesis is arranged as follows:

- **The First Chapter**, we trace the historical development of Cable-Driven parallel robots (CDPRs), highlighting their evolution, essential components, and versatile applications. The impact of CDPRs across various sectors underscores their significance in enhancing our understanding of robotics and its real-world implications.

- **The Second Chapter**, explores the innovative use of a pyramid-shaped structure in robot design, discussing its unique features and visual appeal. It contrasts the

durability of this structure with conventional designs and examines its application in rehabilitation. The research behind the pyramid's shape and its cable integration is covered, along with a qualitative analysis of materials to optimize its construction. This scrutiny enhances our understanding of the pyramid structure's potential for diverse applications.

- **The Third chapter**, explores the use of cables for precision in parallel robot movement. It analyzes cable arrangement, lengths for accuracy (geometric aspect), studies motion patterns influenced by cable adjustments (kinematic aspect), and examines forces, torques, and behavior during operation (dynamic aspect). Integrating these aspects is crucial for effective design and control in diverse applications.

- **And Fourth Chapter**, introduces performance-enhancing control strategies, with a focus on commonly used methods. It details the integration of these chosen controls into the graphical interface using the software. The chapter also outlines planned rehabilitation applications intended for implementation with the robot.

- **The Fifth Chapter,** showcases results from robust control strategies applied to introduced models for maneuvers and rehabilitation tasks in drawing and writing. MATLAB simulations for a three-stage model are presented, along with open-loop and PID control outcomes through a LabView graphical interface. Experimental open-loop control results demonstrate gradual point-to-point movement, followed by an efficacy analysis.

Finally, Results from robust control strategies applied to introduced models for drawing, writing, and rehabilitation were demonstrated. The success of the approach was evident in open-loop and PID control unit outcomes via a LabView interface. Experimental model results showed gradual point-to-point movement, with potential for future improvement through refined control and design enhancements for uniform cable force distribution.

Chapitre 1

I.1 Introduction

A cable-driven parallel robot (CDPR) is a specific type of parallel robot that operates using cables or flexible components as its primary method for controlling the robot's movement. This contrasts with traditional robotic systems that rely on rigid links and joints. CDPRs utilize tensioned cables, which create a connection between the robot's moving part, known as the end-effector or platform, and fixed anchor points. This innovative approach to actuation allows for precise and controlled motion.

CDPRs offer a wide array of advantages. These include a favorable payload-to-robot mass ratio, which means they can carry a substantial load. Additionally, CDPRs possess an expansive workspace, enabling them to cover a significant area during their operation. Their unique design also grants them the ability to generate intricate and customized motion patterns, making them adaptable to various tasks and scenarios.

The applications of CDPRs span across diverse industries. They find utility in aerial robotics, where their lightweight yet capable structure is crucial for efficient flight. In the medical field, CDPRs can be employed in surgical procedures and medical interventions, capitalizing on their precision and controlled motion. Even in the entertainment industry, CDPRs have a role to play, contributing to the creation of captivating visual effects and dynamic displays.

in this chapter, our focus was on exploring the historical evolution of the Cable-Driven parallel robot. By tracing its development through different phases, we aimed to provide insight into its origins and growth. Moreover, we delved into the essential components that shape the configuration of these robots. Understanding these constituents enables us to categorize and characterize the CDPR effectively. Furthermore, we highlighted the diverse domains where CDPRs find application, underscoring the significance of their contributions. The impact of CDPRs is substantial across various sectors, and recognizing their potential adds depth to our understanding of robotics and its real-world implications.

I.2 A Historical Overview of the CDPR

As early as 1984, within the landscape of technological development, researchers Lands Berger and Sheridan put forth pioneering concepts that revolved around the utilization of

cable-controlled parallel linked robotic devices. These groundbreaking ideas were not only documented in their master's thesis under reference (Landsberger, 1984) but were also expounded upon in subsequent references (Landsberger, 1985) (Landsberger S. E., 1987.). The core innovation of their robotic contrivances lay in their exclusive reliance on cable-based actuation, a distinctive feature that set them apart. However, it's worth noting that these devices also leaned on an auxiliary strut to provide supplementary support, adding to the intricacies of their design. Concurrently, during the same temporal span, the domain of cable-based innovations witnessed a significant contribution. In this context, the patent application for the widely renowned Skycam, a camera system centered around cable mechanisms, was formally submitted by innovator Brown (Brown, 1987) (Cone, 1985). This system has garnered recognition as one of the scant instances where cable robots have found practical applications within commercial realms. Within this overarching narrative, there emerged two notable developments. Firstly, Tanaka (Tanaka, 1988) embarked on a pioneering analysis focused on the kinetostatic aspects of systems that bore resemblance to Skycap. This investigation marked a pivotal step in the academic exploration of such cable-based setups. Secondly, Higuchi (Higuchi, 1988), in a parallel line of thought, conceptualized the prospective utilization of multi-cable cranes in the capacity of robotic entities, particularly within the context of construction-oriented tasks. This conceptual proposition extended the potential applications of cable-controlled systems beyond traditional spheres, hinting at their adaptability and versatility within diverse industries.

In the subsequent year of 1989, a significant milestone was reached as the RoBoCrane system made its debut at the National Institute of Standards and Technology (NIST) (Dagalakis, 1989) . This event marked a pivotal moment in the evolution of cable-based robotics, representing one of the earliest instances of a larger-scale prototype in this domain. Notably, the RoBoCrane was at the forefront of innovation, and the groundwork for this breakthrough had already been laid the year prior. In 1988, Albus, a trailblazer in this field, had filed an initial patent for the RoBoCrane, setting the stage for the system's eventual unveiling.

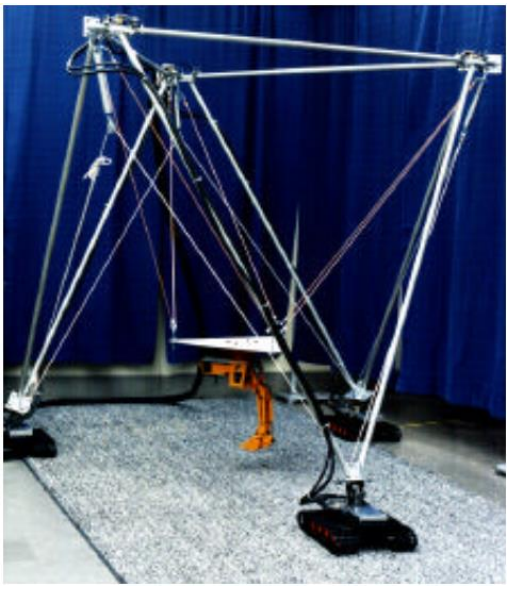

Figure I. 1. *RoBoCrane the first parallel robot has been designed***(ROGER BOSTELMAN, 2015)**

The design of the RoBoCrane drew inspiration from the well-established Stewart-Gough platform, a renowned kinematic mechanism known for its precision and versatility. However, the RoBoCrane introduced a novel twist to this concept, redefining the traditional structural arrangement. Unlike the standard setup, where the mobile platform typically rests atop fixed anchor points, the RoBoCrane ingeniously inverted this arrangement. By situating the mobile platform underneath the fixed anchor points, a unique advantage was realized tension in the cables could be more effectively maintained. This innovative approach paved the way for the utilization of cables as primary load-bearing elements in place of rigid struts. Furthermore, this novel structural arrangement also meant that the connecting legs now only needed to exert pulling forces, simplifying the mechanical requirements.

The RoBoCrane potential was put to the test through its evaluation for large-scale handling tasks, with a specific emphasis on shipbuilding applications (Albus, 1992) (Albus, The NIST ROBOCRANE, 1993) (Dagalakis, 1989). This marked a pioneering foray into applying cable-based robotics in practical, industrial contexts. In parallel, the field of space robotics was abuzz with innovative ideas, with the proposal of using a cable robot as a haptic interface (Lindemann, 1989) a clear example of the far-reaching possibilities that cable-based systems could offer. As the exploration of cable-based systems continued, Kurtz's study in 1991 delved into the mechanics of these systems, leading to a crucial insight. His work established that a rigid body with n degrees-of-freedom required n+1 cables for complete constraint. Building upon this understanding, Kawamura (Kawamura, 1993) presented the initial concepts for a seven-cable parallel robot, envisioning its applications in teleportation.

During this period, Ming and Higuchi (Ming, 1994) introduced a classification scheme designed to categorize cable robots based on the number of cables and degrees-of-freedom they possessed. This effort provided a structured framework for comprehending the diverse landscape of cable-based robotic designs. Subsequently, Kawamura (Kawamura S. C., 2003) unveiled the Falcon prototype, capitalizing on cable robots' remarkable dynamic capabilities to enable rapid and precise pick-and-place operations. This breakthrough was further validated in 1995, when it was demonstrated that cable robots could generate accelerations exceeding 144 m/s^2, a testament to their exceptional performance potential. Pushing the boundaries of cable robot applications, Tadokoro ventured into the realm of disaster response, developing a mobile cable robot system designed for post-earthquake rescue missions (Maeda, 1999) (Tadokoro, 1999). This innovation showcased the adaptability of cable-based systems in addressing critical real-world challenges, underscoring the system's potential to be lightweight and easily deployable.

With the turn of the millennium came a significant surge in cable robot research, encompassing not only Japan and the USA but also extending to Europe, China, and Iran. LA Fourcade's work introduced the concept of ultra-light cable robot structures for motion generation within wind tunnels (Lafourcade, 2002) (Lafourcade P. Z.-Q., 2003), demonstrating the versatility of these systems across diverse applications. In parallel, the University of Duisburg-Essen, Germany, introduced the Segesta prototype a lightweight research system designed to study kinematics, control, and design (Bruckmann, 2010) (Fang, 2005) (Hiller, 2005) (Verhoeven, 2004). Impressively, this prototype achieved experimental accelerations of up to 200 m/s^2 while carrying a small payload of 150g.

Meanwhile, the University of Rostock, Germany, unveiled the Cable prototype a scaled-down model tailored for handling and automating container cranes (Heyden, 2006) (Maier, 2004). This comprehensive exploration of cable robots signified a notable evolution in the field, exemplifying the expanding horizons of cable-based robotics and its global dissemination. In the midst of an extensive exploration focused on parallel robots, conducted within a dedicated program in Germany, a series of initiatives emerged with the goal of constructing a cable robot with potential application as a machine tool (Kraft, 2005) (Uhlmann, 2008). This marked a strategic effort to extend the capabilities of cable-based robotics into the realm of machine tools, showcasing the versatility of these systems in practical industrial contexts.

Figure I. 2. *automatic container cranes.* **(**Technology, 2017**)**

Following this trajectory, the Fraunhofer Institute for Production Systems and Design Technology (IPK) situated in Berlin, Germany, introduced a groundbreaking innovation known as the String-Man robot. This cutting-edge development found its purpose in the domain of gait rehabilitation. Notably, the emphasis of this endeavor lay in achieving exceptional precision in force control and dedicating attention to safety considerations (Surdilovic, 2004) (Surdilovic D. Z., 2007). The String-Man robot stood as a testament to the fusion of advanced robotics technology with the pressing need for effective rehabilitation solutions. Running in parallel, the INRIA research institution in France contributed to the exploration of cable robotics through the introduction of the Marionet robot family. This collection of innovations encompassed a range of applications, including a compact prototype optimized for high-speed operations, a portable crane designed for rescue missions, and modular components crafted to assist individuals in various capacities (Merlet, 2008). This comprehensive approach underscored the adaptability of cable-based systems across diverse scenarios. Turning attention to Canada, noteworthy contributions emerged as Otis undertook the development of a locomotion system (Otis, 2010) (Otis M. J.-D.-L., 2009) . This endeavor showcased the international nature of cable robot research, highlighting the global drive to unlock the potential of these systems in various applications. Simultaneously, at the Swiss Federal Institute of Technology (ETH Zurich) in Switzerland, a motion simulator tailored for sports devices was brought to fruition (Rauter, 2010) (Zitzewitz, 2009) (Zitzewitz J. V., 2010). This innovation bridged the realms of cable robotics and sports technology,

demonstrating the interdisciplinary possibilities that arise from the integration of advanced robotics concepts. Meanwhile, in China, a remarkable initiative took shape—the creation of the world's largest cable robot. This endeavor was specifically aimed at positioning the colossal reflector of the renowned FAST telescope (Five-hundred-meter Aperture Spherical Telescope) (Baoyan, 2008). The scale and ambition of this project highlighted the extraordinary capacity of cable-based systems to address complex and substantial engineering challenges. In a distinct geographical context, researchers in Iran embarked on an in-depth study of KNTU cable robots (Aref, 2009) . This underlined the global nature of research in this field, emphasizing the international collaboration and cross-cultural exchange that drives the advancement of cable-based robotics technology.

While the highlighted instances provide a glimpse into the expansive landscape of cable-based robotics, it's important to recognize that numerous other prototypes have contributed to this evolution as well. These prototypes, collectively, have propelled the field forward, enriching the spectrum of possibilities for cable-based robotic systems..

I.3 Structures

The primary defining feature of a cable robot's geometry is primarily dictated by the positioning of its anchor points in relation to both the stationary machine frame and the movable platform. Initially, we will differentiate between geometries referred to as "generic" and "non-generic." A non-generic configuration adheres to specific geometric constraints, such as having all platform points lie within a single plane or along a straight line. On the other hand, a generic design typically maintains its characteristics even when its geometric parameters undergo tiny adjustments. In contrast, a non-generic design only exhibits particular characteristics as long as explicitly defined constraints are satisfied. Illustrative examples of such constraints encompass (Pott A. , 2018).

The described constraints include:

- All anchor points on the platform or base lying within a shared plane.
- Uniform lengths or equidistant spacing among the anchor points.
- Designs featuring point or axis symmetry.
- Instances with two or more anchor points coinciding either on the platform or the frame.

According to mechanism analysis, these constraints introduce an intriguing dimension. Several documented instances highlight the capacity of these constraints to yield more

straightforward kinematic equations or even solutions for equations that become unmanageable within the broader context. From a practical standpoint, it's important to note that non-generic designs are primarily theoretical in nature, assuming a robot's construction and assembly are flawless. Moreover, they neglect various sources of disruption, including elasticity, clearance, component wear, and thermal effects. On the flip side, non-generic designs offer valuable architectural outlines, serving as initial approximations that can be customized to precise requirements.

Assumptions come into play with non-generic designs, underscoring the significance of algorithms compatible with generic designs. These algorithms tend to exhibit greater robustness against imperfect modeling or manufacturing variations, and they can be fine-tuned through comprehensive calibration procedures. Approaches tailored to non-generic designs can harness more specialized presumptions. Consequently, as long as these assumptions remain valid, the resulting algorithms demonstrate greater ease of implementation and enhanced operational speed.

I.3.1 Symbolic Representation for Anchor Attachment Points

As previously discussed, a commonly held assumption is that two or more cables share a shared anchor point, situated either on the base or the mobile platform. This categorization reflects significant conditions employed within kinematic analysis. To delineate setups featuring these shared anchor points, the X - Y notation is employed. This notation signifies the presence of X distinct points on the frame and Y distinct points on the platform, subject to the constraints $X \leq m$ and $Y \leq m$, where m denotes the number of cables. As an example, an 8 – 4 robotic configuration represents a typical arrangement with eight distinct anchor points on the machine frame and four distinct anchor points on the platform. It's worth noting that this notation can create ambiguity, as it doesn't specify which cables share a common anchor point or the quantity of cables converging at a single point.

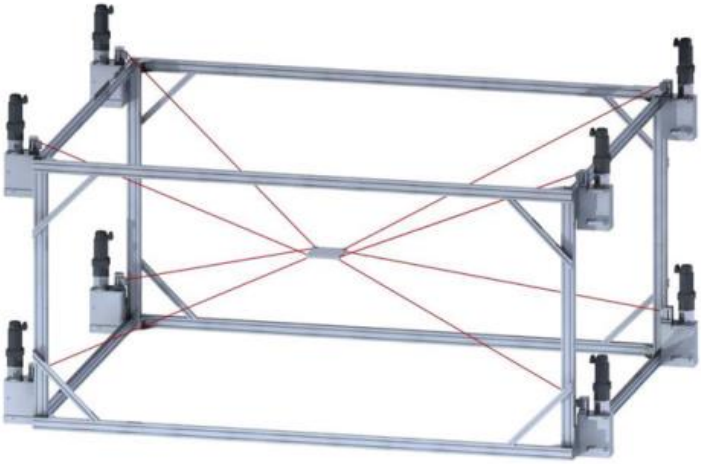

Figure I. 3. *CAD model of the cable robot IPAnema 1.* (A. Pott, 2015)

In the case of the 8 - 4 configuration, various realizations are possible. For instance, it could be established through a two-to-one connection (as depicted in Fig. 3) or by an uneven distribution where five cables link to the initial anchor point while the remaining connections adopt a one-to-one scheme between the base and the mobile platform. Regarding cable robots, it's often assumed that shared anchor points exclusively exist on the mobile platform. Similarly, a notation employing hyphens is prevalent, indicating the number of cables converging at a common point on the platform. Without sacrificing generality, this number can be arranged in descending order. For instance, the Segesta robot (illustrated in Fig. 4) adopts (a 4-2-2) As you can see in Figure 4, four cables are attached to one part of the end effector, with two cables attached to each of the other parts of the end effector, configuration for its platform. This signifies that four cables converge at the first vertex of the triangular platform, while the remaining two vertices are each linked to two winches.

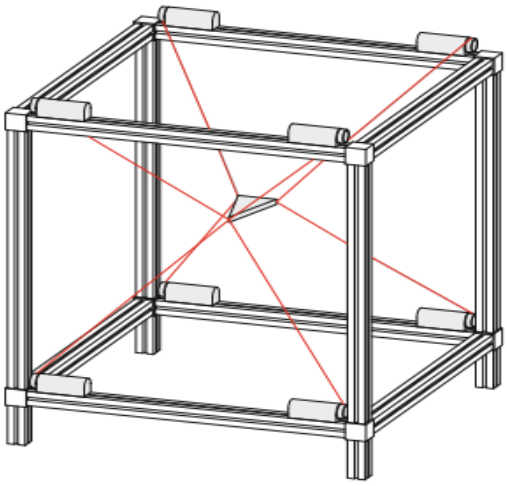

Figure I. 4. *Schematic setup of the Segesta prototype with eight cables in 8-3 configuration* (Pott A. , 2018)

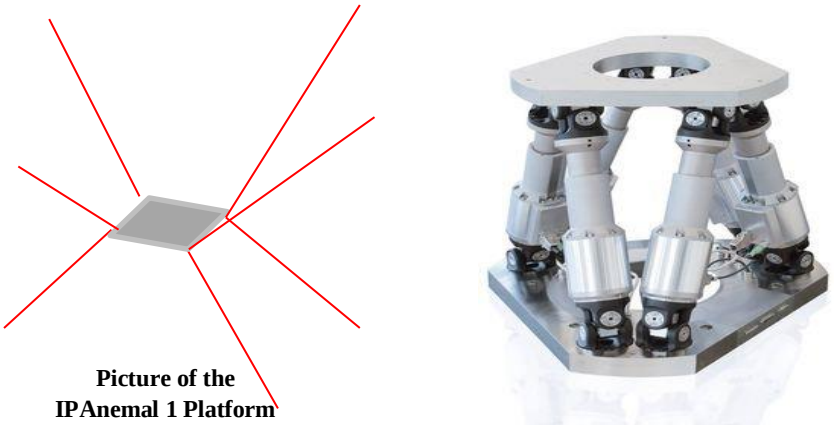

(A) **(B)**

Figure I. 5. *Mobile platforms of the IPAnema robot. A. the cables are directly clamped to the IPAnema. B. the cables are connected in a crossed cable (*Philipp TempelPhilipp Tempel, 2017)

In contrast, the IPAnema 1 system (depicted in Fig. 5) showcases a 2-2-2-2 configuration. Here, each of the four corners of the platform connects to two distinct winches.

I.3.2 Fixed Structure of Machine

In the majority of robot prototypes, the anchor points for winches are confined to geometric primitives. Geometric shapes with prismatic qualities offer distinct advantages, as they can be constructed conveniently using frameworks, and bars made from materials like aluminum or steel are well-suited for anchoring the winches securely. Several publications have emphasized that cable robots possess inherent reconfigurability. This feature has led to the inclusion of test-beds that facilitate the movement of winches along the bars of the framework. Notably, many cable robot prototypes incorporate a frame with a box-shaped configuration, exemplified by designs such as Segesta, IPAnema, and CoGiRo. In these instances, all base anchor points align with or near the box's surface, streamlining the need for intricate mounting mechanisms.

A significant portion of these designs confines the anchor points to the edges or even the corners of the box-like frame. In addition to prismatic arrangements, polar configurations are also favored. These polar setups define the anchor point positions through a radius and angles, effectively distributing the anchor points around a central point. For instance, a trisymmetric structure named ReelAx 8, introduced by Izard (Izard, 2012) , mounts all winches on three or four vertical poles, showcasing this polar design approach. When considering planar robots, they are predominantly operated within closed rectangular frames.

I.3.3 Moving Base

When considering the Moving Base concept in robotics, it's a widely adopted approach to utilize planar platforms. In such configurations, it's not uncommon for specific cables to share the same anchor points on the platform. This design choice offers several distinct advantages. As Verhoeven points out in their work (Verhoeven, 2004), one of the significant benefits is the substantial reduction in the potential for cable-cable interferences. This reduction has a direct consequence of enabling a larger workspace for the robotic system. The practice of using common anchor points helps create a more organized cable arrangement that minimizes the risk of cables coming into undesirable contact with each other during operation.

Additionally, the incorporation of shared anchor points on the platform has implications for other critical aspects of the robot's functionality. Singularities, which are certain configurations in which the robot's kinematics becomes degenerate, are influenced by the distribution of anchor points. Having common anchor points can strategically affect the location and occurrence of these singular configurations. This can be advantageous for controlling the robot's movements and avoiding problematic situations.

Furthermore, the computational aspect of robotics benefits from the use of common anchor points. Calculating the forward kinematics, which involves determining the robot's end-effector position based on joint configurations, is simplified when certain anchor points are shared. This simplification arises from the reduction in the number of independent variables involved in the calculations, streamlining the mathematical procedures and potentially improving computational efficiency. Works by authors such as (Pott, 2008)(Thomas, 2002) delve into the technical details of how these shared anchor points impact the forward kinematic computations.

Expanding into the realm of spatial platforms, which operate beyond the constraints of a single plane, prismatic or cylindrical designs are commonly encountered. These arrangements allow for multi-dimensional movement, adding complexity and versatility to the robot's operational capabilities. Alongside these, star-shaped platforms emerge as another prevalent design choice. These platforms exhibit multiple arms radiating from a central point, facilitating a balanced distribution of forces and movements across various directions.

I.4 Division and classification of the CDPR

Within this segment of our discourse, we embark on an exhaustive exploration of the diverse categorizations that form a fundamental foundation for our research. The significance of these categorizations resonates across the methods and algorithms expounded upon in this

study. This interdependency arises due to the tailored nature of numerous methods designed to address specific subsets within the domain of cable robots. Consequently, delving into these categorizations not only deepens our comprehension of the landscape but also unveils the contextual framework that governs the deployment of diverse methodologies. The inherent connection between these categorizations and the subsequent applicability of methods underscores the pivotal role these categorizations assume in molding the trajectory of our research.

I.4.1 Magnitude, Load Handling, and Motion Dynamics

Next, we consider some limiting factors for magnitude, load handling, and motion dynamics. ultimate limits for the length of the cables are given by:

- The cable material's specific strength, denoted as l R, sets an upper threshold for the length of a suspended cable subjected to gravity. This measure is quantified in meters. Should a cable exceed this limit, its weight surpasses its breaking load, rendering it incapable of supporting any external load. Notably, Zylon and Dyneema (polyethylene) exhibit remarkably high breaking lengths, approximately 350 km and 400 km respectively. Carbon fibers exhibit a somewhat lower strength at 250 km, while steel's breaking length is markedly lower, at around 25 km. Comparatively, graphene and carbon nanotubes (CNT) offer the potential for significantly enhanced values, approximately tenfold that of Dyneema. However, these materials, namely graphene and CNT, come with elevated costs and, as far as the author is aware, cables composed of CNT are not currently being manufactured.
- Conversely, cables constructed from Dyneema and Zylon are readily accessible in the market at reasonable expenses, setting a current practical boundary for size at approximately 350 km. This estimate holds when considering scenarios without the necessity to bear supplementary payloads and without accounting for safety margins. Importantly, this restriction does not hold true for applications in space robotics, where the influence of gravity is negated.

An intricate interplay exists among size, material choice, and dynamics in the context of exceedingly large robots. Notably, when the cable length significantly surpasses the sonic speed within the cable material, a notable reduction in response time occurs during swift movements at the actuator. This is attributed to the cable behaving akin to a spring, effectively functioning as a first-order low-pass filter. In Fig. 6, pivotal metrics are visually represented,

illustrating the ultimate size constraints stemming from fiber strength, designated by the shaded region. To account for commonly required safety factors, this zone is expanded by a factor of ten.

Shifting focus to the maximum payload aspect, contemporary large-scale cranes permit loads in the realm of thousands of tons, constituting a technological threshold. These substantial load capacities are realized through intricate systems of pulley tackles, featuring a considerable number of pulleys to manage the mechanical advantage and load distribution effectively.

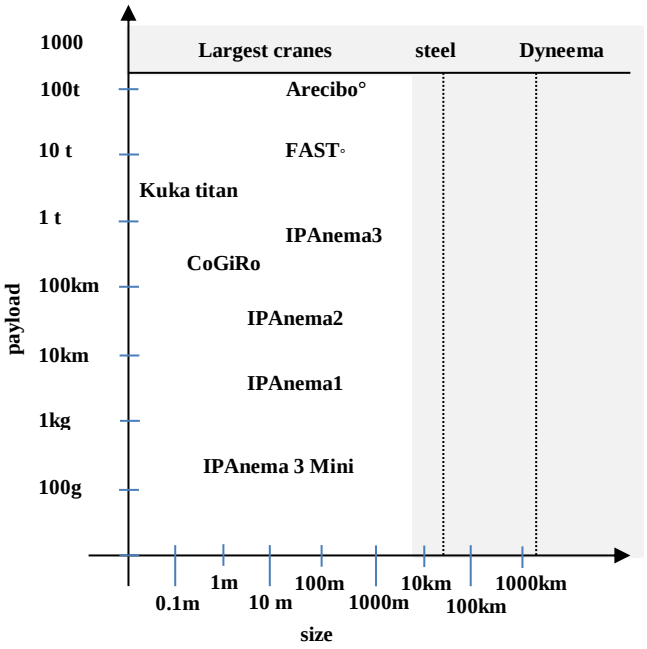

Figure I. 6. *comparison of various robots and cable configurations in terms of payload and size.*

The area on the right side of the graph correlates with the specific strength of common cable materials. The payload axis is confined within the range of the largest cranes' capabilities.

The operation of pulley tackles for the suspension cables of a cable robot introduces complexity to the system's construction. As far as available information suggests, no such design has been documented in existing literature. Consequently, it's reasonable to anticipate that effective payload limits might be somewhat lower than anticipated.

Maximum acceleration constraints are influenced by the capabilities of the available motors. Standard servo drives can achieve accelerations within the range of 20 to 1000 m/s² at the motor shaft's surface. In theory, achieving the specified cable acceleration is possible by directly coiling very lightweight cables onto this surface.

However, real-world mechanical design considerations introduce additional inertia when realizing the cable drum. Opting for larger drums results in escalated motor inertia, despite the advantageous increase in acceleration from a larger diameter. As the inertia of a solid cylinder is proportional to the fourth power of the diameter while velocities scale linearly with diameter, it becomes apparent that smaller drums are more preferable to attain higher maximum accelerations.

I.4.2 Motions Typology

A simple and direct method of classification revolves around the assessment of two key factors: the number of cables, labeled as "m," and the number of controllable degrees-of-freedom linked to the mobile platform, represented as "n." This classification approach was first introduced by Ming and Higuchi (Ming, 1994), thereby establishing its origins. Moreover, this classification introduces the concept of degree-of-redundancy, denoted as "$r = m - n$." This methodology allows us to differentiate between the following categories:

- **Number of Cables (m)**

The number of cables (m) refers to the total number of cables attached to the end-effector or mobile platform. The number of cables is an important factor in determining the robot's ability to control and stabilize the end-effector.

- **Controllable Degrees of Freedom (n)**

The number of controllable degrees of freedom n is the number of independent movements the mobile platform can perform. This typically includes translations along the x, y, and z axes, and rotations about these axes (roll, pitch, and yaw).

- $m < n \leq 6$: The robot operates within an under-constrained framework, making it incapable of withstanding arbitrary applied wrenches denoted as "w_P" When gravitational or other external forces and torques come into play, the robot might exhibit stable or unstable equilibrium at one or multiple configurations. However, it's important to note that certain degrees-of-freedom cannot be governed by the cables in a generalized manner. The count and orientation of these controllable degrees-of-freedom exhibit variations across the workspace. This category of robots is referred to as an "incompletely restrained positioning mechanism" (IRPM), as introduced by Ming and Higuchi (Ming, 1994). Refer to Figure 3 for visual representation.

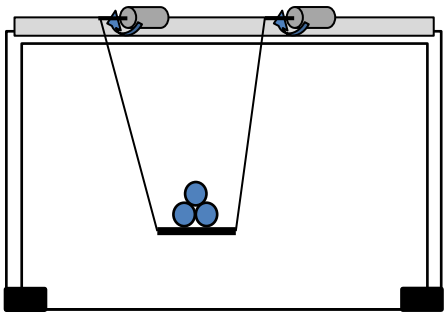

Figure I. 7 *Planer IRPM (m=2, n=3).*

- $n = m$: The robot is endowed with complete kinematic constraints, yet the equilibrium of forces hinges on external factors, including gravitational forces. The robot's capacity to endure forces and torques is bounded, contingent upon the intensity and orientation of these external forces. In the classification proposed by Ming and Higuchi, these robots are categorized within the IRPM class due to their reliance on external forces. However, it's worth noting that other scholars (Fang, 2005) have introduced a distinct classification to encompass such robots.
- $n + 1 = m$: The robot achieves complete constraint through its cables within distinct configurations. Various modes of motion are elucidated in detail in refer. The robot's ability to withstand forces relies on the span between its minimum and maximum cable forces, visually represented in Figure 8. These robots fall into the category termed "completely restrained positioning mechanisms" (CRPM). This nomenclature underscores their capability to attain comprehensive constraint by means of the cable system.

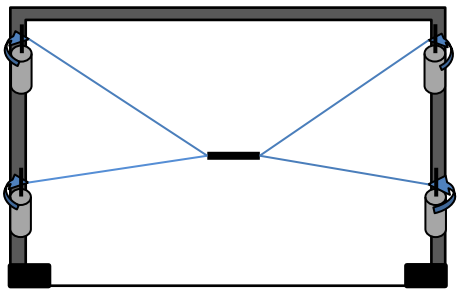

Figure I. 8. *Planer CRPM (m=4, n=3).*

- $n + 1 < m$: The robot operates with excessive constraints, necessitating the distribution of forces among the cables. These robots fall under the category of redundantly restrained positioning mechanisms (RRPM), illustrated in Figure 9. It's important to note, as highlighted by Merlet, that these robots don't possess kinematic

redundancy due to having only a single solution for the inverse kinematics problem. Instead, the redundancy pertains to the count of kinematic constraints, which in turn impacts their actuation mechanism as the constraints outnumber the degrees of freedom. Consequently, the static forces exerted by the robot typically remain undefined. Moreover, when considering the direction of the ith cable as "mu_i," a platform configuration is termed "suspended" when, for all cable i .

$$\cdot \; \boldsymbol{g} < \mathbf{0}, i = \mathbf{1}, \ldots, m\boldsymbol{u}_i$$

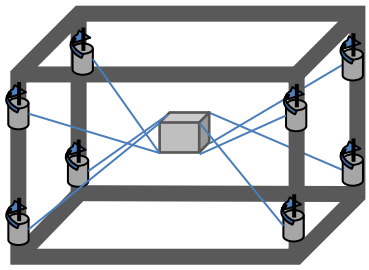

Figure I. 9. *Spatial RRPM (m=8, n=6).*

This statement remains valid, where "g" signifies the direction of gravitational force. In cases where the robot primarily operates in suspended configurations, it is customary to refer to the cable robot as suspended or in a crane configuration, signifying its reliance on gravity for stability. The term "suspended" serves as a convenient descriptor, indicating that the robot's workspace is predominantly situated beneath its frame, and its operation mimics that of a crane. Consequently, the design of the robot takes significant account of the influence of gravity, particularly to facilitate an expansive operational workspace. It's important to note that the inherent attribute of being "suspended" doesn't necessarily apply to the robot's design itself, but rather depends on its usage. Some robot designs are suited solely for suspended configurations, while others accommodate both fully-constrained and suspended operation modes. It's worth mentioning that all categories of robots outlined above (IRPM, CRPM, and RRPM) have the capability to operate in suspended configurations.

I.4.3 Divisions of Actuation

The majority of cable robots utilize winches as their actuation mechanism, where the cables are wound around drums (Albus, 1992) (Fang, 2005) (Kawamura S. &., 1993) (Pott A. M., 2012). This concept, borrowed from cranes, proves particularly effective in handling extensive cable lengths. Winches are established as compact, well-contained components (as shown in Fig. 10). Their mechanical design is both straightforward and cost-efficient. In the realm of cable robots, most winches employ servo motors to regulate cable length via

cascaded position control. Given that winches are typically affixed to larger structures, there exists minimal constraint on the size of applicable motors, with cost considerations being a limiting factor. This makes winches an optimal choice for tasks requiring high forces and dealing with long cables.

An alternative approach to cable length control is the utilization of linear drives in conjunction with pulley tackles (Merlet, 2008) (Merlet J.-P. &., 2007) (Surdilovic D. &., 2004). This technique involves moving either the cable end or one or more pulleys along a linear path to achieve the desired cable length adjustment. Notably, gear mechanisms integrated into the pulley tackles enable linearly actuated cable robots to access a substantial workspace. Linear drive systems coupled with cable tackles offer the potential for the highest cable velocities and accelerations. However, the maximum forces achievable may be constrained due to the limitations of available linear actuation setups.

An innovative proposition (Shoham, 2005), later patented (Shoham, 2006), involves changing cable length through cable twisting. This approach allows for exceedingly small increments in cable length adjustments, albeit with a constrained maximum length change. The twisting of cables effectively introduces a very high gear reduction, resulting in substantial forces generated with relatively modest velocities. However, this method is associated with substantial cable wear due to the twisting process. Despite this, it presents applicability for generating highly precise motion. It's worth noting that twisted cables introduce not only contraction forces but also torque on the platform, potentially necessitating consideration in the system's design and operation.

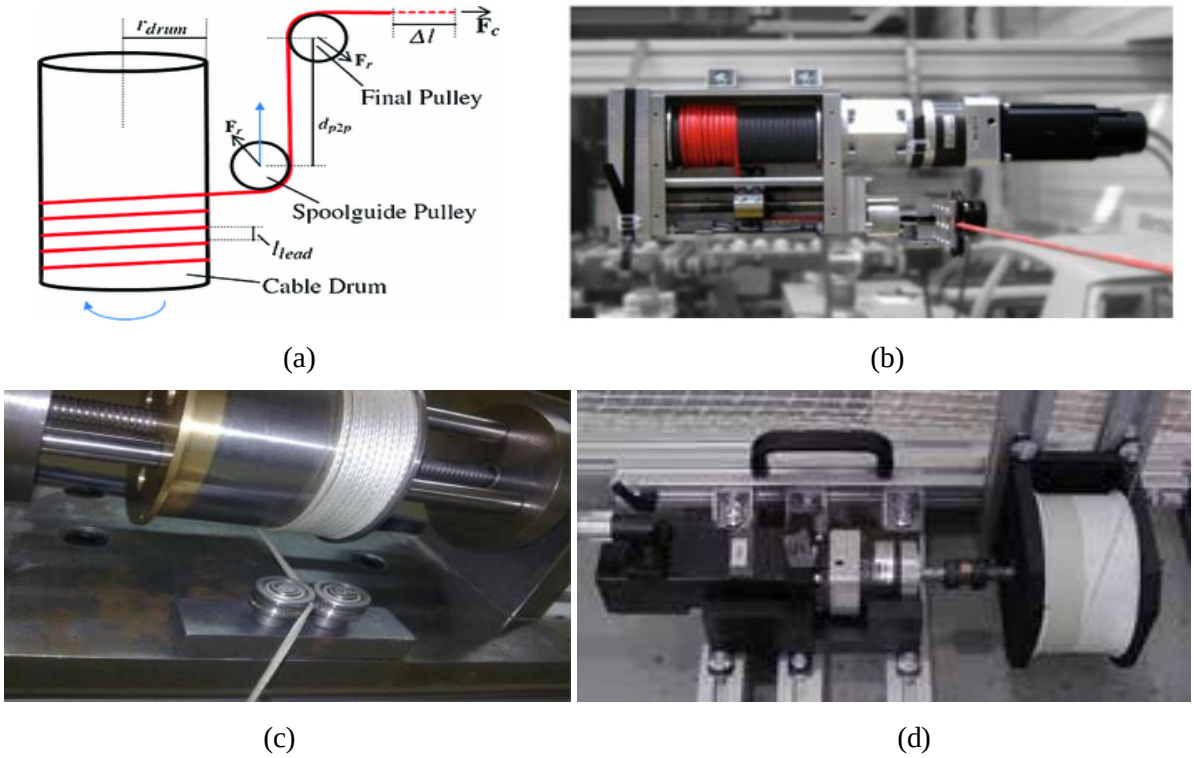

Figure I. 10. *Different concepts for actuation of cable robots with winches* (Mohamed Tazi, 2018) (Marceau Metillon, 2020)

The provided image showcases a preliminary design for a winch system, featuring an IPAnema1 winch integrated with a cable guidance system. The system comprises a servo drive (M), a gearbox (G), a single-layer and unidirectional pulley mechanism drum (T), and a dedicated cable guidance system (S).

Ultimately, kinematic ideas akin to those of Delta robots (Clavel, 1988) were put forth. These concepts involve attaching cables of constant length to rotating levers, mirroring the kinematic arrangement of Delta robots. To account for the inherent use of Delta robots in applications with relatively compact designs and light payloads, a telescopic strut accompanied by a spring is connected to the mobile platform. This design ensures the cables remain taut. Maeda (Maeda, 1999) introduced a prominent example of this approach in the form of the well-recognized demonstrator called WARP.

Additional methods for actuation also exist within this domain. The Cablev system, for instance, incorporates movable winches on a guideway (Maier, 2004) (Maier T. &., 2001) (Woernle, 2012). The planar IPAnema 2 system (Pott A. M., 2012) adopts cable-driven pulleys in conjunction with linear direct actuators, enabling the platform to maintain an isotropic configuration across a rectangular workspace (Pott A. , 2013). Bruckmann introduced a robotic system closely resembling cable robots; however, in this case, slim rigid

legs replace the cables (Bruckmann T. M.-M., 2009). The proximal anchor points of the winches are adjusted via linear guideways. Although akin to the well-known Linaglide architecture used in parallel robots, here, the focus is on maintaining positive forces or permitting only minimal pushing forces in the legs. Nevertheless, despite a promising conceptual study, the constructed machine employed cables and was utilized as a manipulator in a wind tunnel.

Recently, a cable robot characterized by restraining cables and linear springs was introduced (Duan, 2014). In this setup, the springs were employed to shape the workspace through the application of an artificial potential field.

I.4.4 Taxonomy of Function

The term "robot" inherently suggests a device designed to handle or manipulate various objects. Within the context of cable robots, several distinct functions can be discerned, including but not limited to:

- Motion Generation: The primary purpose of most cable robots is to generate controlled motion of the mobile platform. This involves achieving specific positions and orientations in a predetermined sequence. The trajectories between these poses are often well-defined in terms of velocity and acceleration, depending on the control system in place. This is a typical control scheme akin to conventional robots and machine tools. Cable robots that are fully or redundantly constrained tend to have well-defined motion behaviors due to their over-constrained equations (Fig. 11-a).
- Force-Torque Generation: Cable robots can be programmed to produce precise forces and torques at the mobile platform. This functionality is useful for tasks such as production processes or acting as force feedback systems. The platform's motion is influenced by its interaction with the surrounding environment, particularly the exerted wrench on the mobile platform (Fig. 11-b).
- Force-Torque Measurement: Cable robots have the capacity to measure cable forces. These measurements can be obtained through motors, additional sensors integrated into the cables, or the cables themselves. Such measurements enable the derivation of applied forces and torques on the mobile platform, effectively creating a multi-directional force/torque sensor (Fig. 11-c).
- Motion Measurement: Cable robots can determine the position of their platform even when it's moved by external factors such as humans, other machinery, or environmental forces. This can be achieved through sensors that estimate the current

pose of the platform. In scenarios where motors are replaced with contracting springs, position measurement systems can be applied to the winches to determine cable length. Using forward transformations, the pose of the mobile platform can be reconstructed from these measurements. The expansive workspace and relatively low inertial mass of the mobile platform in cable robots make them suitable for large-scale spatial measurement tasks, such as motion tracking and calibration (Figs. 11-d).

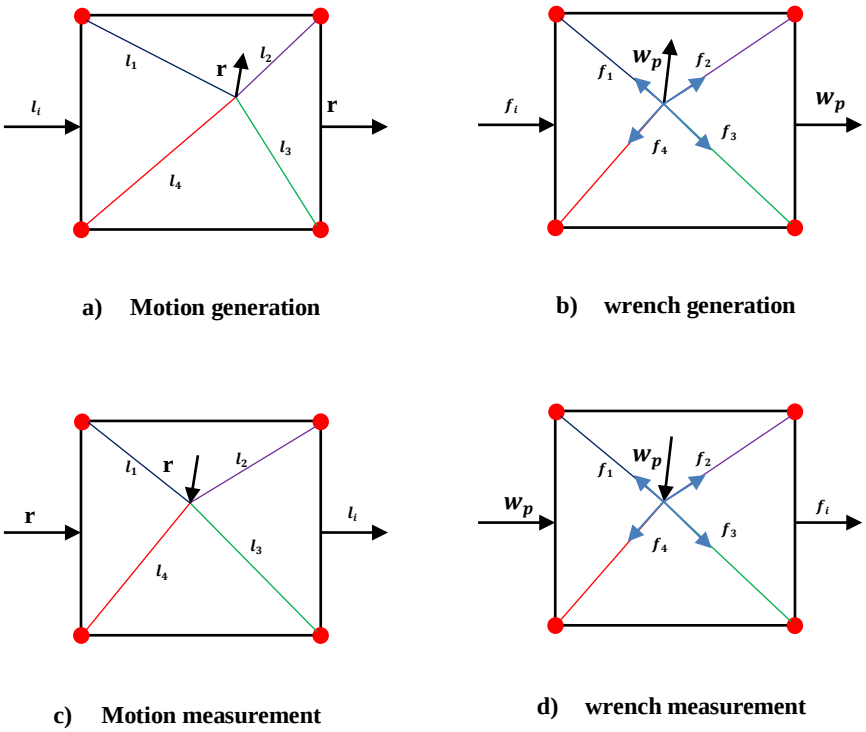

Figure I. 11. *Illustration of the four basic functions of a cable robot*.

Indeed, practical applications often involve the simultaneous utilization of multiple functions within cable robots. For instance, consider a positioning system employed for assembly tasks. This system could effectively harness its force-torque measurement capabilities to enhance process control and ensure precise assembly operations. This integration of functions underscores the versatility and adaptability of cable robots in meeting complex operational demands.

I.4.5 Cable Robot Movement Strategies

The motion pattern of a robot delineates a subset of generalized virtual displacements, denoted as δy, that can be achieved by the end-effector while adhering to its kinematic constraints. Within this framework, a virtual displacement δy represents a composite of translation and rotation, manifesting rigid body motion in three-dimensional space. In the SE3

spatial Euclidean motion group, there exist six autonomous virtual displacements, thereby establishing the maximum degrees-of-freedom n for a mobile platform as six. Notably, a motion pattern is denoted by an abbreviation in the format n RRn TT, where R signifies nR rotational degrees-of-freedom, and T denotes nT translational degrees-of-freedom.

It's worth noting that not all robots can realize all six independent virtual displacements. For instance, robots with fewer than six degrees-of-freedom, such as planar robots (n = 2 or n = 3) or spatial translational robots (n = 3), highlight that the degree-of-freedom isn't a sole determinant for distinguishing platform motion patterns. Consider n = 3 as an illustrative example.

In the context of n = 3, we encounter motion patterns like the planar rigid body motion (1R2T), entailing two translational and one rotational degrees-of-freedom, motion of a point in space (3T) involving three translational degrees-of-freedom, and the spherical motion (3R) that aligns with the special orthogonal group SO3.

The motion pattern of a platform generally relies on its pose-dependent property, implying variations across its workspace, characterized by the loss or acquisition of degrees-of-freedom, in other words the loss or acquisition of degrees of freedom in statistics relates to the reduction or increase in the number of independent parameters that can vary freely, impacting the precision and reliability of statistical analyses. are notable challenges in motion patterns. Apart from changes in the number of degrees-of-freedom for end-effector motion, the direction of available virtual displacements might alter with configuration. In practice, a well-defined motion pattern is preferable, motivating robot designers to concentrate on such designs.

For clarity, the subsequent discussion pertains to motion patterns expressed through the superposition of purely translational and rotational displacements. These directions are arbitrarily aligned with translation along and rotation about the axes of a Euclidean coordinate system.

In notation, translational motions are abbreviated as T, and rotational motions as R, leading to notations like 1R2T for the planar rigid body motion with one rotational degree-of-freedom and two translational degrees-of-freedom. Verhoeven (Verhoeven, 2004) compiled an exhaustive catalog of potential motion patterns for fully parallel cable robots (Fig. 12 and13), substantiating its comprehensiveness. However, these conclusions rest on strict assumptions, assuming independent cable actuation. Notably, it was proven that motion patterns lacking translational degrees-of-freedom (e.g., 1R, 2R, and 3R) are unachievable within this context. Additionally, it's not possible to create Schönflies-motion (1R3T) generators based on fully

parallel cable robots, as established by Verhoeven. However, this limitation can be circumvented by adding cables without actuation or by mechanical constraints. Fixing certain cables at a constant length permits pure rotations (3R). A cable robot can be constructed by combining the 3T and 3R3T robots from Fig. 13 into one robot with m = 11 cables, with four cables of the 3T robot considered to be of constant length without actuation. This setup enables orientation changes of the platform without translation due to the fixed cable length of the 3T component.

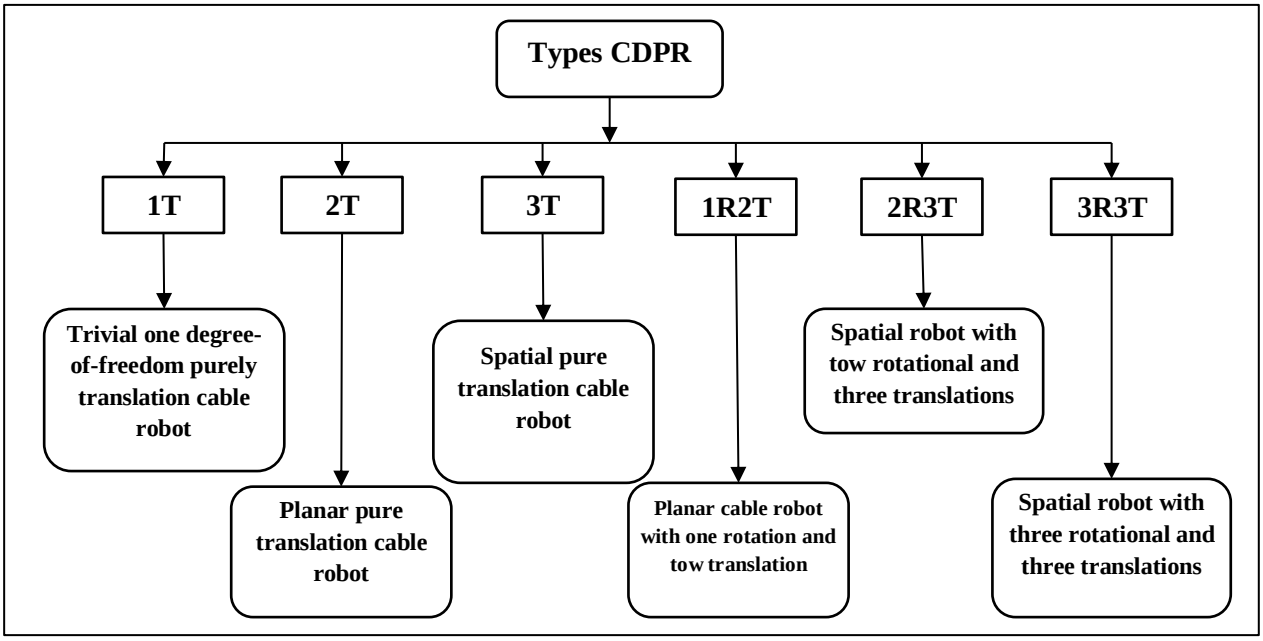

Figure I. 12. *plane complete element of all possible motion patterns for parallel cable-driven robot.*

T represents translation degrees-of –freedom, while R represents rotational degree-of-freedom in the acronyms of the motion patterns.

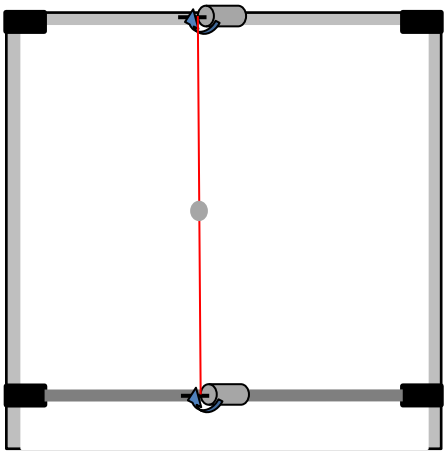

$1T : m = 2, n = 1$

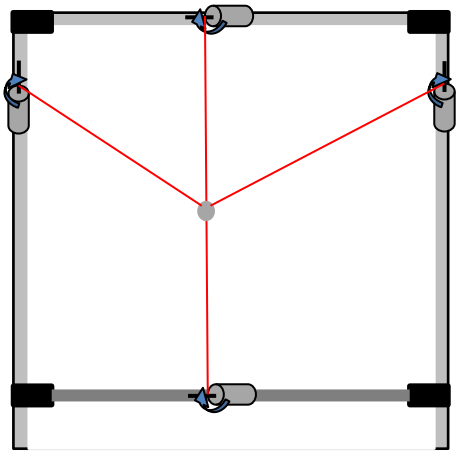

$2T : m = 4, n = 2$

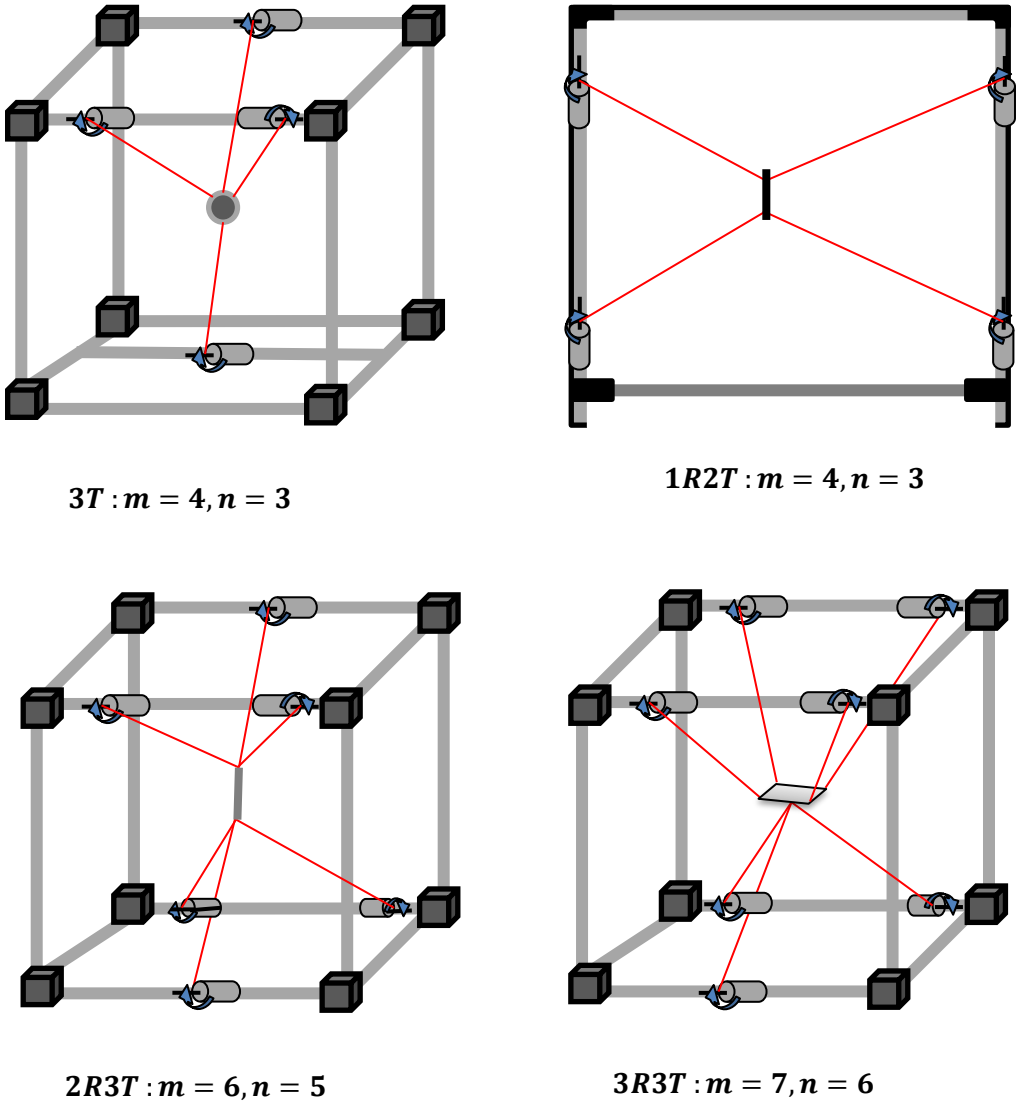

Figure I. 13. *All possible motion patterns for fully parallel cable robots with the number of cables m.*

I.5 Advantages and Disadvantages of cable driven robot

We outline the positive attributes and drawbacks related to cable-driven robots:

I.5.1 Advantages:

- Large Workspace: Cable-driven robots can offer a significantly larger workspace compared to traditional rigid-link robots. This makes them suitable for applications that require extended reach and access to hard-to-reach areas.
- High Payload Capacity: Despite their lightweight design, cable-driven robots can handle substantial payloads. This makes them well-suited for tasks that involve moving heavy objects or performing tasks with significant forces involved.

- Lightweight Design: Cable-driven robots have a lightweight structure due to the absence of heavy rigid links. This feature makes them easier to transport, deploy, and operate, especially in applications that require mobility or aerial capabilities.
- Energy Efficiency: Cable-driven robots can be more energy-efficient than traditional robots because they use lightweight cables and pulleys to transmit forces, reducing the overall power requirements.
- Redundancy and Safety: Many cable-driven robots have redundant actuation, meaning they have more cables than strictly necessary for task execution. This redundancy provides increased safety and reliability as the robot can continue operating even if some cables fail.
- Smooth Motions: Cable-driven robots can achieve smooth and precise motions due to their cable-based transmission system. This characteristic is essential for applications that require accurate positioning and gentle interactions.

I.5.2 Disadvantages:

- Complex Control: The control algorithms for cable-driven robots can be more complex than those used in traditional robots due to the non-linear nature of cable dynamics and the need to manage cable tensions accurately.
- Calibration and Maintenance: Cable-driven robots require precise calibration of cable lengths and tension control to ensure accurate motion. Additionally, maintaining the tension in cables and ensuring they remain in good condition over time can be challenging.
- Sensitivity to External Disturbances: Cable robots can be sensitive to external disturbances, such as wind or external forces acting on the end effector, which may affect the robot's stability and accuracy.
- Limited Accuracy with small dimension structure: While cable-driven robots can achieve impressive accuracy, they may not be as precise as some high-end traditional robots with rigid links. The compliance in the cable system can introduce some level of uncertainty.
- Restricted Speed: Cable-driven robots may have limitations in achieving high-speed motions due to the dynamics of the cables and the need to manage tensions carefully.
- Complex Design and Cost: The design of cable-driven robots can be more complex and require specialized engineering knowledge, making them potentially more challenging and expensive to develop and build.

Overall, the choice to use a cable-driven robot depends on the specific requirements and constraints of the application at hand. These robots are particularly advantageous in scenarios where a large workspace, high payload capacity, and lightweight design are essential, but they may require careful consideration of control, maintenance, and design complexity.

I.6 Application Domains

Cable robots have emerged as versatile candidates for an extensive array of applications. Similar to various other robotic systems, the innovation of novel applications predominantly stems from the drive to automate processes formerly reliant on manual or mechanized methods. This transition towards full automation is a hallmark of robotic solutions and has been exemplified across numerous industrial scenarios, showcasing their potential to curtail labor costs, enhance process precision, and expedite cycle times. Consequently, cable robots are positioned to venture into unexplored realms of application, particularly addressing challenges where traditional industrial robots face limitations related to workspace dimensions, payload capacities, and cycle time requirements.

Nonetheless, cable robots offer additional benefits such as occupying minimal installation space, facilitating straightforward transportation and deployment, and enhancing overall quality. This positions cable robots as potential assistant devices, especially in scenarios where conventional robotic systems may not be suitable.

I.6.1 Organization and construction work

The construction requirements share some connection with the demands associated with various applications. Cable robots, once again, demonstrate their advantage in cost-efficient large-scale systems. However, in the context of these expansive systems, the emphasis on achieving high-speed motion takes a back seat. Instead, cable robots can capitalize on their inherent flexibility and adjust to specific construction tasks through geometrical configuration.

One of the initial applications proposed for the RoboCrane was in ship and bridge building (Albus, 1992) (Albus, 1993) (Bostelman, 1992) (Bostelman R. V., 1996). Cable robots were also put forward as potential robotic cranes for constructing large-scale solar power plants (as depicted in Fig.14) (Pott A. M., 2010). More recently, Izard explored the deployment of a cable robot on a building's facade (Izard J.-B. G., 2012) (Izard J.-B. G., 2012). This endeavor encompassed various potential tasks, including cleaning and advertising. A slightly distinct approach was presented by Voss (Voss, 2012) (Voss, 2013), outlining the use of a cleaning or

inspection unit designed to traverse vast glass surfaces. Emmens (Emmens, 2014) introduced the concept of utilizing a cable robot with constraints for cleaning facades and buildings. To prevent any relative motion between the cables and the surface, the proposal suggests installing motors on the mobile platform. Preliminary results were obtained from a small-scale mock-up.

Figure I. 14. *Vision of assembly of parabolic reflector panels with a mobile large-scale cable-driven parallel robot.*

I.6.2 Logistical Services

Cable robots hold significant promise in the domains of handling and logistics. They can fully leverage two primary advantages: designing cost-efficient robots for extensive workspaces and achieving exceptional dynamics, enabling substantial throughput for tasks such as handling, sorting, and palletizing.

The concept of constructing ultra-high-speed pick-and-place manipulators using cable-driven robots was explored as early as the 1990s. Notably, the FALCON robot developed by Kawamura (Kawamura S. C., 1995) (Kawamura S. K., 2000) and the Warp system proposed by Tadokoro (Maeda, 1999) both tackled this idea. The integration of cable robots with automated cranes emerged as a solution for handling very heavy loads. For instance, the Cablev system (Heyden T. , 2006)(Heyden T. &., 2006) at the University of Rostock, Germany, aimed to automate container crane operations. It employed an under-constrained cable robot with additional linear axes for controlling the winches.

Figure I. 15. *Cable robot IPAnema 3 for large-scale handling of collector modules shown.* (man, 2020)

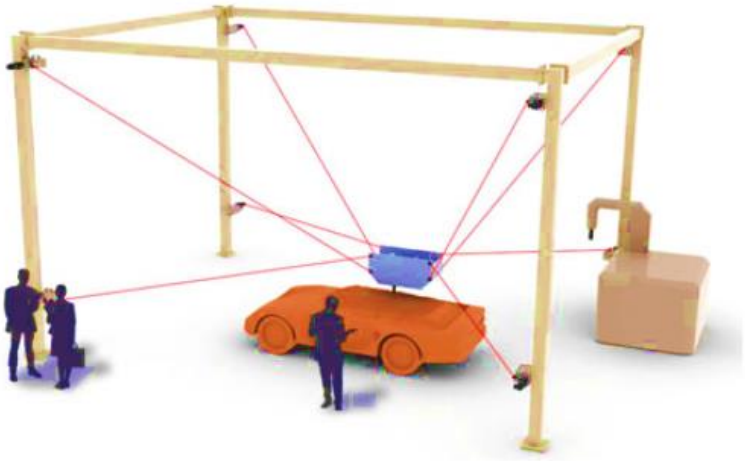

Figure I. 16. *Concept for additive manufacturing of mockups using a large-scale cable robot equipped with an extruder. Source: Pott and Grzesiak (*Pott A. , 2018*)*

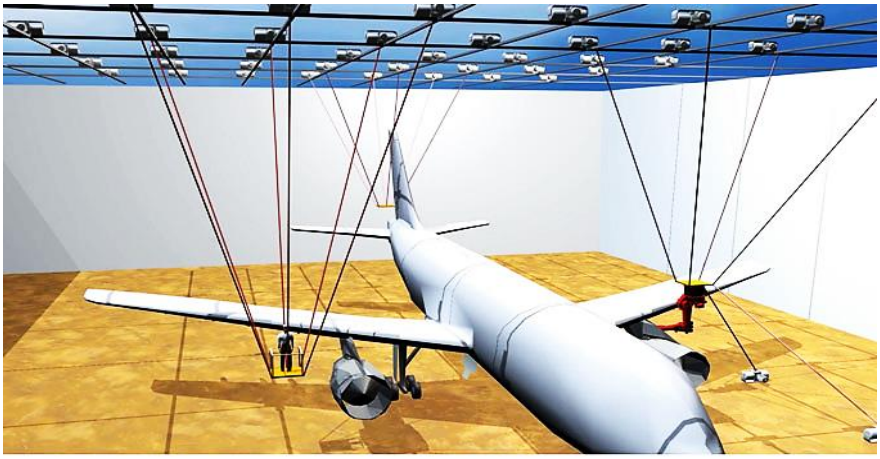

Figure I. 17. *Application concept for painting, cleaning, and maintenance of aircrafts with cable robots (top). (Mijangos, 2013)*

The CABLAR system, developed by Bruckmann (illustrated in Fig. 18), served as a storage retrieval machine (Bruckmann T. L., 2013) (Bruckmann T. L., 2012) (Lalo, 2013) . Merlet later introduced a portable crane designed for heavy-load handling and rescue operations, utilizing an aerostat-like mechanism to anchor pulleys mid-air (Merlet J.-P. &., 2010). Addressing a civil engineering challenge of transporting individuals across a river, Castelli (Castelli, 2009) (Castelli G. O., 2014) also explored cable robots.

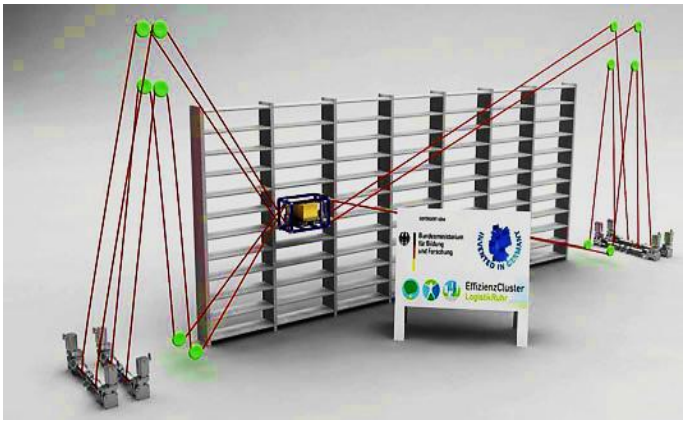

Figure I. 18. *The large-scale cable robots as storage retrieval machine, The University of Duisburg-Essen has extensive experience with cable-driven robots(*Jadhao, 2016 *)*

Given their lightweight structure, cable robots were proposed for use as sensor platforms across various scenarios. Bauer's patent (Bauer, , 2011) capitalized on the extensive workspace of cable robots to maneuver optical and radio sensors through shelf storage systems, enabling the inspection and localization of stored goods.

I.6.3 Rehabilitation Applications

A cluster of applications is dedicated to the simulation and measurement of various movements. Among these, a significant domain is found within medical and rehabilitation applications. Here, the implementation of an ultra-lightweight cable robot emerges as a valuable tool for both guiding and precisely gauging limb motion. Additionally, the potential application extends to stabilizing the upper body during the process of gait rehabilitation. Ishii (Ishii, 1994) pioneered this concept by introducing a straightforward robot configuration consisting of four cables, serving as a sophisticated 3D haptic interface. Surdilovic further expanded this notion with the introduction of the String-Man system (Klatte, 1993)[448]. This inventive system involves suspending a subject using a harness that, in turn, is supported by cables (depicted in Fig.19). By implementing advanced force control mechanisms, the

perceived mass is effectively reduced, offering the possibility of gait training with significantly diminished stress on the body and lower extremities.

Moreover, the cable robot effectively prevents patients from falling, adding a significant safety aspect. A similar concept was subsequently explored by Castelli (Castelli G. O., 2009) (Castelli G. &., 2014), who introduced a device aimed at assisting elderly individuals in transitioning from a seated position in a wheelchair to standing. For over a decade, Agrawal has been dedicated to investigating the versatile applications of cable robots in rehabilitation contexts (Brackbill, 2009) (Mao, 2010) (Mao, 2011), wherein both cable robots and cable-driven exoskeletons were subjects of scrutiny. Merlet conducted a series of practical tests involving the Marionet robot, demonstrating its capability to lift elderly and disabled individuals within a controlled assisted living setting (depicted in Fig.20). The utilization of cable robots for generating and tracking motion in athletic activities such as rowing was examined at ETH Zurich by Zitzewitz and Rauter (Rauter G. Z.-W., 2010) (Zitzewitz J. V., 2009) (Zitzewitz J. V., 2010). Presently, a recently established company offers a novel rail-based cable robot known as the "float" (Free Levitation for Overground Active Training), designed as an assistive tool for rehabilitation (Vallery, 2013) (Engineering., 2015).

Certain researchers have put forward the concept of constructing motion simulator platforms utilizing cable robots. The potential for a notably expansive workspace coupled with impressive dynamic capabilities has been recognized as a pivotal advantage of cable robots over alternative structural solutions. Notably, the application of motion generation and precise positioning within aerodynamic and hydrodynamic test facilities has garnered significant attention.

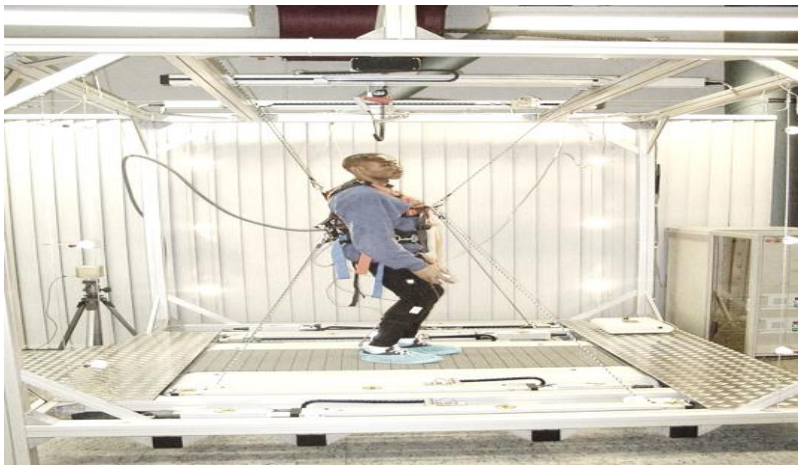

Figure I. 19. *The cable robot String-Man is designed for use in gait rehabilitation.* (Pott A. , 2018)

Lafourcade proposed a compelling application by suggesting the integration of a cable robot into an airplane wind tunnel (Lafourcade P. L., 2002) . This innovative approach leverages the

minimal airflow disturbance caused by the cables, making it conducive to precise testing. Similarly, Bruckmann adopted a comparable strategy, introducing a cable robot tailored for positioning ship hulls (Bruckmann T. M.-M., 2009). Most recently, there is a development involving the design of a cable robot for a distinct purpose: to serve as the motion base for experimental research into human vestibular senses. Additionally, this same cable robot is being considered for use as a flight simulator . This demonstrates the remarkable adaptability and versatility of cable robots across varied applications.

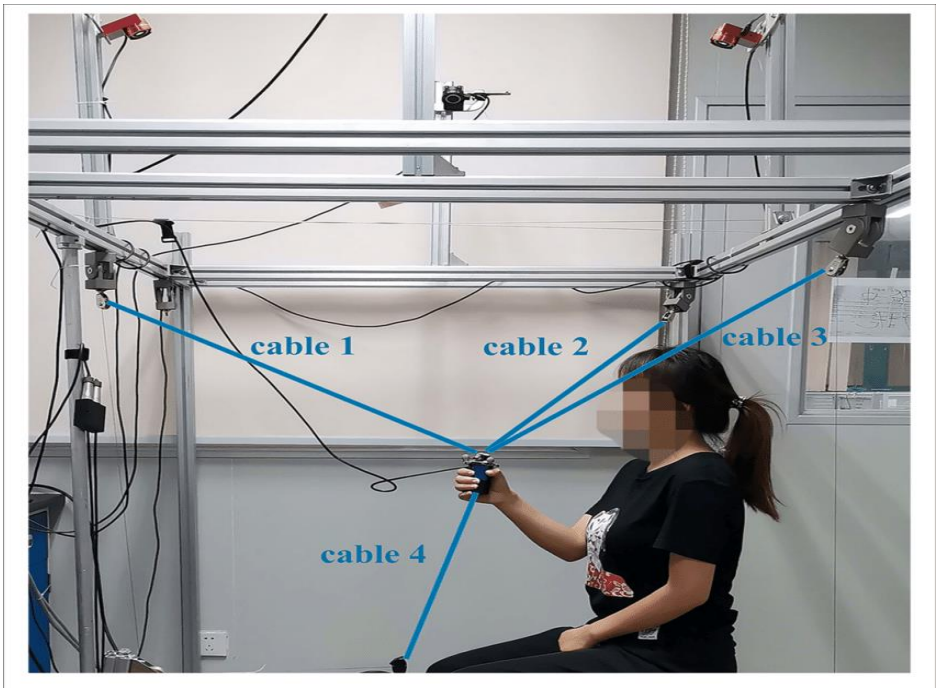

Figure I. 20. *The schematic representation of the cable-driven rehabilitation robot (CDRR)(*Rongrong Tang, 2022*)*

Harnessing the cable robot's capabilities for both motion measurement and force generation has catalyzed investigations into haptic displays and tools designed for virtual reality experiences. Otis (Otis M. J.-D., 2008) introduced an innovative haptic interface tailored for walking simulations. Similarly, Kraus (Kraus, 2015) put forth a sophisticated control framework that enables diverse haptic interaction modes between a cable robot and a human operator. This is achieved through the application of admittance control on the IPAnema 3 Mini robot (depicted in Fig. 21), showcasing the potential for nuanced tactile feedback. Furthermore, the realm of virtual reality has also seen interest in utilizing cable robots. Merlet proposed incorporating them as part of the Marionet robot family to enhance virtual reality applications. This multidisciplinary convergence underscores the wide-ranging impact and applicability of cable robots in cutting-edge technology experiences.

I.6.4 Gauging Equipment

As early as the late 1990s, a position tracking system was introduced by Jeong (Jeong, 1998) (Jeong, 1999) . In a bid to enhance the precision of this system, Jeong put forth the idea of mitigating length errors that result from the sagging of cables. Subsequently, Ottaviano and Thomas (Thomas, 2002) delved into the kinematics of a comparable tracking setup. A parallel line of inquiry involving robot calibration was pursued by Pott (Pott A. M., 2012), who devised the IPAnema measurement apparatus. This device was constructed using industrial cable length sensors, further contributing to advancements in the field.

I.6.5 Manufacturing Techniques

The majority of robots deployed globally find their application within the production and manufacturing sector. In this domain, robots have proven highly effective in automating industrial processes, particularly in tasks such as handling, welding, painting, and assembly. Consequently, a significant portion of research endeavors centered around cable robots has been directed toward exploring their potential in various production-related tasks.

Within the University of Berlin's research endeavors, an innovative machine tool emerged from the integration of a cable robot (Kraft, 2005). This machine tool featured a platform housing a spindle, suspended by eight cables that facilitated its movement around the workpiece. The primary goal of this research was to achieve high-speed motion utilizing the cable robot. However, the outcome revealed a limitation: the system lacked the necessary stiffness required for precision machining.

Bosscher introduced an intriguing application of cable robots known as counter crafting (Bosscher, 2007) (Bosscher P. M., 2010.). This concept involved the development of a mobile frame that could navigate between construction sites. In a detailed patent (Bosscher P. M., 2010.), Bosscher outlined a cable robot employing as many as twelve cables. Notably, a set of eight lower cables were situated on vertical guideways. This innovative arrangement allowed for continuous configuration adjustments, effectively preventing any clashes between the lower cables and the ongoing construction. Additionally, Pott delved into the realm of handling and assembling large-scale products, such as collectors for concentrated solar power (CSP) plants (Pott A. M., 2010). This research was showcased at the Automatica 2010 trade fair in Munich, Germany. These instances underscore the diverse and forward-looking applications of cable robots in various industrial contexts.

Various production tasks necessitate the precise positioning of specialized equipment around substantial workpieces or products, encompassing items like ships, airplanes, windmill

blades, as well as sizeable steel structures such as motors, generators, and gearboxes. These tasks typically involve processes such as painting, welding, grinding, or blast cleaning. Cable robots offer a particularly advantageous solution for these scenarios, especially in non-contact processes. They lend themselves well to tasks involving measurements for inspection, maintenance, or quality control due to their flexibility.

One notable initiative in this direction is the CableBOT research project, supported by the European Commission (Afshari, 2007). This project explored the utilization of cable robots for the intricate task of painting aircraft. Furthermore, a conceptual study was conducted by Pott and Grzesiak, focused on the potential application of cable robots in additive manufacturing. This exploration aligns with the growing interest in 3D printing and its potential implications for the manufacturing industry.

I.6.6 Leisure Activities

As early as the 1920s, the concept of suspending a camera by cables to facilitate its movement was put forth by l'Argent. He devised a setup where both the camera and its operator were positioned on a mobile platform suspended by cables. It's noteworthy that during this era, the operation of the cables was manual. Nevertheless, the fundamental notion, along with its advantages, has been recognized for nearly a century.

Moving forward in the timeline of cable robot development, an essential milestone was the filing of a patent for the SkyCam (Cone, 1985) by Brown (Brown, 1987). Brown, known for inventing the renowned steadicam for stabilizing camera motion, introduced a computer-controlled system for the SkyCam. The patent outlines a suspended camera setup employing three cables, featuring an intricate mechanism on the platform to orient the camera precisely as desired. This establishes the SkyCam as a 3T cable robot system.

Subsequently, the company CableCam Limited submitted a series of patents related to the CableCam concept, a prime example being (Rodnunsky, 1991). Beyond camera applications, the cable robot concept extended to the realm of thrill rides. Various entities, including Disney (Crawford, 2012.), presented patent applications for amusement rides rooted in cable robot technology. A preliminary design of a thrill ride incorporating a suspended cable robot is illustrated in Fig. 21. Moreover, several safety mechanisms tailored for such systems were developed to ensure operational security.

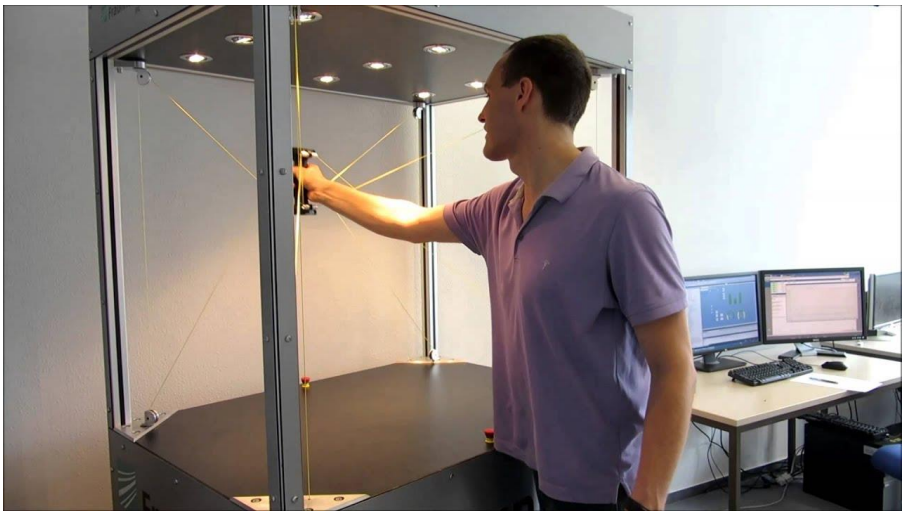

Figure I. 21. *IPAnema 3 Mini for haptic interaction ,the Fraunhofer Institute for Manufacturing Engineering and Automation IPA (*Matt, 2017 *)*

I.7 Conclusion

In this chapter, we discussed a historical overview of the emergence of the Cable-Driven parallel robot through historical stages. Additionally, we explained its essential components that are important in the robot's configuration, through which we can classify and label the robot. We also mentioned the field of applications of these types of robots, given their significant importance in various domains. We will provide more details about how this type of robots operates in the upcoming chapters.

Chapitre 2

II.1 Introduction

In this chapter, we delve into the significance of selecting the pyramid structure's shape, which represents a pioneering approach in designing a robot with such unique characteristics. The choice of this shape is not only novel but also adds an appealing factor for potential users. We explore the durability of the pyramid structure in comparison to other commonly used designs in numerous research endeavors.

Moreover, we discuss the research that led to the determination of this specific shape and how the cables are precisely connected to the end effector. Additionally, we highlight the various rehabilitation applications that this robot can effectively perform.

To thoroughly evaluate the structure's performance, a qualitative analysis was carried out by testing several materials. This analysis aimed to identify the most suitable material and necessary elements required to construct this robot. Through this examination, we intend to enhance our understanding of the pyramid structure's capabilities and potential for successful implementation in various applications.

II.2 Problematic research

Dysgraphia, a writing difficulty experienced by children, is acknowledged as one of the learning challenges affecting young learners worldwide. This disorder significantly impacts children's development across diverse cultural backgrounds. Dysgraphia encompasses difficulties with handwriting, spelling, and expressing coherent thoughts on paper. Failure to acquire this fundamental skill adequately during childhood can result in reduced communication abilities, hindering overall educational progress and social interactions.

Dysgraphia is a multifaceted condition observed in children, irrespective of gender, presenting substantial challenges across various writing aspects, such as spelling, calligraphy, or both. This specific difficulty is commonly identified as “dysgraphia.”

Dysgraphia is classified among the group of disorders related to writing expression and falls under the category of learning disorders. Children with dysgraphia encounter challenges not

only in the physical act of writing but also in effectively conveying their thoughts and ideas on paper. Moreover, difficulties in writing often coincide with other learning disorders, such as dyslexia, which can worsen the overall learning challenges for the affected children.

In summary, dysgraphia is a multifaceted condition that hinders a child's ability to write fluently and accurately, involving challenges in spelling, handwriting, and written expression. Being part of the broader spectrum of learning disorders, it may coexist with other conditions like dyslexia, emphasizing the need for personalized support and interventions to assist these children in overcoming their difficulties and achieving academic success (twinkl, 2017).

The symptoms of this disorder vary, and among the most prominent are the following:

- Handwriting that is inconsistent or illegible, making it difficult to read.
- Difficulty in accurately determining the spaces between words and phrases.
- grammatical problems
- Improper pencil grip.

II.2.1 Reasons for writing difficulties

a) Child-specific difficulties

- ✓ Mental retardation or academic delay can lead to a decreased intelligence level in children, causing a delay in their school entry. Several factors contribute to such difficulties, encompassing mental aspects like cognitive limitations, physical factors such as diseases and disabilities, and environmental factors like family disintegration and other related issues. These factors can collectively contribute to conditions like dysgraphia and other learning challenges.
- ✓ Kinetic control disorder, commonly referred to as dyspraxia, denotes the child's struggle in adequately controlling the movement of their body, head, arms, and hands, leading to challenges in tasks like copying and accurately writing letters. These difficulties arise due to impaired coordination of motor skills, hindering the child's writing abilities. Nevertheless, the child's reading skills may remain intact.
- ✓ The disorder of visual perception manifests as the child's inability to differentiate between the shapes of numbers and letters, despite having no underlying visual problems. In these instances, the child may lack motivation to learn writing, and this situation can worsen in the absence of encouragement from parents or teachers at school. As a result, the child may display a greater interest in playing and seeking enjoyment instead of focusing on learning to write.

b) environmental difficulties

- ✓ The inadequate teaching method overlooks the individual differences and abilities of students, failing to offer adequate encouragement. Moreover, it may lack suitable approaches to effectively teach writing.
- ✓ Left-handedness can also play a role in causing writing difficulties.
- ✓ Insufficient interest and lack of follow-up at home with the child can have negative consequences, as depending solely on school may not always be enough.

II.3 Objective of this research

In this research, we will focus on finding a solution to the aforementioned problem, which involves developing a Pyramid cable-driven robot for which various scientific studies will be conducted. Among these studies is a medical investigation to ensure the safety of this robot for children, ensuring that it does not pose any harm while in operation. Furthermore, the research aims to prevent any potential negative consequences or new disabilities that could arise for the child during the learning process. This robot was also examined from a structural standpoint to determine an ideal and appealing design that sparks the child's interest and enhances their engagement with it for learning purposes. The goal is to ensure that the child continues to use this robot for educational activities. Many robots in the past have had a negative impact on users due to their designs lacking safety features, leading to neglect of such robots. Thus, it is crucial to select a design that prioritizes user safety and encourages positive interaction. however, the structure has been studied from an engineering perspective to ensure its adaptability to the classroom table or a table at home, enabling continuous practice in the learning process.

This topic was also examined from an economic standpoint, aiming to make the robot affordable and accessible for all individuals to acquire and utilize it at home. Although designing the shape and implementing a robust control algorithm might involve some complexity, the actual usage of this robot remains straightforward, allowing anyone to operate it with ease.

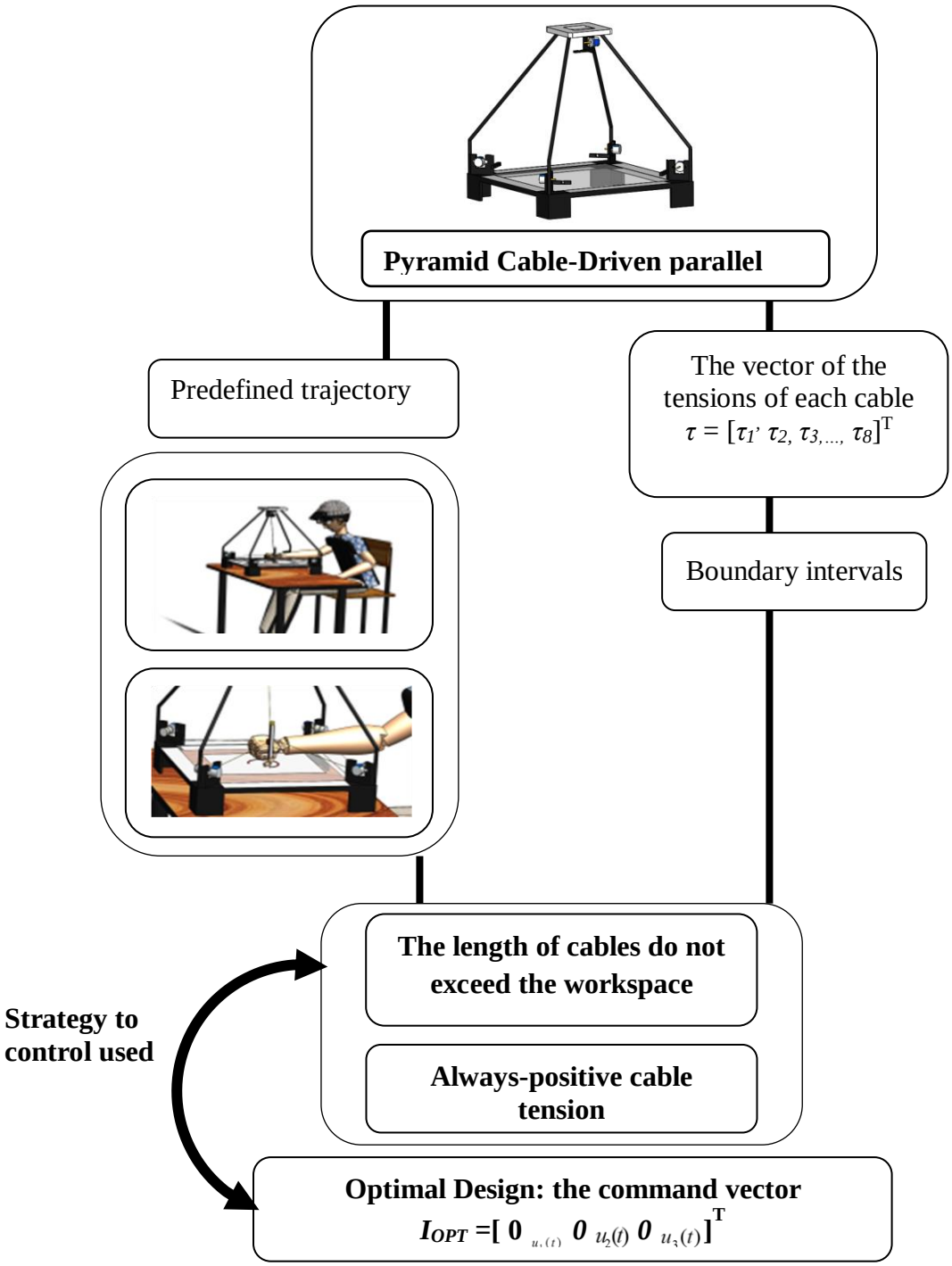

***Figure II.* 22.** *a partial diagram of the operation of this robot.*

In Figure 22, a partial diagram of the operation of this robot is depicted, starting with the pyramid structure, followed by the method of controlling the final effector through cable tension regulation. The diagram also illustrates the robot's positioning and its functionality for use at home or in the classroom.

II.4 A brief summary of the pyramid shape.

The pyramid shape is a three-dimensional geometric figure characterized by a polygonal base and triangular faces that meet at a single point called the apex. This shape is commonly found in various structures, such as ancient pyramid, architectural designs, and natural formations. It exhibits stability and strength due to its structural integrity and has been utilized for practical and aesthetic purposes throughout history (Horning, 2018).

The pyramid shape is one of the strongest structures that can be relied upon in future engineering, whether for urban or industrial applications. And it was used by the Pharaohs in the past to construct the pyramid, which were classified as one of the seven wonders of the world, thanks to their solid structure and strong engineering, allowing them to endure for centuries without being demolished or distorted (Matić, 2020.). Therefore, this structure has been relied upon as the foundation for designing this robot, enabling it to accommodate varying weights based on the individual undergoing rehabilitation. This specific shape stands as an unprecedented marvel in terms of its remarkable engineering, captivating the admiration of countless students and researchers in numerous forums and occasions. Consequently, the continuous development of this design holds immense significance to ensure optimal efficiency in the future.

II.5 The Importance of Choosing the Pyramid Shape:

These authors discussed a series of research papers related to pyramid parallel robots, each focusing on different aspects of their design, performance, and applications. The papers encompass topics ranging from structure design, degree of freedom analysis, parameter identification, nonparametric calibration, stiffness modeling, and kinematic analysis (Liu W, 2013) (Liao S, 2020). The underlying theme throughout these papers is the exploration of various aspects of the Tri-pyramid Robot, a 3-degree-of-freedom over constrained parallel robot specifically developed for versatile applications. Notably, this robot is designed to excel in scenarios requiring large-angle movement, cross-country road simulation, rapid flexible forming of three-dimensional thin sheets, and enhanced kinematic characteristics compared to other 3-DOF translational parallel manipulators (Zeng Q, 2016). Despite the advancement in the field, challenges and limitations of existing designs are acknowledged (Zeng Q, 2014).
By relying on these studies, we will generalize this new model to other robot designs. For example, our subject is the cable-driven parallel robot, for which we will outline the design stages and present the results of this model in the upcoming sections.

II.6 The proposed design procedure

This paper aims to demonstrate the engineering feasibility and effectiveness of the proposed design solution for the rehabilitation or exercising on human handwriting. The proposed design approach is summarized in the flow-chart that is shown in Figure 1. The proposed design procedure refers to the general approach that is reported in (I.B. Hamida, 2021). In particular, this includes a first step consisting of the identification of the design requirements and constraints of the intended hand-writing rehabilitation/exercising application. The maximum required workspace is to write on a standard A3 paper with size 297 mm x 420 mm with a maximum vertical motion comparable with a standard pen of 185 mm that is used to perform various discontinuous paths such as needed for example when writing text, in particular, as referring to English alphabet letters. A further requirement is to being able to gently suggest following a path while there is no need to replace the human hand or exerting significant forces.

The next step consists of a topology search for both the robot frame and end-effector. It requires identifying the main design choices such as the number of Dofs, actuation, and degree of redundancy. The proposed design solution is further described in section 7. The next steps consist of identifying all the hardware components to achieve the designed design solution. This includes the mechanical parts that we decided to mostly 3D print for obtaining a first proof of concept. This also includes the selection, development and customization of electronics, control hardware and sensors, whose characteristics are further detailed in section 8. Afterwards, we address the software design including the control loop and the user interface. The proposed software is developed using a combination of Matlab and LabVIEW to achieve a user-friendly graphical user interface that can manage the control models that have been developed as reported in chapter V. The last step of the proposed procedure consists of a validation of the proposed design solution as based on both numerical simulations and experimental tests on a built prototype that is available both at University of Skikda and at University of Calabria.

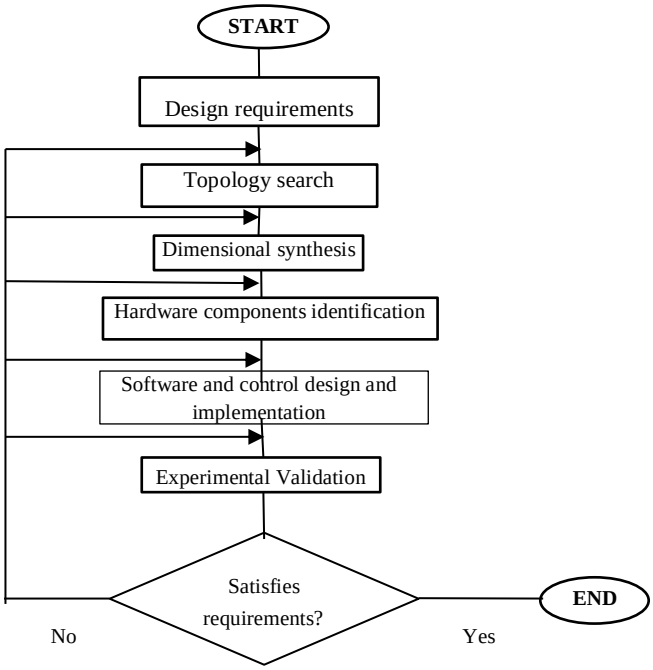

Figure II.23*. A flowchart depicting the proposed design procedure.*

Given the design requirements and intended motion tasks, three degrees of freedom (dofs) are required consisting of X-Y-Z translations. The two horizontal motions are required to enable the motion of a pen along the writing paper. The vertical motion is required to perform non continuous writing tasks where the pen needs to be lifted and placed in a different location. This enables the possibility to make complex drawings and eventually replace the pen with different tools and colors. Also, this can allow a wider range of tasks and rehabilitation exercises to be implemented in future.

There are multiple cable topology solutions that can be suitable for the proposed application as also outlined, for example, in the schemes of Figure 24– (a) first case (a) depicts an under-constrained robot with four cables (F. Inel, (2020)) for three Dofs. Gravity is used in this case to keep the cables in tension, and Figure 24– (b) shows a parallel robot with six cables (G. Carbone, 2018) . Figure 24– (c) describes a cable-driven parallel robot with eight cables (D. Song, 2018) to provide eight Dofs. Figure 24– (d) describes a cable-driven pyramid parallel robot that relies on five motors for controlling the position of the end effector with five Dofs (M. Khadem, 2022). It is worth mentioning that cables cannot exert negative tensions since they can only pull and not push. Therefore, an important condition is to maintain a positive cable in tension. This is usually achieved through redundant cables that keep other cables in tension.

A preliminary analysis was conducted to identify the most convenient topology among

those that are presented in Figure 24 and through this analysis we selected the pyramid topology in Figure 24–(d). It is worth noting that the minimum set of cables to guarantee the required dofs is given by 4 cables, consisting of the 3 dofs plus one additional cable for ensuring that each cable is always pulling. Based on this main consideration we identified the pyramid shape as the most efficient topology allowing the required 3 dofs and motion ranges with a minimum vertical footprint so to make the system easily portable and less bulky. The proposed solution allows the use of two redundant cables with one ensuring that all cables are pulling in the horizontal plane and one setting the vertical configuration of the end-effector. It is worth noting that the proposed solution uses only cables with all motors attached to the fixed frame. This significantly reduces the moving weight and inertia, and it significantly improves the dynamic performance that can be achieved. The proposed solution also avoids using any additional mechanism or actuator for lifting the pen and simplifies the control logic.

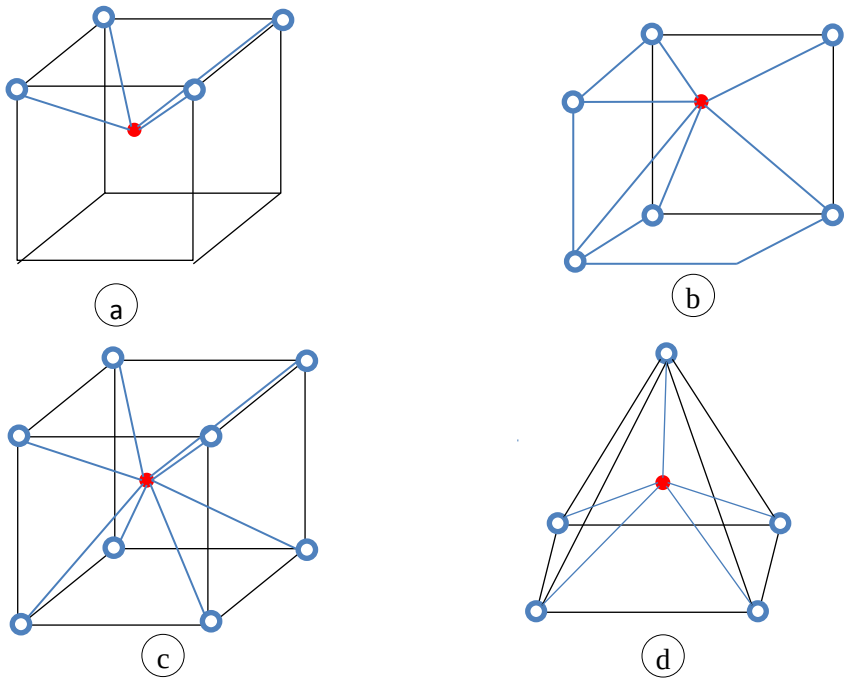

Figure II.24. *Distinct types of cable topologies for CDPRs*

a) four cables attached to the top; b) three cables attached to the top and three cables attached to the bottom; c) four cables attached to the top and four to the bottom; d) pyramid topology.

It is worth noting that the use of highly redundant solutions (i.e., 8 cables) has not been considered, since it significantly complicates the control with a negative impact on the attainable accuracy.

A specific topology search has been conducted also for the attachments of cables to the end-

effector. Figure 25 represents two distinct types of attachment points for the ends of each cable with the end-effector. The first case 25(a) shows the end attachment points of each cable at the center of the end effector. The second case 25(b) shows the cable ends connecting to the vertices and the center of the end-effector. The third case 25(c) shows the cable ends connecting to the vertices, which are on the opposite side and the center of the end-effector. Through the topological studies we conducted, we identified the solution in Fig. 25c, since it ensures higher stability of the end-effector during writing tasks.

The next design step consists of the dimensional synthesis where we can identify and optimize the sizes of our proposed design solution. This design process may require iterative loops to identify an optimal solution, as also outlined in (I.B. Hamida, 2021) .

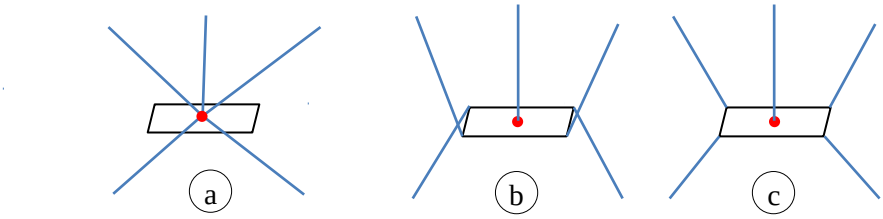

Figure II.25. *Distinct types of attachment for the end-effector.*

II.7 The proposed design solution

In this section, a structure for a cable-operated parallel robot has been developed. The process involved several stages, during which three feasible design patterns were proposed. After evaluating these suggestions, the hierarchical structure was selected to create an experimental pattern. This decision was made to facilitate conducting an in-depth study on the robot's performance and performing several tests, all of which are comprehensively explained in the final chapter of this thesis.

II.7.1 The structure “Planning”

This section introduces a groundbreaking cable-driven parallel robot tailored for intricate 2D printing and artistic tasks see figure 26. Its design features an intentionally unstable base to enhance flexibility, enabling diverse positions for accurate output. The incorporation of four strategic motors at the base's ends empowers precise manipulation through a cable-driven mechanism. This system enables fluid movements crucial for detailed 2D printing and intricate artistic expression, making it a potent tool for creative fabrication (F. Inel L. K., 2014).

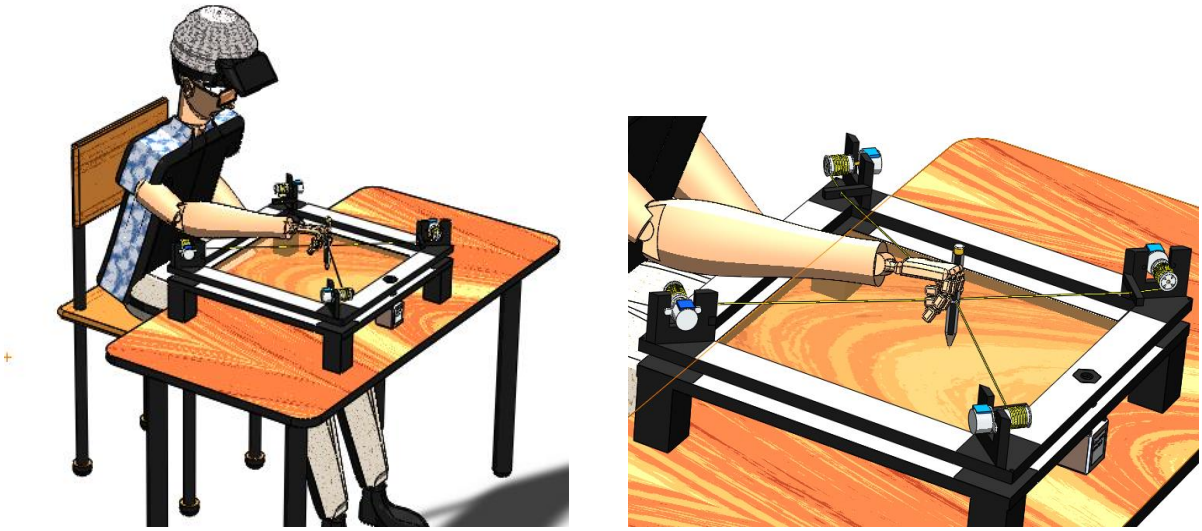

(A) **(B)**

Figure II.26*. (A) prototype design using solidworks software (B) closed-up of the prototype.*

The integration of cable-driven parallel robotics technology in this proposal showcases the potential for highly efficient and versatile robotic systems tailored explicitly for creative and precision-based tasks. As we proceed, we will delve further into the technical aspects of this robot's functioning, including its geometric and kinetic models, and present simulations to demonstrate its capabilities and performance as you can see the final prototype in figure 27.

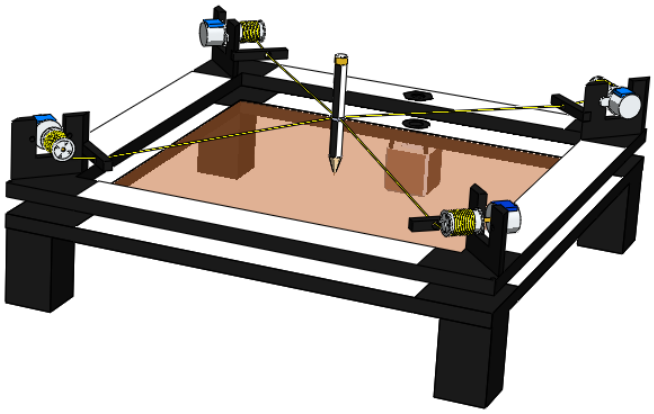

Figure II.27. *general proposed form of the prototype (planning).*

II.7.2 The structure “Cube”

In this section, a novel variation of cable-driven parallel robots has been introduced. The primary function of this innovative robot type revolves around artistic drawing and advanced 3D printing applications. The distinctive feature of this robot lies in its

incorporation of an inherently unstable base, which exhibits controlled movement along the z-axis. This dynamic base configuration is equipped with four individual motors, strategically positioned at its endpoints.

The operational principle of this mechanism involves the utilization of these four motors. Each motor is responsible for winding a cable around a corresponding pulley mechanism. The collective effect of these cable-winding actions culminates in the precise manipulation of the end effector. This design allows for intricate control over the positioning and movement of the end effector, thereby enabling the robot to achieve intricate drawing and complex 3D printing tasks with a high degree of accuracy and finesse see figure.28.

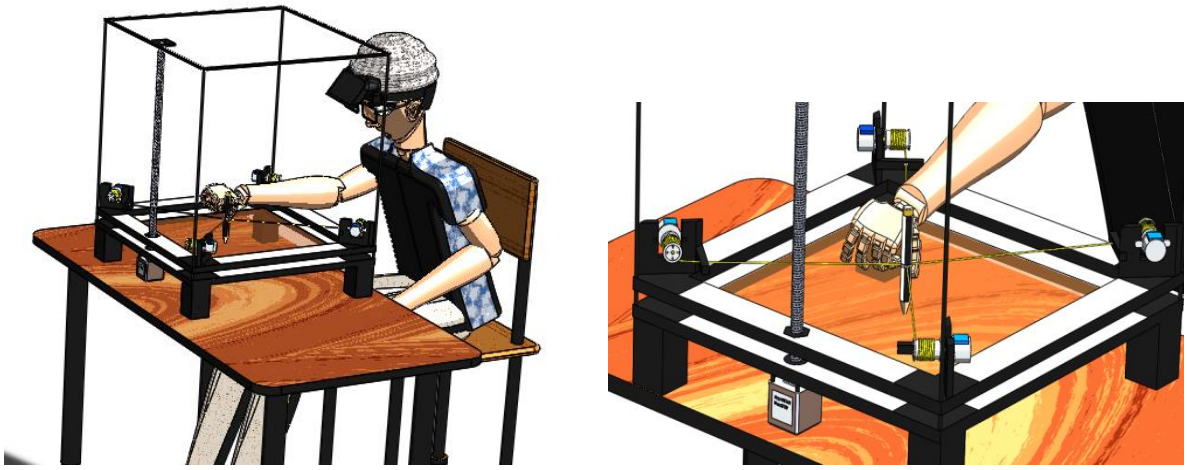

(A) **(B)**

Figure II.28. *(A) prototype design using solidworks software (B) closed-up of the prototype.*

In this section, we describe the initial stages that were used in order to build this robot so that we have a moving base on the Z axis. Four stepper motors are installed on its edges, and each motor has a pulley with a coiled cable. When the motor is running, the cable is pulled around the pulley in order to control the end effector see figure.29 .

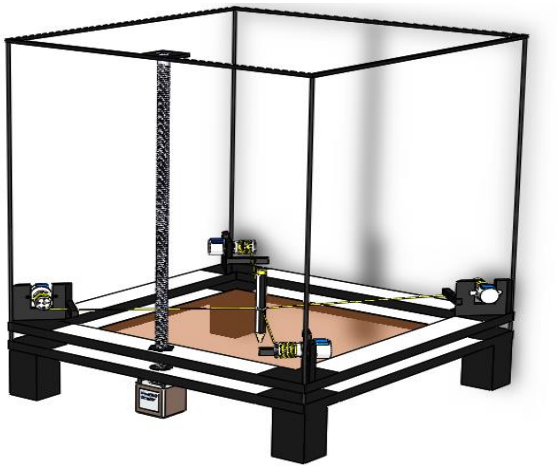

Figure II.29. *general proposed form of the prototype (Cube).*

This robot is designed to work in a space of (size40mm.*40.mm) and (height 450.mm). It was designed in this way in order to facilitate its transfer from one place to another, whether at home or at work.

II.7.3 The pyramid structure

A specific concept design has been proposed based on the design procedure that has been outlined in the previous section. Figure 30 shows an example of the built prototype.

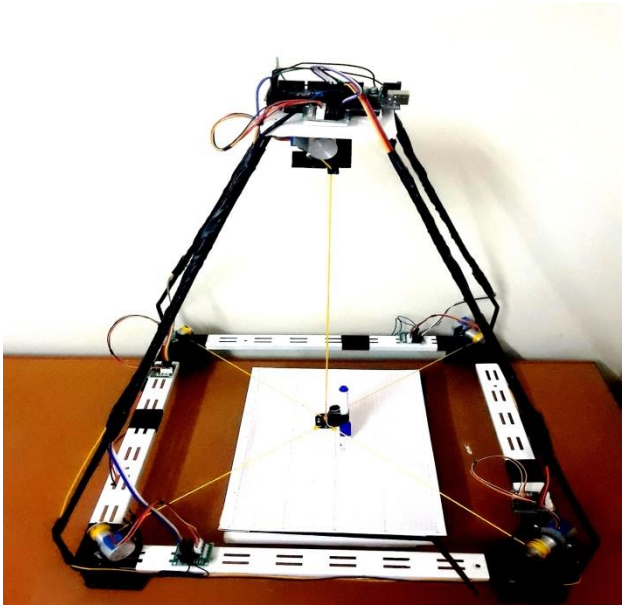

Figure II. 30. *The general proposed prototype of the robot (pyramid CDPR).*

Figure 31(a) and (b) show the structure general of the pyramid robot with dimensional geometric (length of the side and height). This robot's base is square in shape, its length is width is 500 mm x 500 mm, and its height is 558 mm, and it can perform all the intended motion tasks that include rehabilitation applications like drawing and writing. It can also be

used for assisting in arranging shapes, sorting colors, and other applications are required at the preparatory school level as outlined in the 3D cad model proposed in Figure 32(a) and (b). This robot can write letters, draw geometric trajectories, and execute other beginner-level tasks like classifying shapes and colors, for proving performance that is good and accurate this robot. It can also hold twice the weight of a pen in a child's hand. The main geometrical parameters of the prototype have been chosen considering the required workspace and the dimensional constraints given by the standard school tables. Further optimizations are possible and will be considered in future work.

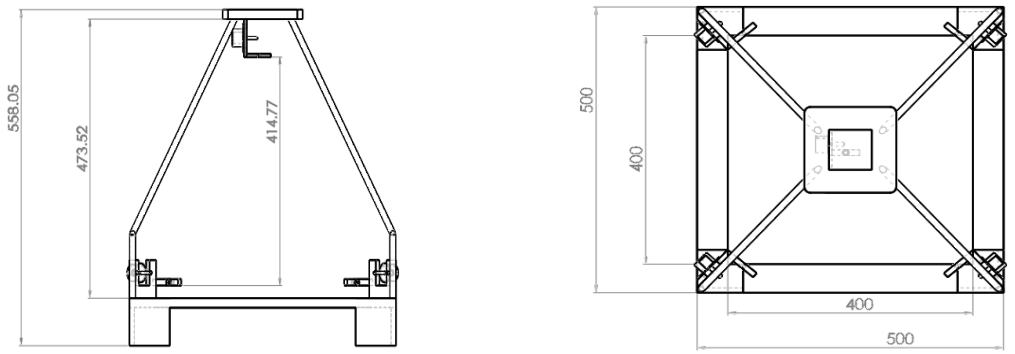

(a) *(b)*

Figure II. 31. *A 2D CAD model of the proposed robot structure (CDPR): a) side view; b) top view.*

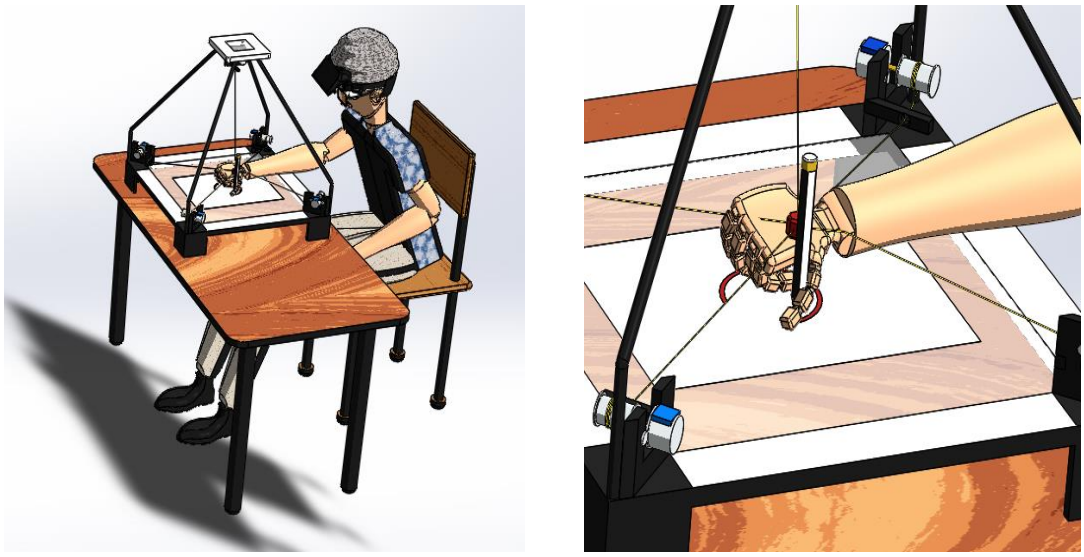

(a) (b)

Figure II. 32. *A 3D CAD model of the proposed robot: a) operation on a primary school desk; (b) a zoom view during a writing assisting task.*

II.8 The Proposed Hardware and Software

II.8.1 Hardware And Components Used in The Design.

The main hardware components are succinctly outlined in Table 2. These components predominantly comprise commercially available elements chosen to align precisely with the specific design requirements, which have been thoughtfully integrated into the proposed robot design see figure 33. Furthermore, the selection of the robot's components is carried out based on a thorough assessment of their quality and performance, ensuring that each chosen element precisely meets the necessary criteria and operational demands.

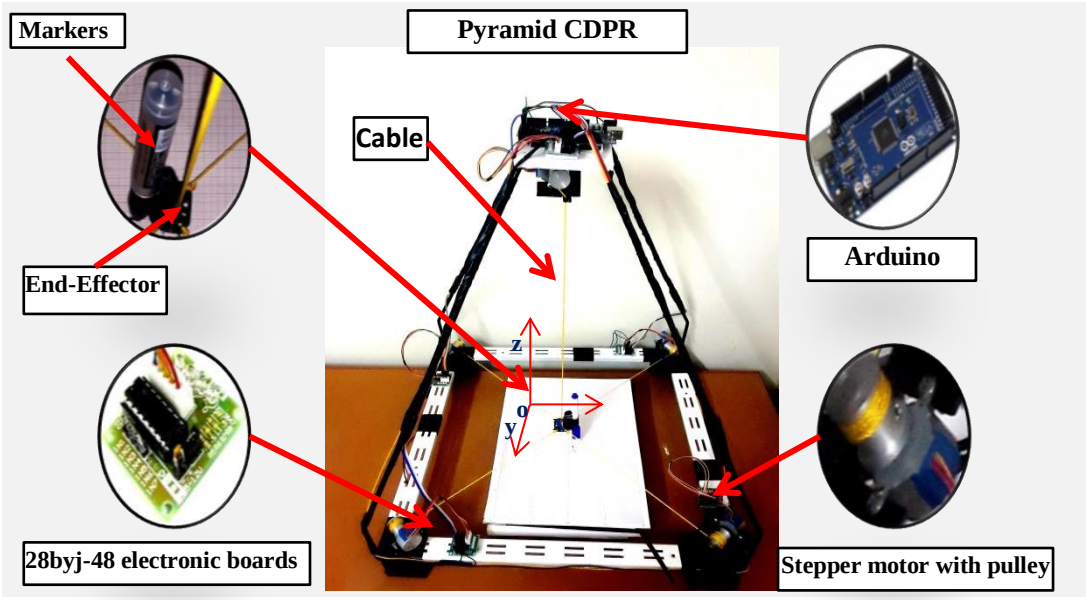

Figure II.33. *The general proposed prototype of the robot (pyramid CDPR).*

II.8.1.1 Arduino Mega 2560

The Arduino Mega 2560 stands as a microcontroller board built around the ATmega2560. It boasts an impressive array of features, including 54 digital input/output pins, with 15 of these capable of functioning as PWM outputs. Additionally, it offers 16 analog inputs and 4 UARTs (hardware serial ports), accompanied by a 16 MHz crystal oscillator, a USB connection, a power jack, an ICSP header, and a reset button. This comprehensive set of components ensures seamless support for the microcontroller's functionality. To begin utilizing the Arduino Mega 2560, one can easily connect it to a computer using a USB cable or power it through an AC-to-DC adapter or battery. It's worth noting that the Mega 2560 board is designed to be compatible with most shields

that were originally intended for use with the Uno, Duemilanove, or Diecimila boards, further enhancing its versatility and potential for integration with various projects (Arduino, 2021).

Figure II.34*. microcontroller arduino mega. Tech specs* ***(Arduino, 2021).***

Table II. 1. *Parameter of the arduino mega.*

Microcontroller	ATmega2560
Operating Voltage	5V
Input Voltage (recommended)	7-12V
Input Voltage (limit)	6-20V
Digital I/O Pins	54 (of which 15 provide PWM output)
Analog Input Pins	16
DC Current per I/O Pin	20 mA
DC Current for 3.3V Pin	50 mA
Flash Memory	256 KB of which 8 KB used by bootloader
SRAM	8 KB
EEPROM	4 KB
Clock Speed	16 MHz
LED_BUILTIN	13
Length	101.52 mm
Width	53.3 mm
Weight	37 g

II.8.1.2 Stepper Motor

A stepper motor represents an electromechanical apparatus that translates electrical pulses

into distinct mechanical movements. When subjected to a series of appropriately sequenced electrical command pulses, the shaft or spindle of the stepper motor rotates in precise step increments.

Figure II. 35. *stepper motor.*

The motor's rotation is directly influenced by the input pulses it receives, establishing several essential relationships. The sequence of applied pulses determines the direction of the motor shaft's rotation, while the frequency of the input pulses correlates with the speed of the motor shaft's rotation. Furthermore, the number of input pulses applied directly corresponds to the extent of rotation achieved by the motor (Electronics, 2023).

Stepper Motor Parameters (Electronics, 2023)

- Rated voltage ： 5VDC
- Number of Phase ： 2
- Stride Angle ： 5.625° /64
- Frequency: 100Hz
- DC resistance ： 50Ω±7% (25℃)
- In-traction Torque >34. 3mN.m(120Hz)
- Self-positioning Torque >34. 3mN.m
- Friction torque: 600-1200 gf.cm
- Pull in torque: 300 gf.cm
- Insulated resistance >10MΩ(500V)
- Insulated electricity power ：600VAC/1mA/1s

II.8.1.3 Driver 28byj-48

The ULN2003, 28byj-48 motor controller is used to interface your stepper motor (in this case, the 28BYJ-48) with your microcontroller (in this example, an Arduino UNO). The motor controller accepts four digital inputs from the microcontroller (IN1 – IN4) and the five wires coming from the 28BYJ-48 stepper motor. Additionally, there is a power input, which can be set to either 5V or 12V. For this specific motor in our example, we would use 5V. The motor controller also features four step indicator LEDs, allowing you to observe the state of the motor's coils as it rotates. However, when running at high speeds, it can be challenging to discern the LED states.

Figure II.36. *28byj-48 motor controller.*

II.8.1.4 Pulley

A pulley was crafted using aluminum material, and this design was precision-engineered with the aid of a lathe machine. The purpose of utilizing the lathe machine was to ensure utmost accuracy in the measurements, preventing any errors that could potentially affect the cable lengths and overall performance of the pulley system. By employing the lathe machine, the manufacturing process was carefully controlled, resulting in precise dimensional specifications for the pulley.

Figure *II.* 37. *A pulley.*

The accurate positioning of the end-effector is of paramount importance to the functionality of the entire system. Therefore, special attention was given to guaranteeing that the end-effector is precisely located at the correct point within the structure. By ensuring the end-effector's accurate placement, the pulley system can operate optimally, enabling seamless and reliable movement of the robot.

Overall, the thoughtful use of aluminum material and the precision-engineering with a lathe machine contribute to a well-crafted pulley, ensuring that it performs flawlessly and meets the necessary specifications for the robot's successful operation.

II.8.1.5 End-effector

An end-effector, also known as an end-of-arm tool or end tool, refers to the specialized tool or device that is attached to the end of a robotic arm, manipulator, or automated system, serving as the crucial interface between the robotic system and the surrounding environment, enabling the robot to interact, manipulate, or perform specific tasks with objects or the surrounding physical world in accordance with its intended purpose and application; the end-effector is carefully selected or designed to suit the particular task requirements, material properties, and desired precision, and it plays a pivotal role in determining the robot's capabilities, versatility, and adaptability to various industrial, manufacturing, assembly, and automation processes, where it can take the form of grippers for grasping and holding objects securely, welding guns for automated welding processes, suction cups for lifting and handling smooth and flat surfaces, spray nozzles for painting or coating applications, screwdrivers for tightening screws in assembly lines, vision systems for object detection and quality control, or laser cutting heads for precise material cutting, among a plethora of other specialized end tools, ultimately making it an indispensable component in modern robotic systems and automation setups.

II.8.1.6 Board Marker Pen

A board marker pen, commonly known as a dry-erase marker or whiteboard marker, is a writing instrument specifically designed for use on smooth, non-porous surfaces like whiteboards, glass boards, and other marker boards. These markers use a special type of ink that can be easily wiped off from the surface using an eraser or a dry cloth, leaving no residue behind.

Figure II. 38. *A board marker pen.*

II.8.1.7 general structure

The pyramid robot has a distinctive geometric structure characterized by a square-shaped base with specific dimensional measurements. The base's sides have a length and width of 500 mm each, forming a perfect square. Additionally, the robot's height stands at 558 mm, measured from the base to its apex.

The robot's pyramid design imparts stability and balanced weight distribution, making it suitable for various applications that require robustness and precise positioning. The square base provides a solid foundation for the robot's movements, while the height determines its reach and working envelope in three-dimensional space.

This particular robot configuration with its specified dimensions offers the potential for versatile use across different industries, such as manufacturing, automation, or research, where its design parameters align with specific task requirements and spatial constraints.

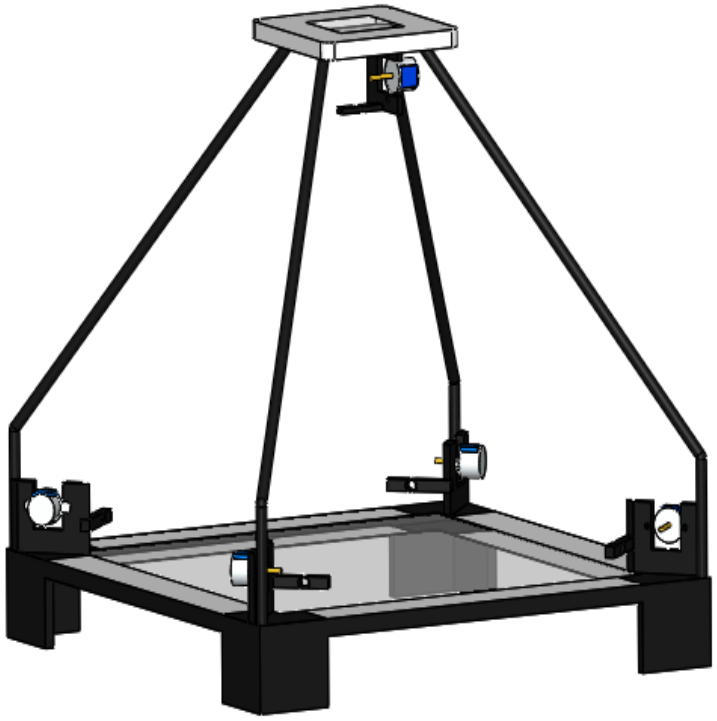

Figure II. 39. *The general of the robot (CDPR).*

II.8.1.8 Cable

The cable used in a cable-driven robot serves as a critical component responsible for transmitting forces and motion between the robot's actuators (motors) and its moving platform or end-effector. This cable is designed to be flexible and possesses high-strength properties, often made from durable materials like steel or synthetic fibers. It acts as the primary means of communication, enabling the robot to execute precise movements and positional adjustments within its three-dimensional workspace. By strategically routing and tensioning the cables through pulleys or guides, the robot can achieve intricate and versatile motion patterns, allowing it to reach various points in its operational range. The cables' tensile strength and flexibility are crucial factors in ensuring their effectiveness and reliability, as they must endure the applied forces and bending during the robot's operation while maintaining their structural integrity and performance. Cable-driven robots find applications in diverse fields, including aerial robotics, medical devices, entertainment systems, and industrial settings, where their lightweight design, high dexterity, and extensive reach make them valuable for specific tasks and operating environments.

Figure II.40. *cable of the robot (CDPR).*

Table II. 2. *the main selected hardware components for the prototype in Figure 12.*

Name	**number**	**Main features**
Arduino mega 2560	**1**	**N° of parts: 1** **N° of pins: 54D,16A** **V: 12v / Weight 37g**
Stepper motor	**5**	**N°: 5** N° of phases: 4 **V: 5v**
driver 28byj-48L5	5	**N°: 5** N° of pins: 4 D **V :5-12v**
pulley	5	**N°: 5** Diameter: 20mm **Length :30mm** **Weight 60g**
End-effector + pen	1	**N°: 5** **Dimensional end-effector (25mm*25mm)** **length :2mm** **Weight: pen 20g +end-effector 50g**
general structure	1	**N°: 1** **dimensions (500mm*500mm, height 558 mm)**
Cable	5	**N°: 5** Diameter: 2mm **$L1_0$= $L2_0$= $L3_0$= $L4_0$ = 280mm** **$L5_0$= 414mm**

II.8.2 The proposed operation logic

The flow-chart in Figure 41 outlines the main operation logic where a graphical user interface GUI is launched on a laptop or tablet device. This

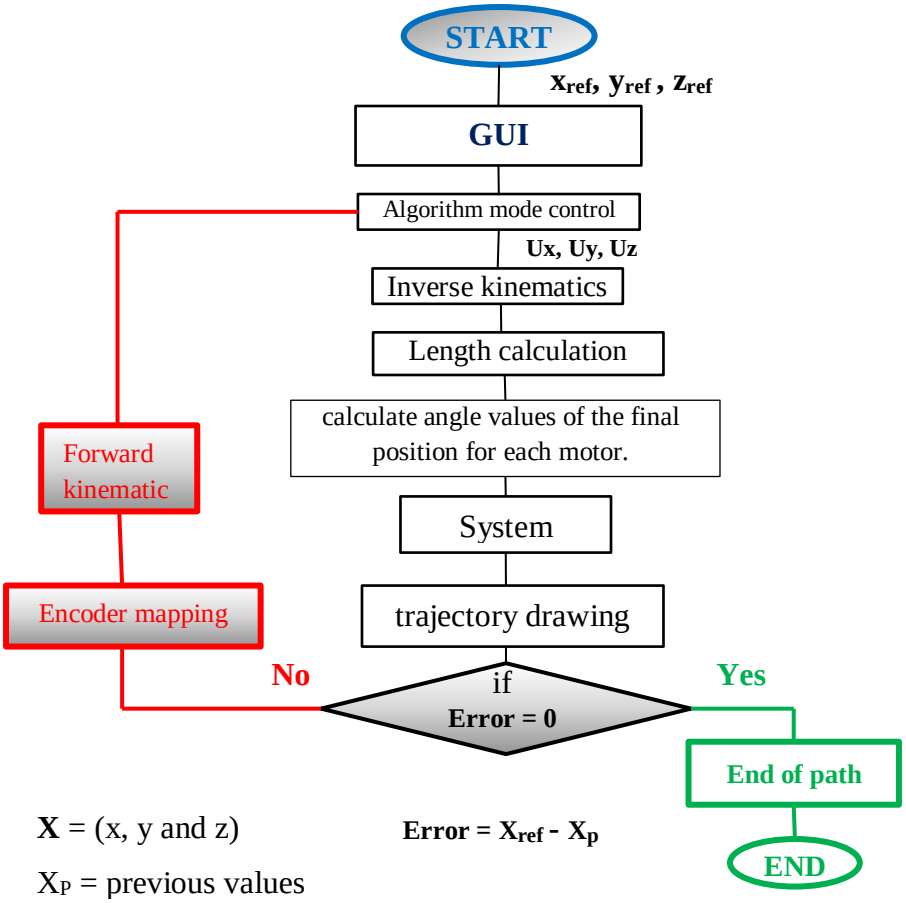

Figure II. 41. *A flowchart for the operation of the proposed robot.*

Figure 41 shows a flowchart of the system algorithm. This process takes place in successive stages. X_{ref}, Y_{ref}, and $Z_{ref.}$ They are the values that are entered from the graphical control interface, and U_X, U_Y and U_Z are values after the process that are entered from the graphical interface. We used LabView software as a key component of this project to design the basic control interface, and it is divided into two parts as follows:

- The upper part sets up the GUI, which defines the Arduino Mega outputs with the 28byj-48 electronic board's inputs to operate the stepper motors (see Figure 42);
- The lower part is the operational part of the system to enter the variables and transfers the end effector from the initial point to the final point (see Figure 43) for more detail about create graphical user interface see ANNEX 01.

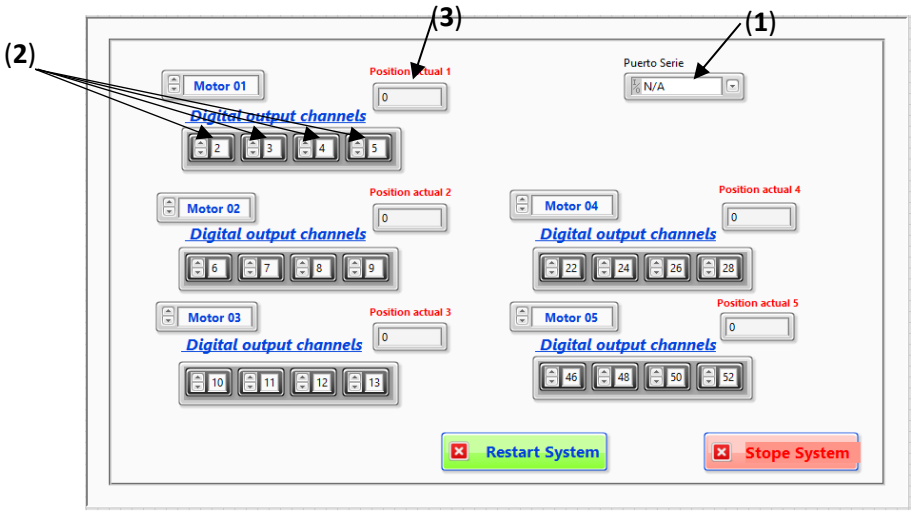

Figure II.42. *upper part of GUI.*

1– Defining the Port (com) to Arduino mega; 2– define the Arduino mega outputs with the 28byj-48 electronic boards inputs for operating the stepper motors; 3– The actual motor position.

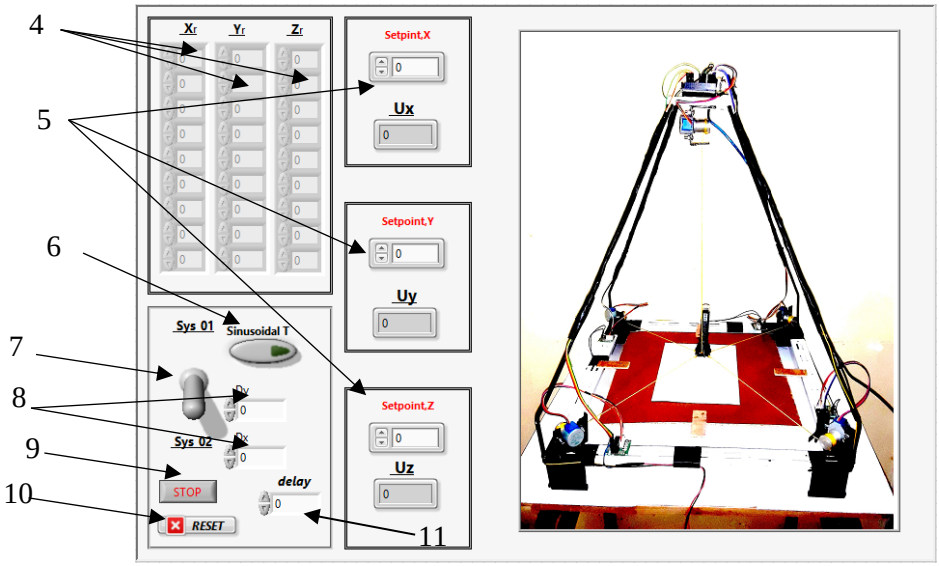

Figure II. 43. *lower part of GUI*

4– Complex paths are determined by entering a set of via points target coordinates X(x, y, z) into the control interface and then the control reads the actual values and performs an interpolation.; 5– Entries values (X setpoint, Y setpoint and Z setpoint) for obtaining point to point trajectories; 6– Button for change the trajectory from linear to sinusoidal; 7– Button to change the trajectory Sys 01 or Sys 02 (Sys-01: simple trajectory and Sys 02: complex trajectory); 8– Dx amplitude along x and Dy amplitude along y for sinusoidal trajectories; 9– Emergency stop; 10– restart system; 11– Delay timer for moving from the first coordinate point to the second coordinate point in complex paths.

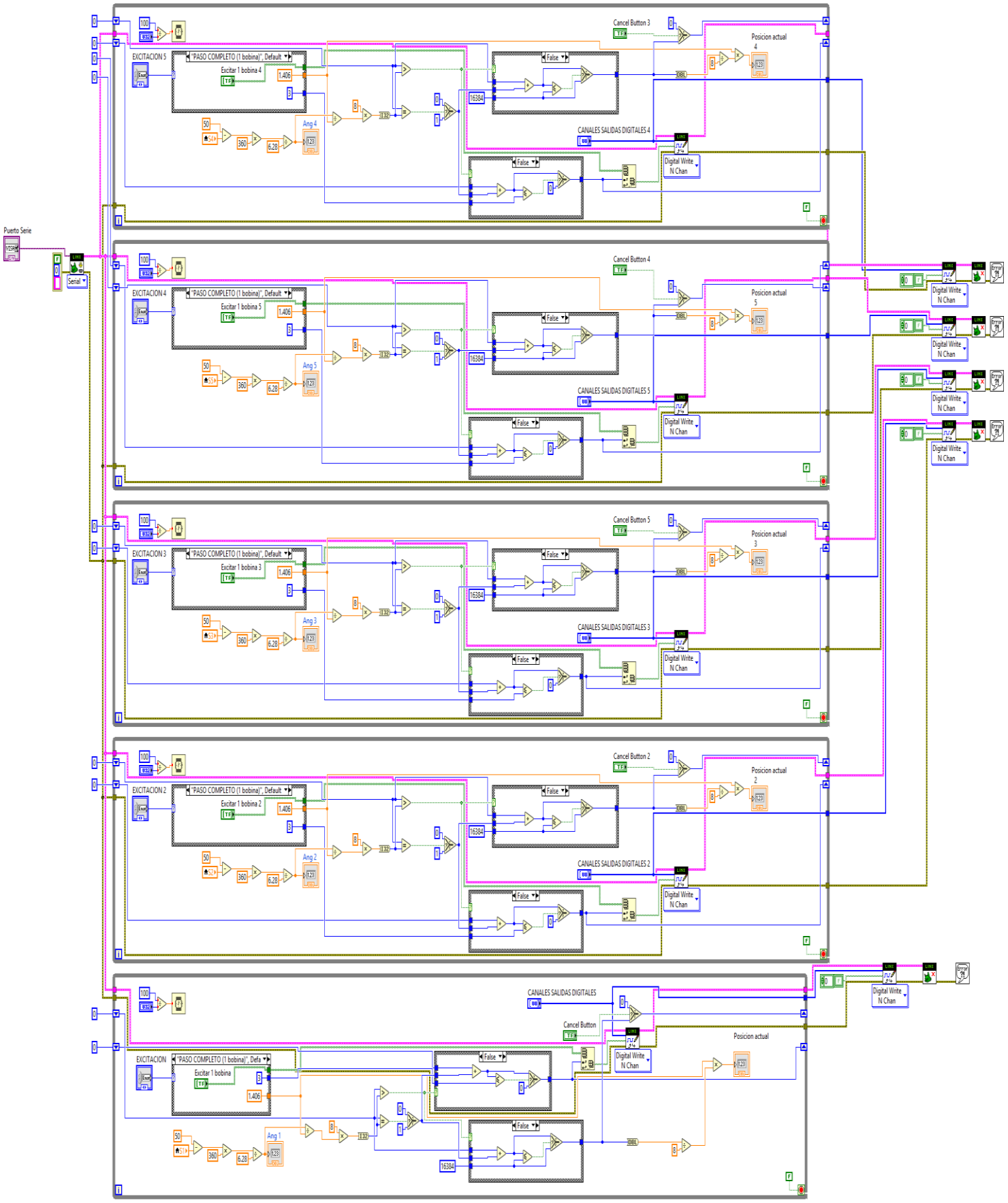

Figure II. 44. *schema bloc of the system.*

In Figure 44, the LabView software displays the "schema block," an essential element of the entire system responsible for facilitating the transmission of control signals to the robot. LabView is a widely used graphical programming environment known for its versatility in automating and controlling various systems, including robotic applications.

The schema block, integrated into the LabView software, serves as a crucial intermediary that establishes seamless communication between the control source (such as a computer or microcontroller) and the robot's actuators. When control signals are generated by the control source, they flow through the schema block, which efficiently directs and regulates the robot's movements and actions based on the received commands.

Within the LabView environment, engineers and developers can easily customize and configure the schema block's functionality to suit specific robotic tasks and applications. This flexibility allows for precise and efficient control over the robot's behavior, making it ideal for a wide range of industries and research fields that demand precise and reliable automation and positioning.

By leveraging the capabilities of LabView and the schema block, the overall system gains a powerful toolset to coordinate and synchronize the robot's actions, leading to smooth and accurate execution of complex tasks. The integration of the schema block in the LabView software significantly contributes to the system's overall efficiency, performance, and adaptability in various robotic applications.

II.9 Simulation and analysis of the structure using solidworks/software

II.9.1 Analysis of the Structure using Carbon

A comprehensive qualitative analysis was conducted on the pyramid structure utilizing simulation through the Solidworks program. In this analysis, the pyramid structure was assumed to be constructed from carbon material. The primary objective was to investigate the structure's ability to withstand external forces. To achieve this, an applied force was simulated and imposed on the structure, enabling a thorough assessment of its load-bearing capacity and response to the external force. The findings from this simulation would provide valuable insights into how the pyramid structure performs under different stress conditions. For a visual reference, please refer to Figure 45.

Name	Type	Min	Max
Displacement1	**URES: Resultant Displacement**	**0 mm Node: 215**	**0.00129639 mm Node: 24112**

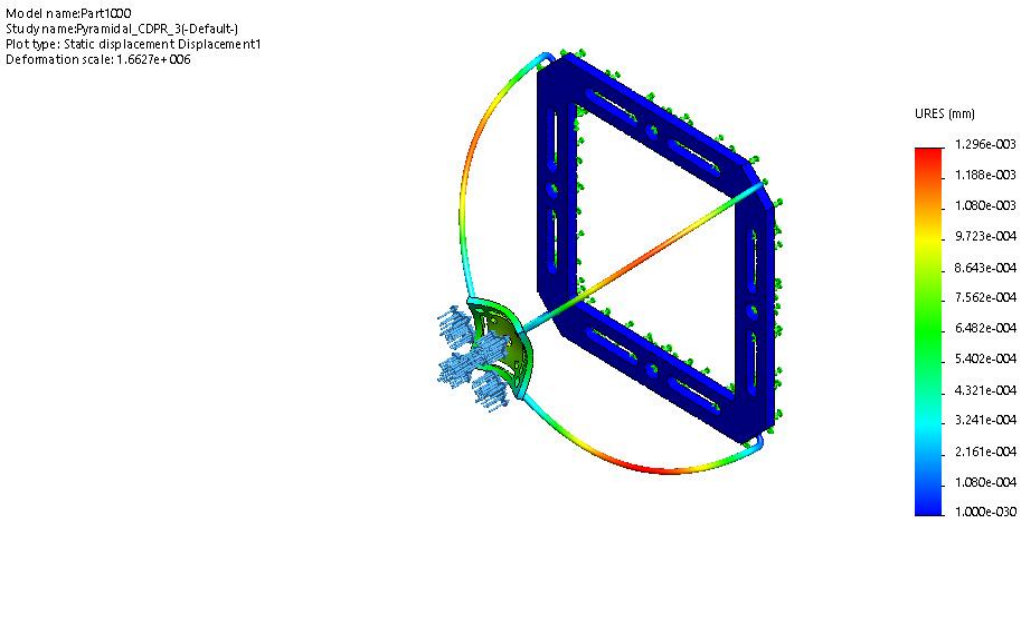

Part1000-Pyramid_CDPR_3-Displacement-Displacement1

Figure II. 45. *Analysis Using Carbon.*

Based on the results obtained, it can be concluded that carbon is a favorable material choice. Carbon is recognized for its lightweight properties in comparison to metals and other materials, making it a suitable option for designing the structure of the robot. Considering its lightweight nature, this carbon-based structure would facilitate ease of movement, allowing seamless transportation from one location to another, and even enabling its transfer to a school or any other desired destination. Consequently, utilizing carbon material in the robot's design could lead to enhanced mobility and versatility, making it a promising consideration for future applications.

II.9.2 Analysis of the Structure Using A286 Iron Base

Utilizing the Solidworks software, a comprehensive qualitative analysis was conducted on the Pyramid structure. In this assessment, it was assumed that the pyramid structure was constructed using A286 Iron material. The main objective of this analysis was to evaluate the structure's ability to withstand external forces. To achieve this, an applied force was simulated and exerted on the structure, allowing for a comprehensive examination of its resilience and how it responds to external pressures. The outcomes obtained from these simulations will provide valuable insights into the performance of the pyramid structure

under various stress conditions. For a visual representation and further details, please refer to Figure ***II***.46.

Based on the results obtained, it can be confidently concluded that A286 Iron stands as an excellent choice for the robot's body design due to its exceptional hardness and heavy-duty properties. Among various metals and materials, A286 Iron is particularly well-suited for such applications.

The solid and durable nature of the A286 Iron-based structure necessitates its permanent placement within the household, as it is expected to be relatively heavy. In scenarios where the user intends to transport the robot to a school or any desired location, the assistance of an adult will be essential, considering the weight of the structure. This is especially important for young children, as compared to a structure designed with carbon, which would likely be much lighter and more manageable for them during transportation.

Name	Type	Min	Max
Displacement1	**URES: Resultant Displacement**	**0 mm Node: 215**	**0.00131702 mm Node: 24112**

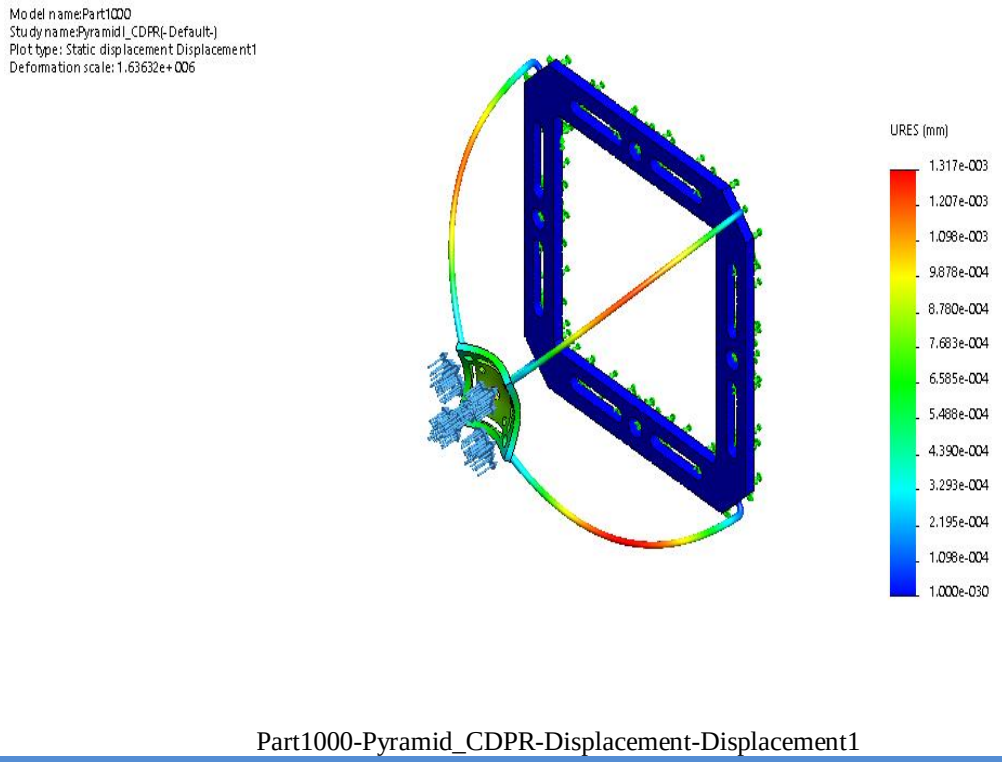

Figure II.46. *Analysis Using A286 Iron Base.*

In summary, the decision to choose iron for the robot's body design is well-founded, owing to its hardness and heavy-duty characteristics. However, the consideration of ease of

transportation and handling should also be taken into account, with carbon presenting itself as a more viable option in situations where mobility is a significant factor.

Therefore, incorporating iron material in the design of this robot holds the potential to significantly enhance its shape, providing increased rigidity and stability, particularly in rehabilitation applications where a stable base is crucial. This makes the utilization of A286 Iron a promising and favorable prospect for future robot applications. The inherent strength and robustness of A286 Iron can contribute to the robot's overall stability and reliability, making it better suited to withstand the demands of rehabilitation tasks, which often require precise and controlled movements. Consequently, the inclusion of iron in the robot's structure ensures that it can effectively support and assist in various rehabilitation activities, thus bolstering its potential for successful implementation in such important applications.

II.9.3 Analysis of the Structure Using ABS plastic

Through the utilization of Solidworks software, an all-encompassing qualitative analysis was conducted on the pyramid structure. For this evaluation, the pyramid structure was presumed to be constructed using ABS plastic. The primary objective of this analysis was to assess the structure's capacity to endure external forces. To achieve this, the applied force on the structure was simulated and studied, enabling a comprehensive examination of its resilience and response to external stresses. The outcomes derived from these simulations will offer valuable insights into the performance of the pyramid structure under diverse stress conditions. For a visual representation and further details, kindly refer to Figure ***II***.47.

Based on the results obtained, it can be confidently concluded that ABS plastic is a favorable material choice for certain robot body designs. ABS plastic is renowned for its lightweight properties, making it notably lighter than metals and various other materials. While ABS plastic possesses a slightly more brittle nature when compared to materials like carbon, it remains a suitable option for robot body design in specific scenarios.

In situations where an exceedingly rigid design is not necessary, or in simple rehabilitation applications that do not require a fixed heavy structure, ABS plastic can serve as an appropriate choice. Its synthetic composition may offer the desired level of flexibility and durability in such applications, while its lightweight characteristics facilitate ease of movement and transportation.

Name	Type	Min	Max
Displacement1	**URES: Resultant Displacement**	**0 mm Node: 215**	**0.129886 mm Node: 403152**

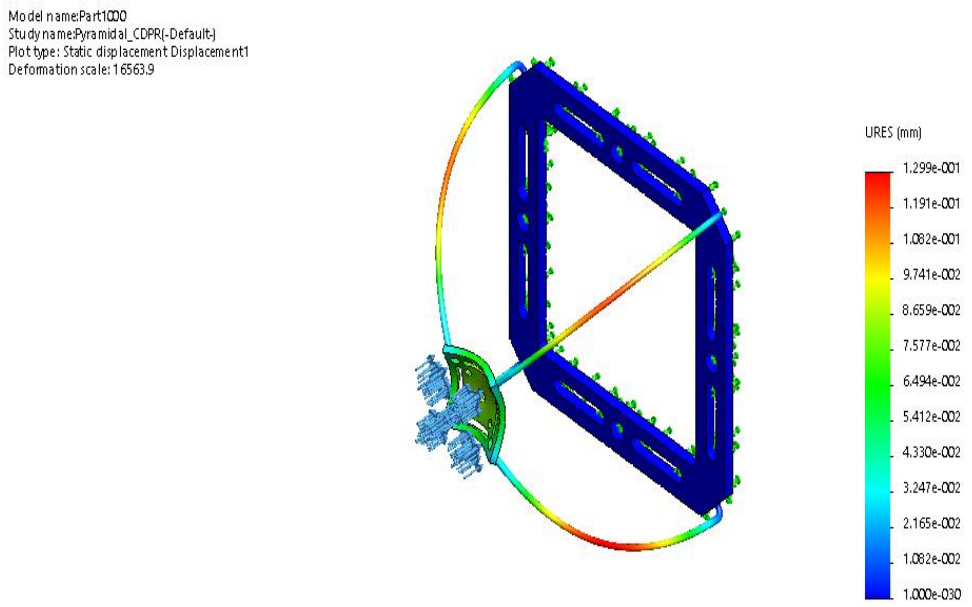

Part1000-Pyramid_CDPR-Displacement-Displacement1

Figure II.47. Analysis Using ABS plastic.

In summary, ABS plastic's advantageous features make it a viable option for robot body design in certain use cases, offering a balance between flexibility and durability, particularly in scenarios where a rigid design is not essential, or when dealing with less complex rehabilitation applications.

Considering its lightweight nature, this robot structure based on ABS plastic will offer exceptional ease of movement, allowing for seamless transportation between different locations. Moreover, its lightness enables effortless transportation to schools or any other desired destinations. Consequently, the use of ABS plastic in robot design can significantly enhance the robot's mobility and versatility, making it a highly promising choice for various future applications. The lightweight attribute of ABS plastic empowers the robot to navigate through different environments with agility and efficiency, making it well-suited for scenarios where mobility and adaptability are critical factors. As a result, ABS plastic contributes to the robot's potential for successful implementation in a wide range of applications that demand efficient movement and transportation.

II.10 Conclusion

In this chapter, we have presented a set of information that highlights the significance of our choice of the pyramid shape in realizing our experimental project. In addition to addressing the issue our research focuses on, we have also explained the steps of designing this robot, from three-dimensional design using software to manufacturing and assembling the components. We have also delved into creating a graphical control interface and its functioning through these stages. The results of these steps will be presented in the following sections.

Chapter 3

III.1 Introduction

A cable-driven parallel robot utilizes cables to achieve precise movement of its components. This entails analyzing the cable arrangement and lengths to ensure accurate positioning (geometric aspect). Within this chapter, the robot's motion patterns are investigated to comprehend how adjustments in cable lengths lead to specific movements (kinematic aspect). Furthermore, the forces and torques exerted on the robot's structure due to cable tensions, elasticity, and inertia are scrutinized to anticipate its behavior during operation (dynamic aspect). The integration of these geometric, kinematic, and dynamic considerations proves essential in the effective design, control, and utilization of cable-driven parallel robots across diverse industries and applications.

III.2 Planar Structure CDPR

III.2.1 Geometric model of the Planar CDPR

III.2.1.1 System structure

Illustrated in Figure 48 is an instance of a parallel robot employing a quadruple-cable configuration. This robot boasts four degrees of freedom, facilitated by a steadfast foundation. The core design involves securing each cable to an individual point on the platform, denoted as A_1, A_2, A_3, and A_4, from which tension is exerted. Through the application of rotational forces by the motors, the cables gracefully wind around the pulleys, culminating in the orchestrated manipulation and precise control of the ultimate end effector's position.

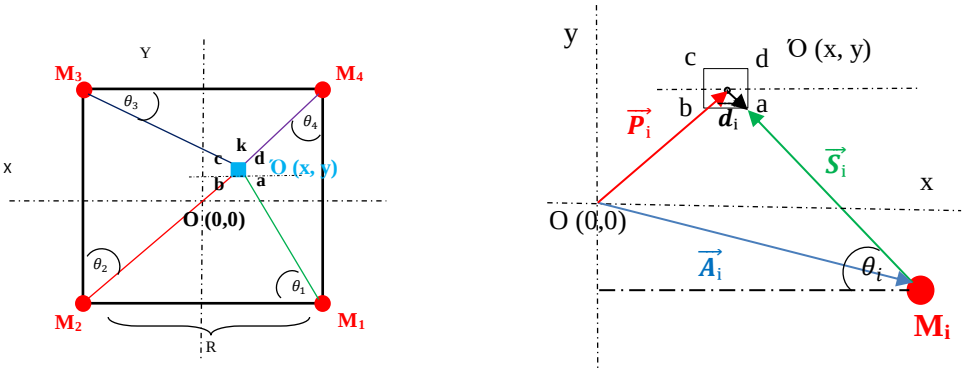

Figure III. 48. *(A) The general geometrical (B). the vector analysis that applies to a part of the robot.*

III.2.1.2 Geometric model

In this section, the geometric model of the robot is established using Figure 48 as a reference. Mathematical relationships are employed to obtain the final equation, which is then presented within this section.

The following aims at determining the length of each cable.

$$\vec{S}i = \vec{P} + \mathcal{R}^*\vec{di} - \vec{A}i \qquad i = 1 \ldots . n \qquad (1)$$

$$\mathcal{R}^* = \begin{bmatrix} 1 & 0 \\ 0 & 1 \end{bmatrix}$$

$$Li = \left\|\vec{Si}\right\| = \sqrt{(x + dix - Aix)^2 + (y + diy - Aiy)^2} \qquad (2)$$

The geometric parameters that define the robot and play a role in describing the geometric model, which in turn determines the cable lengths, are listed as follows:

- L_i: length of the cable;
- $\mathcal{R}^*$ Unitary matrix;
- θ_i: is rotation angel between cable and Y or X axis
- R: side length of the robot base (The shape of the robot base is square);
- H: height between the base and the motor 5;
- M_i: exit point of the cables from the base;
- $\vec{S_i}$: vector $\overrightarrow{(a\,, M_i)}$;
- $\vec{P_i}$: vector $\overrightarrow{(\grave{o}\,, o)}$;
- $\vec{A_i}$: vector $\overrightarrow{(M_i, o)}$;
- $\vec{di}$: vector $\overrightarrow{(a, \grave{o})}$.

- k: is the side length of the end-effector (The shape of the end-effector is square);

III.2.2 Kinematic Planar model CDPR

III.2.2.1 Inverse kinematic model

The inverse kinetic model of the robot is portrayed, serving as the underlying framework for calculating the robot's velocities and accelerations. This model is simplified depicted within a three-dimensional context, enabling the subsequent derivation of equations through the judicious application of mathematical principles. These equations, an outcome of this analytical process, capture and express the characteristics of these identified models, and they are explicitly presented as follows:

$$\begin{pmatrix} x \\ y \end{pmatrix} = \begin{pmatrix} A_i x + L_i \cos(\theta_i) \\ A_i y + L_i \sin(\theta_i) \end{pmatrix} \qquad i = 1 \ldots\ldots 4 \qquad (3)$$

Upon the derivation of Equation 1 $(x\ y\ z)^T$, we arrive at the subsequent velocity equation, which can be expressed as follows:

$$\begin{pmatrix} \dot{x} \\ \dot{y} \end{pmatrix} = \begin{pmatrix} \cos(\theta_i) & -L_i \sin(\theta_i) \\ \sin(\theta_i) & L_i \cos(\theta_i) \end{pmatrix} \begin{pmatrix} \dot{L}_i \\ \dot{\theta}_i \end{pmatrix} \quad i = 1 \ldots . 4 \qquad (4)$$

Inverse equation 4 which obtain as following:

$$\begin{pmatrix} \dot{L}_i \\ \dot{\theta}_i \end{pmatrix} = \begin{pmatrix} \cos(\theta_i) & \sin(\theta_i) \\ \frac{-\sin(\theta_i)}{L_i} & \frac{L_i \cos(\theta_i}{L_i}) \end{pmatrix} \begin{pmatrix} \dot{x} \\ \dot{y}_i \end{pmatrix} \qquad (5)$$

Within this context, we ascertain the kinematic speed corresponding to each individual cable, as formulated in the manner depicted below:

$$\begin{pmatrix} \dot{L}_1 \\ \dot{L}_2 \\ \dot{L}_3 \\ \dot{L}_4 \end{pmatrix} = \begin{pmatrix} \cos(\theta_1) & \sin(\theta_1) \\ \cos(\theta_2) & \sin(\theta_2) \\ \cos(\theta_3) & \sin(\theta_3) \\ \cos(\theta_4) & \sin(\theta_4) \end{pmatrix} \begin{pmatrix} \dot{x} \\ \dot{y} \end{pmatrix} \qquad (6)$$

we can expect a mathematical or descriptive representation to follow, providing specific insight into the process of obtaining these kinematic speeds.

III.2.2.2 Direct kinematic model

In order to derive the direct kinematic model for the envisioned 4-cable design, a pivotal step involves the inversion of the equation represented by $\dot{X} = M^{(-1)}\dot{L}$. However, solving this equation necessitates dealing with a non-square inverse Jacobian matrix M, characterized by dimensions (4 by 2). To navigate through this challenge, we employ the Moore-Penrose pseudo-inverse technique, as outlined in reference (F. Inel L. K., 2014). This method serves as an effective strategy to handle the non-square matrix and obtain a viable solution for the given problem.

We can write this equation in the form

$$\dot{X} = M^{-1}\dot{L} \tag{7}$$

In this context, the term $\boldsymbol{M^{-1}}$ pertains to the inverse Jacobian matrix. The manipulation of the robot's speed and acceleration is facilitated through the utilization of kinematic equations expounded in the paper. These equations enable precise control by incorporating conventional cubic spline interpolations, seamlessly connecting predefined target via points. the role of $\boldsymbol{M^{-1}}$ is provides further insight into how the speed and acceleration control of the robot is achieved, emphasizing the use of kinematic equations and specific interpolation techniques.

III.2.2.3 Static force

In Figure 49, a depiction is presented that showcases the static force free body model of the end-effector. This model distinctly involves the interplay of four cables, each contributing to the equilibrium and stability of the end-effector configuration. This visualization serves as a pivotal representation, offering insights into the cable forces and their distribution, thereby contributing to a comprehensive understanding of the system's mechanical behavior.

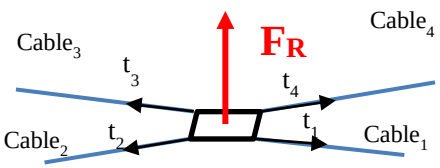

Figure III. 49. *A free body model with static forces.*

The presented equations articulate the manifestation of tensile forces operating on the cables. These equations serve as a pivotal framework, enabling the attainment of complete equilibrium for the ultimate effector. This equilibrium state is of utmost importance, as it guarantees the end effector's stability and operational effectiveness. The forces of 2D plane equations are represented in the following equation as based on reference (F. Inel L. K., 2014).

$$\mathrm{F_R} = \begin{pmatrix} f_x \\ f_y \end{pmatrix} = \begin{pmatrix} \cos(\theta_1) & \cos(\theta_2) & \cos(\theta_3) & \cos(\theta_4) \\ \sin(\theta_1) & \sin(\theta_2) & \sin(\theta_3) & \sin(\theta_4) \end{pmatrix} \begin{pmatrix} t_1 \\ t_2 \\ t_3 \\ t_4 \end{pmatrix} \tag{8}$$

$$S = \begin{pmatrix} cos(\theta_1) & cos(\theta_2) & cos(\theta_3) & cos(\theta_4) \\ sin(\theta_1) & sin(\theta_2) & sin(\theta_3) & sin(\theta_4) \end{pmatrix} \tag{9}$$

$$T = \begin{pmatrix} t_1 \\ t_2 \\ t_3 \\ t_4 \end{pmatrix} = S^{-1} \begin{pmatrix} fx \\ fy \end{pmatrix} \tag{10}$$

The equation (5) lacks constraints, resulting in a multitude of feasible solutions for the cable tension vector T in response to the force F_R. To address this issue, we employ the principles of particular and homogeneous solutions to effectively invert equation (6). This inversion process enables us to express the cable tensions (T) as a function of the applied force (F_R), offering a clear relationship between the two variables dynamic model Planar CDPR

III.2.3 Dynamic model of the end-effector

In this part, the end-effector is expressed by the following expression

$$M\ddot{X} = \mathrm{F_R} \tag{11}$$

$$M = m_e + m_{ch} \tag{12}$$

$$\begin{pmatrix} M & 0 & 0 \\ 0 & M & 0 \end{pmatrix} \begin{pmatrix} \ddot{x} \\ \ddot{y} \end{pmatrix} = \begin{pmatrix} f_x \\ f_y \end{pmatrix} \tag{13}$$

where $F_R = (f_x, f_y)^T$ is the resulting force due to all the cable tensions, M is the total weight, m_e; is weight of the End effector and m_{ch}; is weight of the charge

III.2.4 Dynamic model of the system

Here we first apply the kinematic model and then we use it for calculating the motor torques starting from

$$L_i = \sqrt{(x - A_i x)^2 + (y - A_i y)^2 + (z - A_i z)^2} \qquad i = 1...4 \qquad (14)$$

$$L_{i0} = \sqrt{(A_i x)^2 + (A_i y)^2 + (A_i z)^2} \qquad i = 1...4 \qquad (15)$$

with $\theta_i = \tan^{-1}\left(\frac{y - A_i y}{x - A_i x}\right)$; $\alpha_i = \tan^{-1}\left(\frac{z - A_i z}{\sqrt{(x - A_i x)^2 + (y - A_i y)^2}}\right)$;

$$\beta = \begin{pmatrix} \beta_1(X) \\ \beta_2(X) \\ \beta_3(X) \\ \beta_4(X) \end{pmatrix} = \frac{1}{r}\begin{pmatrix} L_{1,0} - L_1 \\ L_{2,0} - L_2 \\ L_{3,0} - L_3 \\ L_{4,0} - L_4 \end{pmatrix} \qquad (16)$$

By iteratively applying the process of differentiation to equations 16 with respect to time, we derive the following expressions:

$$\dot{\vec{\beta}} = \frac{1}{r}\left[\begin{pmatrix} \dot{\theta}_1 \sin(\theta_1) & -\dot{\theta}_1 \cos(\theta_1) \\ \dot{\theta}_2 \sin(\theta_2) & -\dot{\theta}_2 \cos(\theta_2) \\ \dot{\theta}_3 \sin(\theta_3) & -\dot{\theta}_3 \cos(\theta_3) \\ \dot{\theta}_4 \sin(\theta_4) & -\dot{\theta}_4 \cos(\theta_4) \end{pmatrix}\begin{pmatrix} \dot{x} \\ \dot{y} \end{pmatrix} - \begin{pmatrix} \cos(\theta_1) & \sin(\theta_1) \\ \cos(\theta_2) & \sin(\theta_2) \\ \cos(\theta_3) & \sin(\theta_3) \\ \cos(\theta_4) & \sin(\theta_4) \end{pmatrix}\begin{pmatrix} \ddot{x} \\ \ddot{y} \end{pmatrix}\right] \qquad (17)$$

By replacing the content of equation (16) and (17) into equation (18), we arrive at:

$$J = \begin{pmatrix} J_1 & 0 & 0 & 0 \\ 0 & J_2 & 0 & 0 \\ 0 & 0 & J_3 & 0 \\ 0 & 0 & 0 & J_4 \end{pmatrix}, C = \begin{pmatrix} C_1 & 0 & 0 & 0 \\ 0 & C_2 & 0 & 0 \\ 0 & 0 & C_3 & 0 \\ 0 & 0 & 0 & C_4 \end{pmatrix}$$

we present the diagonal matrices representing the inertias (J) and the viscous damping coefficients (C) of each motor

$$T = \frac{1}{r}\left(\tau - J\ddot{\beta} - C\dot{\beta}\right) \qquad (18)$$

$$T = \frac{1}{r}\left(\tau - J\left(\frac{d}{dt}\left(\frac{\delta\beta}{\delta X}\right)\dot{X} + \frac{\delta\beta}{\delta X}\ddot{X}\right) - C\frac{\delta\beta}{\delta X}\dot{X}\right) \qquad (19)$$

Finally, through the amalgamation of equations (12), and (16), the collection of equations constituting the dynamic model can be formulated into a conventional standard form, commonly applicable to robotic systems (F. Inel L. K., 2014) :

$$M(X)\ddot{X} + N(X,\dot{X}) = S(X)\tau \tag{20}$$

$$\ddot{X}(t) = M^{-1}(X) * N\left(X,\dot{X}\right) + M^{-1}(X) * S(X)\tau \tag{21}$$

Or:

$$M = r * m + S(X)J\frac{\delta\beta}{\delta X}\ and\ N\left(X,\dot{X}\right) = S(X)\left(J\frac{d}{dt}\frac{\delta\beta}{\delta X} + C\frac{\delta\beta}{\delta X}\dot{X}\right)$$

$$M = \begin{pmatrix} M_{11} & M_{12} \\ M_{21} & M_{22} \end{pmatrix}\ and, \qquad N\left(X,\dot{X}\right) = \begin{pmatrix} N_1\left(X,\dot{X}\right) \\ N_2\left(X,\dot{X}\right) \end{pmatrix}$$

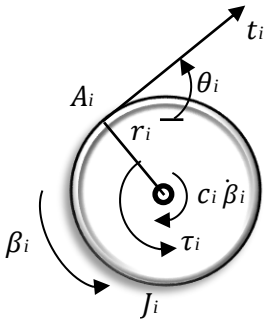

Figure III. 50. *A scheme of the pulley.*

where

- β_i: angle of rotation of the pulleys (Fig.50);
- r_i: radius of the pulley;
- τ_i: torque of the motor;
- J_i: rotational inertia of the shaft-pulley system;
- c_i: viscous damping coefficient of the Motor shaft;
- L_{i0}: initial length of the cable.

It's important to acknowledge that our proposed model doesn't encompass forces and torques attributed to pen holding. This omission is a deliberate safety measure, as pen holders typically exert favorable forces that aid in pen retention on the writing surface. Moreover, our robot's primary function is to assist users by gently guiding their hands along specific trajectories. Gravity's influence on the hand is offset by the desk, which securely holds the paper and has low friction. Consequently, the robot's need for exerting significant forces is minimized.

In this context, operating the robot with a hand holding a pen generally requires comparable forces and torques to those experienced during standalone robot motion. Given the objectives of our work, a preliminary validation sufficed. As such, the conducted experiments centered around a straightforward position control method utilizing cubic interpolation profiles. Various factors were treated as negligible, including dynamic effects, masses, inertia, friction, cable compliance, and sagging.

III.3 Pyramid Structure of CDPR

In this section, we will elaborate on the process of establishing the geometric and kinematic models specifically tailored for the innovative pyramid parallel cable-driven robot that has been put forward. Additionally, we will visually present the overarching design of the robot by drawing upon the illustrative diagrams presented in Figure 51(a) and (b).

The initial focus of this segment is directed towards delineating the geometric model of the proposed pyramid parallel cable-driven robot. This involves a comprehensive description of the physical dimensions, shapes, and spatial relationships that collectively define the robot's structural characteristics. By defining these aspects, we aim to establish a solid foundation for understanding how the various components of the robot come together in a coherent and efficient manner.

Subsequently, we will delve into the kinematic model, which deals with the study of the robot's motion and the relationship between its various parts. This entails elucidating the mathematical representations that encapsulate the robot's motion, such as its joint angles, velocities, and accelerations. A robust kinematic model is crucial for predicting and controlling the robot's movements accurately, which is imperative for its effective operation in real-world scenarios.

To facilitate a better understanding of the aforementioned geometric and kinematic models, we will provide visual aids in the form of schematic diagrams. These diagrams will be sourced from Figure 51(a) and (b), each of which has been thoughtfully crafted to illustrate specific aspects of the robot's structure and operation. By referring to these diagrams, readers will be able to visualize the interplay between different components and gain insights into how the theoretical models translate into the physical construction of the robot.

In essence, this section serves as a comprehensive guide to comprehending the inner workings of the proposed pyramid parallel cable-driven robot. Through a exploration of its geometric and kinematic models, accompanied by visual representations from Figure 51(a) and (b), we aim to provide a clear and thorough understanding of the robot's design and operational principles.

III.3.1 Geometric model of pyramid CDPR

The focus of this section is aimed at outlining the geometric model inherent to the envisioned pyramid parallel cable-driven robot. This encompasses providing a thorough account encompassing the physical measurements, forms, and spatial correlations that collectively shape the fundamental attributes of the robot's structure. Through a detailing of these facets, our objective is to lay a robust groundwork for comprehending how the diverse elements of the robot harmoniously converge, yielding a cohesive and optimized operational framework.

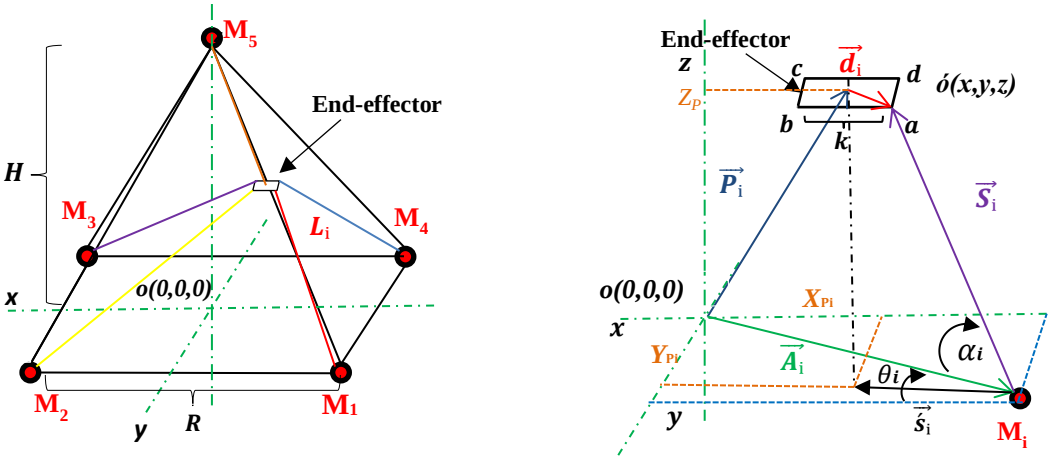

(a) (b)

Figure III. 51. *Schemes of the proposed robot: (a) The geometric model; (b) vector representation of the end-effector position.*

where

- α_i: is the rotation about cable with in the plane (X, Y)
- θ_i: is rotation angel between cable and Y or X axis
- M_i: starting points of the cables on the base frame.
- k: the side length of the end-effector (the shape of the end-effector is square);

- $\overrightarrow{P_i}$: vector between points $(o, \grave{o})$;
- $\overrightarrow{S_i}$: vector between points (M_i, a);
- L_i: length of the cables;
- R: the length of the side of the workspace (The shape of the robot base is square);
- $\overrightarrow{d_i}$: vector between points $(\grave{o}, a)$;
- H: the height between the base and motor axes;
- $\overrightarrow{A_i}$: vector between points (o, M_i);
- i: number of cables.

The geometric model of the robot with 3 Dofs along the $(X, Y, and\ X)$ axes is defined in this section. Considering what we discussed in (M. Khadem, 2022), the robot has no rotational motions. This is also due to the selected cable attachments for the end effector (see Figure 51-b). Accordingly, no rotations are allowed and the rotation matrix $(\mathcal{R}^*)$ simplifies into an identity matrix in equation (1)

$$\overrightarrow{\mathbf{S_i}} = \vec{\mathbf{P}} + \mathcal{R}^*\overrightarrow{\mathbf{d_i}} - \overrightarrow{\mathbf{A_i}} \qquad i = 1,\ldots,5 \qquad (22)$$

$$\mathcal{R}^* = \begin{bmatrix} 1 & 0 & 0 \\ 0 & 1 & 0 \\ 0 & 0 & 1 \end{bmatrix}$$

The cable lengths L_i can be calculated as follows

$$L_i = \left\|\overrightarrow{\mathbf{Si}}\right\| = \sqrt{(x + d_i x - A_i x)^2 + (y + d_i y - A_i y)^2 + (z + d_i z - A_i z)^2} \qquad (23)$$

$$\vec{S} = \left[\overrightarrow{S_1}\ \overrightarrow{S_2}\ \overrightarrow{S_3}\ \overrightarrow{S_4}\ \overrightarrow{S_5}\right] \qquad (24)$$

III.3.2 Kinematic model pyramid CDPR

Within this segment, we will delve into the kinematic model, a facet concerned with scrutinizing the motion of the robot and the interrelationships among its assorted components. This endeavor involves explicating the mathematical portrayals that encapsulate the robot's motion, encompassing factors such as its joint angles, velocities, and accelerations. The significance of a robust kinematic model cannot be overstated, as it serves as the bedrock for precisely prognosticating and managing the robot's motions an imperative requisite for seamless functionality within real-world contexts.

III.3.2.1 Inverse kinematic model

The inverse kinematic model for the 3D space is represented with the following equations, signifies that the mathematical relationships governing the inverse kinematics of

a system in three-dimensional space are articulated through a set of equations. These equations serve as a mathematical representation of how the joint variables of a robotic or mechanical system can be determined given a desired end-effector position or pose.

Inverse kinematics is a critical concept in robotics and engineering, particularly in scenarios where one needs to determine the joint configurations required to achieve a specific spatial arrangement of the end-effector. The equations mentioned in the sentence would provide a way to calculate these joint variables based on the desired position or pose, enabling precise control and manipulation of the robotic system in 3D space.

$$\begin{pmatrix} x \\ y \\ z \end{pmatrix} = \begin{pmatrix} A_i x + L_i \cos(\alpha_i) \cos(\theta_i) \\ A_i y + L_i \cos(\alpha_i) \sin(\theta_i) \\ A_i z + L_i \sin\alpha_i \end{pmatrix} \qquad i = 1 \ldots\ldots 5 \qquad (25)$$

If we derive $(x\ y\ z)^T$ it with respect to time, we get:

$$\begin{pmatrix} \dot{x} \\ \dot{y} \\ \dot{z} \end{pmatrix} = \begin{pmatrix} \cos(\alpha_i) \cos(\theta_i) & -L_i \sin(\alpha_i) \cos(\theta_i) & -L_i \cos(\alpha_i) \sin(\theta_i) \\ \cos(\alpha_i) \sin(\theta_i) & -L_i \sin(\alpha_i) \sin(\theta_i) & L_i \cos(\alpha_i) \cos(\theta_i) \\ \sin(\alpha_i) & L_i \cos(\alpha_i) & 0 \end{pmatrix} \begin{pmatrix} \dot{L}_i \\ \dot{\alpha}_i \\ \dot{\theta}_i \end{pmatrix} i = 1 \ldots . 5 \ (26)$$

$$\begin{pmatrix} \dot{L}_i \\ \dot{\alpha}_i \\ \dot{\theta}_i \end{pmatrix} = \begin{pmatrix} \cos(\alpha_i) & \cos(\alpha_i) \sin(\theta_i) & \sin(\alpha_i) \\ \frac{-\cos(\theta_i)}{L_i \cos(\alpha_i)} & \frac{\cos(\theta_i)}{L_i \cos(\alpha_i)} & 0 \\ \frac{-\sin(\alpha_i) \cos(\theta_i)}{L_i} & \frac{\sin(\alpha_i) \cos(\theta_i)}{L_i} & \frac{\cos(\alpha_i)}{L_i} \end{pmatrix} \begin{pmatrix} \dot{x} \\ \dot{y} \\ \dot{z} \end{pmatrix} \qquad (27)$$

where we get the kinematic speed for each cable, as form following:

$$\begin{pmatrix} \dot{L}_1 \\ \dot{L}_2 \\ \dot{L}_3 \\ \dot{L}_4 \\ \dot{L}_5 \end{pmatrix} = \begin{pmatrix} \cos(\alpha_1) \cos(\theta_1) & \cos(\alpha_1) \sin(\theta_1) & \sin(\alpha_1) \\ \cos(\alpha_2) \cos(\theta_2) & \cos(\alpha_2) \sin(\theta_2) & \sin(\alpha_2) \\ \cos(\alpha_3) \cos(\theta_3) & \cos(\alpha_3) \sin(\theta_3) & \sin(\alpha_3) \\ \cos(\alpha_4) \cos(\theta_4) & \cos(\alpha_4) \sin(\theta_4) & \sin(\alpha_4) \\ \sin(\alpha_5) \cos(\theta_5) & \sin(\alpha_5) \sin(\theta_5) & \cos(\alpha_5) \end{pmatrix} \begin{pmatrix} \dot{x} \\ \dot{y} \\ \dot{z} \end{pmatrix} \qquad (28)$$

The inverse kinematic equations can vary depending on the type of robot, its degrees of freedom, and the coordinate systems used. They generally involve trigonometric functions, geometric relationships, and sometimes numerical optimization methods to find suitable solutions.

III.3.2.2 Direct Kinematic Model

In order to derive the direct kinematic model for the envisaged configuration employing five cables, it is necessary to reverse the equation represented by $\dot{X} = M^{-1}\,\dot{L}$. This solution entails computing the inverse of the non-square Jacobian matrix M, which has dimensions of 5 by 3. Due to this non-standard matrix dimensionality, the challenge is addressed by resorting to the Moore-Penrose pseudo-inverse method, as outlined in reference (F. Inel M. M., 2020) .

We can write this equation in the form

$$\dot{X} = M^{-1}\dot{L} \tag{29}$$

where, M^{-1}: is the inverse Jacobian matrix. Through the kinematic equations presented in the paper, the speed and acceleration of this robot are controlled considering standard cubic spline interpolations among the predefined target via points.

III.3.2.3 Static force analysis

In Figure 52, a visual representation is provided that illustrates the static force-free body model of the end-effector. This model pertains to the configuration where five cables are attached to the end-effector. The illustration offers insights into the equilibrium state of forces acting on the end-effector when it is at rest, with the tension and distribution of forces in the cables being the primary focus. By depicting this static scenario, the figure elucidates how the forces are distributed across the cables in order to maintain the end-effector in a stable, motionless condition.

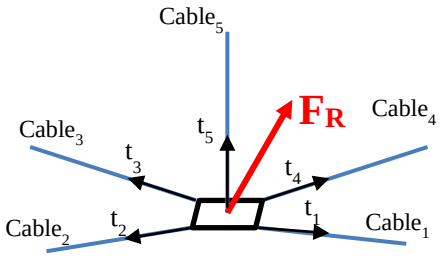

Figure III. 52. *A free body model with static forces.*

The forces characterized by the equations within the three-dimensional plane are succinctly expressed through the subsequent equation, drawing from the foundation established in reference (B. Billel, 2014). This equation encapsulates the mathematical

representation of the forces acting within the three-dimensional plane, providing a link to the principles and concepts detailed in the cited reference (B. Billel, 2014).

$$F_R = \begin{pmatrix} f_x \\ f_y \\ f_z \end{pmatrix} = \begin{pmatrix} \cos(\alpha_1)\cos(\theta_1) & \cos(\alpha_2)\cos(\theta_2) & \cos(\alpha_3)\cos(\theta_3) & \cos(\alpha_4)\cos(\theta_4) & \sin(\alpha_5)\cos(\theta_5) \\ \cos(\alpha_1)\sin(\theta_1) & \cos(\alpha_2)\sin(\theta_2) & \cos(\alpha_3)\sin(\theta_3) & \cos(\alpha_4)\sin(\theta_4) & \sin(\alpha_5)\sin(\theta_5) \\ \sin(\alpha_1) & \sin(\alpha_2) & \sin(\alpha_3) & \sin(\alpha_4) & \cos(\alpha_5) \end{pmatrix} \begin{pmatrix} t_1 \\ t_2 \\ t_3 \\ t_4 \\ t_5 \end{pmatrix} \quad (30)$$

$$S = \begin{pmatrix} cos(\alpha_1)cos(\theta_1) & cos(\alpha_2)cos(\theta_2) & cos(\alpha_3)cos(\theta_3) & cos(\alpha_4)cos(\theta_4) & sin(\alpha_5)cos(\theta_5) \\ cos(\alpha_1)sin(\theta_1) & cos(\alpha_2)sin(\theta_2) & cos(\alpha_3)sin(\theta_3) & cos(\alpha_4)sin(\theta_4) & sin(\alpha_5)sin(\theta_5) \\ sin(\alpha_1) & sin(\alpha_2) & sin(\alpha_3) & sin(\alpha_4) & cos(\alpha_5) \end{pmatrix} \quad (31)$$

$$T = \begin{pmatrix} t_1 \\ t_2 \\ t_3 \\ t_4 \\ t_5 \end{pmatrix} = S^{-1} \begin{pmatrix} fx \\ fy \\ fz \end{pmatrix} \quad (32)$$

Equation (30) emerges as an unconstrained formulation, signifying that a multitude of potential solutions exist for the vector of cable tension, T, in response to the application of force FR. In addressing this scenario, we employ the principles of both particulate and homogeneous solutions to effectively reverse this equation. The objective here is to transform the equation (30) in a way that allows us to express the cable tensions (T) as a function of the applied force FR. By leveraging the notions of particulate and homogeneous solutions, we aim to derive a comprehensive understanding of how cable tensions adapt in reaction to external forces. This analytical approach facilitates the determination of the interplay between cable tensions and applied forces, shedding light on the intricate dynamics at play in this physical system.

III.3.3 dynamic model pyramid CDPR

III.3.3.1 Dynamic model of the end-effector

In this dedicated segment, the dynamic model of the end-effector is concisely presented through the following expression. This expression encapsulates a comprehensive description of the end-effector's dynamic behavior, encompassing various factors such as forces, accelerations, and interactions that influence its motion. By providing this explicit expression, a thorough insight into the intricate dynamics governing the end-effector's movement and response to external influences is conveyed, enabling a comprehensive understanding of its behavior within the system under study.

$$M\,\ddot{X} = \mathrm{F_R} \tag{33}$$

$$\begin{pmatrix} M & 0 & 0 \\ 0 & M & 0 \\ 0 & 0 & M \end{pmatrix} \begin{pmatrix} \ddot{x} \\ \ddot{y} \\ \ddot{z} \end{pmatrix} = \begin{pmatrix} f_x \\ f_y \\ f_z \end{pmatrix} \tag{34}$$

$$M = m_e + m_{ch}$$

Here, the term "where" introduces a crucial contextual relationship. The vector $(F_R = (f_x, f_y, f_z))^T$ embodies the aggregate force resultant from the combined effects of cable tensions. This vector encapsulates three components, specifically $f_x, f_y, and\ f_z$, which respectively represent forces acting along the $x, y,$ and z axes. The superscript "T" indicates that the vector is transposed. This resultant force vector, F_R, captures the net influence of the combined cable tensions acting on the end-effector. It stands as a pivotal factor in comprehending the overall force interactions within the system, thus playing a central role in the subsequent analyses and discussions, M is the total weight, m_e; is weight of the End effector and m_{ch}; is weight of the charge.

III.3.3.2 Dynamic model of the system

In this methodology, the sequence unfolds as follows: we commence by implementing the kinematic model, a foundational step that furnishes us with essential information about the system's spatial relationships. Subsequently, this kinematic model serves as the basis for computing the motor torques. These torques are pivotal in quantifying the forces that drive the system's motion. This cumulative process culminates in the determination of the system's dynamic model. The journey commences with the application of the kinematic framework and advances seamlessly into calculating motor torques, eventually resulting in the establishment of the dynamic model that encapsulates the intricate interplay of forces and motions within the system.

$$\mathrm{L_i} = \sqrt{(\mathrm{x} - \mathrm{A_i x})^2 + (\mathrm{y} - \mathrm{A_i y})^2 + (\mathrm{z} - \mathrm{A_i z})^2} \qquad i = 1...5 \tag{35}$$

$$\mathrm{L_{i0}} = \sqrt{(\mathrm{A_i x})^2 + (\mathrm{A_i y})^2 + (\mathrm{A_i z})^2} \qquad i = 1...5 \tag{36}$$

with $\theta_\mathrm{i} = \tan^{-1}\left(\frac{\mathrm{y} - \mathrm{A_i y}}{\mathrm{x} - \mathrm{A_i x}}\right)$; $\alpha_\mathrm{i} = \tan^{-1}\left(\frac{\mathrm{z} - \mathrm{A_i z}}{\sqrt{(\mathrm{x} - \mathrm{A_i x})^2 + (\mathrm{y} - \mathrm{A_i y})^2}}\right)$;

$$\beta = \begin{pmatrix} \beta_1(X) \\ \beta_2(X) \\ \beta_3(X) \\ \beta_4(X) \\ \beta_5(X) \end{pmatrix} = \frac{1}{r} \begin{pmatrix} L_{10} - L_1 \\ L_{20} - L_2 \\ L_{30} - L_3 \\ L_{40} - L_4 \\ L_{50} - L_5 \end{pmatrix} \quad (37)$$

$$\dot{\beta} = \frac{\partial \beta}{\partial x}\dot{x} = -\frac{1}{r}\left[\begin{pmatrix} \cos(\alpha_1)\cos(\theta_1) & \cos(\alpha_1)\sin(\theta_1) & \sin(\alpha_1) \\ \cos(\alpha_2)\cos(\theta_2) & \cos(\alpha_2)\sin(\theta_2) & \sin(\alpha_2) \\ \cos(\alpha_3)\cos(\theta_3) & \cos(\alpha_3)\sin(\theta_3) & \sin(\alpha_3) \\ \cos(\alpha_4)\cos(\theta_4) & \cos(\alpha_4)\sin(\theta_4) & \sin(\alpha_4) \\ \sin(\alpha_5)\cos(\theta_5) & \sin(\alpha_5)\sin(\theta_5) & \sin(\alpha_5) \end{pmatrix} \begin{pmatrix} \dot{x} \\ \dot{y} \\ \dot{z} \end{pmatrix} \right] \quad (38)$$

$$\ddot{\beta} = \frac{d}{dt}\left(\frac{\partial \beta}{\partial x}\right)\dot{x} + \frac{\partial \beta}{\partial x}\ddot{x} \quad (39)$$

The scheme of the pulley to this robot as showing in figure 50 and, the parameter is presented in the Section 2.2.5

It's worth observing that our formulated model intentionally excludes considerations of forces and torques stemming from the act of holding the pen. This design choice aligns with safety measures, as conventional pen holders tend to exert forces that facilitate pen retention on the writing surface. Moreover, our robot's fundamental objective revolves around supporting users by gently guiding their hand along a predefined trajectory. The influence of gravity on the hand is offset by the desk that holds the paper, which features minimal friction.

Given these factors, the robot's exertion of substantial forces isn't warranted. This is particularly true since the forces involved when the hand holds a pen generally mirror those required for the robot's motion in isolation. The scope of our work is primarily focused on a preliminary validation, and as such, the conducted experiments adopt a straightforward position control strategy using cubic interpolation profiles.

Notably, various factors have been intentionally treated as negligible in this context. These include dynamic effects, masses, inertia, friction, cable compliance, and sagging. These simplifications are rationalized by the specific goals of this study and the nature of the implemented experiments, providing an initial validation for the proposed model and its application.

III.4 Structure "Cube CDPR"

III.4.1 Geometric model "Cube CDPR"

III.4.1.1 Structure model

In this section, we will provide a comprehensive explanation of a 3D parallel robot that utilizes cables for its operation. The fundamental design of the robot involves a dynamic base that can undergo changes along the Z-axis. Furthermore, the robot incorporates a system of cables that play a crucial role in its functioning. Each cable is affixed to one of the endpoints on the platform, specifically denoted as A_1, A_2, A_3, and A_4. Additionally, there is a distinct point labeled as A_5, which serves the pivotal function of effecting alterations in the positions of the points on the Z-axis.

The operational mechanism of the robot is intricately tied to motor movements. As these motors exert force, the cables are coiled around pulleys in a controlled manner. This mechanism facilitates precise manipulation of both the position and orientation of the robot's end-effector. A visual representation of the entire setup is provided in Figure 06, which visually outlines the arrangement and interplay of the various components described above. This graphical representation serves as a helpful reference for understanding the interrelationships and functionalities of the 3D parallel robot and its cable-based control system.

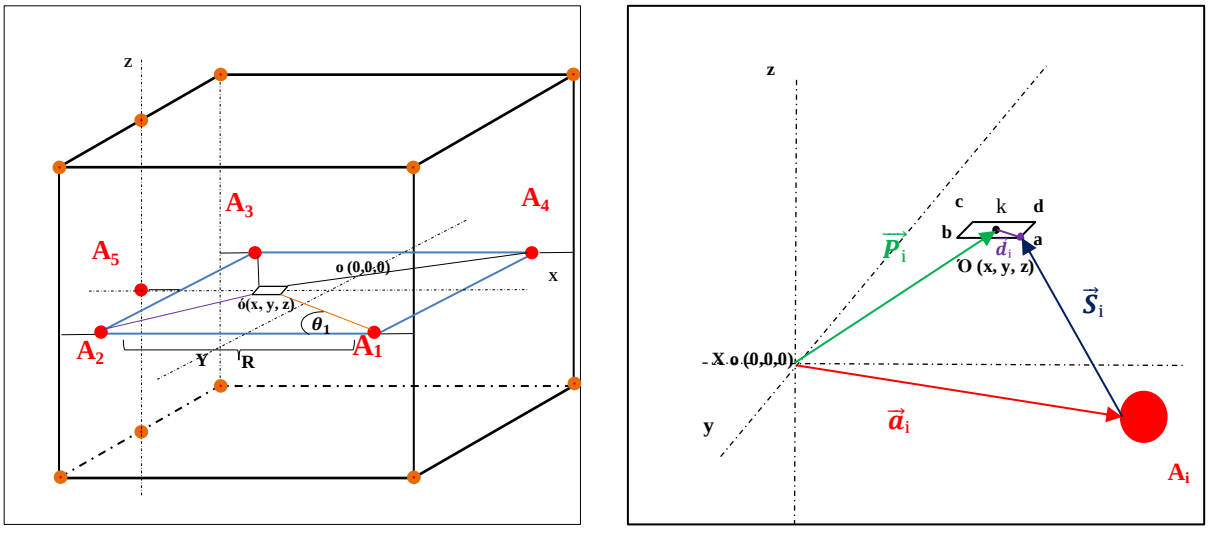

(a) **(b)**

Figure III. 53*. (a). The general geometrical (b). the vector analysis that applies to a part of the robot.*

Indeed, the provided information in the text highlights the significance of the figures in elucidating the characteristics of the robot. Figure 53 (a) provides a comprehensive depiction of the overall geometrical and analytical configuration of the ideal robot. This figure serves as a visual representation that captures the fundamental structural layout, showcasing the interplay of various components and their spatial relationships. It presents a holistic view of the robot's design, enabling observers to glean insights into its essential geometry and fundamental characteristics. On the other hand, Figure 53 (b) delves into the realm of vector analysis, offering a specialized examination of a specific segment or portion of the robot. This vector analysis is a powerful analytical tool used to dissect and comprehend the intricate forces and motions at play within the robot's mechanism. By breaking down complex interactions into vectors, this analysis allows for a more focused investigation into the behavior of the selected robot component. It aids in dissecting the intricate forces, displacements, and orientations that contribute to the overall operation of the robot.

Together, these two figures play a complementary role in enhancing our understanding of the robot's functionality. Figure 53 (a) offers a bird's-eye view of the overarching design, while Figure 53 (b) hones in on a specific aspect through vector analysis. The combination of both visuals provides a comprehensive insight into the intricate interplay of geometrical, analytical, and dynamic elements that collectively define the behavior and performance of the ideal robot.

III.4.1.2 Geometric model

In this particular section, our focus is directed towards the establishment of a comprehensive geometric model tailored specifically for the Cable Parallel Robot. This model serves as a fundamental framework for understanding the robot's spatial configuration and maneuverability. Notably, the Cable Parallel Robot boasts a distinct set of degrees of freedom, amounting to a total of three. These degrees of freedom encapsulate the range of motion and manipulation capabilities that the robot can exhibit within its operational context. To facilitate the precise control of these degrees of freedom, a strategic arrangement of motors has been integrated into the robot's base. Specifically, a total of four motors have been positioned on the base of the robot. These motors play a pivotal role in governing the robot's movement along both the x and y axes. Their

coordinated actions ensure seamless and controlled displacements within the horizontal plane.

In addition to the motors dedicated to the x and y axes, an additional fifth motor holds the responsibility of orchestrating movements along the z axis. This z-axis motor, referred to as motor 5, contributes significantly to the robot's ability to maneuver and manipulate its position vertically. To provide a visual aid in comprehending this intricate setup, Figure 2 has been included. This graphical representation serves as a succinct visual summary, offering a glimpse into the arrangement of the motors and their specific roles. By referencing this figure, readers can gain a clearer understanding of how the motorized components work in unison to govern the Cable Parallel Robot's degrees of freedom along the x, y, and z axes, thereby shaping its overall operational capabilities.

$$\vec{S}i = \vec{P} + \mathcal{R}^*\vec{di} - \vec{a}i \qquad i = 1 \ldots .4 \qquad (40)$$

$$\mathcal{R}^* = \begin{bmatrix} 1 & 0 & 0 \\ 0 & 1 & 0 \\ 0 & 0 & 1 \end{bmatrix}$$

$$Li = \left\|\vec{Si}\right\| = \sqrt{(x + dix - aix)^2 + (y + diy - aiy)^2 + (z + diz - aiz)^2} \qquad (41)$$

$$\left\|\overrightarrow{S_1}\right\| = \sqrt{(\mathrm{x} + \mathrm{k}/2 - \mathrm{R}/2)^2 + (\mathrm{y} - \mathrm{k}/2 + \mathrm{R}/2)^2}$$

$$\left\|\overrightarrow{S_2}\right\| = \sqrt{(\mathrm{x} - \mathrm{k}/2 + \mathrm{R}/2)^2 + (\mathrm{y} - \mathrm{k}/2 + \mathrm{R}/2)^2}$$

$$\left\|\overrightarrow{S_3}\right\| = \sqrt{(\mathrm{x} - \mathrm{k}/2 + \mathrm{R}/2)^2 + (\mathrm{y} + \mathrm{k}/2 - \mathrm{R}/2)^2}$$

$$\left\|\overrightarrow{S_4}\right\| = \sqrt{(\mathrm{x} + \mathrm{k}/2 - \mathrm{R}/2)^2 + (\mathrm{y} + \mathrm{k}/2 - \mathrm{R}/2)^2}$$

$$\mathrm{z(t)} = \mathrm{z}_{set}$$

$$\vec{S} = \left[\overrightarrow{S_1}\ \overrightarrow{S_2}\ \overrightarrow{S_3}\ \overrightarrow{S_4}\ z\right] \qquad (42)$$

The list that follows outlines and elucidates the essential geometric parameters that define the intricate structure and configuration of the robot:

- $\overrightarrow{d_i}$: vector $\overrightarrow{(a, \grave{o})}$.
- *R:* side length of the robot base (The shape of the robot base is square);
- A_i: exit point of the cables from the base;
- $\mathcal{R}^*$ Unitary matrix;
- $\overrightarrow{P_i}$: vector $\overrightarrow{(\grave{o}, o)}$;

- $\overrightarrow{a_i}$: vector $\overrightarrow{(Ai, o)}$;
- $\overrightarrow{S_i}$: vector $\overrightarrow{(a, Ai)}$;
- L_i: length of the cable;
- k: is the side length of the end-effector (The shape of the end-effector is square);

Each parameter serves as a crucial building block in comprehending the robot's spatial characteristics and its interplay with its operational environment. These geometric parameters collectively contribute to the robot's overall shape, dimensions, and maneuverability. By providing a detailed account of these parameters, readers can attain a comprehensive understanding of how the robot is positioned, oriented, and capable of interacting within its designated workspace. The description of these geometric parameters serves as a foundational step in unraveling the complexities of the robot's design and functioning, offering insights into its mechanical layout and its potential applications.

III.4.2 Kinematic model "Cube CDPR"

In this section, we will explore the kinematic model a realm dedicated to analyzing the movement of the robot and the intricate connections between its various elements. This pursuit entails unraveling the mathematical descriptions that encompass the robot's motion, encompassing elements such as its joint angles, velocities, and accelerations. The importance of a well-constructed kinematic model cannot be emphasized enough, as it forms the foundation for accurately predicting and controlling the robot's movements an essential necessity for ensuring smooth operation in real-world scenarios.

III.4.2.1 Inverse kinematic model

The depiction of the inverse kinematic model within three-dimensional space is elucidated through the subsequent equations. This elucidation conveys that the intricate mathematical connections governing the reverse kinematics of a system operating in a three-dimensional environment are articulated using a defined set of equations. These equations function as a mathematical framework that illustrates how the various joint parameters of a robotic or mechanical system can be deduced, given a desired endpoint position or orientation.

Inverse kinematics holds a pivotal role in the domains of robotics and engineering, particularly in situations where the objective is to ascertain the precise joint configurations necessary to attain a specific spatial alignment of the end-effector. The equations referenced in the statement offer a systematic means to compute these joint parameters based on the intended position or orientation, thereby enabling control and manipulation of the robotic system within the expansive scope of three-dimensional space.

$$\begin{pmatrix} x \\ y \\ z \end{pmatrix} = \begin{pmatrix} A_i x + L_i \cos(\theta_i) \\ A_i y + L_i \sin(\theta_i) \\ z_{(t)} \end{pmatrix} \qquad i = 1 \ldots\ldots 4 \qquad (43)$$

If we derive $(x\ y\ z)^T$ it with respect to time, we get:

$$\begin{pmatrix} \dot{x} \\ \dot{y} \\ \dot{z} \end{pmatrix} = \begin{pmatrix} \cos(\theta_i) & -L_i \sin(\theta_i) & 0 \\ \sin(\theta_i) & L_i \cos(\theta_i) & 0 \\ 0 & 0 & 1 \end{pmatrix} \begin{pmatrix} \dot{L}_i \\ \dot{\theta}_i \\ \dot{z_{(t)}} \end{pmatrix} \quad i = 1 \ldots . 5 \qquad (44)$$

where we get the kinematic speed for each cable, as form following:

$$\begin{pmatrix} \dot{L}_1 \\ \dot{L}_2 \\ \dot{L}_3 \\ \dot{L}_4 \\ \dot{z_{(t)}} \end{pmatrix} = \begin{pmatrix} \cos(\theta_1) & \sin(\theta_1) & 0 \\ \cos(\theta_2) & \sin(\theta_2) & 0 \\ \cos(\theta_3) & \sin(\theta_3) & 0 \\ \cos(\theta_4) & \sin(\theta_4) & 0 \\ 0 & 0 & 1 \end{pmatrix} \begin{pmatrix} \dot{x} \\ \dot{y} \\ \dot{z} \end{pmatrix} \qquad (45)$$

III.4.2.2 Direct kinematic model

In order to derive the direct kinematic model tailored for the specific design incorporating four cables, a crucial step involves the inversion of a particular equation, resulting in the formulation $\dot{X} = M^{-1}\dot{L}$. This equation serves as a representation of the velocity relationship between the variables X and L, where X represents the end-effector velocity and L signifies the cable lengths.

The process of solving this equation necessitates the computation of the inverse Jacobean matrix denoted as M. Notably, this Jacobean matrix is non-square in nature, possessing dimensions of 4 by 3. This asymmetry arises due to the distinct characteristics of the system under consideration.

Addressing this non-square matrix dilemma, an effective solution strategy is employed. Specifically, the Moore-Penrose pseudo-inverse technique, as referenced from source (F. Inel, 2014), is harnessed to overcome this challenge. The Moore-Penrose pseudo-inverse provides a method to compute the inverse of a non-square matrix, enabling effective calculations and solutions even in cases where traditional matrix inversion is not feasible.

This mathematical manipulation allows us to rewrite the aforementioned equation in a revised format, enhancing its clarity and comprehensibility within the context of the proposed design. This step is integral to the overall process of establishing the direct kinematic model for the five-cable design, a model that will play a pivotal role in understanding and controlling the motion of the system within its operational parameters.

$$\dot{X} = M^{-1}\dot{L} \tag{46}$$

In this context, M^{-1} corresponds to the inverted Jacobean matrix. Utilizing the kinematic equations outlined in the paper, the robot's velocity and acceleration are managed by employing conventional cubic spline interpolations that connect the predetermined target waypoints.

III.4.2.3 Static force

Within Figure 54, there exists a visual portrayal that effectively depicts the static force-free body model affiliated with the end-effector. This particular model is tailored to a configuration involving the attachment of four cables to the end-effector. The visual representation serves as an enlightening avenue for comprehending the equilibrium state characterized by forces exerted upon the end-effector during its state of rest. The pivotal point of focus pertains to the intricacies surrounding the tension and dispersion of forces within the cables. Through the illustration of this static scenario, the figure clarifies the precise manner in which forces are allocated across the cables, culminating in the maintenance of the end-effector in a stable, motionless state.

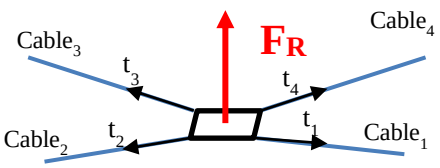

Figure III. 54. *A free body model with static forces.*

The forces corresponding to the equations that operate within the three-dimensional (3D) plane are explicitly defined through the subsequent equation, building upon the

framework established in reference (B. Billel, 2014) . This equation serves as a concise representation that encapsulates the intricate interplay of forces acting within the 3D space, drawing upon the principles and insights provided in the referenced source. Through this equation, a clear and formal connection is forged between the forces involved and the theoretical underpinnings outlined in the cited reference, aiding in a comprehensive understanding of the forces' effects and interactions within the broader 3D context.

$$\mathrm{F_R} = \begin{pmatrix} f_x \\ f_y \\ f_z \end{pmatrix} = \begin{pmatrix} \cos(\theta_1) & \cos(\theta_2) & \cos(\theta_3) & \cos(\theta_4) & 0 \\ \sin(\theta_1) & \sin(\theta_2) & \sin(\theta_3) & \sin(\theta_4) & 0 \\ 0 & 0 & 0 & 0 & 1 \end{pmatrix} \begin{pmatrix} t_1 \\ t_2 \\ t_3 \\ t_4 \\ \tau \end{pmatrix} \tag{47}$$

$$S = \begin{pmatrix} cos(\theta_1) & cos(\theta_2) & cos(\theta_3) & cos(\theta_4) & 0 \\ sin(\theta_1) & sin(\theta_2) & sin(\theta_3) & sin(\theta_4) & 0 \\ 0 & 0 & 0 & 0 & 1 \end{pmatrix} \tag{48}$$

$$T = \begin{pmatrix} t_1 \\ t_2 \\ t_3 \\ t_4 \\ \tau \end{pmatrix} = S^{-1} \begin{pmatrix} fx \\ fy \\ fz \end{pmatrix} \tag{49}$$

Equation (44) exhibits an unconstrained nature, implying a scenario where the vector of cable tension, denoted as T, possesses an infinite array of possible solutions when subjected to the application of force F_R. To navigate this intricate landscape, we draw upon the principles of particulate and homogeneous solutions, employing them to reverse the equation's direction. This inversion process serves the purpose of articulating the tensions in the cables, represented as T, as a function dependent on the exerted force, F_R. By doing so, we gain a structured understanding of how the cables' tensions correlate to the applied force, unveiling a deeper comprehension of the system's response and behavior.

III.4.3 dynamic model “Cube CDPR”

III.4.3.1 Dynamic model of the end-effector

Within this specific section, a profound exploration unfolds as the dynamic model governing the end-effector's behavior takes center stage. The dynamic intricacies inherent to the end-effector's operation are revealed through a concise yet comprehensive expression that follows. This expression serves as a mathematical representation that

encapsulates the multifaceted interplay between forces, accelerations, and motion within the end-effector's domain. By unveiling this expression, a profound insight is cultivated into the intricate dynamics that shape the end-effector's response to dynamic forces and external influences. Through this endeavor, a deeper comprehension emerges, shedding light on the nuanced ways in which the end-effector navigates and adapts to dynamic scenarios.

$$M\,\ddot{X} = \mathrm{F_R} \tag{50}$$

$$\begin{pmatrix} M & 0 & 0 \\ 0 & M & 0 \\ 0 & 0 & M \end{pmatrix} \begin{pmatrix} \ddot{x} \\ \ddot{y} \\ \ddot{z} \end{pmatrix} = \begin{pmatrix} f_x \\ f_y \\ f_z \end{pmatrix} \tag{51}$$

$$M = m_e + m_{ch}$$

The significance of this equation comes into focus as it describes the resulting force, denoted as $F_R = (f_x, f_y, f_z)^T$, which is a vector representing the combined effects of cable tensions. This vector encapsulates the force components acting along the $x, y\ and\ z$ directions, manifesting from the collective tension exerted by multiple cables. Each element in the vector (f_x, f_y, f_z) reflects the specific force magnitude exerted in its respective direction. The equation's transpose operation (^{T}) emphasizes the transformation of the vector into a column matrix, enhancing its mathematical representation.

The equation's underlying significance lies in its role as a foundational connection between cable tensions and the resultant force that emerges within the specified three-dimensional coordinate system. By consolidating these cable tensions into a single force vector, the equation provides a succinct representation of the cumulative effects generated by the cables. This holistic viewpoint contributes to a more profound understanding of how cable tensions collectively influence and shape the overall forces experienced by the system, enriching our comprehension of the system's equilibrium and behavior.

III.4.3.2 Dynamic model of the system

To derive the dynamic model for the system, a two-step approach is employed. First, the kinematic model is applied, providing foundational information about the system's motion and configuration. This kinematic understanding forms the basis for the second

step: calculating the required motor torques. By utilizing the kinematic model's insights, precise torque values are determined, driving the system's motion accurately and efficiently. This sequential process ensures that the system's geometry and dynamics are interconnected, enabling effective control and operation within its environment.

$$L_i = \sqrt{(x - A_i x)^2 + (y - A_i y)^2 + (z - A_i z)^2} \qquad i = 1...4 \qquad (52)$$

$$L_{i0} = \sqrt{(A_i x)^2 + (A_i y)^2 + (A_i z)^2} \qquad i = 1...4 \qquad (53)$$

$$z_{(t)} = z_{set}. \qquad (54)$$

With $$\theta_i = \tan^{-1}\left(\frac{y - A_i y}{x - A_i x}\right); \qquad (55)$$

$$\beta = \begin{pmatrix} \beta_1(X) \\ \beta_2(X) \\ \beta_3(X) \\ \beta_4(X) \\ \beta_5(X) \end{pmatrix} = \frac{1}{r}\begin{pmatrix} L_{10} - L_1 \\ L_{20} - L_2 \\ L_{30} - L_3 \\ L_{40} - L_4 \\ z_0 - z_{ref} \end{pmatrix} \qquad (56)$$

The scheme of the pulley to this robot as showing in figure 50 and, the parameter are presented in the Section 2.2.5

It's important to recognize that our proposed model intentionally excludes the consideration of forces and torques arising from pen holding. This decision is made as a safety precaution, as pen holders typically exert helpful forces that aid in pen stability on the writing surface. Moreover, our robot's primary role is to gently guide the user's hand along a specified trajectory, where the desk's support counteracts gravitational effects. This setup minimizes the need for strong forces from the robot.

In scenarios where the hand holds a pen, the forces and torques involved are typically comparable to those generated by the robot's motion alone. Given the specific objective of our study, a preliminary validation sufficed. Thus, the experiments executed a basic position control with cubic interpolation profiles. Certain factors such as dynamic effects, masses, inertia, friction, cable compliance, and sagging were intentionally treated as negligible due to the scope of this work.

III.5 Mechanical Structure of Motors

The mechanical structure of motors serves as the foundation upon which their dynamic behavior is anchored. This dynamic behavior, encapsulating the intricate interactions between various components and forces, is succinctly encapsulated in the equation that follows. This equation embodies the mathematical representation of how the motor responds to inputs, external influences, and its inherent characteristics. The mechanical structure, encompassing components such as rotor, stator, and associated mechanical elements, plays a critical role in shaping the motor's responsiveness and overall performance. The equation acts as a gateway to comprehending the motor's motion, torque generation, and response to applied forces, thereby offering crucial insights into the intricate interplay between mechanical components and dynamic behavior.

The dynamic behavior of motor is expressed by the equation:

$$J\ddot{\beta} + C\dot{\beta} = \tau - rT \tag{57}$$

$$J =, \begin{pmatrix} J_1 & 0 & 0 & 0 & 0 \\ 0 & J_2 & 0 & 0 & 0 \\ 0 & 0 & J_3 & 0 & 0 \\ 0 & 0 & 0 & J_4 & 0 \\ 0 & 0 & 0 & 0 & J_5 \end{pmatrix}, and\ C = \begin{pmatrix} C_1 & 0 & 0 & 0 & 0 \\ 0 & C_2 & 0 & 0 & 0 \\ 0 & 0 & C_3 & 0 & 0 \\ 0 & 0 & 0 & C_4 & 0 \\ 0 & 0 & 0 & 0 & C_5 \end{pmatrix}$$

The matrices $J\ and\ C$ paramount significance, as they constitute diagonal matrices portraying the inertias (J) and viscous damping coefficients (C) of each individual motor. This distinction is crucial, for it encapsulates the inherent dynamics and resistance to motion characterizing each motor's behavior.

A notable simplification within our analysis arises from the assumption that all pulley radii are uniform, denoted as $r_i = r$ (where i ranges from 1 to 4). This assumption streamlines the system's complexities, allowing for a more streamlined consideration of the system's dynamics see figure 03 for showing the structure the pulley.

At the heart of this system's operation, the torque vector $T(t_1, t_2, t_3, t_4, t_5)$ signifies the cumulative torques applied by the motors, acting as a decisive driver for the system's movement. Additionally, the cable voltage vector $V(t_1, t_2, t_3, t_4, t_5)$ wields a profound influence, dictating the system's response to applied voltages.

To encapsulate the angular orientation of the pulley, we introduce the variable θ. As the pulley rotates, it imparts motion and direction to the system, profoundly impacting the motor dynamics and ensuing cable movements.

The intricate relationships highlighted in this comprehensive depiction underscore the interplay of various elements, elucidating the complex dynamics and control mechanisms governing the system's behavior. This analytical framework is substantiated by reference [54], further enriching its credibility and significance within the broader context of motor and pulley systems.

So: $$T = \frac{1}{r}(\tau - J\ddot{\beta} - C\dot{\beta}) \quad (58)$$

III.6 Conclusion

In conclusion, the exploration of cable-driven parallel robots encompasses a comprehensive understanding of their fundamental aspects: geometric, kinematic, and dynamic. By strategically employing cables, these robots achieve precise and intricate movements of their components. The analysis of cable arrangement and lengths guarantees accurate positioning, while the study of motion patterns clarifies the relationship between cable adjustments and specific movements. Additionally, delving into the forces and torques induced by cable tensions, elasticity, and inertia offers valuable insights into the robot's operational behavior. The successful integration of these considerations—geometric, kinematic, and dynamic—proves pivotal in crafting efficient designs, implementing effective controls, and harnessing the potential of cable-driven parallel robots across a myriad of industries and applications. As technology advances, this interdisciplinary approach will continue to push the boundaries of robotics, enabling innovative solutions for complex tasks and challenges.

Chapter 4

IV.1 Introduction

Controlling cable-driven robots involves developing strategies to command their movement with precision and efficiency. These strategies encompass a range of techniques, algorithms, and feedback systems that address the unique challenges posed by cable-driven mechanisms. By orchestrating the tensions and lengths of the cables, these control strategies ensure accurate positioning, manage complex movements, and optimize the robot's overall performance. The goal is to seamlessly integrate the geometric, kinematic, and dynamic aspects of the robot to achieve desired outcomes across various applications and industries.

In this chapter, we will propose some control strategies that can be used to enhance the robot's performance, focusing on the most common ones used. Additionally, we will explain how to integrate the selected control units with the graphical control interface in the software utilized to create this interface. Furthermore, applications of rehabilitation will be elaborated, intended to be implemented through this robot, and their results will be presented in the final chapter of this memorandum.

IV.2 Strategy to control cable-driven robots

The objective for applying algorithms to control cable-driven robots is to achieve precise and efficient manipulation of the robot's movements and interactions with the environment. Cable-driven robots, also known as cable robots or wire-driven parallel robots, use flexible cables as their primary actuation mechanism. These robots offer several advantages, such as high payload capacity, workspace flexibility, and lightweight design.

Here are some specific objectives for applying algorithms to control cable-driven robots:

- Trajectory Planning: Develop algorithms that can generate smooth and optimized trajectories for the robot's end-effector. The goal is to efficiently move the robot from one point to another while avoiding obstacles and adhering to motion constraints.

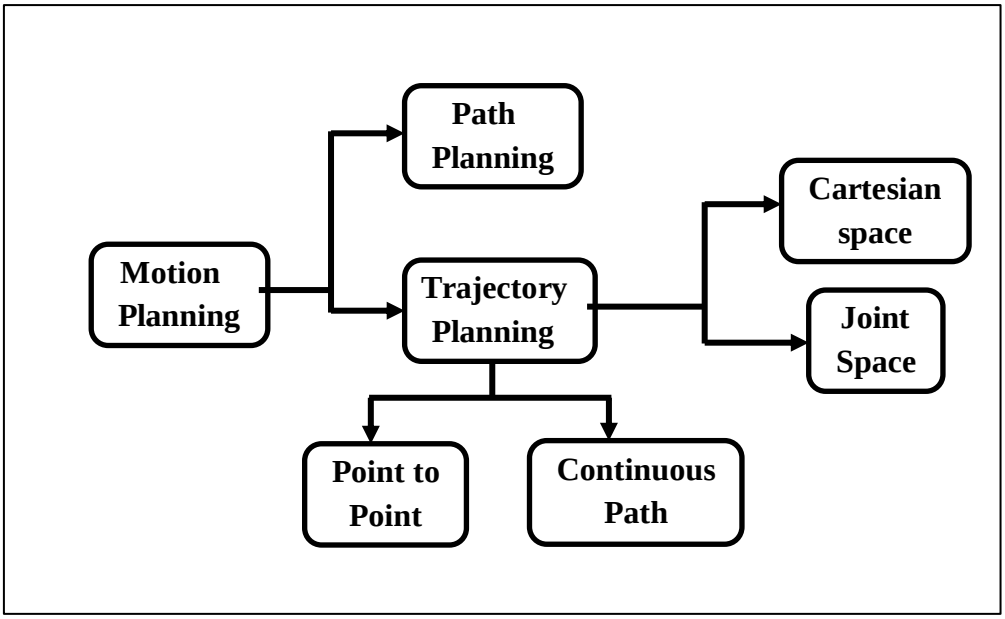

Figure IV. 55. *blocks diagram to control the system.*

- Kinematic Control: Create algorithms to control the robot's kinematics, ensuring that the cables are actuated properly to achieve the desired end-effector position and orientation accurately.
- Dynamic Control: Design control algorithms that consider the dynamic behavior of the cable-driven robot. Dynamic control takes into account the robot's mass, inertia, and cable compliance to achieve stable and responsive motion.
- Cable Tensioning: Develop algorithms to maintain proper tension in the cables. Appropriate tensioning is essential to prevent slackness or excessive strain on the cables during operation, which could lead to inaccuracies or even mechanical failure.
- Force and Torque Control: Implement control algorithms that enable the robot to apply specific forces or torques on objects it interacts with. This is crucial for tasks such as grasping, lifting, and manipulating objects in a controlled manner.
- Singularity Avoidance: Devise algorithms to avoid singular configurations, where the robot's motion becomes highly sensitive or difficult to control. Singularity avoidance enhances the robot's stability and improves its operational range.

- Workspace Optimization: Optimize the robot's workspace utilization to maximize its reach and dexterity. Algorithms can be used to find the best cable lengths and orientations to cover a desired working area effectively.
- Sensor Integration: Integrate sensors, such as cameras, force/torque sensors, or range finders, and develop algorithms to use the sensor data for feedback control. This can improve the robot's perception of the environment and enable more sophisticated manipulation tasks.
- Safety and Redundancy: Implement safety features and redundancy strategies in the control algorithms to ensure the robot can handle unexpected situations or cable failures without compromising safety.
- Real-time Control: Optimize the algorithms for real-time performance, allowing the robot to respond quickly to changes in the environment or adapt to dynamic tasks.

Overall, the objective of applying control algorithms to cable-driven robots is to enhance their precision, reliability, and versatility in various applications, such as industrial automation, surgical robotics, entertainment, and more. These algorithms can enable cable-driven robots to perform complex tasks with high accuracy and efficiency, expanding their potential uses in diverse fields.

IV.3 The objective of searching a control strategy

The primary objective of the search for a suitable control strategy for the cable-driven parallel robot is to achieve precise control over the robot's performance. This goal is pursued through the continuous monitoring of output signals and the prompt correction of errors caused by various external factors. Some of these factors include cable stretching, the weight of the final effector, variations in the operation of the motors, and other potential influences. To address these challenges and optimize the robot's performance, a comprehensive control strategy is sought. By closely examining the output signals generated during the robot's operation, valuable data can be obtained to understand its behavior and response to different inputs. This data will play a crucial role in the design and implementation of an effective control scheme. Among the external factors affecting the robot's performance, cable stretching can introduce imprecisions in its movements. Therefore, the control strategy will include compensation techniques to account for and mitigate the effects of cable stretching, thus ensuring more accurate and reliable operations.

Additionally, the weight of the final effector, the part of the robot that interacts with the environment, can influence its motion and stability. The control strategy will incorporate algorithms to manage the weight and optimize the robot's movements, maintaining a balance between efficiency and accuracy.

Moreover, the variation in the operation of the motors can impact the robot's performance, leading to deviations from the desired behavior. To address this issue, the control strategy will encompass adaptive control methods, enabling the robot to adjust its parameters in response to changing motor characteristics. The selection of this specific control strategy is based on previous research conducted by experts in the field. Extensive studies and experimentation have been carried out to evaluate various control approaches, and the most effective and simplest strategy has been identified as the optimal choice.

IV.4 The proposed control strategy

In this section, we will demonstrate several powerful control algorithms that can be relied upon to enhance the performance of cable-operated robots. Additionally, we will explore various research studies that have experimented with and studied the effectiveness of these control algorithms specifically for cable-driven robots.

IV.4.1 PID Control

The Proportional-Integral-Derivative (PID) control method combines three control techniques, primarily using PID control due to its benefits from each method. This fusion leads to faster responses through the P-only component and reduced offset via derivative and integral components. Research examples employing PID control are highlighted, such as tension management in cable-driven robots (Mohammad A. Khosravi, 2014), visual-based control (Reza Babaghasabha), addressing elasticity (M. A. Khosravi, 2016) , and fuzzy-PID comparison (M. Carpio, 2021). These studies emphasize PID's efficacy in cable robot control. Incorporating the Derivative (D) control boosts responsiveness when combined, anticipating disturbances, but is slower alone. Despite PID's suitability, cost limits adoption to precise and stable processes. PID control relates controller output, error, integral, and derivative, as shown in Equation 58

$$c(t) = Kc\,(e(t) + \frac{1}{Ti}\int e(t)dt + Td\,\frac{de}{dt}) + C \qquad 58$$

Where

- c(t) = controller output
- K_c = controller gain
- e(t) = error
- T_i = integral time
- T_d = derivative time constant
- C = intitial value of controller

As demonstrated in the equation above, PID control integrates all three control types. In this equation, the gain is applied to the integral and derivative components, alongside the proportional element. This is due to the interconnected nature of the PID composite control, where the gain influences both the I and D actions. Due to the presence of derivative control, PID control is unsuitable for processes with high noise levels, as the noise could disrupt its predictive, feedforward nature. Nevertheless, PID control is selected for scenarios demanding minimal offset and rapid response times. Below, (Figure 58) illustrates a visual representation of the PID controller's output following a step increase in input at time t0. This graphical depiction resembles the combined characteristics of P-only, I-only, and D-only responses.

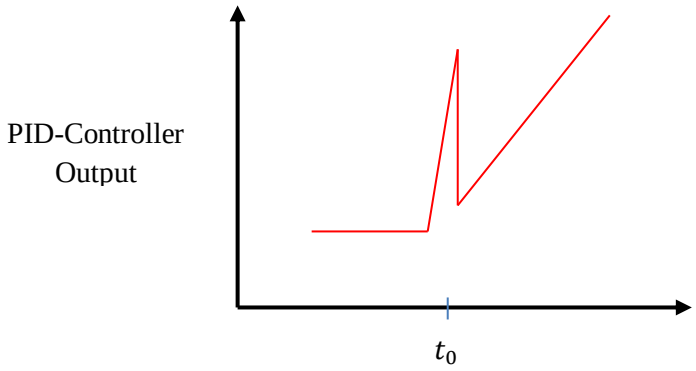

Figure IV. 56. *PID-controller output for step input.*

In addition to PID-control, the P-, I-, and D- controls can be combined in other ways. These alternative combinations are simplifications of the PID-control.

IV.4.2 Optimal Control

Optimal Control, situated at the intersection of control engineering and applied mathematics, is concerned with devising optimal control inputs for dynamic systems to achieve specific objectives, while considering system dynamics and constraints. The

primary goal is to improve a performance measure, often represented as a cost function, while adhering to system requirements. In a foundational Optimal Control scenario, key elements include:

- Dynamical System: Described by mathematical equations, it captures the system's evolution over time, influenced by control inputs and external forces.
- Control Inputs: Managed by the controller, these steer the system's behavior and objective achievement, whether they're continuous or discrete.
- Objective Function (Cost Function): Quantifies the desired outcome, aiming to minimize or maximize performance measures.
- Constraints: Imposed to maintain system behavior within acceptable limits, constraining control inputs and state variables.

Addressing an Optimal Control challenge involves finding control inputs that optimize the objective function while adhering to constraints and system dynamics within a defined timeframe. Techniques encompass calculus of variations, Pontryagin's maximum principle, dynamic programming, optimization methods, and numerical approaches.

Optimal Control finds applications across diverse fields like engineering, finance, robotics, aerospace, and manufacturing. It enhances the effective management of complex systems, leading to improved performance and resource utilization.

Shifting focus to research, one exemplary instance stands out in the work titled Real-Time Motion Planning of Legged Robots: Tracking the Optimal Path with Admissible Error in a Closed-Loop Manner While Carrying the Highest Load (M. H. Korayem1, 2012) . This study introduces a novel path planning approach, seeking an optimal trajectory within an acceptable error margin using a closed-loop method. Notably, these tackles scenarios involving the highest load previously unexplored. By adopting this strategy, precision in the final destination improves significantly compared to open-loop methods, reducing Dynamic Load Carrying Capacity (DLCC). Optimal control exists in open-loop and closed-loop forms. For cable robots, Wang minimizes cable tension through open-loop optimization, while others use the Method of Approximate Programming (MAP) to optimize parallel systems (K. T. Oen, 2007). The Hamilton-Jacobi-Bellman (HJB) method plans the optimal cable robot path, focusing on DLCC (M. H. Korayem, 2009.) . Closed-loop optimal control calculates the max dynamic load capacity of cable robots, integrating feedback linearization and Linear Quadratic Regulator (LQR) optimization (F. Lin, 2007) . This integration enhances the system's ability to handle dynamic loads. Overall, these studies underscore

optimal control's efficacy in skillfully managing the intricacies of cable-driven robots, emphasizing its effectiveness and problem-solving capabilities in this context.

IV.4.3 Model Predictive Control (MPC)

Model Predictive Control (MPC) is an advanced control strategy used to guide dynamic systems within a limited time horizon, achieved by iteratively solving an optimization problem. It relies on predictive modeling to anticipate a system's behavior based on mathematical models and then optimizes control inputs accordingly to meet predefined objectives. Key aspects of MPC comprise:

- Model-Based Approach: MPC requires a dynamic mathematical model of the system, describing how its state variables evolve in response to inputs and external factors.
- Prediction Horizon: Operating within a future time interval, the prediction horizon forecasts the system's behavior using current state and models.
- Control Horizon: A subset of the prediction horizon, the control horizon optimizes control inputs, often applying initial ones.
- Receding Horizon Control: At each control step, MPC optimizes over the control horizon but implements only the initial control input. The control horizon shifts as time progresses.
- Objective Function: MPC's optimization aims to minimize or maximize an objective function, often a cost function, including various criteria.
- Constraints: MPC handles input, state, and soft constraints, ensuring inputs and behavior remain feasible and safe.

MPC finds applications across industries, like process control, robotics, and energy management. Its real-time consideration of predictions and constraints makes it adept for complex systems, although solving the optimization problem at each step requires efficient algorithms and hardware.

In this context, examples of MPC's application are highlighted, such as, Real-Time Motion Planning of Legged Robots: A Model Predictive Control Approach (F. Farshidian, t 2017), integrating SLQ algorithm and multi-processing for efficiency. Another instance is Data-Driven Model Predictive Control for Trajectory Tracking with a Robotic Arm, (A Carron, 2019) , combining inverse dynamics feedback linearization and data-driven error model for trajectory tracking.

Furthermore, Nonlinear Model Predictive Control for Rough-Terrain Robot Hopping (M. Rutschmann, 2012) explores a look-ahead strategy for rough terrains, and "Point Stabilization of Mobile Robots with Nonlinear Model Predictive Control (F. Kuhne, July 2005) [12] addresses point stabilization for nonholonomic wheeled robots. Model Predictive Control of a Mobile Robot Using Linearization (Jr, 2004.) focuses on wheeled robot control, while "An integrated system for real-time Model Predictive Control of humanoid robots (Tom Erez, June 28, 2013.) demonstrates autonomous humanoid operations. "Mobile Robot Trajectory Tracking Using Model Predictive Control (F. Kühne, 2005) targets nonholonomic wheeled mobile robot tracking.

In conclusion, these research endeavors highlight MPC's potential across various domains, particularly in controlling cable robots. Researchers validate its success, emphasizing its impact on desired tasks.

IV.4.4 Adaptive Control

Adaptive Control is a specialized strategy employed in systems characterized by varying or uncertain parameters. Unlike traditional methods with fixed control parameters, Adaptive Control adjusts its control law continually based on real-time system feedback.

Its core objective is to adapt control parameters to account for shifts in system dynamics, uncertainties, or external influences. This ability allows the control system to maintain desired performance amid changing conditions or unknown parameters.

Essential features of Adaptive Control include:

- Parameter Estimation: Adaptive Control uses techniques to estimate time-varying or unknown system parameters affecting behavior.
- Adaptive Law: The algorithm has an adaptive law updating control parameters based on parameter estimation, ensuring stability.
- Adaptation Mechanism: Observes system behavior, comparing it with predicted behavior using estimated parameters to adjust control.
- Robustness: Designed to counter uncertainties and disturbances, mitigating modeling errors and unmolded dynamics for reliability.

Adaptive Control finds utility in various fields, particularly where parameters are uncertain. Examples include aircraft flight, automotive control, robotics, and process control.

It's noteworthy that applying Adaptive Control to Robot Manipulators with uncertain kinematics and dynamics has been explored. Adaptive approaches for tracking task-space trajectories despite uncertainty were detailed in reference (Wang, 2016).

Further investigations delve into Adaptive Control, such as "Experimental Results on the Robust and Adaptive Control of Robot Manipulators Without Velocity Measurements (Marco A. Arteaga-Pérez, 2019), discussing outcomes in the absence of velocity measurements. "Adaptive Control of Robot Manipulator Using Fuzzy Compensator (Byung Kook Yoo, 2000) integrates fuzzy compensators for improved adaptability. "Adaptive Robust Control of Fully Constrained Cable Robots via a Singular Perturbation Approach (Reza Babaghasabha M. A., 2016) proposes adaptive robust control for cable robots, and "Adaptive Control of a Flexible Robot Using Fuzzy Logic (A. Green∗, 2005) explores fuzzy logic in flexible robot control.

Numerous studies concentrate on "Adaptive Control" (M. Honegger, 1997.) (Rogelio Lozano, 1992) (Hao-Bo Kang, 2015) (Mehdi Narimani, 2009) , highlighting its relevance across contexts (Jin Yang, 2016) (Dongeun Seo a, 2009) (Zi-Jiang Yang, 2012.). Such prominence underscores its applicability in cable-based robotic systems and Robot Manipulators. This significance is further underscored by prior references, affirming the pivotal role Adaptive Control plays in the field.

IV.4.5 Sliding Mode Control

The paragraph introduces a sliding mode control approach inspired by references (K.D. Young, 1999) (G. El-Ghazaly, 2014) for nonlinear systems, aiming to enhance robot performance in path tracking. It defines the 3D sliding mode controller's surface across X, Y, and Z axes. This leads to a discussion of research employing sliding mode control principles (Gamal El-Ghazaly, Aug 2014) (Y. Shtessel, 2015) (Agrawal, 2004) (Levant, 2012). Particularly notable is the work titled "Real-Time Motion Planning of Legged Robots: Adaptive Fast Terminal Sliding Mode Control of a Suspended Cable–Driven Robot" (M. I. Hosseini, 2019), introducing a Fast Terminal Sliding Mode (FTSM) controller for accurate path tracking in dynamic uncertainty scenarios. Another study focuses on neural network-based sliding mode adaptive control for robot manipulators, merging techniques for precise trajectory tracking (Tairen Sun, 2011). The application shifts to overhead cranes, demonstrating adaptive sliding mode control accommodating varying cable lengths, even without prior knowledge (Tuan, 2013). A robust adaptive

sliding mode controller for a cable-driven derusting robot in marine environments is discussed (Chen Y., 2022), aiming to improve positioning accuracy. Cable-driven redundancy parallel robots, incorporating cable-length sensor feedback, are explored (Wei Lv, 2017), leading to enhanced control accuracy. In essence, these collective research endeavors underscore sliding mode control's effectiveness in adeptly addressing cable-driven robot control challenges. These studies serve as testament to the success of sliding mode control strategies in this context. The sliding surface of a common sliding mode controller has been defined as.

$$s_{2dx} = C_{12dx} \times (x_{12d}(t) - x_{ref}) + C_{22dx} \times x_{22d}(t) \quad (59)$$

$$s_{2dy} = C_{12dy} \times (x_{22d}(t) - y_{ref}) + C_{22dy} \times x_{42d}(t) \quad (60)$$

$$s_{2dz} = C_{12dz} \times (x_{32d}(t) - z_{ref}) + C_{22dz} \times x_{62d}(t) \quad (61)$$

where C_{12dx} ; C_{22dx} ; C_{12dy} ; C_{22dy}; C_{12dz}; C_{22dz}; C_{22dz} are parameters that need determination to achieve the desired tracking performance encompass the end-effector's trajectory planning parameters: xref, yref, and zref. A method of synthesis was applied to establish the order of the laws, following the approach outlined in (A. Zaatri, 2014.), thereby enabling the formulation of the following expression.

$$\dot{s}_{2dx} = -K_{2dx}s_{2dx} - Q_{2dx}\text{sign}(s_{2dx}) \quad (62)$$

$$\dot{s}_{2dy} = -K_{2dy}s_{2dy} - Q_{2dy}\text{sign}(s_{2dy}) \quad (63)$$

$$\dot{s}_{2dz} = -K_{2dz}s_{2dz} - Q_{2dz}\text{sign}(s_{2dz}) \quad (64)$$

where K_{2dx}, s_{2dx}, K_{2dy}, s_{2y}, Q_{2dx}, Q_{2dy}, Q_{2dz}: are parameters established through simulation. The motion paths are guided to remain close to a predetermined absorbent sliding surface, with the discontinuous control input derived from the sign function's limited switching around the sliding surface, taking values of either +1 or -1. Implementation of the control necessitates addressing a nonlinear dynamic equation (equation 13), making the utilization of the Runge-Kutta method essential due to its effectiveness in solving nonlinear partial differential equations.

IV.4.6 Nonlinear Control

Nonlinear Control, a specialized field within control engineering, focuses on designing and analyzing control systems for nonlinear dynamic systems. Unlike linear control, which deals with linear equations, nonlinear control systems handle intricate relationships between state variables and control inputs. The goal of Nonlinear Control is to develop control strategies that stabilize, track references, and regulate the behavior of nonlinear systems while accounting for their complexities and nonlinearities.

Characteristics of Nonlinear Control encompass handling nonlinear system dynamics, designing nonlinear control laws tailored to system complexities, stability analysis using methods like Lyapunov stability analysis, feedback linearization to transform nonlinear systems into linear ones, adaptive control for uncertain parameters, and robustness against uncertainties and disturbances. Nonlinear Control finds applications in various fields such as aerospace, robotics, power electronics, and biological systems.

This paragraph highlights the utilization of Model Predictive Control in research studies. A study on a flexible parallel humanoid arm joint robot (L. Jiang, 2017) addresses vibration control, while research on an offshore boom crane (Yongchun Fang, 2014.) develops a high-performance nonlinear controller for trajectory tracking. Another study (M. Zarei a, 2018) presents an approach to dampen oscillations in nonlinear systems, illustrated through an under-actuated cable-driven parallel robot. The underlying theme across these research endeavors revolves around applying the control principles to cable robots, with successful evaluations confirming its effectiveness in cable robot control tasks.

IV.5 The Strategy to Control Cable-Driven Robot

IV.5.1 Open loop control

Open-loop control is a type of control system in which the control action is not influenced by feedback from the output or the system's current state. In an open-loop control system, the control input is determined based on a predefined set of commands or a predetermined sequence of actions, without considering the actual output or the system's response.

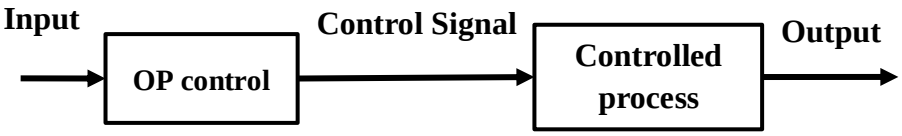

Figure IV. 57. *blocks diagram to open loop control.*

In this setup, there is no mechanism to measure the system's performance or correct deviations from the desired behavior. As a result, open-loop control is typically used in situations where the system's behavior can be accurately predicted, and external factors or disturbances do not significantly affect the process.

It is essential to note that open-loop control lacks the ability to respond to changes or uncertainties during operation, making it less flexible and potentially prone to errors if the system's dynamics deviate from what was initially assumed. Due to these limitations, open-loop control is less common in complex or critical control applications, where feedback-based control (closed-loop control) is often preferred for its stability and robustness.

IV.5.1.1 Implementing open-loop controller on software

we can implement an open-loop controller, have set up a control system where the control action is based on predetermined commands or a fixed sequence of actions, without using any feedback from the system's output or current state. The control input is determined in advance, and the controller does not make adjustments based on how the system responds to these inputs.

IV.5.1.1.1 Implementing open-loop controller by using LabView/software

In order to activate the open-loop control module on the LabView interface we need to follow several key steps through which the overall system control interface is created. Firstly, we need to determine all the parameters specific to the robot, such as the dimensions of the structure, initial cable lengths, and necessary transformations. Afterward, we input these parameters into the graphical control interface, as shown in Figure 60.

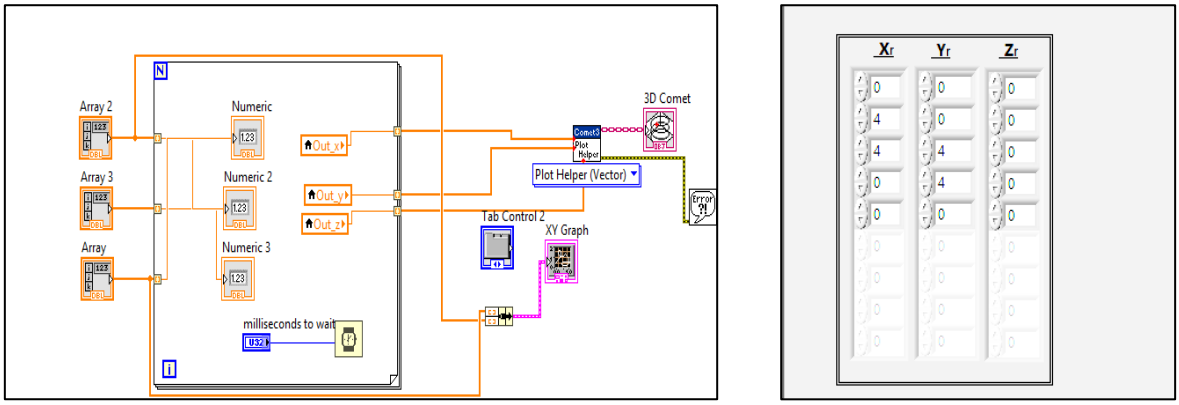

(a) (b)

Figure IV. 58. *(a) Variables dented (x, y and z), (b) an array input.*

Create a source for the variables that control the final responder's position. We have inputs dedicated to point-to-point paths, as well as inputs for continuous paths composed of a set of points, as shown in Figure 60. This is done in order to create a complex path formed by a series of points. When it finishes at point 1, it moves directly to the next point.

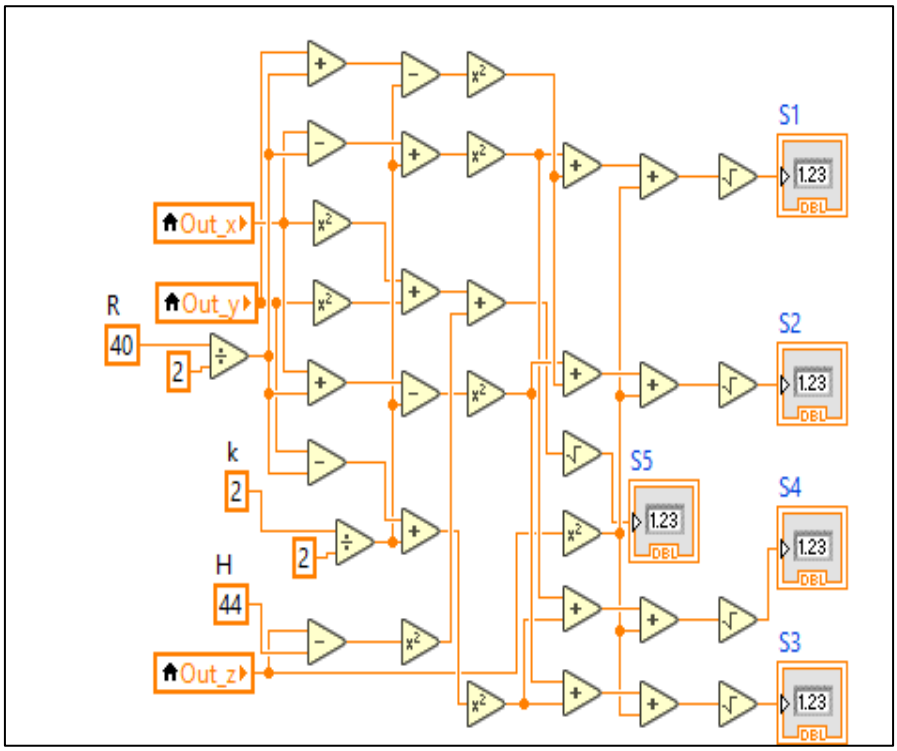

Figure IV. 59. *Geometric model in schema blocs .*

In Figure 61, a detailed representation of the robot's geometric model is presented. This model serves as the basis for calculating the precise cable lengths required for each intended position of the end effector. Once the cable lengths are calculated, a specific algorithm comes into play. This algorithm's primary function is to compute the exact

number of motor revolutions necessary for achieving the desired destination at each new point. By accurately determining these revolutions, the robot can efficiently navigate its path while maintaining precision and accuracy in its movements.

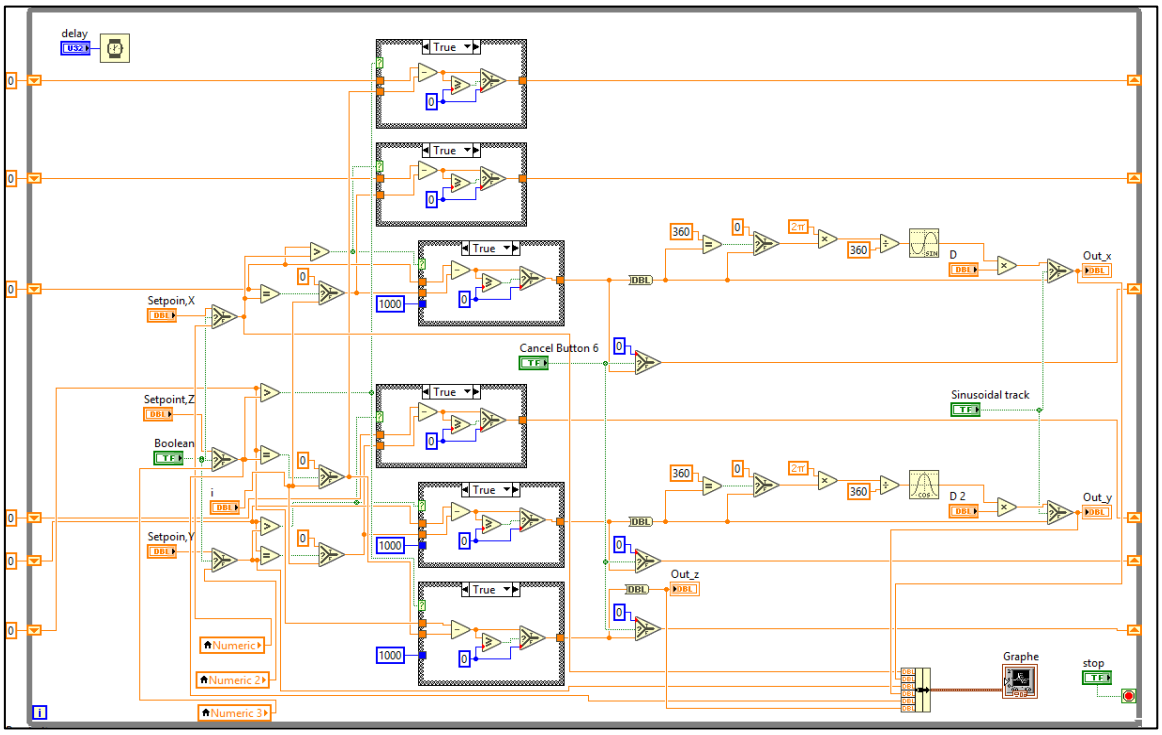

Figure IV. 60. *Functional linear block (open-loop control).*

In Figure. 62, there is a graphical representation of a functional block comprising various programming components, collectively constituting the open-loop control unit. This block embodies a linear mathematical function expressed as $C = i + B$, which plays a crucial role in transforming the predefined path from a straightforward line into a sequence of distinct points. The variable "i" undergoes incremental changes by a constant value of +1. This gradual alteration results in the progressive movement of the end effector, occurring at a controlled pace. Importantly, this synchronized motion guarantees the concurrent operation of all motors, ensuring that their actions remain harmonized and consistent without introducing any discrepancies.

IV.5.1.1.2 Implementing open-loop controller by using Arduino IDE

In this section, we will explain how to activate the open-loop controller within the Arduino interface. This will allow us to position point control the path of the robot's end effector through a series of steps.

boucle_Open

```
float Tr1=0,Tr2=0,Tr3=0,Tr4=0,Tr5=0;
int R1=40,R2=40,H=45,K=0,Tp1=0,Tp2=0,Tp3=0,Tp4=0,Tp5=0;
int Xrf,Yrf,Zrf,Xp,Yp,Zp;
int x=0,y=0,z=0;
```

Figure IV. 61.*initial parameters of the robot*

Initially, we define the robot's parameters and establish fixed values for certain aspects of the robot. For instance, this includes determining the dimensions of the structure and the total lengths of the cables, as depicted in Figure IV-07.

```
AccelStepper stepper1(AccelStepper::FULL4WIRE, 2, 4, 3, 5);
AccelStepper stepper2(AccelStepper::FULL4WIRE, 10, 12,11,13);
AccelStepper stepper3(AccelStepper::FULL4WIRE, 22,26,24,28);
AccelStepper stepper4(AccelStepper::FULL4WIRE, 34, 38,36,40);
AccelStepper stepper5(AccelStepper::FULL4WIRE, 46, 50,48,52);
```

Figure IV. 62. *identify pins of the motors with arduino*

Subsequently, we proceed to define the inputs of the Arduino. A distinct program code is assigned to each motor, and these codes are numbered based on their respective positions on the chassis, as illustrated in Figure IV-08.

```
////////////_______ Input _______ ///

  int a = analogRead(A0)/10.23;
  int b = analogRead(A2)/10.23;
  int c = analogRead(A4)/10.23;
  int d = analogRead(A7)/10.23;
```

(a)

```
double X[]={0  ,0 , 0,0 , 0 , 2, };
double Y[]={0  ,0 , 0,0 , 0 , 2, };
double Z[]={0  ,0 , 0,0 , 0 , 2, };
```

(b)

Figure IV. 63. *(a) variables denoted (x, y, z), (b) utilizing an array*

Following that, we establish the inputs for the variables denoted as 'ah,' as depicted in Figure 65. (a). This approach applies both when transitioning between points and when aiming to execute a complex path, utilizing an array as shown in the same Figure 65. (b).

```
////////////_______ Open loop Control _______ ///////,

  if(a>x) {x=x+1;}if(a<x) {x=x-1;}if(a=x) {x=a;}
  if(b>y) {y=y+1;}if(b<y) {y=y-1;}if(b=y) {y=b;}
  if(c>z) {z=z+1;}if(c<z) {z=z-1;}if(c=z) {z=c;}
```

Figure IV. 64. *Functional linear (open-loop control) .*

To implement the controller, we employ a linear function represented as a + b = c, as illustrated in Figure 66. This enables us to transform the extended path into a functional representation, ensuring synchronized execution by all motors.

```
////////////_______Geometric Model _______ /////,

S1=sqrt(sq(x+K/2-R1/2)+sq(y-K/2+R2/2)+sq(z));
S2=sqrt(sq(x-K/2+R1/2)+sq(y-K/2+R2/2)+sq(z));
S3=sqrt(sq(x-K/2+R1/2)+sq(y+K/2-R2/2)+sq(z));
S4=sqrt(sq(x+K/2-R1/2)+sq(y+K/2-R2/2)+sq(z));
S5=sqrt(sq(x)+sq(y)+sq(z-H));
```

Figure IV. 65. *geometric model.*

To determine the trajectory fed into the control interface, it's essential to ascertain the length of each cable at the intended destination point. The calculation of cable lengths is achieved using the geometric model outlined within a program code, as depicted in Figure 67.

```
////////////_______ Number_Of_Step _______ ////////.

stepper1.moveTo( (S0t-S1)*w  ), stepper1.run();
stepper2.moveTo( (S0t-S2)*w  ), stepper2.run();
stepper3.moveTo( (S0t-S3)*w  ), stepper3.run();
stepper4.moveTo( (S0t-S4)*w  ), stepper4.run();
stepper5.moveTo( (S0t-S5)*w  ), stepper5.run();
```

Figure IV. 66. *functionality of the motor.*

Upon the culmination of the outlined procedure, all motors commence operating collectively to maneuver the end effector towards the desired destination. Each motor operates based on a distinct command, either retracting or extending the cable from the pulley. This functionality is achieved through the utilization of the program code depicted in Figure 68.

Implementing an open-loop controller can be relatively straightforward, as it does not require feedback sensors or the complexity of monitoring the system's behavior. However, open-loop control is best suited for situations where the system's behavior is predictable and external disturbances are minimal. In cases where the system's dynamics are subject to change or uncertainties, open-loop control may not be the most effective choice, and closed-loop control (feedback-based control) is usually preferred for better performance and robustness.

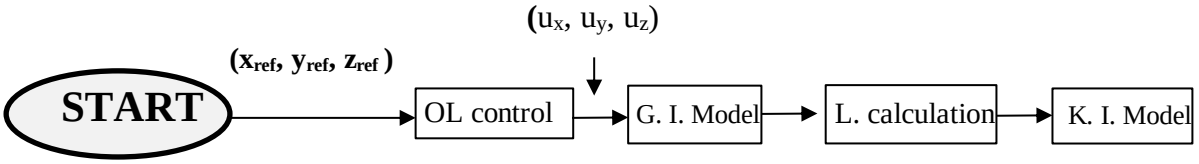

Figure IV.67. *Open loop Controller architecture for the proposed robot system.*

IV.6 PID control strategy

IV.6.1.1 PID control

The PID controller is a control algorithm that combines Proportional, Integral, and Derivative gains to regulate a system's behavior. The feedback control system, as shown in Fig. 70, utilizes this PID controller to achieve the desired control objectives. In this context:

- X: represents the reference signal, which is the target value or setpoint that the system aims to achieve.
- e: stands for the error signal, which is the difference between the reference signal "r" and the actual output of the system.
- u: corresponds to the controller output, which is the calculated control signal generated by the PID controller based on the error signal "e" and the PID gains.
- S: denotes the controlled variable, which is the actual output of the system being controlled.

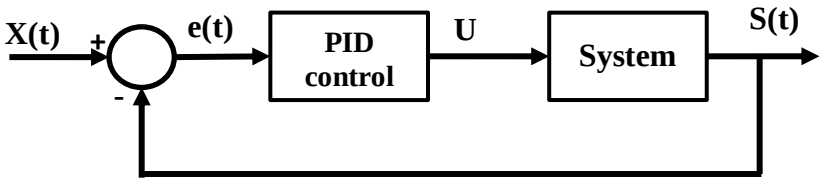

Figure IV. 68. *PID Controller architecture.*

Together, the PID controller continually adjusts the control signal "u" to minimize the error "e" and drive the controlled variable "S" towards the desired reference value "X," thus achieving effective control over the system's behavior.

IV.6.1.2 Implementing PID controller

The implement controller consists of a conventional proportional-derivative (PD) control integrated into a closed-loop system, as depicted in Fig. 70. The control architecture, shown in the block diagram of Fig. 71, comprises three elements in the forward path: the PD controller, the calculation of cable tensions, and the cable-based robot. In the feedback path, two elements are present: the encoder mapping and the forward kinematics.

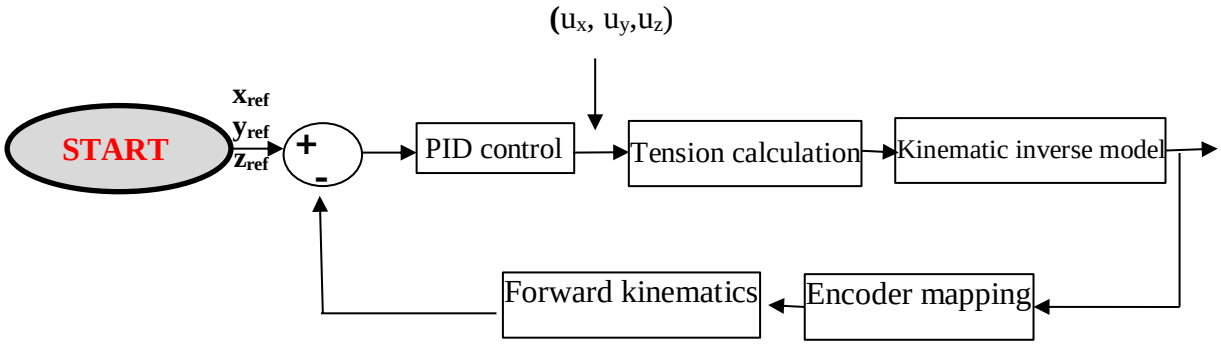

Figure IV. 69. *Controller architecture for the proposed robot system.*

In our system, we do not directly measure the Cartesian position of the end-effector. Instead, we obtain the rotation angles β_i of the pulleys and convert them into cable lengths L_i. These lengths serve as inputs to the forward kinematics, allowing us to derive the Cartesian position X (M. A. Khosravi, 2016).

The control law (U_x, U_y and U_z) along the x and y directions is then established as follows:

$$\begin{cases} U_x = K_P e_x + K_I \int_0^t e_x + K_D \dfrac{de_x}{dt} \\ U_y = K_P e_y + K_I \int_0^t e_y + K_D \dfrac{de_y}{dt} \\ U_z = K_P e_z + K_I \int_0^t e_z + K_D \dfrac{de_z}{dt} \end{cases}$$

The validation of the PID controller considers the constraints related to cable tensions, ensuring that they remain positive and within the bounds of T_{min} and T_{max}. To determine the appropriate coefficients K_P, K_I and K_D for the controller, we employ a trial-and-error method during the validation the experimental prototype. For a satisfactory balance, the following values have been selected:

$$\begin{cases} K_P = 1.00 \\ K_I = 0.048 \\ K_D = 0.000 \end{cases}$$

We have conducted tests of the validation the experimental prototyping involving point-to-point commands and the tracking of various trajectories. To demonstrate the effectiveness of our controller, we provide examples of tracking typical trajectories, including circular, triangular, and sinusoidal paths. Graphical representations of the temporal evolution of the desired path compared to the actual followed path, the cable lengths, and the tensions applied to the cables are presented for each case in chapter 05.

IV.6.1.2.1 implementing of a PID controller on the Arduino board

Crafting and implementing a PID (Proportional-Integral-Derivative) controller on the Arduino board entails a step-by-step sequence that empowers you to attain sophisticated management over a system's operational characteristics. Below is a moderately comprehensive elucidation of this procedural pathway:

- we connect the Arduino board to our computer and open the Arduino IDE development environment;
- To ensure that we have the PID library installed in our Arduino IDE, we can achieve this by navigating to the "Sketch" menu, then selecting "Include Library," and finally clicking on "Manage Libraries." Within the library manager, we can locate the "PID" library and proceed to install it.

```
#include <PID_v2.h>
```

Figure IV. 70. *Bibliotic PID control in arduino IDE.*

- We initiate the declaration of essential variables for the PID controller, encompassing tuning coefficients (Kp, Ki, Kd), setpoint, current values, and outputs.

```
float kp=0.00; //
float ki=0.0014; //
float kd=0.000006; //
```

Figure IV. 71. *PID gin in arduino IDE.*

- Inside the setup () function, we perform the initialization of the necessary input and output pins on the Arduino in accordance with our requirements. For instance, if we're utilizing a sensor to measure a process variable, we designate the pertinent pin

as an input. Similarly, if we're managing an actuator, we designate the relevant pin as an output.

- Within the loop () function, we execute the subsequent actions:
  - We begin by reading the current value of the process variable using the sensors connected to our Arduino.

```
int X_input =  analogRead(A0)/102.3;
int Y_input =  analogRead(A2)/102.3;
int Z_input =  analogRead(A4)/102.3;
```

Figure IV. 72. *Input values on the system.*

  - Next, we calculate the error as the difference between the current value and the setpoint.
  - Utilizing the PID library, we perform computations to determine the controller output using the specified tuning coefficients and the calculated error.

```
//////////////////////___Error___//////////////////
  X_error = X_setpoint - X_input;
  Y_error = Y_setpoint - Y_input;
  Z_error = Z_setpoint - Z_input;
```

Figure IV. 73. *Determining Error in arduino IDE.*

  - This resulting output is then utilized to govern the actuator connected to our Arduino.
  - As part of the iterative process within the loop () function, we consistently repeat these outlined steps during each iteration.

```
//////////////////////////___PID___//////////////////
    //____P
  P_X = kp * X_error;
  P_Y = kp * Y_error;
  P_Z = kp * Z_error;
    //____D
   float dist_diference_X = X_error - X_previous_error;
  D_X = kd*((X_error - X_previous_error)/elapsedTime);
  float dist_diference_Y = Y_error - Y_previous_error;
  D_Y = kd*((Y_error - Y_previous_error)/elapsedTime);
  float dist_diference_Z = Z_error - Z_previous_error;
  D_Z = kd*((Z_error - Z_previous_error)/elapsedTime);
    //____I
    /////////// 1 ////////////////
    if(-25 < X_error && X_error < 25){I_X = I_X + (ki * X_error);}else{I_X = 0;}
   ////////////// 2 ///////////////////////
    if(-25 < Y_error && Y_error < 25){I_Y = I_Y + (ki * Y_error);}else{I_Y = 0;}
  ////////////// 3 ///////////////////////
    if(-25 < Z_error && Z_error < 25){I_Z = I_Z + (ki * Z_error);}else{I_Z = 0;}
```

Figure IV. 74. *PID code in arduino IDE.*

- Following successful code development, we proceed to upload it to our Arduino board and closely observe the ensuing operation of the PID controller.

```
////////////////////////////////////____PID_T____/////////////////////////////////
  PID_X = P_X + I_X +D_X ;
  PID_Y = P_Y + I_Y +D_Y;
  PID_Z = P_Z + I_Z +D_Z;
if(PID_X < -25){PID_X = -25;}if(PID_X > 25) {PID_X = 25; }
if(PID_Y < -25) {PID_Y = -25;}if(PID_Y > 25) {PID_Y = 25; }
if(PID_Z < 0){PID_Z= 0;}if(PID_Z > 40) {PID_Z = 40; }
```

Figure IV. 75. *PID output in arduino IDE.*

It's worth noting that the implementation of a PID controller can exhibit variability based on the particulars of our specific application. The fine-tuning of adjustment coefficients (K_P, K_I, K_D) might be necessary to achieve optimal outcomes. Additionally, it's essential to consider supplementary factors like output limitations, filtering mechanisms, and other pertinent considerations that align with the requirements of our unique control system.

IV.6.1.2.2 implementing of a PID controller on the LabView/software

To implement the PID control in a simulated environment containing a manipulator arm, which has been programmed using LabVIEW, and following the setup of the control interface, the procedure progresses through the ensuing series of steps, characterized by moderate elaboration:

- Initiation of Robot Kinematic Modeling: We embark on the process by creating an inverse kinematic model of the robot within the LabVIEW environment. This model encapsulates the articulations, joints, and coordinates essential for delineating the robot's geometry and its motion characteristics.

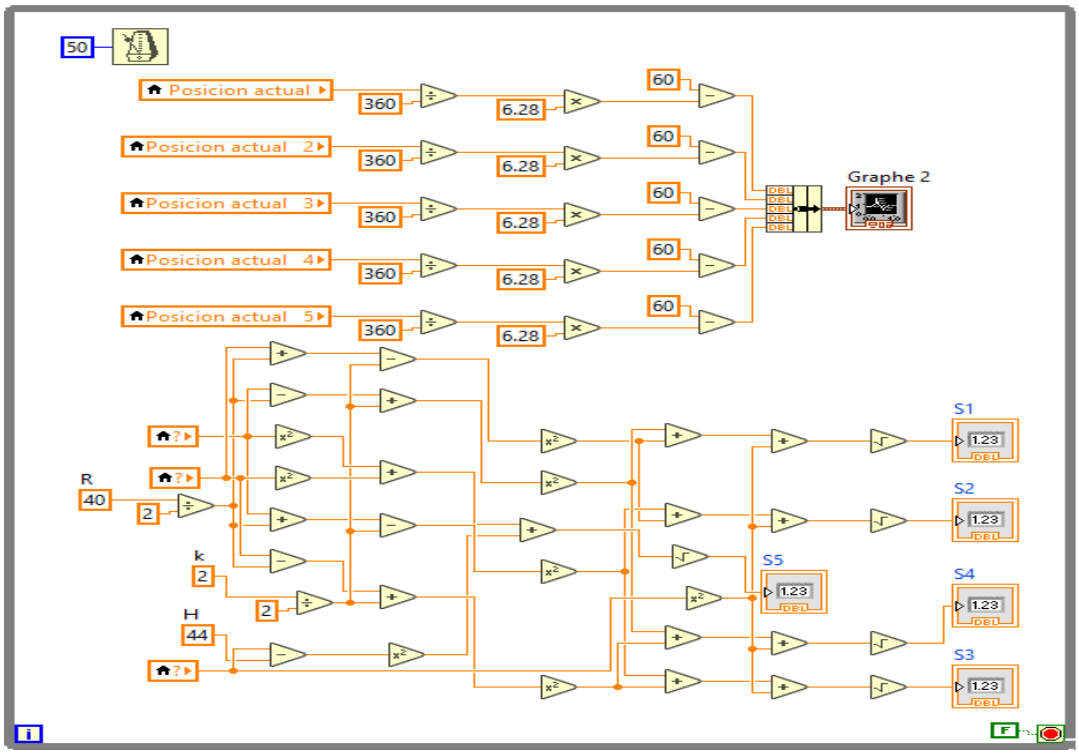

Figure IV. 76. *blocks diagram of kinematic model.*

- Parameter Initialization: The next step involves the initialization of pivotal parameters associated with the PID controller. These include the proportional, integral, and derivative gains, along with other vital variables that influence the controller's behavior.

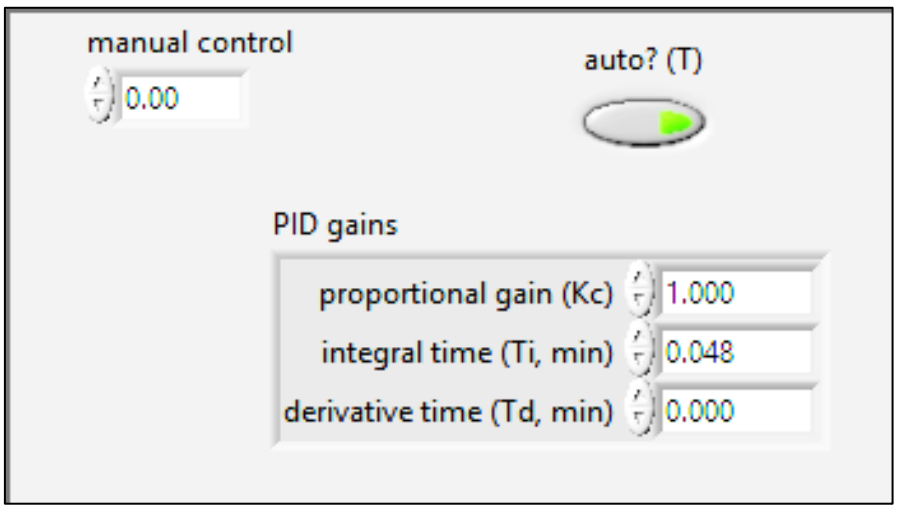

Figure IV. 77. *PID gains*

- Manual Adjustment of PID Parameters: Employing a manual approach, we fine-tune the PID gains to ascertain optimal performance. This entails iteratively modifying the proportional, integral, and derivative coefficients.
- Computation of Error: A critical facet involves comparing the collected data with the desired reference values, enabling us to compute the error an indicator of the deviation between the two datasets.
- Values Update: To prepare for the ensuing iteration of the PID controller, we proceed to update crucial values. This encompasses variables such as the prior error magnitude and the cumulative sum of errors.

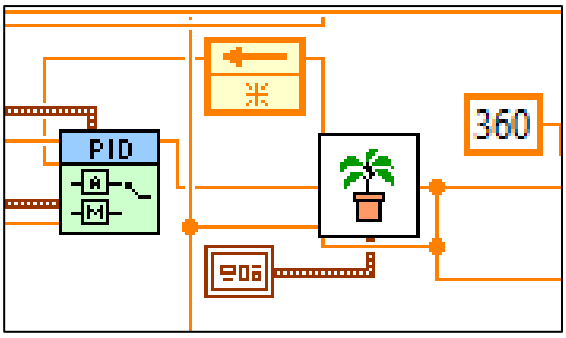

Figure IV. 78. *PID block.*

- Implementation of the Core Loop: The preceding steps are recurrently executed within the confines of a principal loop. This overarching loop facilitates the continuous gathering of data, fine-tuning of PID parameters, and updating of relevant values.

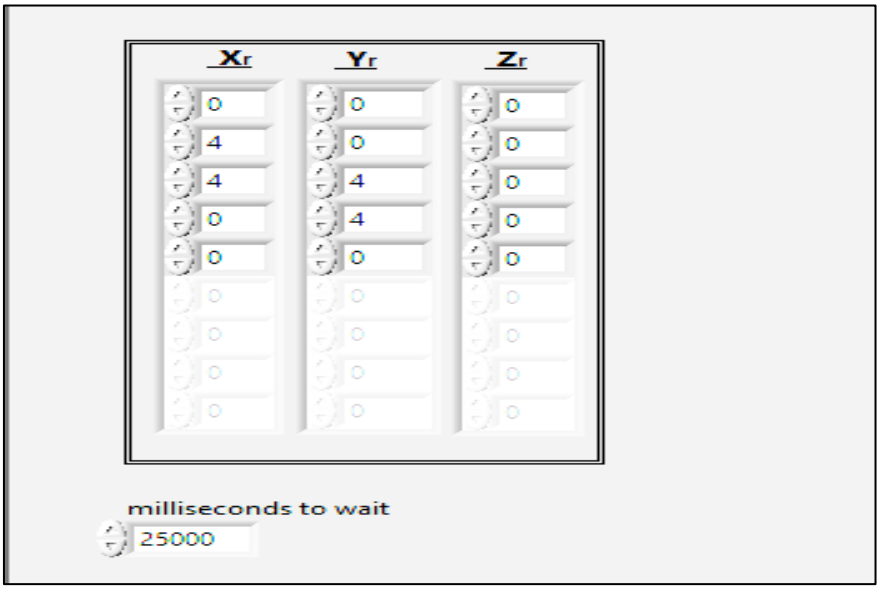

Figure IV. 79. *Array input.*

- Result Visualization: Harnessing LabVIEW's array of visualization tools, including graphs, we present the outcomes of our endeavor. These visual representations encompass the system's response dynamics, the extent of error, the command issued to the output, and more.
- By methodically engaging in these actions, we facilitate the effective integration of PID control into a LabVIEW-programmed robot with a simulated environment. This empowers us to observe, evaluate, and optimize the robot's behavior in response to our control efforts.

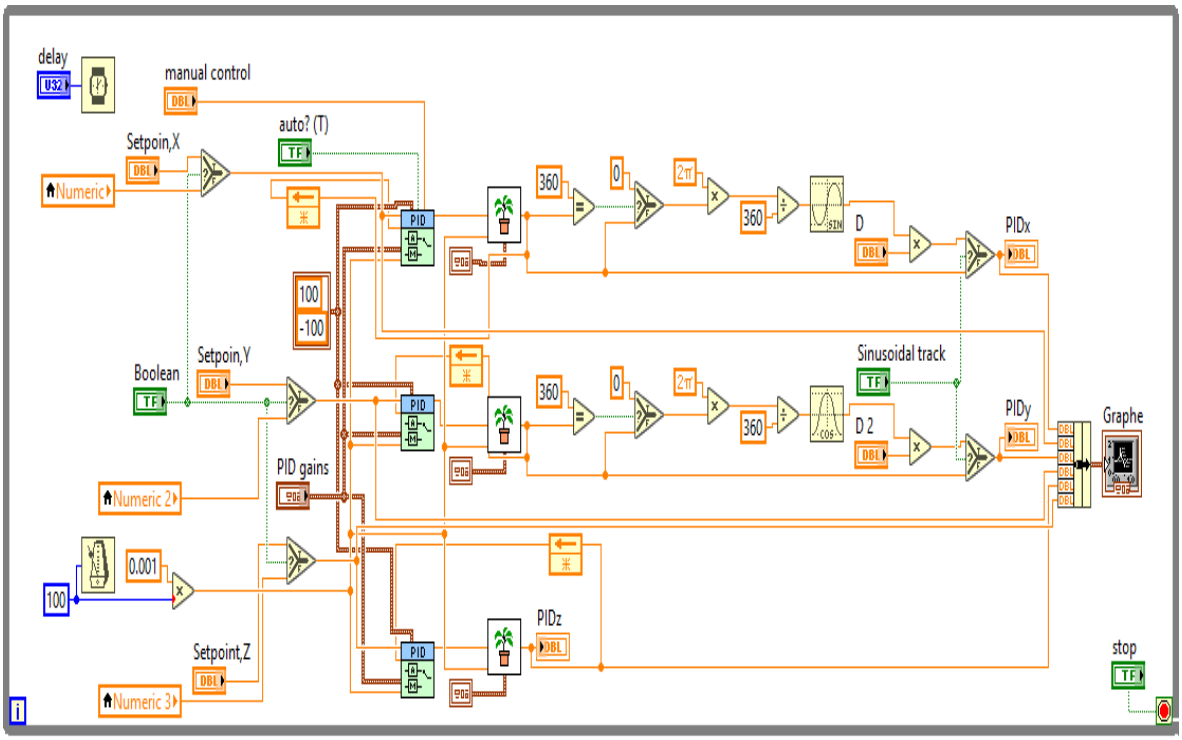

Figure IV. 80. *blocks diagram of PID control.*

Accurate configuration of the PID controller gains for each individual joint in the robot is crucial to attain the targeted control proficiency. These gains can be calibrated either through manual adjustments or by employing automated tuning techniques, such as the closed-loop Ziegler-Nichols method.

IV.7 Rehabilitation Task Proposed of Prototypes

In this section, we propose some tasks that we will strive to implement in the future, using three types of cable-driven parallel robots. Through this idea, we aim to integrate routine tasks with technology, aiming for a qualitative leap in technology and the integration of new skills

in the field of medical robotics. Furthermore, we also aim, through this concept, to provide new services in the world and keep up with the advancements of modern technology.

IV.7.1 Rehabilitation Task of Planning CDPR

In this section, we propose some tasks that we will strive to implement in the future, using a Plane Cable driven parallel robot. These tasks encompass routine applications such as writing and drawing on school boards. With this idea, we aim to integrate routine school or household tasks with technology, thereby reducing the role of educators in teaching the young ones, as you can see in Figure 83. A robot is available to perform their routine tasks, and the user follows the path of the robot that has been predefined by the programmer. Through this concept, we aim to provide new technological services, keeping up with progress and the current era.

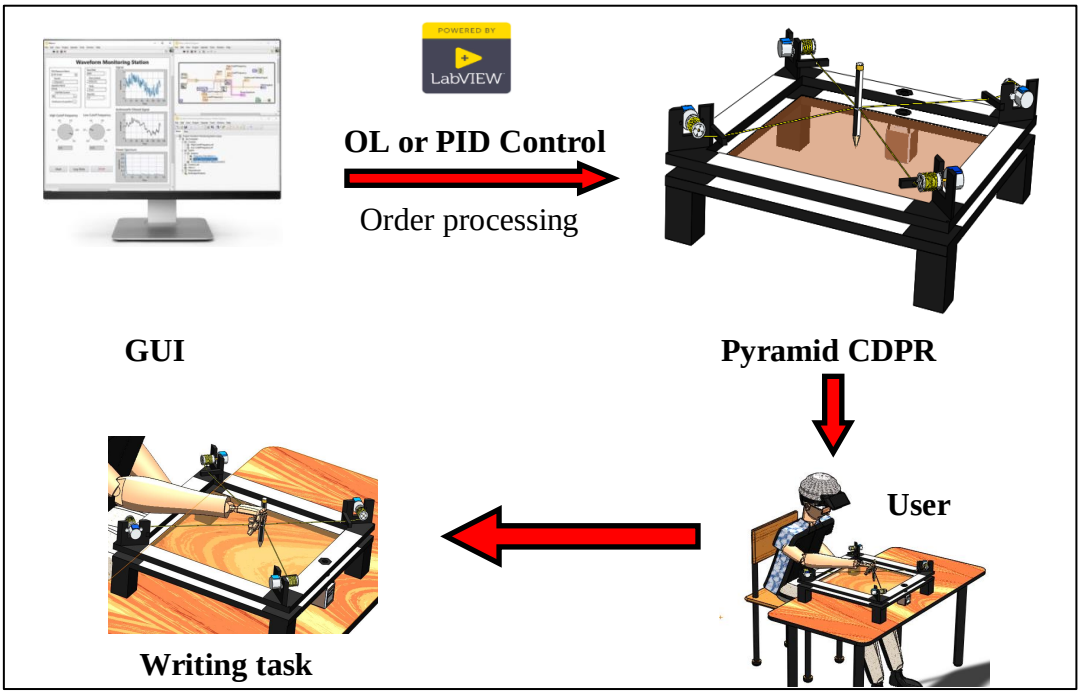

Figure IV. 81. *Rehabilitation Task Proposed of Planning CDPR.*

IV.7.2 Rehabilitation Task of Cube CDPR

In this section, we propose some tasks that we will strive to implement in the future, using a cub-shaped Cable Parallel robot that operates in a three-dimensional workspace. These tasks encompass routine applications such as writing and drawing on school boards, both at home and in school. Additionally, it will be utilized in 3D printing (see in Figure 84). With this experimental model, we can create large three-dimensional shapes, as this type of robot is

capable of operating in extremely spacious areas. Through this idea, we aim to integrate construction and routine tasks with modern technology, allowing us to expand the realm of three-dimensional work and routine exercises at home. Furthermore, our goal with this concept is to introduce new technological services and keep up with the advancements of the new era.

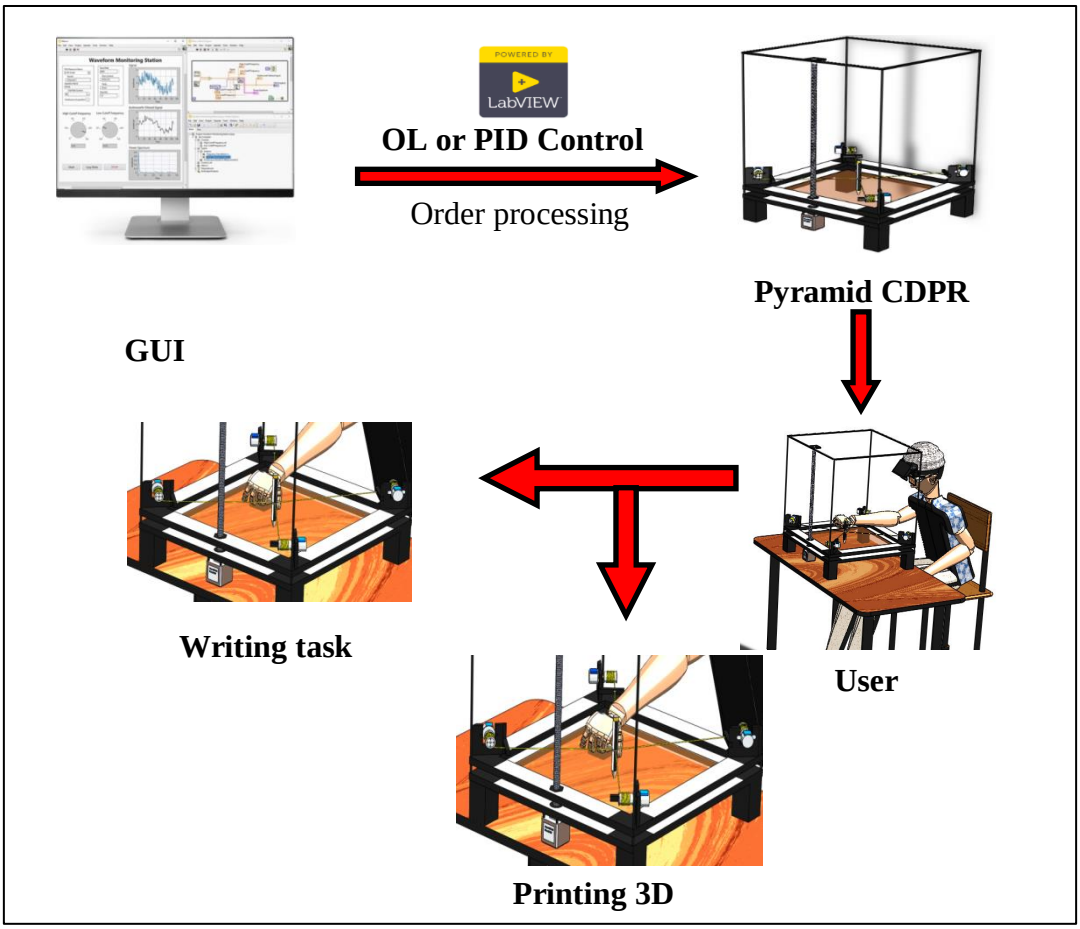

Figure IV. 82. *Rehabilitation Task Proposed of Cube CDPR.*

IV.7.3 Rehabilitation Task of Pyramid CDPR

In this section, we present a comprehensive explanation of various rehabilitation applications that are targeted for integration into our robot's repertoire of tasks, aimed at their prospective implementation. The overarching objective is to empower the robot with a fresh set of skills. For instance, one notable skill is the incorporation of hand rehabilitation procedures. This entails the systematic execution of repetitive hand exercises, tailored to align with the individualized needs of each user. By methodically adapting the exercises based on the user's specific requirements, our intention is to facilitate optimal recovery and enhancement.

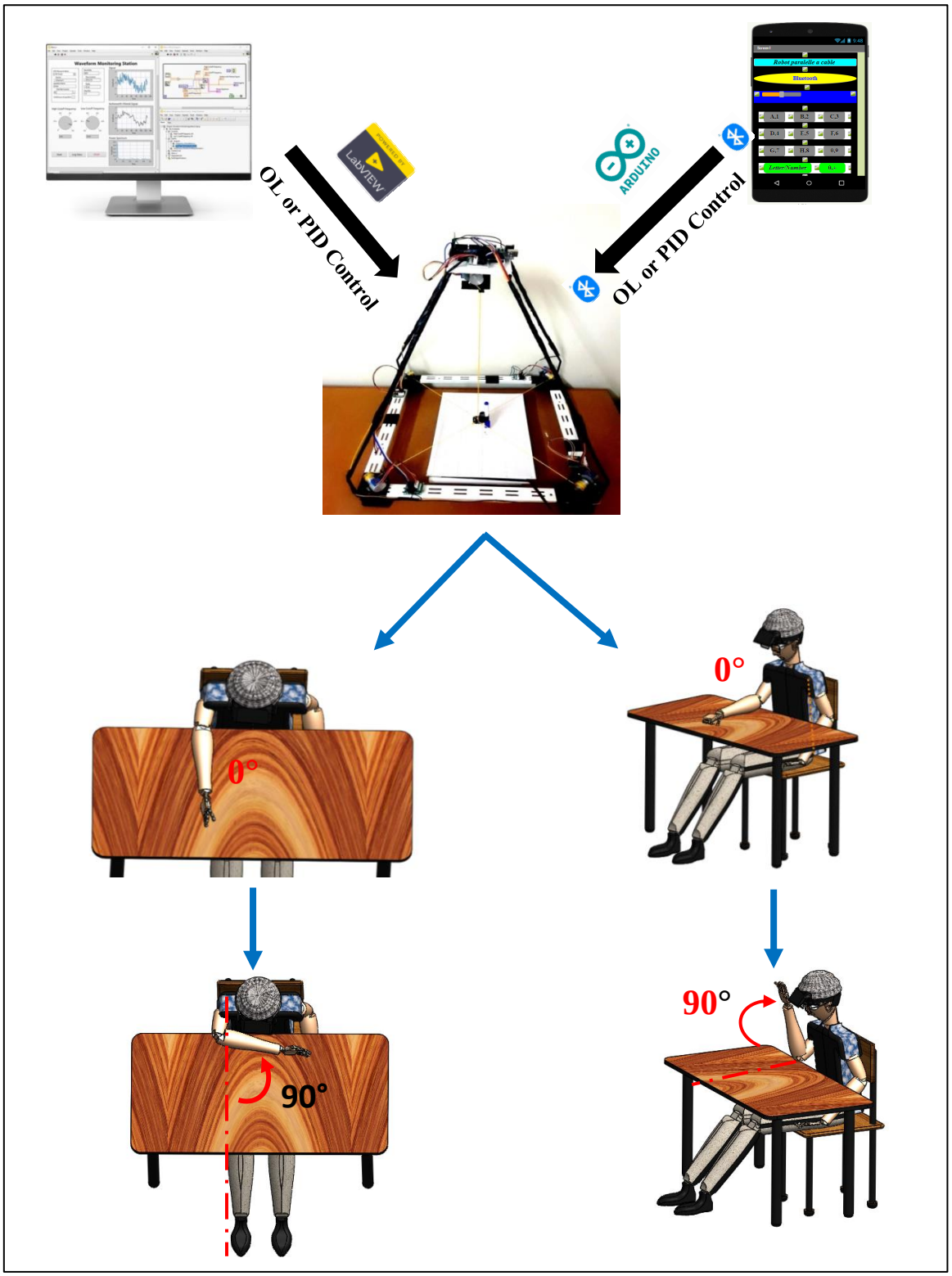

Figure IV. 83. *Rehabilitation Task Proposed of Pyramid CDPR.*

IV.8 Exercising Rehabilitation Task CDPR

IV.8.1 Application rehabilitation task of pyramid CDPR

Within this section, we delve into comprehensive details concerning the array of rehabilitation applications well within the capabilities of our robot. The overarching purpose is to imbue the robot with an entirely novel skillset.

For instance, consider the incorporation of hand rehabilitation methodologies, where the robot engages in repeated hand exercises involving drawing and writing. These exercises are designed to be conducted multiple times, aligning precisely with the specific requirements of each individual user. By tailoring the exercises in accordance with the unique needs of each user, our intention is to facilitate optimal recovery and skill acquisition for more detail about create graphical user interface see ANNEX 01 and ANNEX 02.

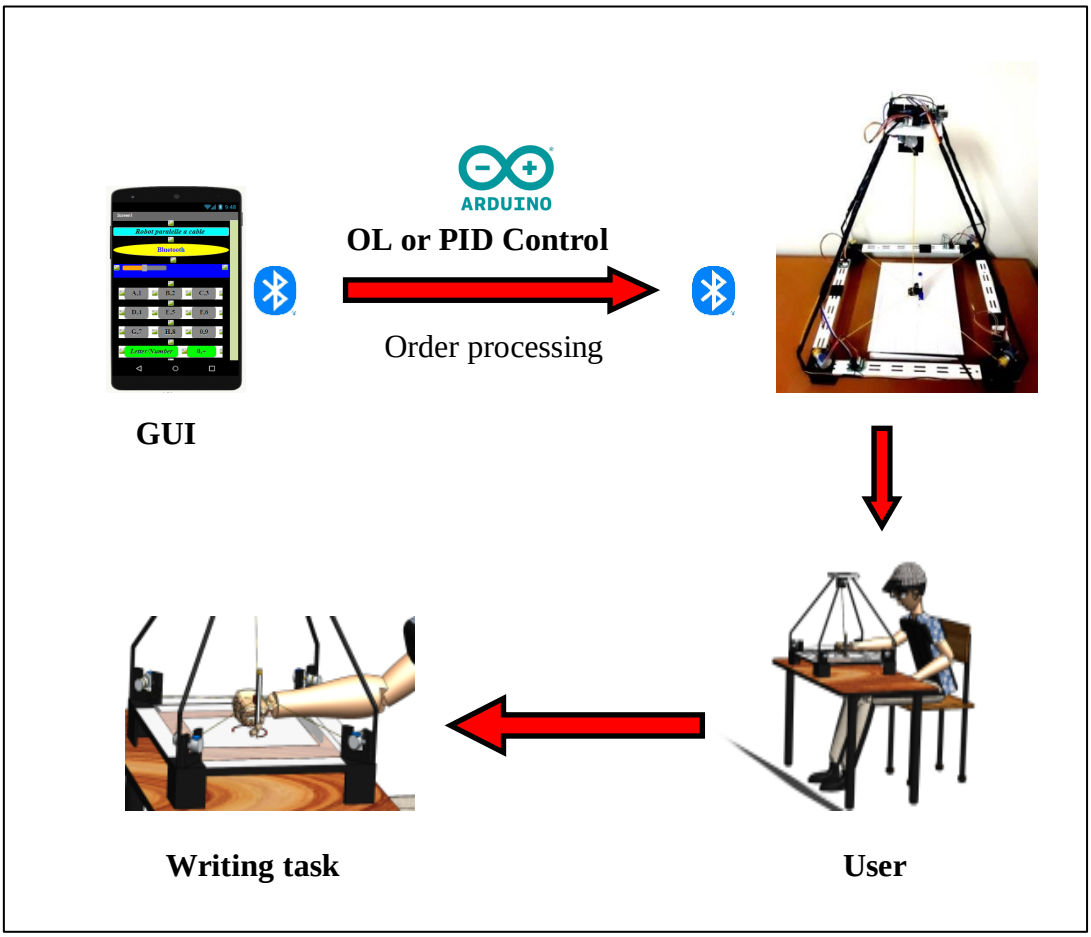

Figure IV. 84. *App. Android for control Pyramid CDPR.*

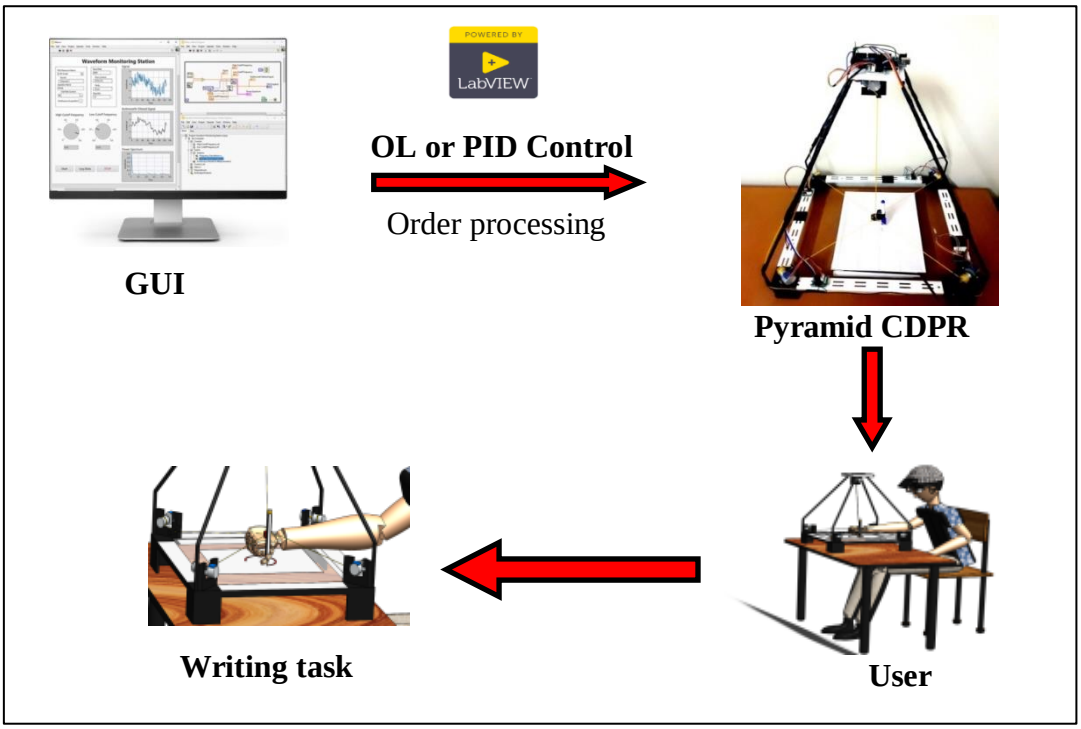

Figure IV. 85. *GUI (LabView software) for control Pyramid CDPR.*

In this section, we have Figure 86. illustrating the process of controlling the robot using an Android application through a smartphone. This application is developed using Model MIT inventor for creating mobile applications. Additionally, to control the robot, we need to write programming code using the Arduino IDE. Afterward, the control unit with an open loop () is activated or PID control, as shown in Figure 86. In Figure 87, we have the same model, but it's controlled through a graphical control interface created using LabView software. The open loop () or PID control unit is integrated into it to enhance the robot's performance. In Figure 87, we also present some tasks that this model offers. Through these tasks, we were able to expand the scope of three-dimensional work and routine exercises at home. Our goal with this concept is to introduce new technological services and keep up with the advancements of the new era, and we will present the results of this model in the final chapter.

IV.9 Conclusion

In conclusion, the aim of searching for a suitable control strategy for the cable-driven parallel robot is to exert precise control over its performance, rectifying errors stemming from external factors like cable stretching, effector weight, motor operation variations, and others. Through the application of a well-designed control strategy, guided by insights from prior research, the robot's capabilities will be enhanced, allowing it to operate more accurately, efficiently, and reliably across a range of applications and tasks.

Chapter 5

V.1 Introduction

In this chapter, we present the results obtained through the activation of strong control strategies for the introduced models in order to conduct several maneuvers and applications of rehabilitation in drawing and writing. Firstly, we presented simulation results using MATLAB software for the model developed through three regular stages. Then, the results of the open-loop control unit and the PID Control unit displayed through the graphical control interface created using LabView software. Finally, the results of the experimental model, which was controlled using the open-loop control unit, were presented. Its output is in the form of a linear path to gradually move from one point to another, in addition to analyzing these results to determine their effectiveness.

V.2 Simulation of the proposed writing tasks

V.2.1 Simulation test of the proposed "Planar CDPR"

In the present section, we have chosen multiple uncomplicated as well as intricate trajectories with the primary objective of assessing the reliability of simulating a planar robot through the utilization of the MATLAB software. These chosen trajectories can be categorized into two distinct types: a discrete point-to-point path and a continuous trajectory composed of an assemblage of points. The intended purpose of these trajectories is to facilitate the depiction of alphabetic characters as well as intricate geometric shapes. The sequential outcomes of the simulations, which are visually presented in Figures 1 to 4, effectively demonstrate the tangible outcomes stemming from the hands-on implementation of the methodologies expounded upon within this specific section. In this section, we depending on the on the geometric and kinematic models, we simulated the 2D of Cable driven parallel robots using Matlab/ Software.

V.2.1.1 Point to point test

Within this section, our methodology hinged on the utilization of both geometric and kinetic models, which enabled us to conduct simulations of the proposed robot using the Matlab/Software platform, in which a point-to-point trajectory was simulated.

Fig. 88 (a) and (b) show the transition of the final responder from the first point to the second point.

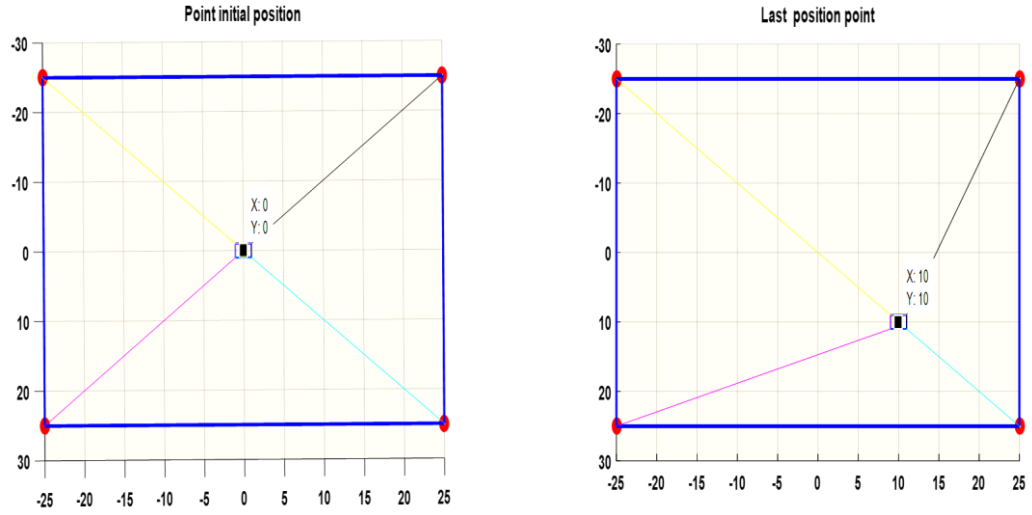

(a) ***(b)***

Figure V. 86. *(a) Plot of the end effector to initial point position. (b) Plot of the end effector to second point position.*

V.2.1.2 Trajectories continue test

In the context of this section, our approach was anchored in employing both geometric and kinetic models. This combination allowed us to carry out simulations of the envisioned robot's behavior using the Matlab/Software platform. Notably, the simulations included the emulation of a continuous trajectory, adding a specific focus to our analysis.

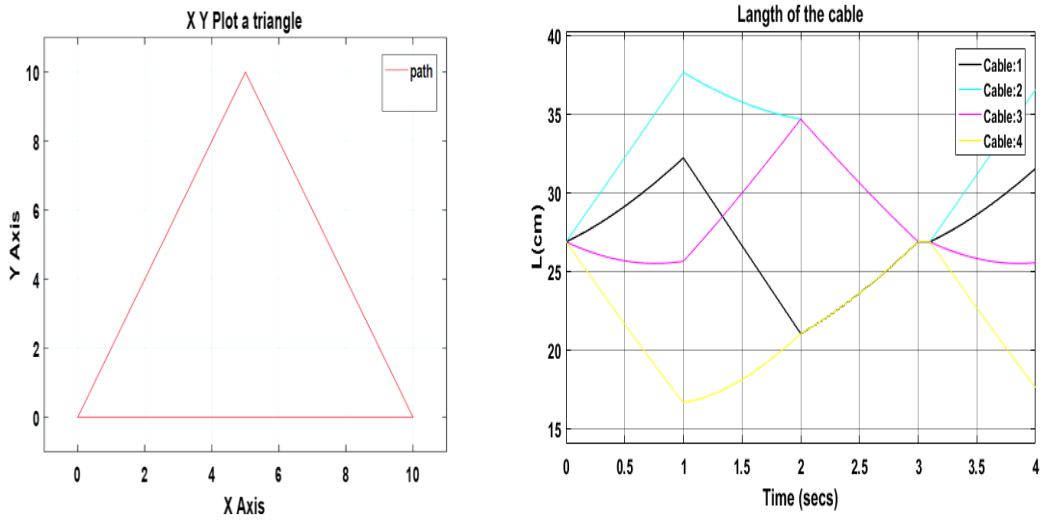

(a) ***(b)***

Figure V. 87. *(a) Simulation of a triangle in matlab (b) The cables lengths (L1, ...L4).*

Fig. *V*. 89–a shows the transmission of the final effector in a continuous path in a triangle shape and Fig. *V*. 89-b plot lengths of the cables.

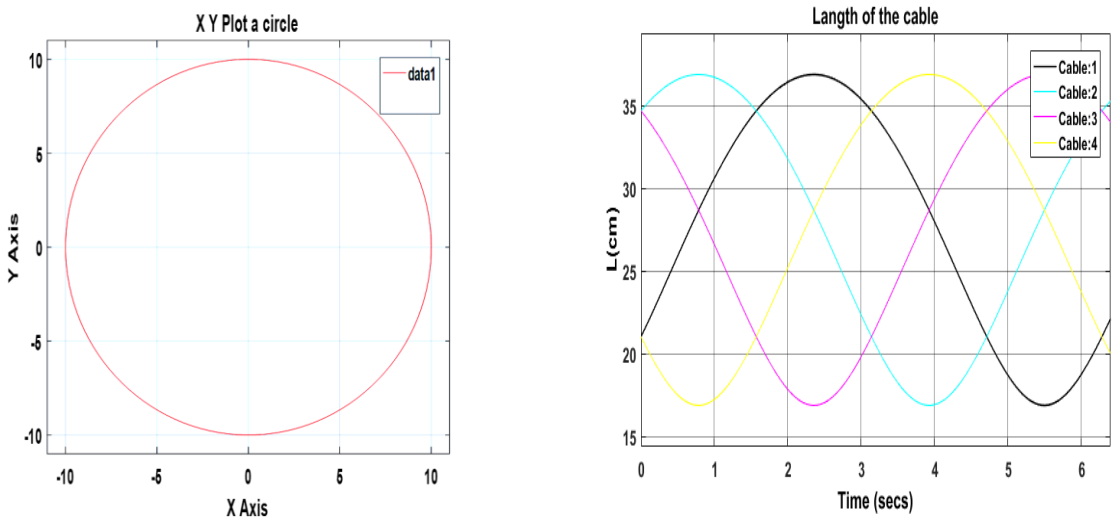

(a) ***(b)***

Figure V. 88. *(a) Simulation of a circle in matlab. (b) The cables lengths (L1, ...L4).*

Fig. *V*. 90–a shows the transmission of the final effector in a continuous path in a circle shape and Fig. *V*. 90-b plot lengths of the cables.

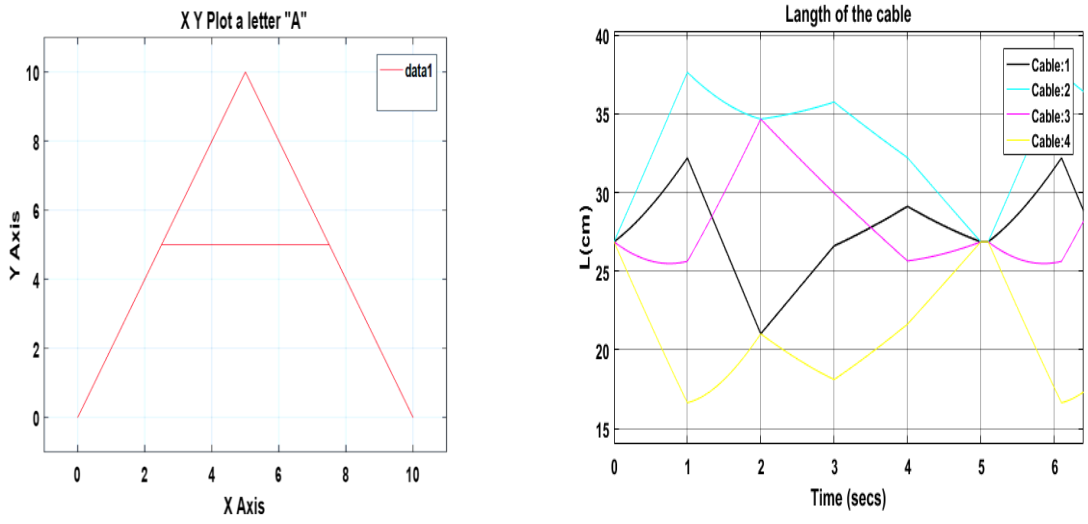

(a) ***(b)***

Figure V. 89. *(a) Simulation of a letter "A" in matlab. (b) The cables lengths (L1, ...L5).*

Illustrations in Figures *V.* 88 to *V.* 91 offer a graphical exposition of the simulated outcomes originating from a cable-driven robot designed for planar motion. The configurations identified by the marker 'a' offer a strikingly vivid representation of the trajectories that trace a variety of letters. These carefully chosen shapes serve a dual purpose: firstly, as a means to assess and verify the precision of the active geometric models, and secondly, to confirm their validity. In contrast, the figures annotated with the label 'b' provide a comprehensive exhibition of the dynamic variations in the robot's cable lengths as it traverses its trajectory, concurrently reproducing these distinctive letters and shapes. This comprehensive depiction allows for a detailed observation of how the cable lengths adapt and change during the robot's motion, lending further insight into its mechanical behavior and performance.

The outcomes obtained serve as robust confirmation of the accuracy embedded within both the geometric and inverse kinematic models. This verification not only instills a deep sense of confidence but also encourages the utilization of these models to construct a durable control algorithm. This algorithm, once developed, holds the potential to greatly augment and supervise the operational prowess of the robot. Moreover, these models, now validated, lay the crucial groundwork for the construction of experimental frameworks. These frameworks are central to the subsequent stages of research, serving as the basis upon which further investigations and conclusions are established. This pivotal aspect will be comprehensively elaborated upon in the subsequent section dedicated to presenting the ultimate and conclusive findings of the study.

V.2.2 Simulation test of the proposed "Cube CDPR"

In this section, we selected a wide range of different trajectories for simulation using Matlab software. We have two trajectories, simple (point-to-point) and complex (continuous trajectories) for drawing letters and geometric shapes such as reported in the simulation results in Figures *V.* 92 to *V.* 97 that have been obtained by implementing the models in chapter 3 section 4.2.

V.2.2.1 Point to point test

in this part, our approach centered on the utilization of both geometric and kinetic models. Employing the Matlab/Software platform, we conducted simulations involving the envisioned robot. This strategic choice allowed us to explore and evaluate the robot's behavior based on the interplay of these models, facilitating a comprehensive understanding of its dynamics and performance.

Fig. *V.* 92–a. and Fig. *V.* 92-b shows the transition of the final responder from the first point to the second point.

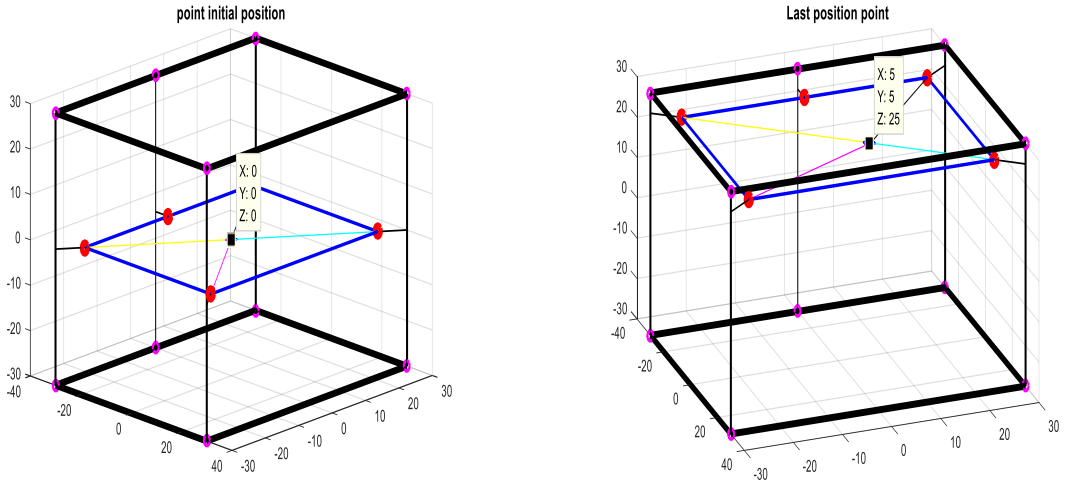

(a) ***(b)***

Figure V. 90. *(a) Plot the end effector to initial point position. (b) Plot the end effector to second point position.*

V.2.2.2 Test of continue trajectories

In the confines of this section, our methodology was predicated on harnessing both geometric and kinetic models. This synergy facilitated the execution of simulations for the envisaged robot via the Matlab/Software platform. Notably, these simulations

encompassed the emulation of a continues trajectory, accentuating a specific facet of our investigation.

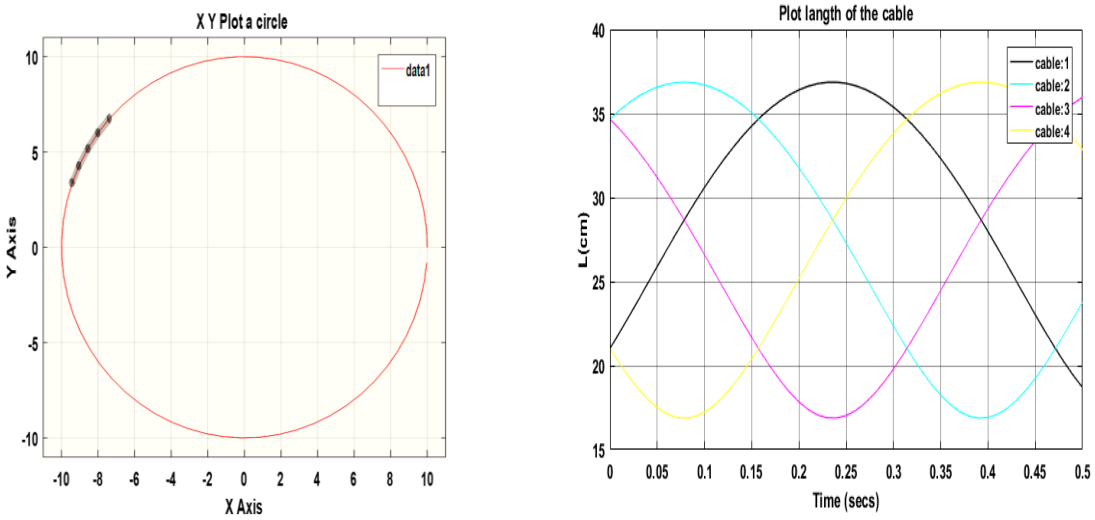

(a) ***(b)***

Figure V. 91. *(a) Simulation of a circle in matlab (b) The cables lengths (L1, ...L4).*

Fig. *V*.93–a. shows the transmission of the final effector in a continuous sinusoidal path and Fig. *V*. 93–b shows the lengths of the cables.

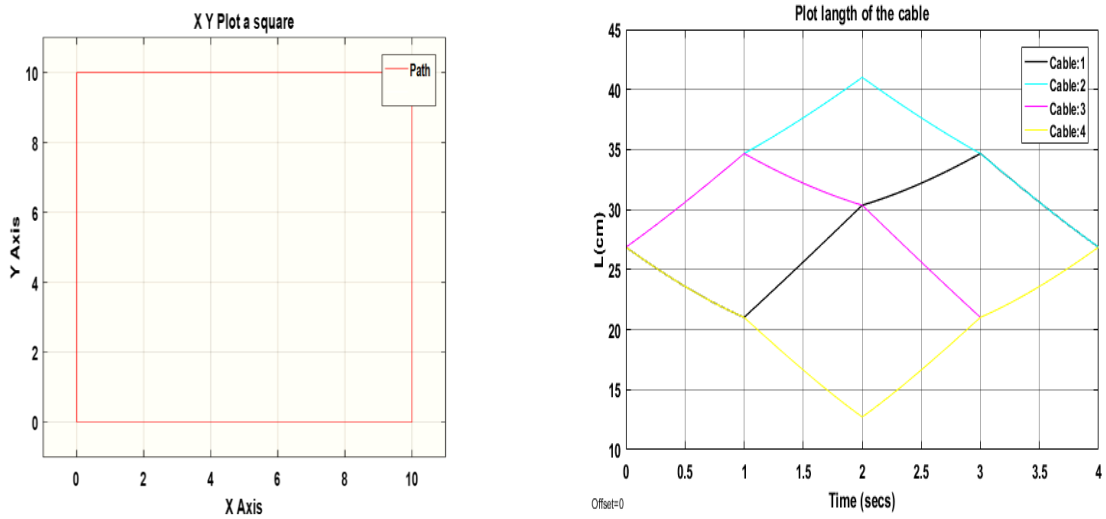

(a) (b)

Figure V. 92. *(a). Simulation of a square in matlab (b) The cables lengths (L1, ...L4).*

Fig. *V*. 94–a shows the transmission of the final effector in a continuous path in a square shape and Fig. *V*. 94-b plot lengths of the cables.

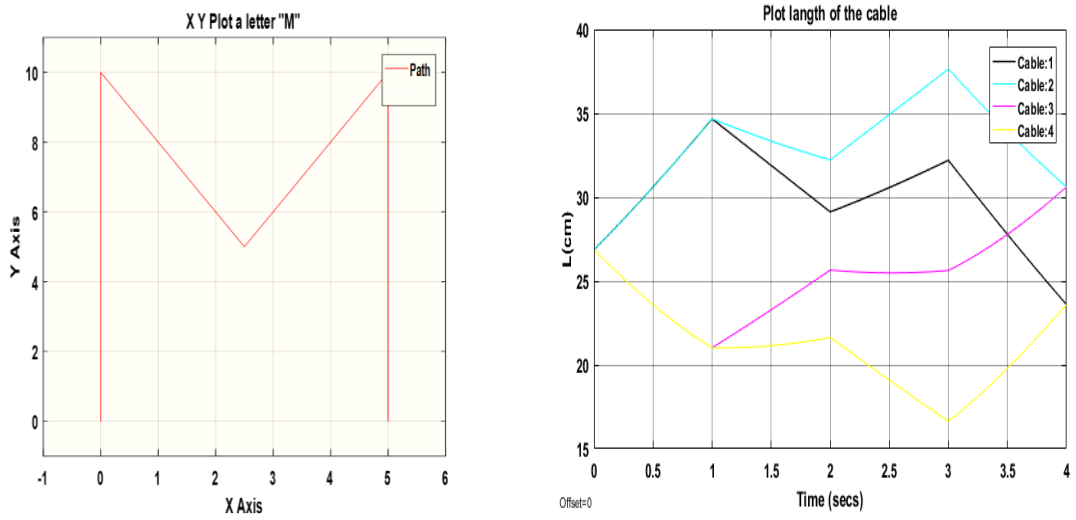

(a) ***nn*** ***(b)***

Figure V. 93. *(a) Simulation of a letter "M" in matlab (b) The cables lengths (L1, ...L4).*

Figures *V.* 92 to *V.* 97 provide visual representation of the simulated results stemming from a cubic cable-driven robot. The shapes designated by the identifier 'A' vividly illustrate the paths tracing various letters. These specific shapes were thoughtfully chosen to serve as a means of assessing and confirming the accuracy of the geometric models in play. In contrast, the figures labeled with the marker 'B' offer a comprehensive display of the robot's cable length variations over the course of its trajectory while reproducing these distinct letters and shapes.

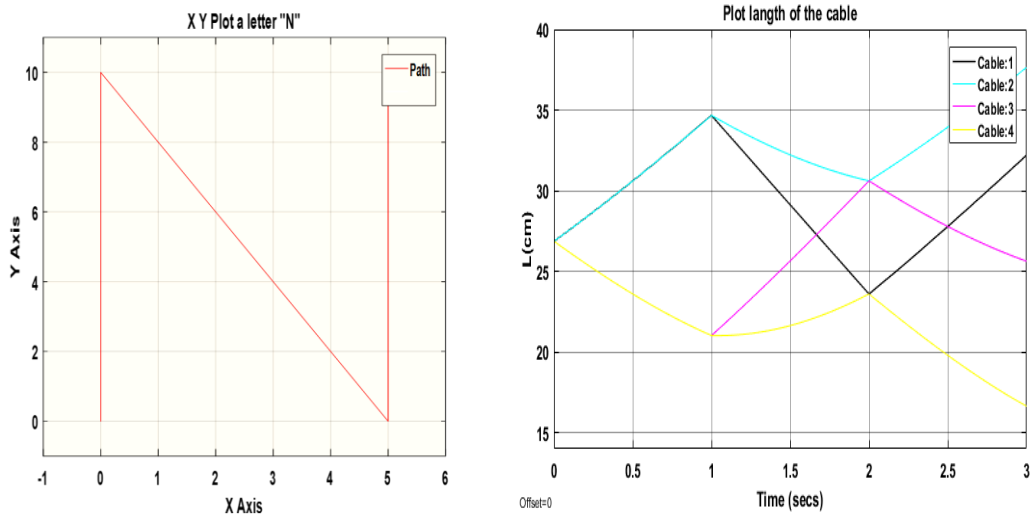

(a) (b)

Figure V. 94. *(a) Simulation of a letter "N" in matlab (b) The cables lengths (L1, ...L4).*

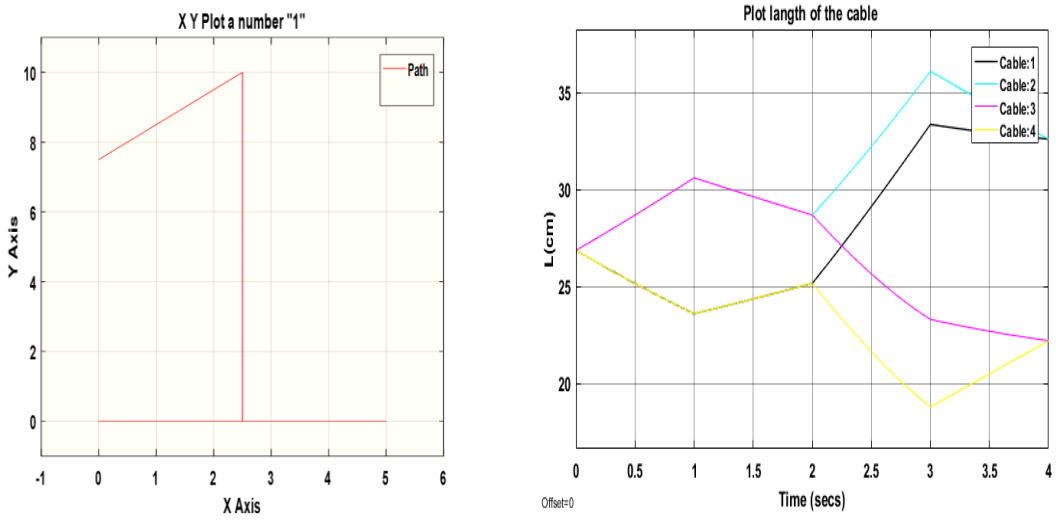

(a) ***(b)***

Figure V. 95*. (a) Simulation of a number "1" in matlab (b) The cables lengths (L1, ...L4).*

The attained results provide strong validation for the precision of both the geometric and inverse kinematic models. This validation imbues a sense of assurance in harnessing these models to craft a resilient control algorithm that can effectively enhance and oversee the robot's operational capabilities. Furthermore, these validated models establish a cornerstone upon which experimental frameworks are built, a topic that will be expounded upon in the last section devoted to presenting the conclusive findings.

V.2.3 Simulation test of the proposed “pyramid CDPR”

In this section, a diverse selection of trajectories was carefully chosen for simulation using the Matlab software to thoroughly test the simulation capabilities of the pyramid cable-driven parallel robot. The trajectories encompass two distinct categories: the first involves simple point-to-point movements, while the second entails more intricate continuous trajectories. These trajectories serve the purpose of illustrating the robot's ability to create both letters and complex geometric shapes. The simulation results, depicted in Figures 98 to 104, were achieved by effectively implementing the geometric and kinematic models within the Matlab software environment.

V.2.3.1 Point to point test

In this section, we rely on the inverse geometric model. Figures 98-a and 98-b visually demonstrate the movement of the end effector, which transitions from its initial position to the designated coordinates. These coordinates are introduced through a control interface tailored for precision.

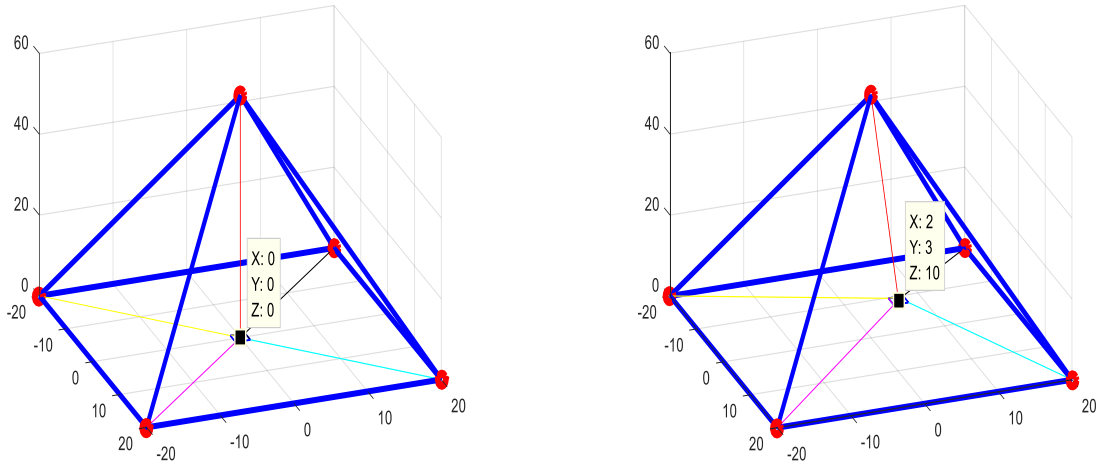

(a) ***(b)***

Figure V. 96. *(a) Plot the displacement of the end effector point to point initial position. (b) Plot the displacement of the end effector point to point second position.*

V.2.3.2 Trajectories continue test

Within the scope of this section, our approach was rooted in the utilization of both geometric and kinetic models, working in tandem. This collaboration streamlined the process of conducting simulations for the envisioned robot through the Matlab/Software platform. Of particular note is that these simulations replicated a continuous trajectory, thereby emphasizing a specific aspect of our investigative focus.

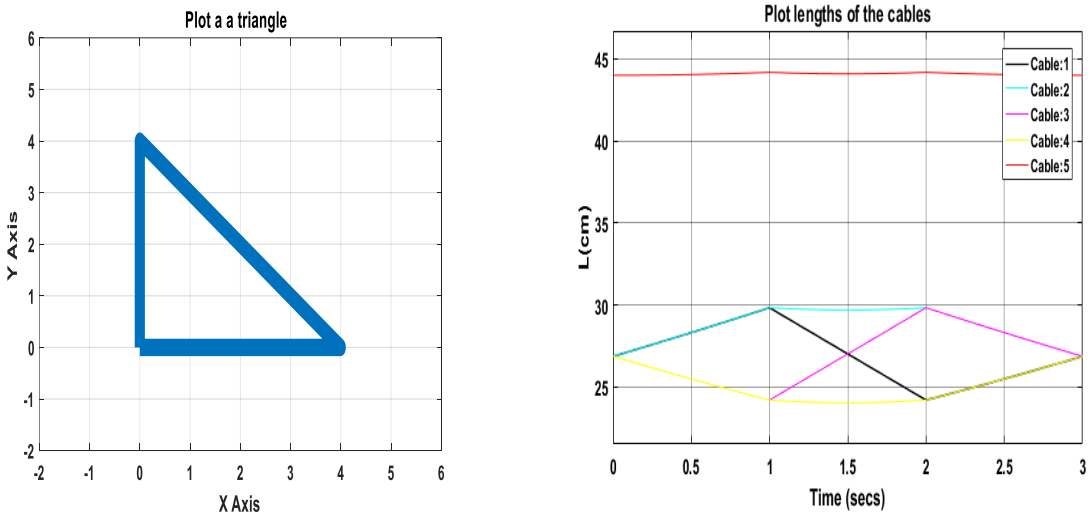

(a) **(b)**

Figure V. 97. *Obtained simulation results: (a) Plotting a continued triangle trajectory; (b) calculated evolution of cable lengths versus time to achieve the path in Fig.99(a).*

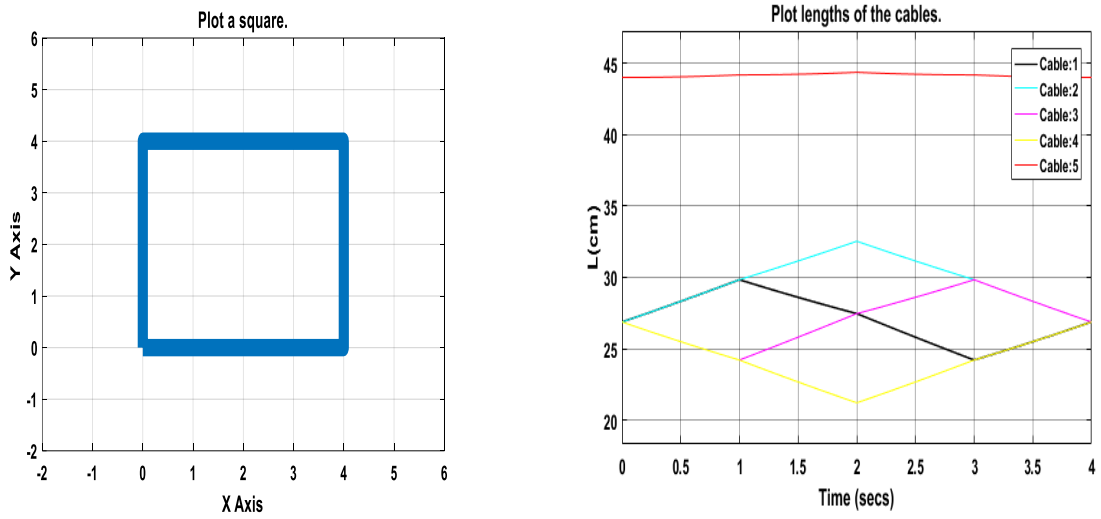

(b) (b)

Figure V. 98. *Obtained simulation results: (a) Tracking of square trajectories; (b) calculated evolution of cable lengths versus time to achieve the path in Fig.100(a).*

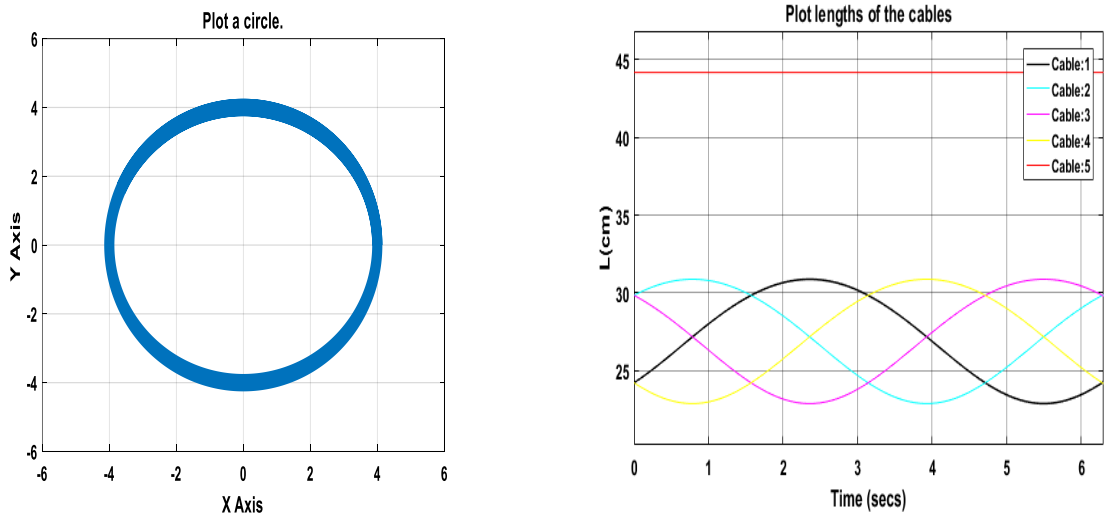

(a) **(b)**

Figure V. 99. *Obtained simulation results: (a) Tracking of the circular path; (b) calculated evolution of cable lengths versus time to achieve the path in Fig.101(a).*

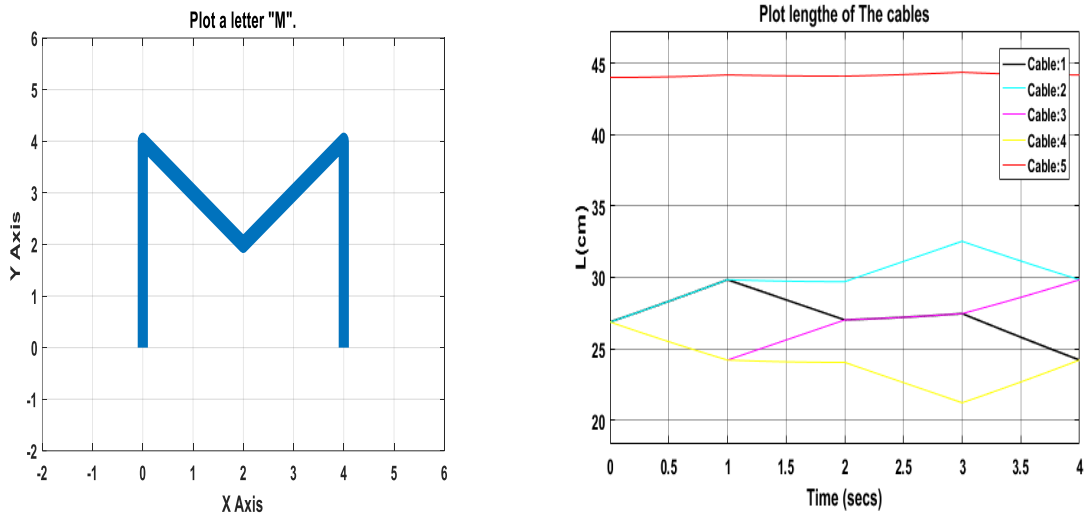

(a) **(b)**

Figure V. 100. *Obtained simulation results: (a) Tracking of the letter "M" path ;(b) calculated evolution of cable lengths versus time to achieve the path in Fig.102(a).*

Figures ***V***. 97 to ***V***. 104 portray the simulated outcomes of a hierarchical cable-driven robot. The shapes denoted by the letter 'A' depict the trajectories corresponding to letters, which were deliberately selected to validate the geometric models. Conversely, the figures labeled with the letter 'B' showcase how the robot's cable lengths evolved over time as it traced these letters and shapes.

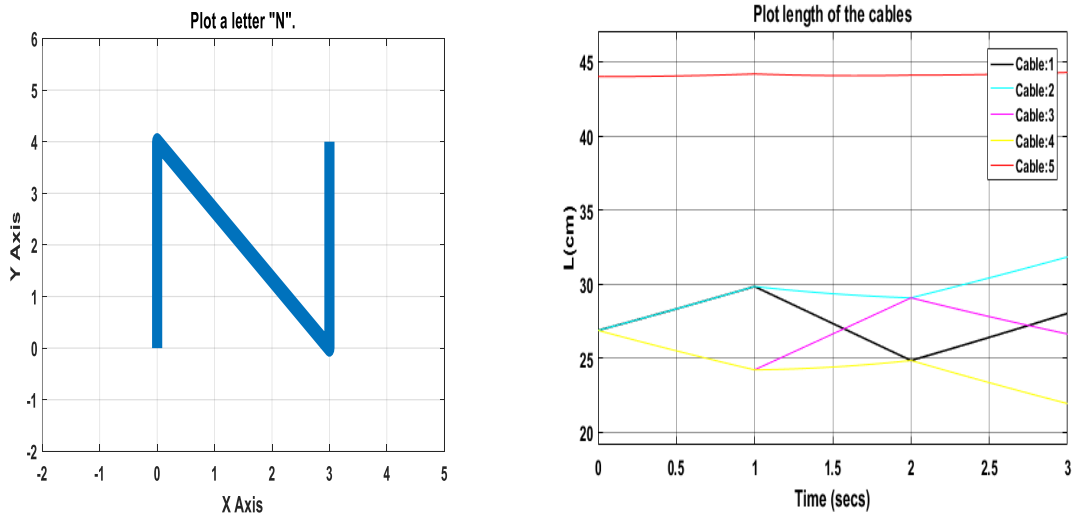

(a) ***(b)***

Figure V. 101. *Obtained simulation results: (a) writing of the letter "N" trajectories; (b) calculated evolution of cable lengths versus time to achieve the path in Fig.* ***V.****103(a).*

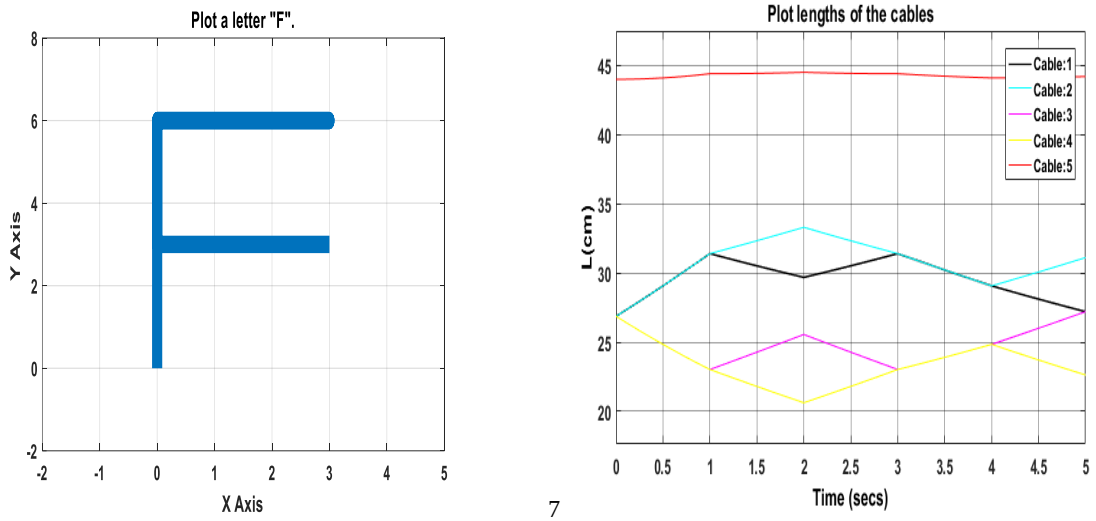

(a) ***(b)***

Figure V. 102. *Obtained simulation results: (a) Tracking of the letter "F" path; (b) calculated evolution of cable lengths versus time to achieve the path in Fig. V.104(a).*

The achieved outcomes validate the accuracy of both the geometric and inverse kinematic models. These results instill confidence in utilizing these models to develop a robust control algorithm for enhancing and managing the robot's performance. Additionally, these models serve as a foundation for the experimental constructs, which will be elaborated upon in the forthcoming section dedicated to the final results.

V.3 Trajectories test using LabView/Software

V.3.1 Trajectories test using Open Loop control

In this section, a series of tests will be executed on the pyramid cable-Driven robot. These tests aim to validate the robot's performance in accurately reproducing various letters and shapes. The chosen assortment of letters and shapes serves the purpose of assessing the robot's drawing capabilities. The control mechanism employed throughout this segment is an open loop system. To comprehensively evaluate the robot's performance under this control scheme, efforts were directed towards minimizing the transitional deviation between successive points along the trajectory. This approach ensures precise path tracking, thereby yielding optimal results. This procedural methodology will be elaborated upon in the ensuing sections.

V.3.1.1 Test of point-to-point trajectories

In this section, a point-to-point transmission test was conducted by employing the open-loop console. This procedure entailed the input of specific values into a graphical control

interface developed using the LabView software. The purpose of this test was to assess the seamless transmission of data between distinct points, thus evaluating the robustness and effectiveness of the open-loop system. The careful execution of this test allowed for a comprehensive analysis of the system's performance in facilitating accurate and reliable point-to-point motion.

V.3.1.2 Trajectories test, complex drawing “shapes “

In this part, an extensive evaluation encompassing the drawing of intricate geometric shapes was executed. This evaluation was carried out through the utilization of the open-loop console. The methodology entailed a comprehensive analysis of the designated shapes and letters, breaking them down into determined coordinates. These coordinates were then systematically fed into a graphical control interface that was constructed using the LabView software.

The data presentation was structured in a sequential manner, ensuring an organized input of values. These values were organized in an Array format, thereby streamlining the process of automatically generating a complex path. This approach was a departure from the conventional practice of individually inputting each value. The innovative automation allowed for the efficient creation of intricate paths, further underscoring the systematic approach adopted in this evaluation.

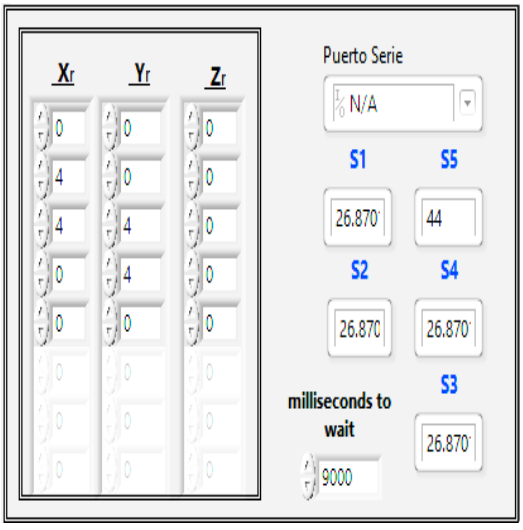

(a)

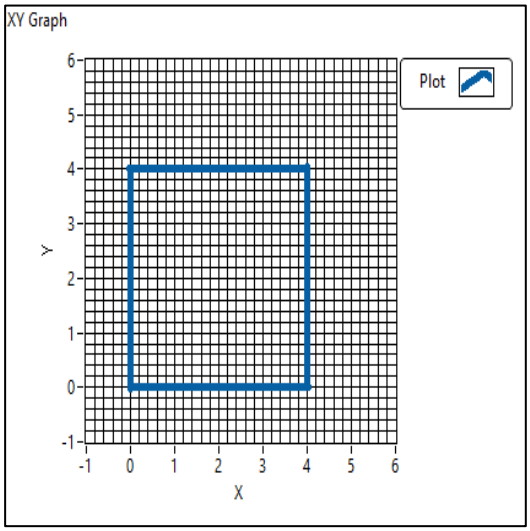

(b)

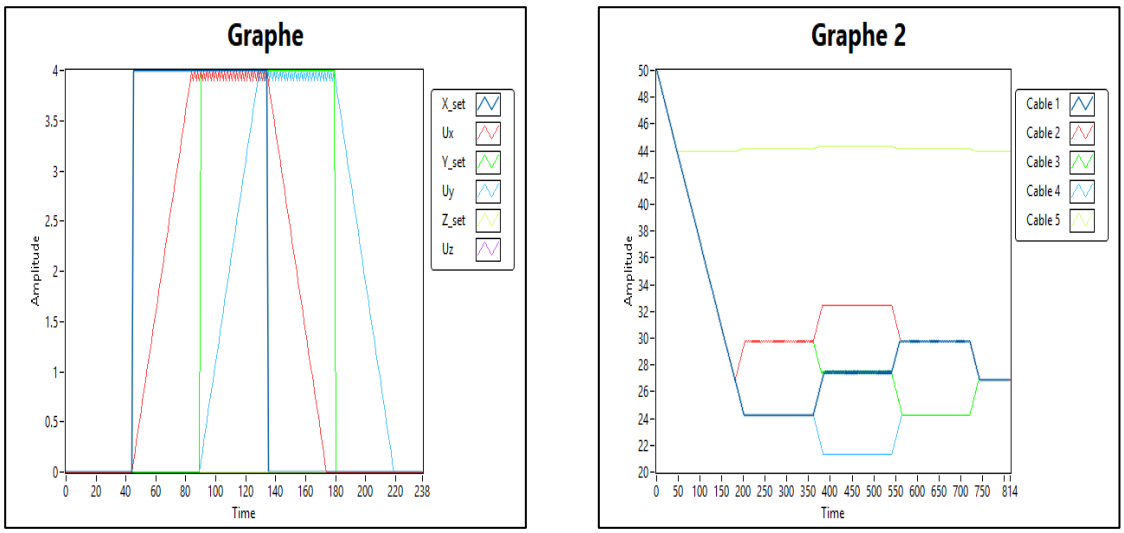

(c) ***(d)***

Figure V. 103. *Obtained results using the GUI: (a)values input;(b) Tracking of square trajectories; (c)the values after processing; (d) calculated evolution of cable lengths versus time to achieve the path in Fig.105(a).*

Figure *V.* 105 depicts a procedure for conducting a square drawing test within the context of activating an open-loop controller. In this depiction, (a) signifies the representation of coordinates entered via the control interface, organized as an array. Meanwhile, (b) visually demonstrates the intended drawing path or the trajectory of units (x, y and z). Additionally, (c) presents a graph illustrating the variations in reference input values over time, in comparison to the values processed by the control unit. Furthermore, (d) displays a graph showcasing the temporal changes in cable lengths. Alongside these graphical elements, a questionnaire is included to investigate the influence of the control unit on the observed alterations in cable lengths.

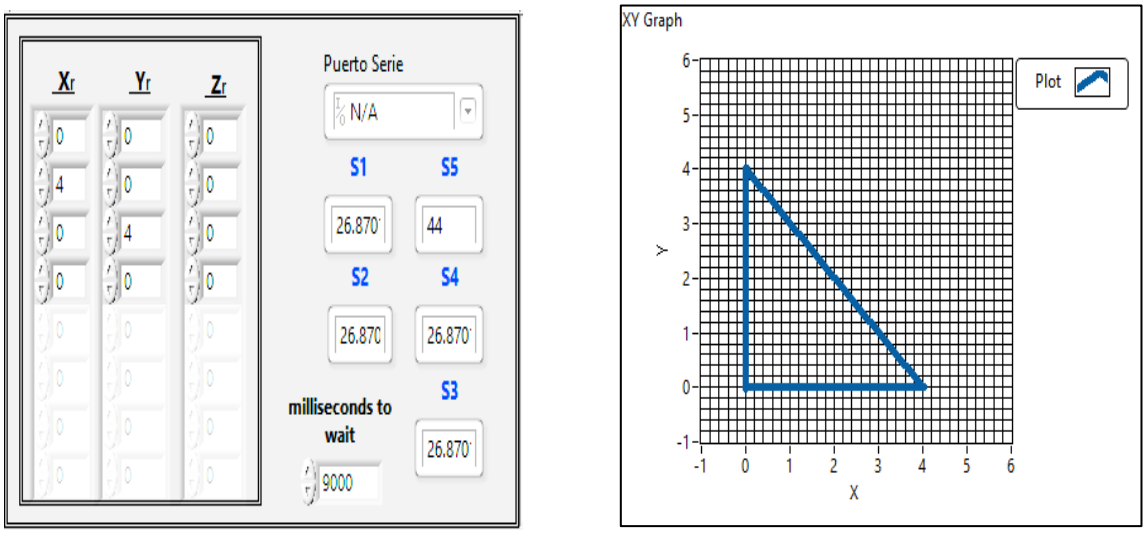

(a) ***(b)***

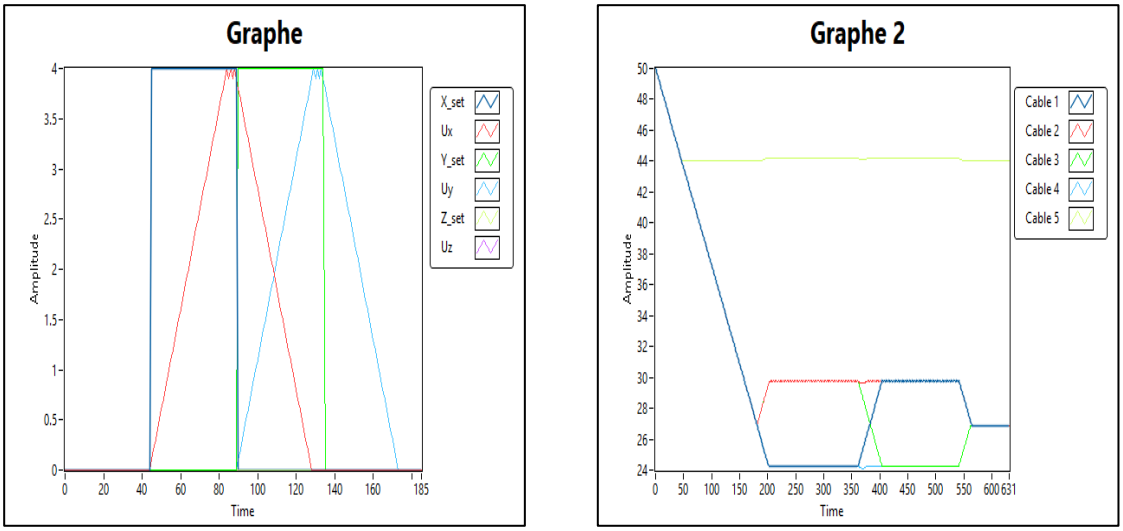

(c) ***(d)***

Figure V. 104. *Obtained results using the GUI: (a) values input; (b) Tracking of triangle trajectories; (c) values after processing; (d) calculated evolution of cable lengths versus time to achieve the path in Fig.106(a).*

Figure *V.* 106 illustrates the procedural steps for conducting a triangle drawing test while engaging the open-loop controller. Within this depiction, (a) represents the visualized coordinates inputted via the control interface and structured as an array. Simultaneously, (b) visually portrays the intended drawing trajectory or the path followed by units (x, y and z). Moreover, (c) depicts a graph that highlights variations in reference input values over time, in contrast to the values processed by the control unit. Additionally, (d) exhibits a graph that presents the temporal evolution of cable lengths. Alongside these visual components, an accompanying questionnaire is integrated to probe the impact of the control unit on the observed shifts in cable lengths.

The visual representations presented within this section offer a visual portrayal of diverse pathways comprising both uncomplicated and intricate geometric shapes. The selection of these specific shapes was purposeful, designed to serve as a means of rigorously testing the robot's performance capabilities. Furthermore, these figures enable a comprehensive assessment of the outcomes resulting from the utilization of the open-loop control unit, which played a pivotal role in achieving the showcased performance. The examination also extends to the variations in cable lengths over time, providing valuable insights into the system dynamics.

The exhibited shapes notably demonstrated commendable performance, thus validating the efficacy of the mathematical analysis incorporated into the control unit. Moreover, the chosen console itself proved to be proficient in execution, despite the occasional occurrence of minor deviations or abrupt movements along certain trajectories. Importantly, these imperfections had minimal impact on the overall results, affirming the robustness of the system and the viability of the chosen control approach.

V.3.1.3 Trajectories test, complex drawing "letters"

Furthermore, within this segment, a comprehensive examination was carried out involving a letter-writing assessment, facilitated by the operational deployment of the open-loop console. This procedure involved a deconstruction of both letters, dissecting them into precise sets of coordinates. These coordinates, once organized, were systematically introduced in a sequential manner through the graphical control interface developed using LabView software.

The presentation of these coordinates in a sequential order was crucial to ensure a methodical input of values. These values were thoughtfully structured in an Array format, a configuration chosen to enable the automated generation of intricate paths. This innovative strategy deviated from the traditional practice of inputting individual values in isolation. Through this automated approach, the creation of complex paths was streamlined, exemplifying the strategic and systematic nature of this evaluation.

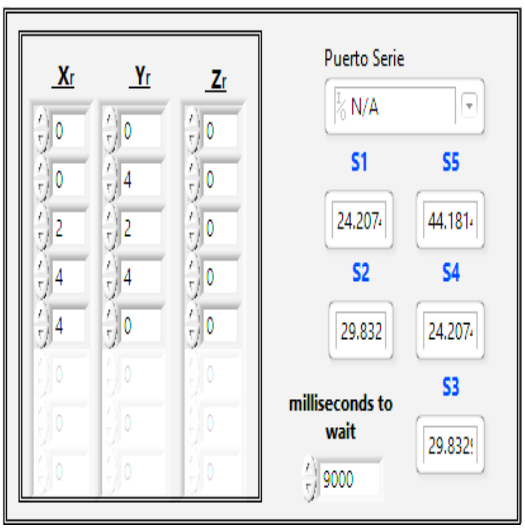

(a)

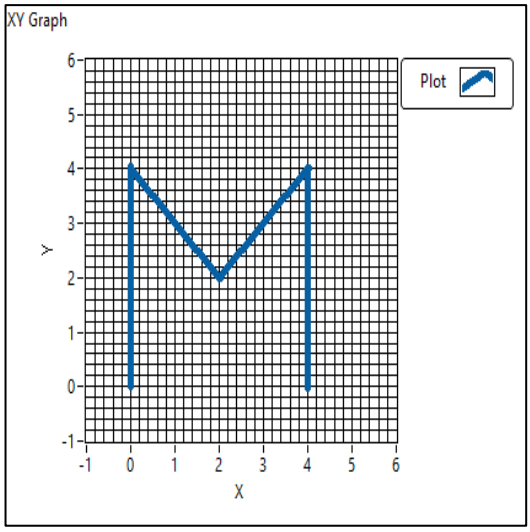

(b)

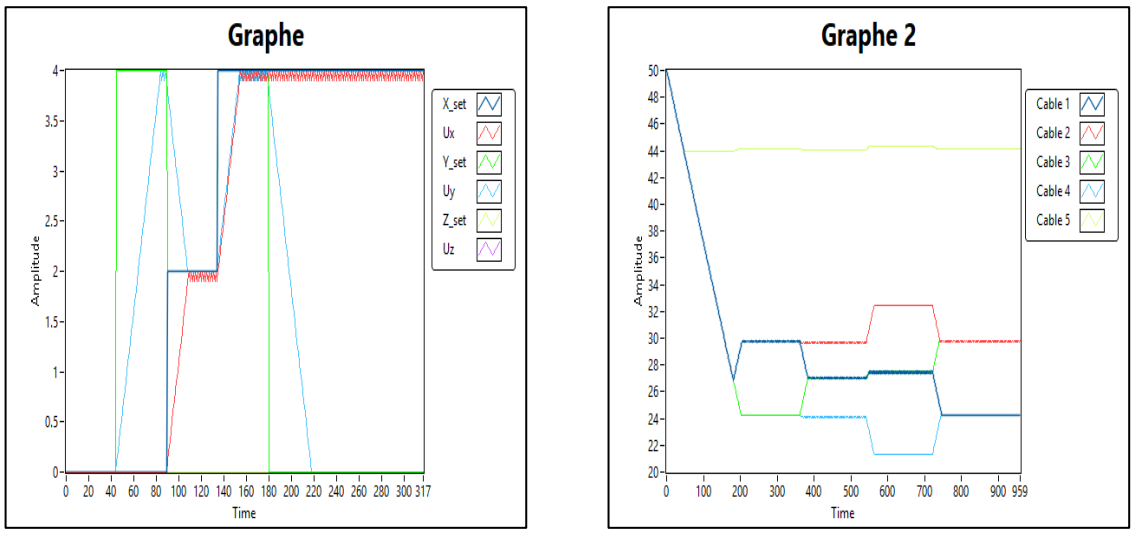

(c) ***(d)***

Figure V. 105. *Obtained results using the GUI: (a)values input; (b) Tracking of the letter "M" path;(c) values after processing; (d) calculated evolution of cable lengths versus time to achieve the path in Fig.107(a).*

Figure *V*. 107 illustrates the process of writing the letter 'M' while operating in the open-loop console mode. In this depiction, (a) signifies the depiction of coordinates necessary for rendering the letter 'M,' entered via the control interface in an array format. Meanwhile, (b) visually demonstrates the trajectory followed by the character during its execution, or alternatively, the path taken by units (x, y and z). Additionally, (c) presents a graph illustrating the variations in reference input values compared to the values processed by the control unit over time. Furthermore, (d) displays a graph showcasing the expansion and contraction of cable lengths over time. Accompanying these graphical elements is a questionnaire designed to explore the impact of the control unit on the changes in cable lengths.

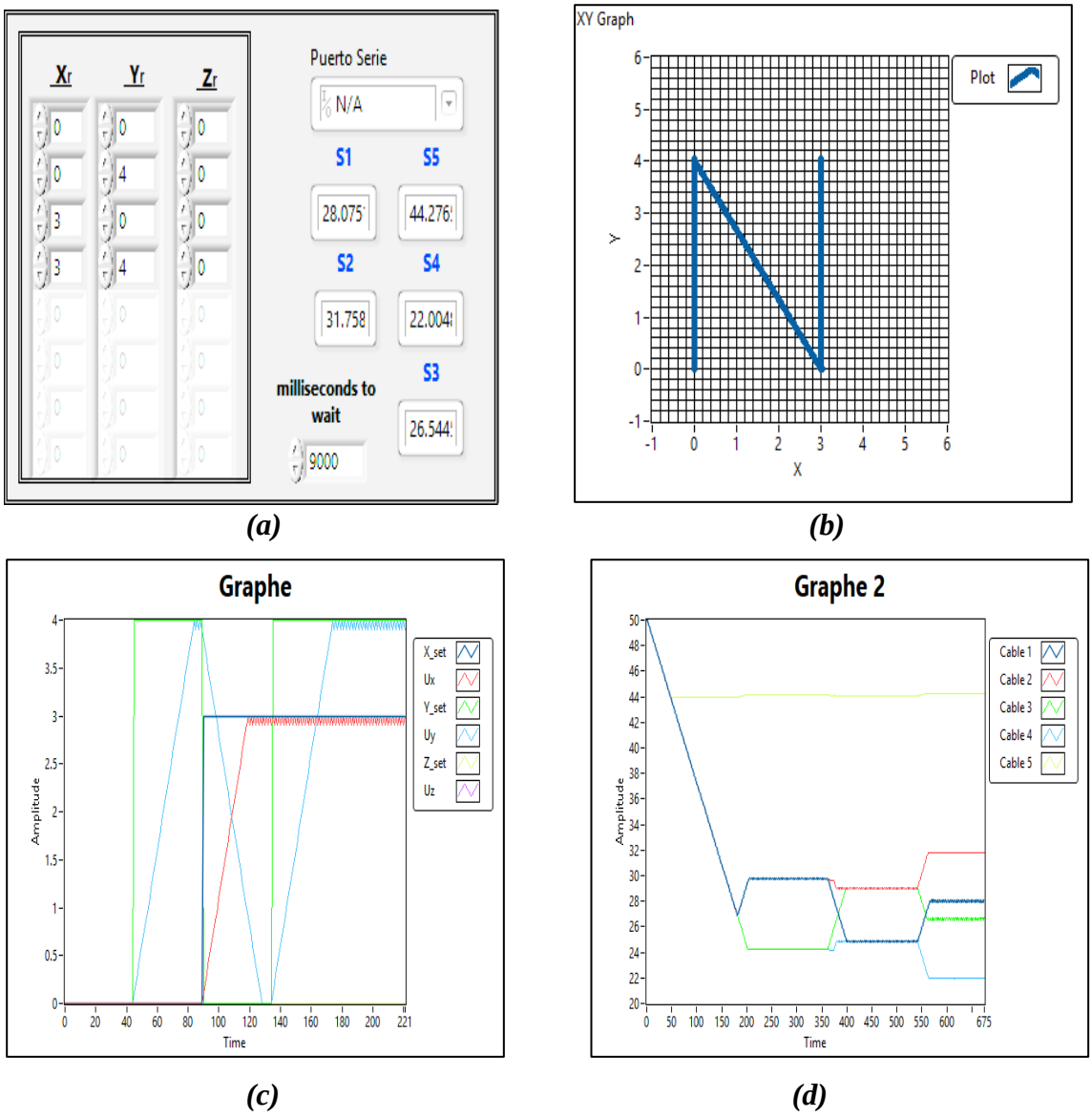

Figure V. 106. *Obtained results using the GUI:(a) values input; (b) Tracking of the letter "N" path;(c) values after processing; (d) calculated evolution of cable lengths versus time to achieve the path in Fig.108(a).*

Figure 108 depicts the sequential process of composing the letter 'N' within the operational framework of the open-loop console mode. In this visual representation, (a) conveys the essential coordinates needed for crafting the letter 'N,' inputted through the control interface and structured as an array. Concurrently, (b) visually traces the character's execution path, capturing the trajectory of units (x, y, and z). Moreover, (c) presents a graph illustrating the dynamic fluctuations in reference input values, juxtaposed against the values processed by the control unit over time. Furthermore, (d) exhibits a graph showcasing the temporal expansion and contraction of cable lengths. Complementing these

graphical elements is an integrated questionnaire, designed to explore the impact of the control unit on cable length variations.

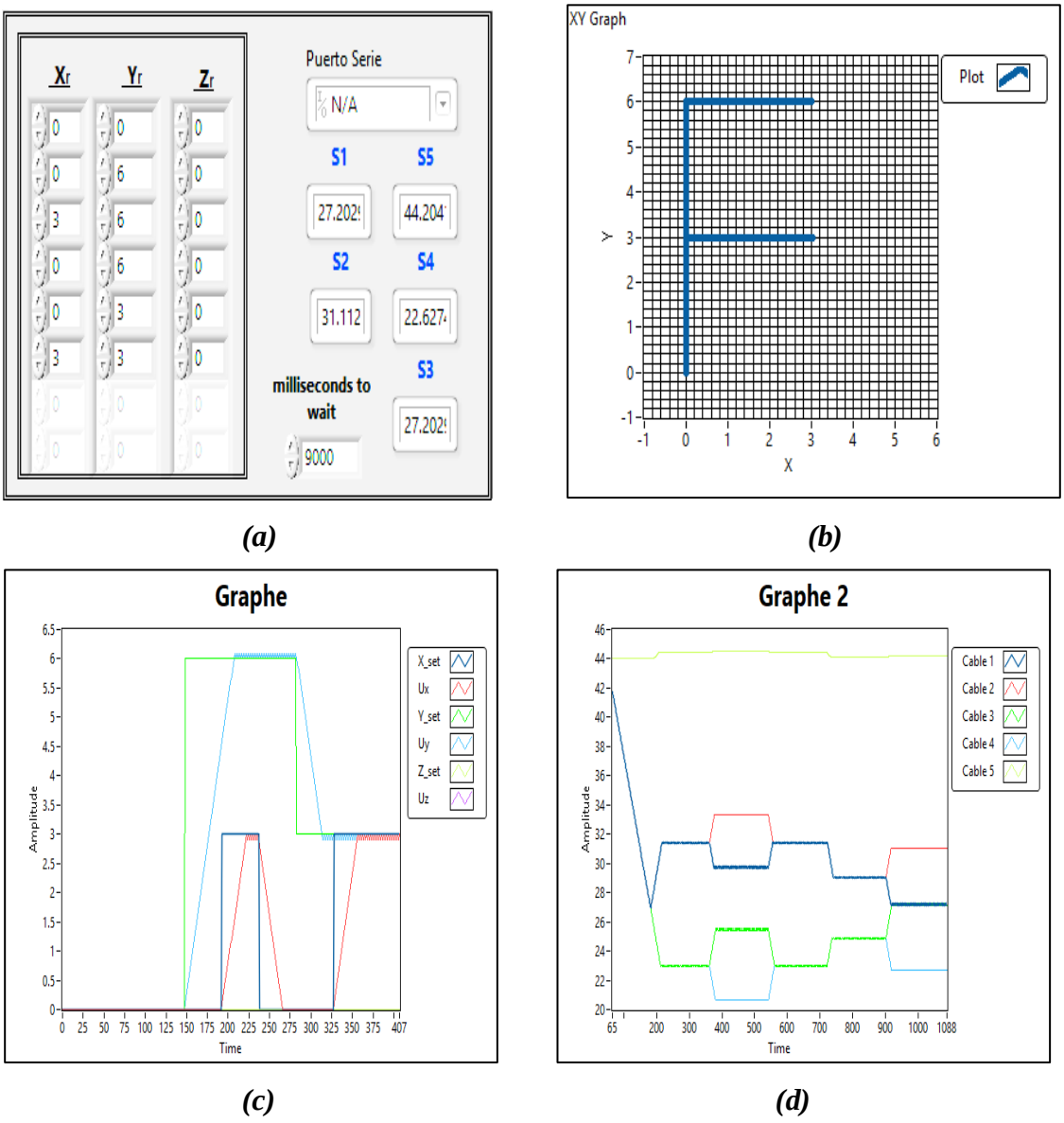

Figure V. 107. *Obtained results using the GUI: (a)values input;(b) Tracking of the letter "F" path; (c)values after processing; (d) calculated evolution of cable lengths versus time to achieve the path in Fig.109(a).*

Figure *V*. 109 portrays the sequential steps for composing the letter 'F' within the context of activating the open-loop console mode. In this visual representation, (a) delineates the requisite coordinates essential for crafting the letter 'F,' which are input via the control interface and organized in an array format. Simultaneously, (b) visually traces the trajectory of the character's execution, capturing the journey of units (x, y, and z). Furthermore, (c) features a graph illustrating the dynamic shifts in reference input values

compared to the values processed by the control unit, observed over time. Additionally, (d) exhibits a graph that vividly demonstrates the fluctuation in cable lengths, showcasing their expansion and contraction throughout time. Augmenting these graphical elements is an incorporated questionnaire, aimed at investigating the influence of the control unit on the variations in cable lengths.

V.3.1.4 Comment general;

The illustrations presented in this section vividly depict the trajectory of multiple paths, intricately forming both uncomplicated and intricate letters. The deliberate selection of these particular paths served the dual purpose of rigorously evaluating the robot's operational prowess and assessing the effectiveness of the employed open-loop control unit. Concurrently, the variations in cable lengths over time were tracked, contributing to a comprehensive understanding of the system's dynamic behavior.

The demonstrated shapes notably exhibited commendable performance, thereby substantiating the efficacy of the mathematical analysis seamlessly integrated into the control unit. Additionally, the chosen control console exhibited commendable proficiency, successfully orchestrating the execution of tasks. While occasional minor errors or slight disruptions were encountered along certain trajectories, these imperfections did not significantly impact the overall outcomes of the evaluation. This resilience further underscores the reliability of the selected control methodology and its ability to deliver substantial results.

V.3.2 Trajectories test using PID control

Within this section, a pivotal transition has been effectuated, shifting the control methodology from open loop control to closed loop control, specifically utilizing the Proportional-Integral-Derivative (PID) configuration. This strategic alteration was undertaken with the explicit intention of enhancing the robot's operational efficacy during the execution of designated tasks.

A series of carefully selected paths, encompassing both elementary and intricate trajectories, were employed in this phase. Subsequent to their execution, a thorough analysis ensued, drawing comparisons against preceding results. This rigorous examination enabled the identification of novel approaches and solutions, tailored to the unique performance

attributes of each control unit. The revelations derived from these results are poised to be expounded upon in this very section, shedding light on the multifaceted improvements and insights arising from the adoption of the closed loop PID control mechanism.

V.3.2.1 Point-to-point trajectories test

The inaugural examination entailed subjecting the PID controller to a rigorous assessment, achieved through the formulation of a point-to-point transition trajectory. It's important to note that these preliminary trials were exclusively conducted within the realm of the graphical control interface. This initial phase serves as a crucial validation step before the integration of this comprehensive interface with the PID control unit, directly interfacing it with the robot itself. This integration is contingent upon the satisfactory completion of the preliminary tasks. As part of this evaluation, a series of illustrative depictions has been generated, capturing the outcomes of these initial trials. The subsequent analysis of these visual representations is a focal point of this section, offering a detailed exploration of the performance and behavior of the PID controller within the context of the transition path experiment.

V.3.2.2 Trajectories test, complex drawing “shapes “

A comprehensive examination was undertaken using the PID console, entailing the generation of diverse pathways aimed at depicting both straightforward and intricate geometric shapes. These evaluation procedures were initially carried out exclusively within the realm of the graphical control interface. This preliminary phase serves as a deliberate measure to verify the console's ability to effectively fulfill its designated tasks.

Upon confirming the successful execution of these initial tasks, the integrated interface, which seamlessly aligns the graphical control interface with the PID controller, is then seamlessly interfaced with the robot. This pivotal linkage is established once the console's proficiency has been substantiated.

The designated geometric shapes were translated into precise sets of coordinates. This preparatory process was essential for their systematic entry into the control interface. These coordinates were carefully arranged to ensure a sequential input, adopting the structure of an array. Following the execution of these assessments, the obtained results underwent analysis. The subsequent sections will delve into an exhaustive exploration of

these findings, offering a comprehensive understanding of the PID controller's performance in orchestrating the creation of geometric shapes and its subsequent direct integration with the robot

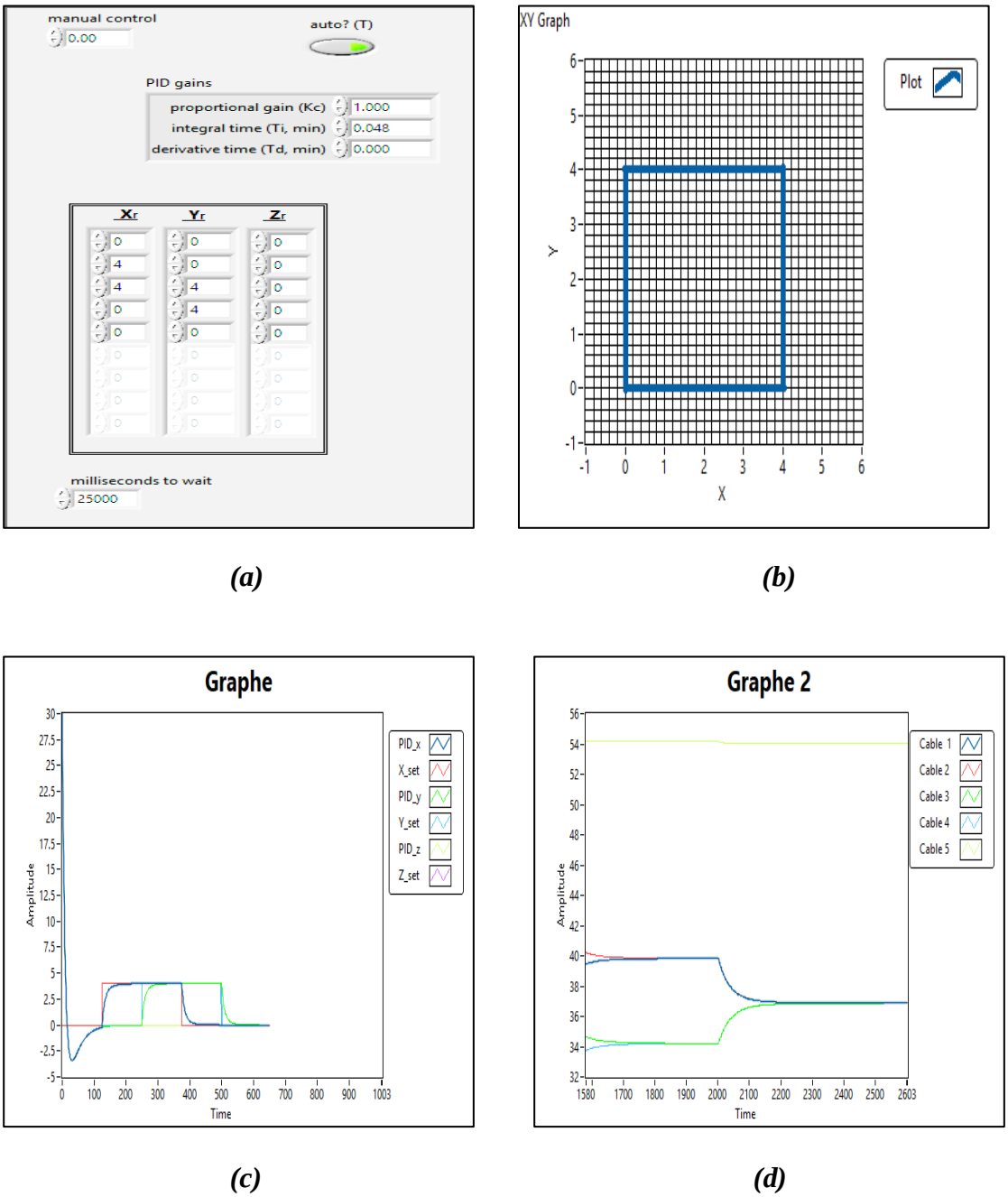

(a) ***(b)***

(c) ***(d)***

Figure V. 108. *Obtained results using the GUI: (a)values input;(b) Tracking of square trajectories;(c) values after processing (c) calculated evolution of cable lengths versus time to achieve the path in Fig.110(a).*

In our study, Figure *V*. 110 serves to illustrate the assessment of drawing a square shape while operating under an activated PID controller mode. In this context: (a) The figure highlights the coordinates necessary for drawing a square shape. These coordinates are to

be entered via the Array method in the graphical control interface, including the console constants Kp, Ki, and Kd. (b) Simultaneously, the figure defines the intended drawing path of the shape, simplifying it as the trajectory followed by units (s, k, and z). (c) Additionally, the figure displays a graph representing shifts in the reference input values and compares them with the values processed by the PID controller as time changes. (d) Moreover, the figure presents a graph illustrating changes in cable length as a function of time. These graphic elements are accompanied by a related questionnaire designed to explore the effects of the PID controller on cable length changes over time.

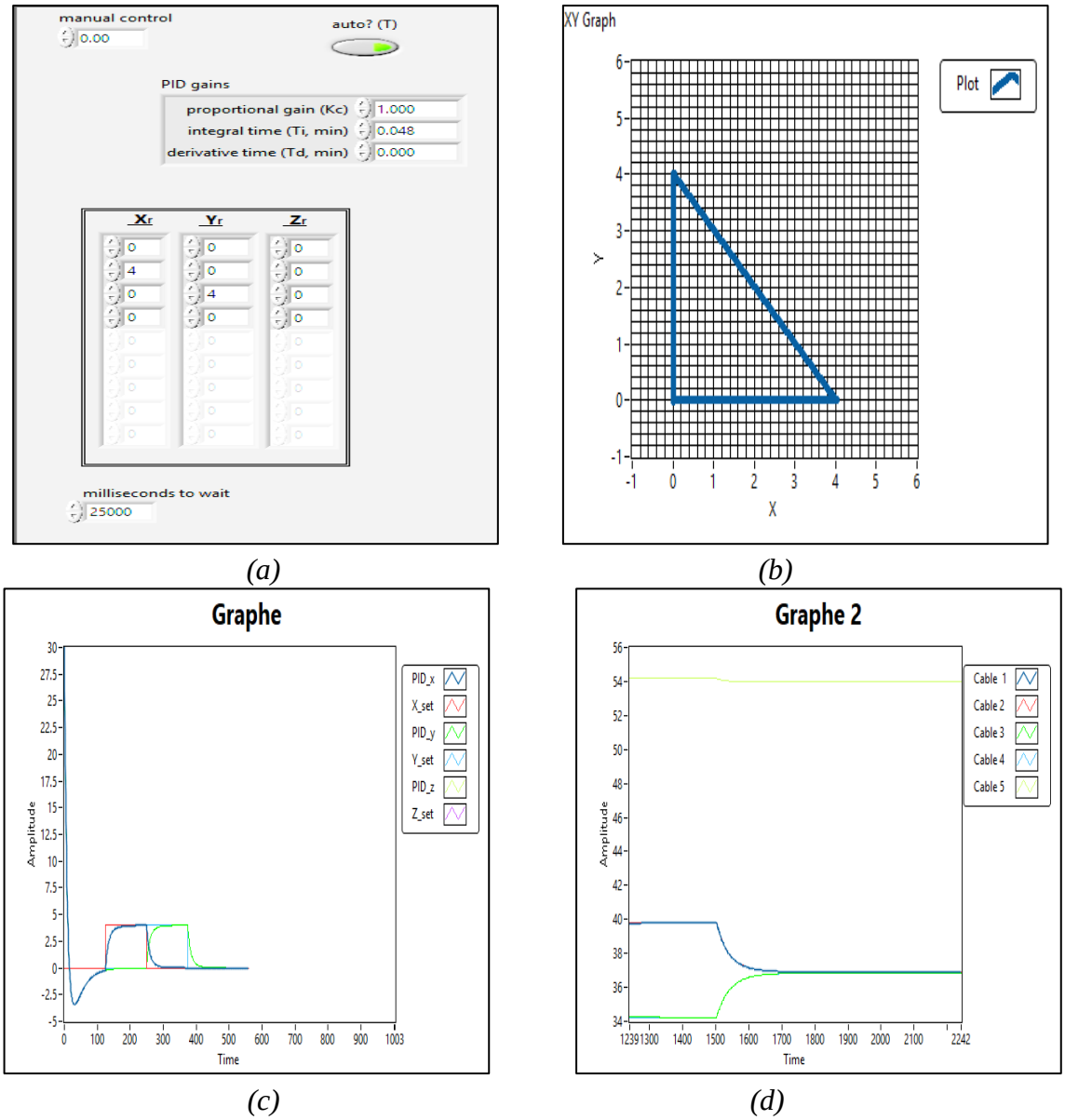

Figure V. 109. *Obtained results using the GUI: (a) values input;(b) Tracking of triangle trajectories; (c) values after processing; (d) calculated evolution of cable lengths versus time to achieve the path in Fig.111(a).*

Within our research, Figure *V.* 111 plays a crucial role in illustrating the assessment of drawing a triangle shape while operating within an activated PID controller mode. In this specific context: (a) The figure brings attention to the essential coordinates required for accurately drawing a triangle shape. These coordinates are inputted via the Array method in the Graphical User Interface (GUI), and they incorporate the console constants Kp, Ki, and Kd to ensure precise control. (b) Concurrently, the figure establishes a clear definition of the intended drawing trajectory for the triangle shape. To simplify, this trajectory represents the precise route followed by individual units (s, k, and z). (c) Moreover, the figure visually presents a graph that effectively captures the shifts occurring in the reference input values. This graph serves as a comparative tool, contrasting these shifts with the values processed by the PID controller as time progresses. (d) Furthermore, the figure offers an insightful graph that graphically showcases the changes in cable length over time. This graph sheds light on the dynamic relationship between cable length and time. These illustrative graphical elements are thoughtfully paired with an accompanying questionnaire. This questionnaire is thoughtfully designed to delve into the intricate effects that the PID controller has on the fluctuations in cable length over time.

V.3.2.3 Trajectories test, complex drawing “letters”

An evaluative procedure was carried out using the PID console, involving the deliberate formulation of diverse trajectories to render both uncomplicated and intricate characters in written form. These assessments were initially confined to the domain of the graphical control interface. This preliminary phase was executed to ensure the console's adeptness in effectively accomplishing its designated tasks.

Upon validating the successful completion of these initial tasks, the integrated interface, harmoniously unifying the graphical control interface with the PID controller, is seamlessly interfaced with the robot. This significant connection is established upon confirming the console's proficiency.

The designated characters were systematically translated into precise sets of coordinates. This preparatory process was instrumental in their orderly input into the control interface. These coordinates were organized, ensuring sequential entry and adopting the structured format of an array. Following the execution of these assessments, the garnered results underwent a thorough analysis. The ensuing sections will delve extensively into the

exploration of these findings, furnishing a comprehensive comprehension of the PID controller's role in orchestrating the creation of written characters and its subsequent direct integration with the robot.

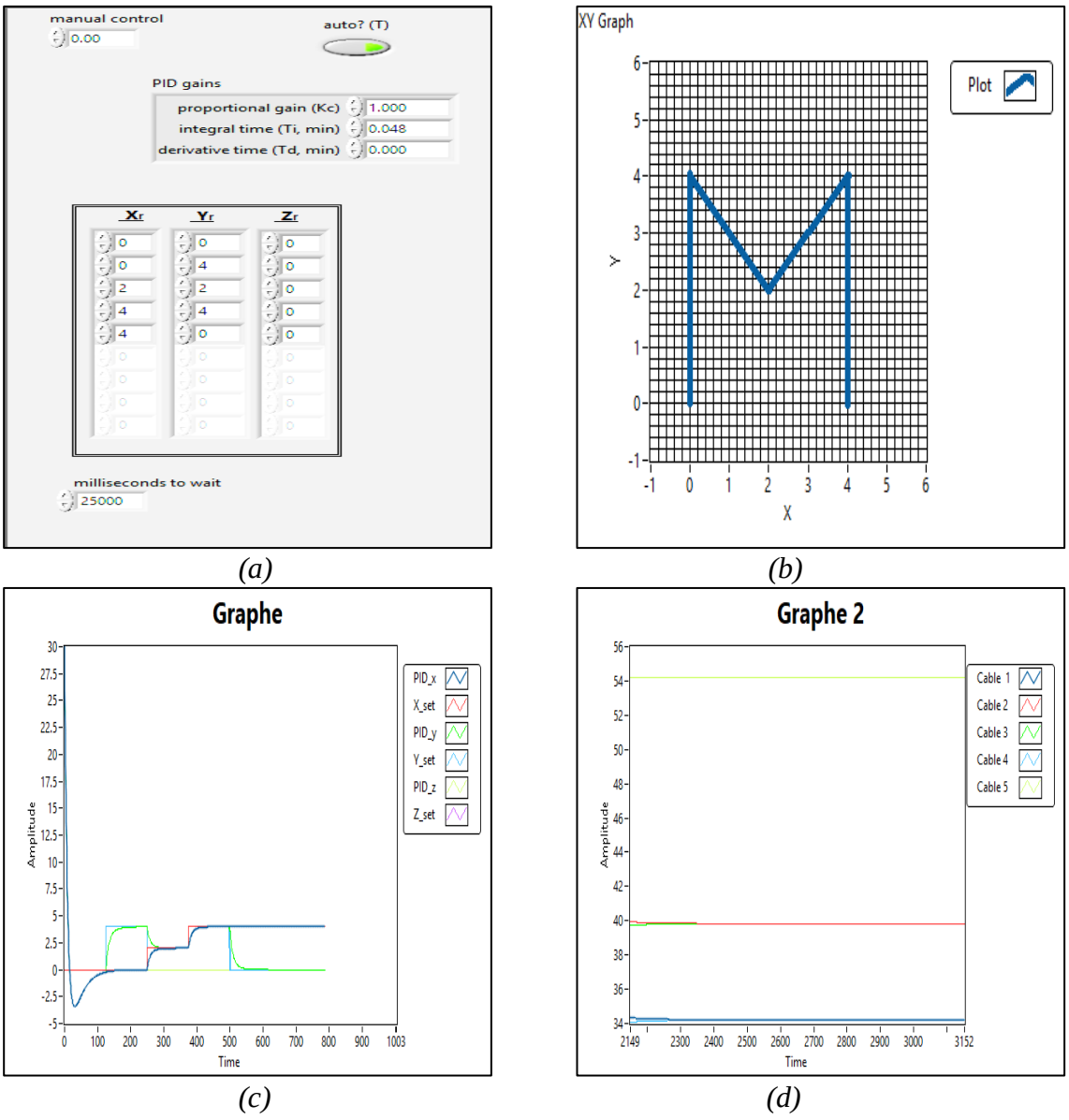

Figure V. 110. *Obtained results using the GUI:(a) values input; (b) Tracking of the letter "M" path; (c) values after processing; (d) calculated evolution of cable lengths versus time to achieve the path in Fig.112(a).*

After activating the PID console, we obtained multiple outcomes along with a variety of shapes representing diverse pathways for drawing letters and both simple and intricate designs. Figure *V.* 112 illustrates the letter 'M' writing test conducted within the framework of the activated PID console mode. In this context, (a) signifies the necessary coordinates for crafting the letter 'M,' entered via the Array method within the graphical control interface, alongside the console constants Kp, Ki, and Kd. Concurrently, (b)

indicates the character's drawing path, effectively tracing the trajectory of units (s, k, and z). Additionally, (c) portrays a graph showcasing the fluctuations in reference input values compared to the values processed by the PID controller over time. Furthermore, (d) presents a graph illustrating the temporal expansion and contraction of cable lengths. Accompanying these graphical elements is an included questionnaire, designed to assess the influence of the PID controller on the variations in cable lengths over time.

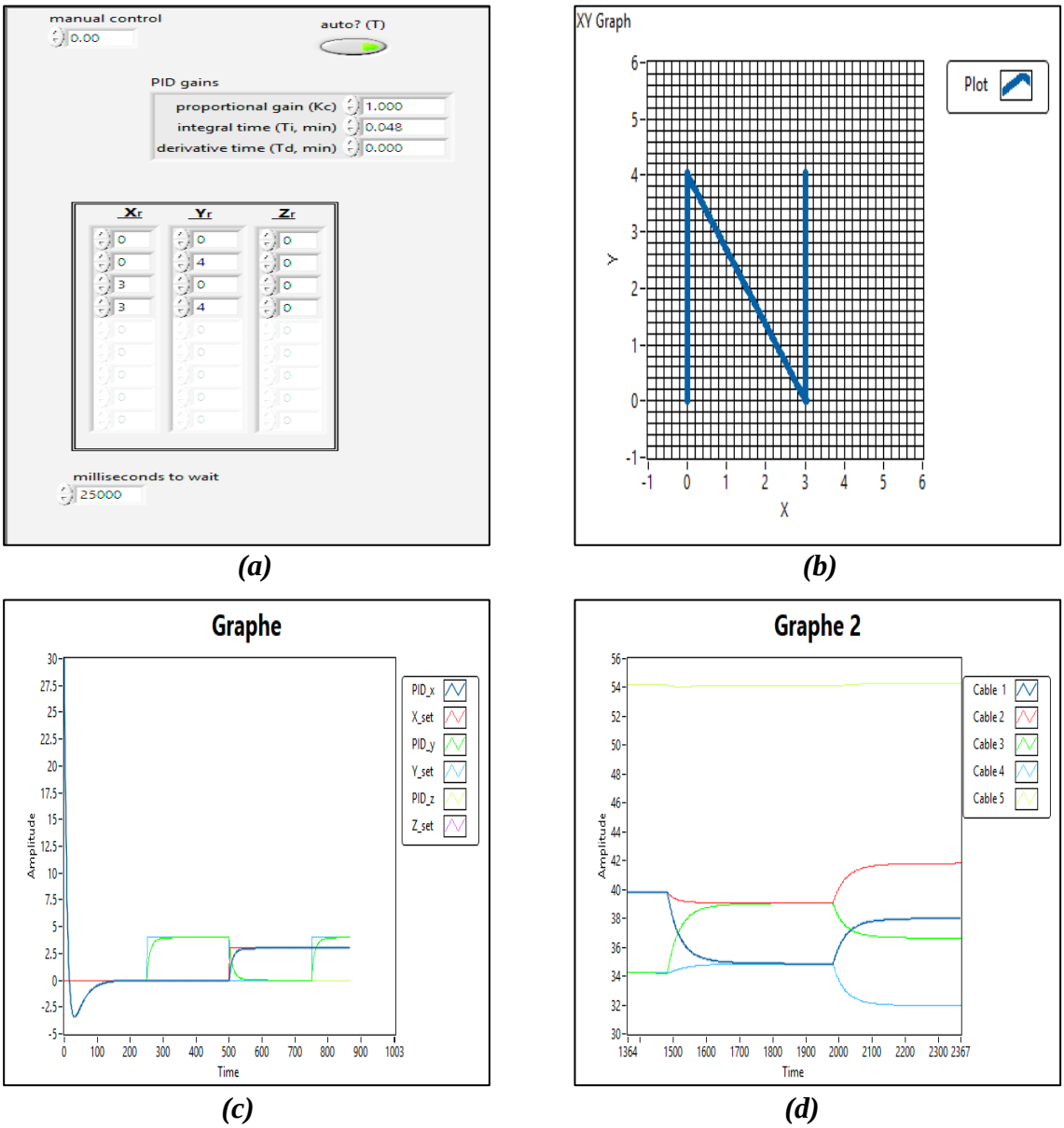

Figure V. 111. *Obtained results using the GUI:(a) value input; (b) Tracking of the letter "N" path; (c) values after processing; (d) calculated evolution of cable lengths versus time to achieve the path in Fig. V. 113(a).*

Within our study, Figure *V.* 113 serves to illustrate the evaluation of writing the letter 'N' while operating under the activated PID console mode. In this context: (a) highlights the coordinates requisite for letter 'N' formation, to be entered via the Array method in the

graphical control interface, alongside the inclusion of console constants Kp, Ki, and Kd. Simultaneously, (b) delineates the character's intended drawing trajectory or, in simpler terms, the path traced by units (s, k, and z). Additionally, (c) showcases a graph that visually represents the shifts in reference input values, contrasting them against the values processed by the PID controller over time. Furthermore, (d) presents a graph illustrating the temporal dynamics of cable length expansion and contraction. Accompanying these graphical elements is an accompanying questionnaire, designed to probe into the effects of the PID controller on cable length variations over time.

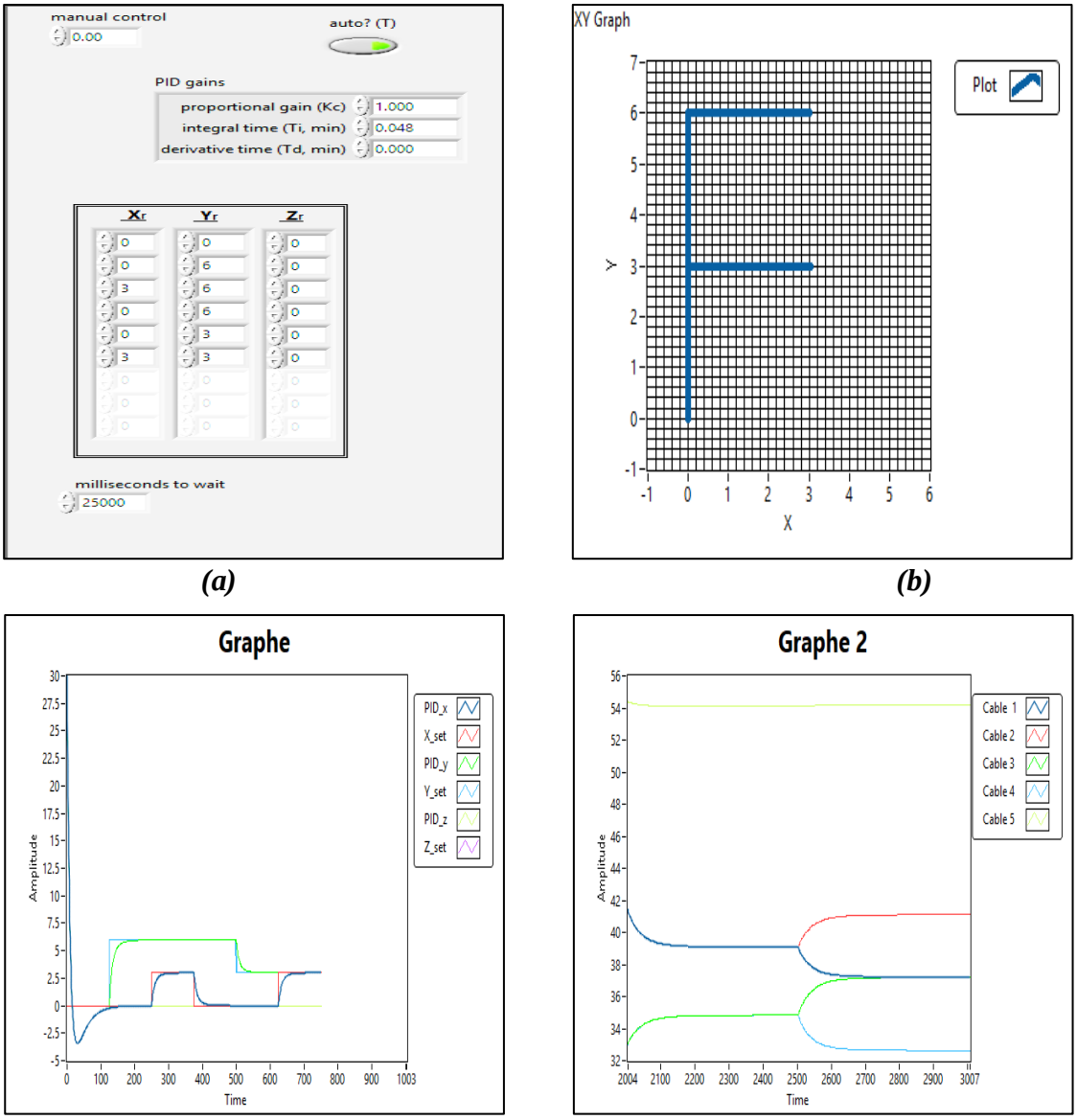

(a) ***(b)*** ***(c)*** ***(d)***

Figure V. 112. *Obtained results using the GUI:(a) values input; (b) Tracking of the letter "F" path; (c) values after processing; (d) calculated evolution of cable lengths versus time to achieve the path in Fig.114(a).*

In the scope of our investigation, Figure *V*. 114 serves as an illustrative tool to depict the assessment of writing the letter 'F' while under the influence of the activated PID console mode. In this scenario: (a) emphasizes the fundamental coordinates necessary for forming the letter 'F,' inputted via the Array method within the graphical control interface, alongside the integration of console constants Kp, Ki, and Kd. Concurrently, (b) outlines the intended trajectory followed during the character's drawing process, or in simpler words, the pathway traced by units (s, k, and z). Furthermore, (c) presents a graphical representation that vividly captures the shifts in reference input values, providing a visual contrast against the values processed by the PID controller over a span of time. Moreover, (d) portrays a graph that visually captures the temporal fluctuations in cable length, demonstrating the dynamics of expansion and contraction. Alongside these visual elements, a corresponding questionnaire is incorporated, strategically designed to investigate the ramifications of the PID controller on the fluctuations in cable length over time.

V.4 Experimental tests

V.4.1 Point to point tests

Empirical experiments have been executed to substantiate the validity of the simulation models put forth and to affirm the practicality of the scripted writing tasks simulated in the preceding section. Specifically, Figure 28 serves as a demonstration of the achievable nature of point-to-point displacement tests involving the end effector. This test effectively showcases the movement of the end effector from its initial location to a designated target point, solidifying the viability of the proposed methodology.

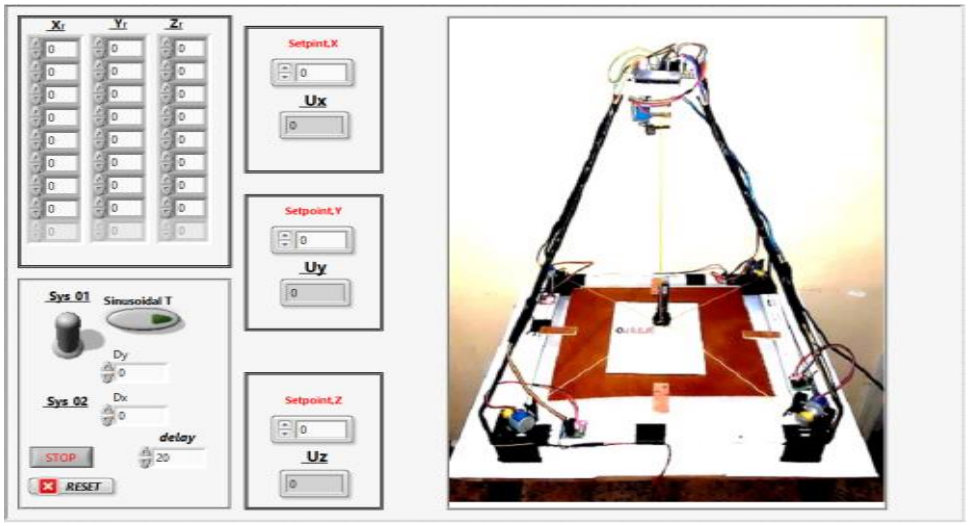

(a)

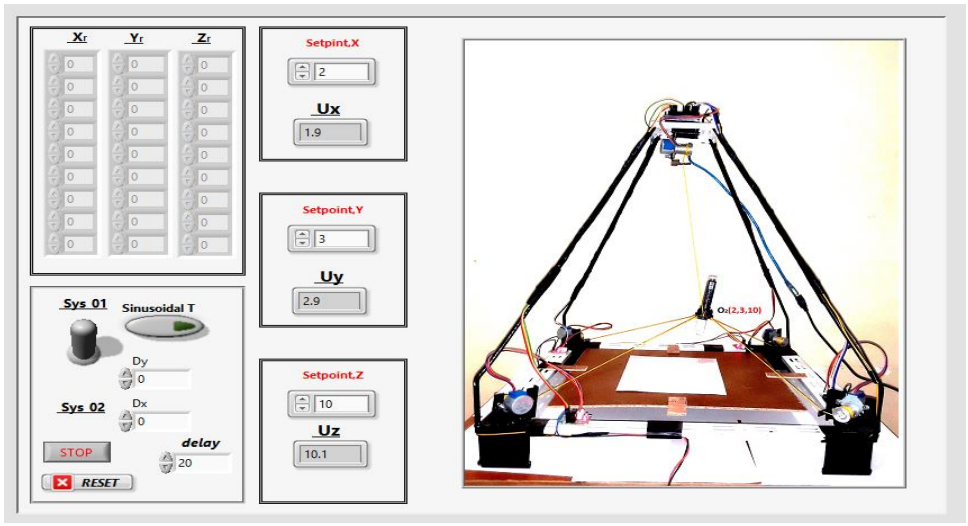

(b)

Figure V. 113. *A point-to-point displacement test of the end effector; a) initial configuration; b) final configuration.*

V.4.2 Tests of continuous trajectories

This section is dedicated to showcasing the outcomes of empirical trials conducted in alignment with the trajectories simulated in Figures *V.* 99 to *V.* 104. The results obtained from these practical experiments are displayed in Figures *V.* 116 to *V.* 121. Through a comparison of the outcomes of simulations and real-world experimental tests, it becomes evident that a commendable alignment exists with the intended writing paths. This observation underscores the engineering viability and efficacy of the prototype hardware and control methodology that have been introduced. The close accord between the

simulated and experimental outcomes provides compelling evidence of the feasibility and effectiveness of the proposed approach.

Illustrated in Figure 116 are the sequential stages involved in sketching a triangular trajectory. This is achieved through the utilization of the experimental model, functioning within the open-loop console operation mode. The figure provides a comprehensive guide on how to precisely input the points that define the trajectory using the graphical control interface.

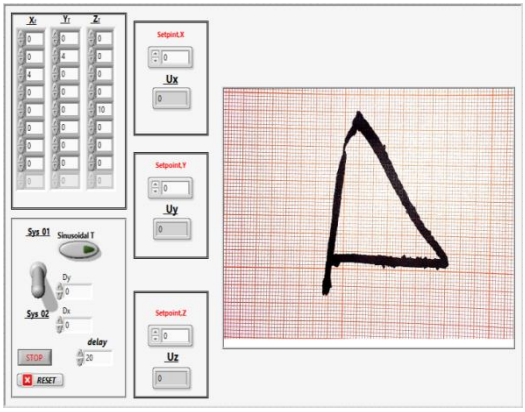

Figure V. 114. *Test drawing of a continuous triangle trajectory using the experimental prototype.*

Depicted in Figure *V*. 117 are the consecutive phases encompassing the creation of a square trajectory. This accomplishment is realized by employing the experimental model, which operates within the open-loop console operation mode. The figure serves as an inclusive manual, offering precise instructions on inputting the defining points of the trajectory using the graphical control interface.

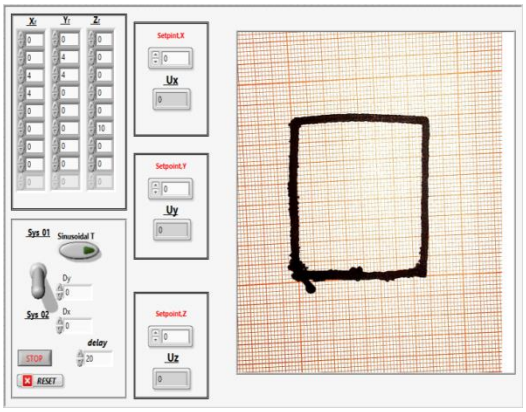

Figure V. 115. *Test drawing of a square trajectory using the experimental prototype.*

Illustrated in Figure 118 are the successive stages involved in crafting a circular trajectory. This achievement is made possible through the utilization of the experimental model, operating within the open-loop console operation mode. The figure functions as a comprehensive guide, providing accurate directives for inputting the pivotal points that delineate the trajectory, all facilitated by the graphical control interface.

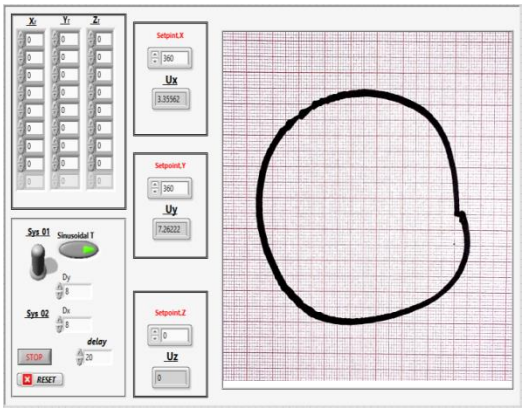

Figure V. 116. *Test drawing of a circle path using the experimental prototype.*

Figure *V.* 119 showcases the procedural steps for composing the letter "M" utilizing the experimental model within the open-loop console operation mode. Additionally, it offers guidance on entering waypoints through the graphical user interface (GUI).

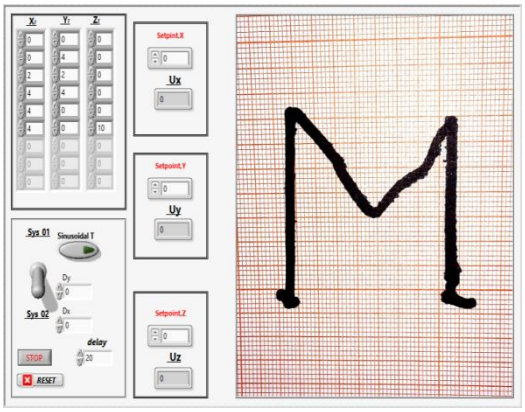

Figure V. 117. *Test drawing of the letter "M "using the experimental prototype.*

In Figure *V.* 120, a visual representation is provided of the sequential process involved in forming the letter "N" through the utilization of the experimental model in the open-loop console operation mode. The figure also includes instructions on how to input waypoints using the graphical user interface (GUI).

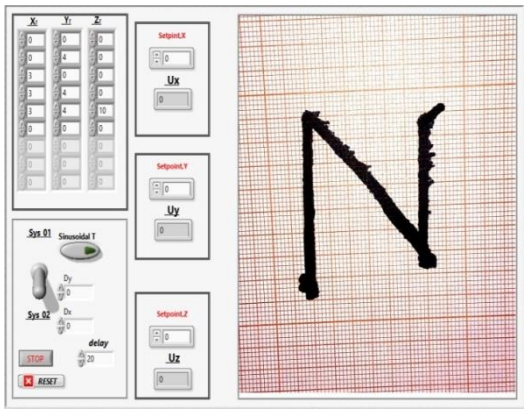

Figure V. 118. *Test drawing of the letter "N "using the experimental prototype.*

Displayed within Figure *V.* 121 are the outlined procedures for generating the letter "F," employing the experimental model within the open-loop console operation mode. The figure further encompasses guidelines on the method for entering waypoints via the graphical user interface (GUI).

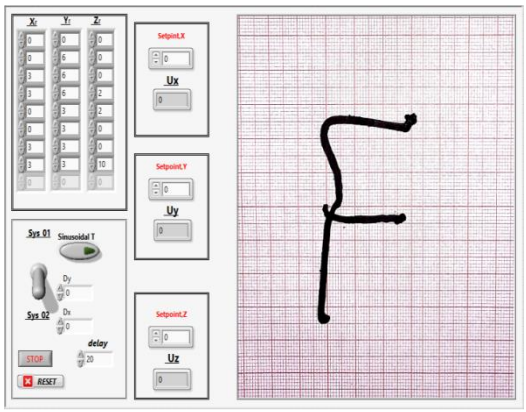

Figure V. 119. *Test drawing of the letter "F "using the experimental prototype.*

The acquired outcomes effectively validate the practicability of the designed solution tailored to the intended application. The executed experimental tests serve as concrete demonstrations of the robot's functionality and the viability of incorporating the prescribed writing exercises. A thorough performance evaluation is earmarked for the horizon, slated for execution upon the construction of an enhanced, optimized prototype. It's important to highlight that the current experimental findings serve as preliminary

evidence substantiating the proposed conceptual design. Subsequent endeavors will necessitate the fabrication of a refined hardware and software prototype.

Given the objectives of this study, certain factors such as pen weight and inertial effects were initially overlooked in the initial tests. By addressing these aspects, alongside considerations of friction on the writing surface and the pen's interaction with the human hand, enhanced tracking precision can be achieved. Future endeavors will encompass the implementation of more precise dynamic control strategies, enabling a quantitative assessment of the robot's precision.

Table V. 3. *List of test video use experimental prototype*

N°	Teste	Video links
1	Test experimental	https://www.youtube.com/watch?v=09cmttble3c&ab_channel=RoboticaAlgeria
2	Test experimental	https://www.youtube.com/watch?v=aLlyUz0hx9s&ab_channel=RoboticaAlgeria
3	Test draw circle	https://www.youtube.com/watch?v=92-YGS5sOMo&list=TLPQMDcwNzIwMjSp4F9E-AgT-g&index=6&ab_channel=RoboticaAlgeria
4	Test draw letter M	https://www.youtube.com/watch?v=BhFsQ4XX7gE&ab_channel=RoboticaAlgeria
5	Test draw letter N	https://www.youtube.com/watch?v=MNplp7wa98A&ab_channel=RoboticaAlgeria
6	Test draw letter E	https://www.youtube.com/watch?v=o7FFuxzdBDs&list=TLPQMDcwNzIwMjSp4F9E-AgT-g&index=1&ab_channel=RoboticaAlgeria
7	Test draw letter K	https://www.youtube.com/watch?v=EOSHgQQ1sHY&ab_channel=RoboticaAlgeria

V.5 Conclusion

All the results obtained through the activation of strong control strategies for the introduced models were presented in order to perform several maneuvers and applications of rehabilitation in drawing and writing. The results served as strong evidence of the success of this idea. This was demonstrated by showcasing the results of the open-loop control unit and the (PID) through the graphical control interface created using LabView software. The results of the experimental model, which was controlled using the open-loop control unit, were presented. Its output is in the form of a linear path to gradually move from one point to another. The effectiveness of this experimental model, as demonstrated by its results through precise path tracking, despite some errors in certain characters, can be improved in the future through the development of the control unit and the creation of new designs for the final responder, ensuring that forces are evenly distributed across all cables.

General Conclusion

General Conclusion

This Thesis provides an extensive and detailed exploration of the design process undertaken to conceptualize and create an entirely novel cable-driven parallel robot tailored to the unique needs of exercising and rehabilitating writing and drawing tasks. At its core, the proposed design solution introduces an innovative and distinct pyramid structure, which is augmented by the inclusion of a redundant set of five cables. This architectural feature is strategically devised to enable not only three-dimensional point-to-point movements but also continuous paths, offering a comprehensive solution to the multifaceted requirements of such tasks. The architectural ingenuity extends further, as the proposed pyramid structure is remarkably compact, ensuring an efficient spatial footprint that seamlessly fits within the confines of primary school or home desks. The added attributes of portability and user-friendliness further enhance its potential applicability across diverse contexts.

In a significant and foundational contribution, this Thesis establishes the principal geometric, kinematic, and dynamic models that underpin the functionality of the proposed design solution. To validate and substantiate the practicality of the developed models, comprehensive simulations are methodically executed, demonstrating the feasibility of diverse exercises, maneuvers, and tasks that this innovative robot can successfully undertake.

An integral aspect of the proposed solution lies in the establishment of a graphical user interface, thoughtfully designed through a harmonious amalgamation of LabView and Matlab technologies. This interface incorporates advanced control strategies, namely Open loop and PID controllers, which collectively empower the robot to navigate complex three-dimensional trajectories with unparalleled accuracy and precision. The prowess of thesis control strategies is not only showcased through simulations but is further bolstered through experimental tests, which validate the effectiveness and viability of the proposed solution in practical scenarios.

This Thesis looks forward to the future with a clear and ambitious vision, expressing the intention to refine and optimize the hardware and software components of the proposed

prototype. This impending phase aims to bridge the gap between theory and implementation, actualizing the potential encapsulated within the design. Furthermore, the Thesis underscores a commitment to exploration and innovation, expressing an explicit intent to uncover and capitalize on additional applications and domains that can benefit from the groundbreaking design.

In summation, this Thesis stands as a comprehensive and seminal contribution to the realm of cable-driven parallel robotics. It marries innovative design principles with rigorous theoretical underpinnings, advanced control strategies, and a clear pathway for future enhancements. Through this exploration, the paper not only pushes the boundaries of knowledge but also lays the foundation for transformative applications in diverse fields.

Referance

A Carron, E. A. (2019). Data-Driven Model Predictive Control for Trajectory Tracking with a Robotic Arm. *IEEE ROBOTICS AND AUTOMATION LETTERS*. https://doi.org/10.1109/LRA.2019.2929987

A. Alikhani, M. V. (2012). Sliding Mode Control of a Cable-driven Robot via Double-Integrator Sliding Surface. *ICCRC, vol.43*, (pp. pp. 1-7). Singapore.

A. Green∗, J. Z. (2005). Adaptive Control of a Flexible Robot Using Fuzzy Logic . *JOURNAL OF GUIDANCE, CONTROL, AND DYNAMICS*. https://doi.org/10.2514/1.6376

A. Pott, V. S. (2015). On the forward kinematics of cable-driven parallel robots. *2015 IEEE/RSJ International Conference on Intelligent Robots and Systems (IROS)*, (pp. Pott, Andreas and Valentin Schmidt. "On the forward kinematics of cable-driven parallel robots." 3182-3187.). https://doi.org/10.1109/IROS.2015.7353818

A. Zaatri, B. B. (2014.). Sliding mode versus PD control for cable-based robots. *World Journal of Engineering* , pp. pp.287-296,. https://doi.org/10.1260/1708-5284.11.3.287

Afshari, A. &. (2007). New jacobian matrix and equations of motion for a 6 d.o.f. cable-driven robot. *International Journal of Advanced Robotic Systems, 4(1)*, (pp. , 63–68.). https://doi.org/10.5772/5709

Agrawal, S.-R. O. (2004). Nonlinear Sliding Mode Control and Feasible Workspace Analysis for a Cable Suspended Robot with Input Constraints and Disturbances. *Proceeding of the 2004 American Control Conference Boston,* . Massachusetts. https://doi.org/10.23919/ACC.2004.1384041

Albus, J. S. (1992). The NIST ROBOCRANE. *Journal of Research at the National Institute of Standards and Technology,*, pp. 373–385.

Arduino. (2021). *Arduino Mega 2560 Rev3*. Récupéré sur © 2021 Arduino S.r.l. - Partita IVA 09755110963.

Aref, M. M. (2009). Optimal design of dexterous cable driven parallel manipulators. *International Journal of Robotics and Automation*, pp. 29–47.

B. Billel, Z. A. (2014). Image-based Control for Cable-based Robots . *International Journal of Control, Automation, and Systems 12(1):*, pp. 118-125.

B. Sheng, W. M. ((2016).). Model based kinematic & dynamic simulation of 6-DOF upper-limb rehabilitation robot. *Proceedings of Asia-Pacific Conference on Intelligent Robot Systems (ACIRS),* , (pp. 21–25). Tokyo, Japan .

Baoyan, D. Q.-Y. (2008). Analysis and experiment of the feed cable suspended structure for super antenna. *IEEE/ASME International Conference on Advanced Intelligent Mechatronics,*. 329–334.

Bauer, C. (, 2011, Jan. 28). Device and method for detecting the inventory of a selling and/or storingdevice, and a storage-managing system equipped with said device. *Patent, WO 2012 101248,*.

Bjekić, M. (2005). , Numerical computation dynamic characteristics of permanent-magnet step motor,. *International PhD Seminar Numerical Field Computation and Optimization in Electrical Engineering, Ohrid, Macedonia,*. pp. 11–16.

Bjekić, M. (2006). Determining static torque characteristics of permanent magnet step motor, . *International PhD Seminar Computational Electromagnetics and Technical Applications,*, (pp. pp. 5–10.).

Bosscher, P. M. (2010., July 13,). Apparatus and method associated with cable robot system. *U.S. Patent No. 7, 753, 642 B2,*.

Bosscher, P. W.-L. (2007). Cable suspended robotic contour crafting system. . *Automation in Construction, ,* pp. 45–55.

Bostelman, R. V. (1992). A robotic crane system utilizing the Stewart platform configuration. *In Proceedings of 4th International Symposium on Robotics and Manufacturing (ASME).*

Bostelman, R. V. (1996). RCS-based robocrane integration. . *In International Conference on Intelligent Systems: A Semiotic Perspective.*

Brackbill, E. A. (2009). Dynamics and control of a 4-dof wearable cable-driven upper arm exoskeleton. . *In IEEE International Conference on Robotics and Automation (ICRA) .*, (pp. pp. 2300–2305).

Brown, G. W. (1987, Dec 1,). Suspension system for supporting and conveying equipment. *such as a camera. U.S. Patent 4*, pp. 710, 819, .

Bruckmann, T. (2010). Auslegung und Betrieb redundanter paralleler Seilroboter. *PhD thesis,Germany: University of Duisburg-Essen.*

Bruckmann, T. L. (2012). Development of a storage retrieval machine for high racks using a wire robot. . *In ASME International Design Engineering Technical Conferences & Computers and Information in Engineering Conference* , (p. p. 771).

Bruckmann, T. L. (2013). Design and realization of a high rack storage and retrieval machine based on wire robot technology. *In Proceedings of the XV International Symposium on Dynamic Problems of Mechanics*, (pp. pp. 771–780).

Bruckmann, T. M.-M. (2009). A novel tensed mechanism for simulation of maneuvers in wind tunnels. *In 33rd ASME Mechanics and Robotics Conference (MECH 2009)* , pp. pp. 17–24.

Byung Kook Yoo, W. C. (2000). Adaptive Control of Robot Manipulator Using Fuzzy Compensator. *IEEE TRANSACTIONS ON FUZZY SYSTEMS.*

Castelli, G. &. (2014). A cartesian cable-suspended robot for aiding mobility. *In Computational Kinematics* . (pp. pp. 369–376). Berlin: Springer.

Castelli, G. O. (2009). .Modelling and simulation of a cable-based parallelmanipulator as an assisting device. *In Computational Kinematics* (pp. pp. 17–24). Berlin : Springer.

Castelli, G. O. (2014). A cartesian cable-suspended robot for improving end-users' mobility in an urban environment. *Robotics and Computer-Integrated Manufacturing*, pp. 335–343.

Chen Y., L. J. (2022). Dynamic Modeling and Robust Adaptive Sliding Mode Controller for Marine Cable-Driven Parallel Derusting Robot. *Sci*, p. 6137.

Clavel, R. (1988). DELTA, a fast robot with parallel geometry. . *In 18th International Symposium on Industrial Robots*, (pp. pp. 91–100).

Cone, L. L. (1985). Skycam, an aerial robotic camera system. *Byte Magazine*, pp. 122–132.

Crawford, D. W. (2012. , April 3,). Amusement park ride with cable-suspended vehicles. . *U.S. Patent No. 8*, , pp. 147, 344 B2.

D. Song, L. Z. (2018). Configuration Optimization and a Tension Distribution Algorithm for Cable-Driven Parallel Robots. *IEEE Access*, pp. pp. 33928-33940.

Dagalakis, N. G.-L. (1989). Stiffness study of a parallel link robot crane for shipbuilding applications. *ASME Journal of Mechanical*, pp. 183–193.

Dongeun Seo a, M. R. (2009). Non-certainty equivalent adaptive control for robot manipulator systems. *Systems & Control Letters* , pp. 304–308. .

Duan, Q. V. (2014, –10 1). Effect on wrench-feasible workspace of driven parallelmanipulator based triple-level spatial positioner. *Advances in Mechanical Engineering*, .

E. Oyman, M. K. (2022). Design and control of a cable-driven rehabilitation robot for upper and lower limbs. *Robotica 40(1)*, , pp. pp.1–37 .

Electronics, F. (2023). *High Quality Unipolar Stepper Motor*. Récupéré sur Future Electronics Egypt.

Emmens, A. R. (2014). Modeling and control of a large-spanredundant surface constrained cable robot with a vision sensor on the platform. . *In Bruckmann,T., & Pott, A., (Eds.), Cable-Driven Parallel Robots. Mechanisms and Machine Science* (pp. pp. 249–260). Berlin: Springer.

Engineering., L. M. (2015). *The float rehabilitation training.* Récupéré sur www.thefloat.ch.

F. Farshidian, E. J. (t 2017, Oc 11). Real-Time Motion Planning of Legged Robots: A Model Predictive Control Approach. . *arXiv*.

F. Inel, L. K. (2014). Comparison performance between PID and PD controllers for three and four cablebased robots. *World Journal of Engineering* , pp. 543-556.

F. Inel, M. N. (2020). 3D cable-based parallel robot simulation using PD control. *IOP Conf. Series: Materials Science and Engineering*, (p. 788).

F. Kühne, J. M. (2005). Mobile Robot Trajectory Tracking Using Model Predictive Control. *II IEEE latin-american robotics symposium*, .

F. Kuhne, W. F. (July 2005). Point Stabilization of Mobile Robots with Nonlinear Model Predictive Control. *Proceedings of the IEEE International Conference on Mechatronics & Automation Niagara Falls* . Canada.

F. Lin. (2007). Robust Control Design an Optimal Control Approach. *Wayne State University, USA and Tongji University, China, Publisher*. England : Wiley.

F. Zhang, W. S. (2021). Calibration of geometric parameters and error compensation of non-geometric parameters for cable-driven parallel robots. *Mechatronics, Vol. 77*, p. paper 102595.

Fang, S. (2005). Design, modeling and motion control of tendon-based parallel manipulators. *PhD thesis, Germany: University of Duisburg-Essen.*

G. Boschetti, G. C. (2019). Cable Failure Operation Strategy for a Rehabilitation Cable-Driven Robot. *MDPI Robotics, Vol.8*, , pp. n.17, .

G. Carbone, B. G. (2018). Design issues for an inherently safe robotic rehabilitation device. *Mechanisms and Machine Science*, pp. pp. 1025 – 1032.

G. El-Ghazaly, M. G. (2014). Adaptive Terminal Sliding Mode Control of a Redundantly Actuated Cable-Driven Parallel Manipulator: CoGiRo. *CableCon: Cable-Driven Parallel Robots, Tobias Bruckmann; Andreas Pott, ,* (pp. pp.179-200). Germany.

G. Rosati, P. G. (2005). Design of a New 5 DOF Wire-Based Robot for Rehabilitation. *9th International Conference on Rehabilitation Robotics, ICORR 2005,* (pp. .pp. 430–433). Chicago,: USA,.

Hao-Bo Kang, J.-H. W. (2015). Adaptive Robust Control of 5 DOF Upper-limb Exoskeleton Robot . *International Journal of Control, Automation, and Systems* , pp. 1-9 .

Heyden, T. &. (2006). Dynamics and flatness-based control of a kinematically undetermined cable suspension manipulator. *Multibody System Dynamics,*, pp. 155–177.

Heyden, T. (2006). Bahnregelung eines seilgeführten Handhabungssystems mit kinematisch unbestimmter Lastführung. *Fortschritt-Berichte VDI, Reihe 8, Nr. 1100. Düsseldorf: VDI Verlag.*

Higuchi, T. M.-y. (1988). Application of multi-dimensional wire cranes in construction. *In 5th International Symposium on Robotics in Construction*, (pp. pp. 661–668).

Hiller, M. F. (2005). Design, analysis and realization of tendon-based parallel manipulators. *Mechanism and Machine Theory,*, pp. 429–445.

Horning, N. (2018). Ancient Egypt: The Land of Pyramids and Pharaohs. *an imprint of greenhaven publishing* . New York, NY 10010.: LLC.

I. Chawla P.M. Pathak, L. N. (2021). Effect of selection criterion on the kineto-static solution of a redundant cable-driven parallel robot considering cable mass and elasticity. *Mechanism and Machine Theory*, pp. Vol.156, 104175.

I. Chawla, P. P. (2021). Workspace analysis and design of large-scale cable driven printing robot considering cable mass and mobile platform orientation. *Mechanism and Machine Theory, Volume 165*, p. paper 104426.

I.B. Hamida, M. L. (2021). Multi-Objective optimal design of a cable driven parallel robot for rehabilitation tasks. *Mechanism and Machine Theory*, p. n.104141.

Ishii, M. &. (1994). A 3D Spatial interface device using tensed strings. *Presence:Teleoperators and Virtual Environments*, pp. 81–86.

Izard, J.-B. G. (2012). Integration of a parallel cable-driven robot on an existing building façade. *In Bruckmann, T., & Pott, A. (Eds.), Cable Driven Parallel Robots. Mechanisms and Machine Science* (pp. pp. 149–164). Berlin: Springer.

Izard, J.-B. G. (2012). A reconfigurable robot for cable-driven parallel robotic research and industrial scenario proofing. *in Bruckmann, T., & Pott, A. (Eds.), Cable-Driven Parallel Robots. Mechanisms and Machine Science* (pp. pp. 135–148). Berlin: Springer.

J Albus, R. B. (1992). The NIST RoBoCrane‖,. *Journal Res. Natl. Inst. Stand. Technol*, pp. pp. 373–384,.

J.P. Merlet. (2019). Some properties of the Irvine cable model and their use for the kinematic analysis of cable-driven parallel robots. *Mechanism and Machine Theory, Vol. 135*, pp. pp.271-280.

Jadhao, K. (2016). *Cable Driven Haptic Gripper*. Récupéré sur delft haptics lab.

Jeong, J. W. (1998). Development of a parallel wire mechanismfor measuring position and orientation of a robot end-effector. *Mechatronics*, , (pp. 845–861.).

Jeong, J. W. (1999). Kinematics and workspace analysis of a parallel wire mechanism for measuring a robot pose. *Mechanism and Machine Theory*,, pp. 825–841.

Jin Yang, H. S. (2016). Adaptive Control with a Fuzzy Tuner for Cable-based Rehabilitation Robot. *International Journal of Control, Automation and Systems* , pp. 865-875 .

Jr, F. K. (2004.). Model Predictive Control of a Mobile Robot Using Linearization. *Proceedings of mechatronics and robotics* .

K. T. Oen, L. C. (2007). Optimal Dynamic Trajectory Planning for Linearly Actuated Platform Type Parallel Manipulators Having Task Space Redundant Degree of Freedom. *J. Mechanism. Machine. Theo.*

K.D. Young. (1999). A control engineer's guide to sliding mode control. *IEEE Transactions on Control Systems Technology* , pp. 328–342.

Kawamura, S. &. (1993). New type of master robot for teleoperation using a radial wire drive system. *In IEEE International Conference on Intelligent Robots and Systems (IROS)*, (pp. pp. 55–60).

Kawamura, S. C. (1995). Development of an ultrahigh speed robot FALCON using wire drive system. *In IEEE International Conference on Robotics and Automation*, (pp. pp. 1764–1850).

Kawamura, S. C. (2003). Development of an ultrahigh speed robot FALCON using wire drive system. *In IEEE International Conference on Robotics and Automation* , (pp. pp. 1764–1850).

Kawamura, S. K. (2000). High-speed manipulation by using parallel wire driven robots. *Robotica*,, pp. 155–177.

Klatte, R. K. (1993). C-XSC - A C++ Class Library for Extended Scientific Computing. *New York.* New York: Springer.

Kraft, M. &. (2005). Simulation and optimisation of a tendon-based Stewart platform. *In Intelligent Production Machines and Systems* , pp. pp. 405–410.

Kraus, W. K. (2015). Pulley friction compensation for winch-integrated cable force measurement and verification on a cable-driven parallel robot. *In IEEE International Conference on Robotics and Automation (ICRA)* ., (pp. pp. 1627–1632).

L. Jiang, B. G. (2017). Design and Nonlinear Control of a 2-DOF Flexible Parallel Humanoid Arm Joint Robot . *Hindawi.*, pp. ID 2762169,14 pages .

Lafourcade, P. L. (2002). Design of a parallel wire-drivenmanipulator for wind tunnels. . *In Workshop on Fundamental Issues and Future Research Directions for Parallel Mechanisms and Manipulators.* . Canada.

Lafourcade, P. Z.-Q. (2003). Stiffness analysis of wire-driven parallel kinematic manipulators. *In Proceedings of 11th World Congress on Theory of Machines and Mechanisms (IFToMM).*

Lalo, W. B. (2013). Optimal control for a wire-based storage retrieval machine. . *Mechanisms and Machine Science* (pp. pp. 631–639). Berlin: Springer.

Landsberger. (1985). A new design for parallel link manipulators. *Cambridge MA: Sea Grant College Program, Massachusetts Institute of Technology*.

Landsberger, S. E. (1984). Design and construction of a cable-controlled, parallel link manipulator. *Master thesis, Cambridge MA: Massachusetts Institute of Technology*.

Landsberger, S. E. (1987., May 19,). Parallel link manipulators. *U.S. Patent No. 4*, pp. 666, 362, .

Levant, A. (2012). Sliding order and sliding accuracy in sliding mode control. *International Journal of Control*.

Liao S, Z. Q. (2020). Parameter Identification and Nonparametric Calibration of the Tri-Pyramid Robot. *IEEE/ASME Transactions on Mechatronics*, pp. 2309-2317.

Lindemann, R. &. (1989). Construction and demonstration of a 9-string 6 DOF force reflecting joystick for telerobotics. *In NASA Techdocs*, pp. pp. 55–63.

Liu W, C. S. (2013). Structure design and performance analysis of six-pyramid parallel robot. *Nanjing Li Gong Daxue Xuebao/Journal of Nanjing University of Science and Technology* , pp. 257-261.

M. A. Khosravi, H. D. (2016). Stability Analysis and Robust PID Control of Cable-Driven Robots Considering Elasticity in Cables . *AIJ - Electrical & Electronics Engineering,*.

M. Bjekić. (2006.). Numerical simulation, measuring and foreseeing dynamic characteristics of the energetic permanent magnet step motor. *51st Internationales Wissenschaftliches Kolloquium,*. Technische Universitat Ilmenau,.

M. Carpio, R. S. (2021). Proposal of a Decoupled Structure of Fuzzy-PID Controllers Applied to the Position Control in a Planar CDPR . *Electronics*, p. 745.

M. Gouttefarde, P. W. (2015). A comparative review of cable-driven parallel robots. *Mechanism and Machine Theory*, pp. pp.133–152.

M. H. Korayem, M. B. (2009.). Optimal Trajectory Planning with Dynamic Load Carrying Capacity of Cable-suspended Manipulator. *IEEE Int. Symposium Mechatronics and its Applications, ISMA*, pp. pp. 1-6.

M. H. Korayem1, H. T. (2012). Optimal Path Planning of Spatial Cable Robot Using Optimal Sliding Mode Control . *International Journal of Advanced Robotic Systems.*

M. Honegger, A. C. (1997.). Adaptive Control of the Hexaglide, a 6 dof Parallel Manipulator. *Proceedings of International Conference on Robotics and Automation, .*

M. I. Hosseini, M. J. (2019). Adaptive Fast Terminal Sliding Mode Control of A Suspended Cable-Driven Robot. *27th Iranian Conference on Electrical Engineering (ICEE)* (pp. pp. 985-990,). Iran: Yazd.

M. Khadem, F. I. (2022). “Design and validation of a novel pyramidal cable-driven robot,”. *Mech. Mach. Sci.*, (pp. 122, 201–208).

M. Korayem, M. Y. (2020). Optimal Control of a Wheeled Mobile Cable-Driven Parallel Robot ICaSbot with Viscoelastic Cables. *, Robotica, Vol.38, Issue 8,*, pp. pp.1513–1537.

M. Rutschmann, B. S. (2012). Nonlinear Model Predictive Control for Rough-Terrain Robot Hopping. *IEEE/RSJ International Conference on Intelligent Robots and Systems* .

M. Zarebidoki, J. S. (2022). A Review of Cable-Driven Parallel Robots: Typical Configurations, Analysis Techniques,and Control Methods. *IEEE Robotics & Automation Magazine, vol. 29, no. 3,*, pp. pp. 89-106, .

M. Zarei a, A. A. (2018). Oscillation damping of nonlinear control systems based on the phase trajectory length concept: An experimental case study on a cable-driven parallel robot . *Mechanism and Machine Theory 126* , pp. 377–396.

M., B. (2004). Numerical methods of solving magnetic circuit of permanent magnet step motor,. *International PhD Seminar Computation of Electromagnetic Field, Budva, Monte Negro,*, (pp. pp. 11–16.).

M.A. Khosravi, H. T. (2013). Experimental performance of robust PID controller on a planar cable robot. . *Mechanisms and Machine Science, vol. 12*, pp. pp. 337-352.

M.A. Laribi, G. C. (2019). On the Optimal Design of Cable Driven Parallel Robot with a Prescribed Workspace for Upper Limb Rehabilitation Tasks. , *J Bionic Eng*, p. 16.

Maeda, K. T. (1999). On design of a redundant wire-driven parallel robot WARP manipulator. *In Proceedings of IEEE International Conference on Robotics and Automation*, (pp. pp. 895–900).

Maier, T. &. (2001). Dynamics and control of a cable suspension manipulator. *In Proceedings of the 9th German-Japanese Seminar on Nonlinear Problems in Dynamical Systems.*

Maier, T. (2004). Bahnsteuerung eines seilgeführten Handhabungssystems. *Fortschritt Berichte VDI, Reihe 8, Nr. 1047. Düsseldorf: VDI Verlag.*

man, r. (2020). *IPAnema 3 Cable Robot with 250kg Capacity*. Récupéré sur robotic gizmos.

Mao, Y. &. (2010). Wearable cable-driven upper arm exoskeleton - motion with transmitted joint force and moment minimization. *In IEEE International Conference on Robotics and Automation (ICRA)* ., (pp. pp. 4334–4339).

Mao, Y. &. (2011). A cable driven upper arm exoskeleton for upper extremity rehabilitation. *In IEEE International Conference on Robotics and Automation (ICRA)* , (pp. pp.4163–4168).

Marceau Metillon, P. C. (2020). A Cable-Driven Parallel Robot with Full-Circle . *The ASME 2020 International Design Engineering Technical Conferences & Computers and Information in Engineering Conference.* United States.: HAL Science.

Marco A. Arteaga-Pérez, J. P.-J. (2019). Experimental Results on the Robust and Adaptive Control of Robot Manipulators Without Velocity Measurements. *IEEE TRANSACTIONS ON CONTROL SYSTEMS TECHNOLOGY*, (pp. 1063-6536).

Matić, U. (2020). Ethnic Identities in the Land of the Pharaohs. *Published online by Cambridge University Press*.

Matt. (2017 , October 17,). *mini cable robot IPAnema-haptic*. Récupéré sur MATT'S HOMEPAGE.

Mehdi Narimani, S. N. (2009). Robotics Vision-based System for an Underwater Pipeline and Cable Tracker. *OCEANS 2009-EUROPE*.

Merlet, J.-P. &. (2007). A new design for wire-driven parallel robot . *In 2nd International Congress, Design and Modelling of Mechanical systems.* . Monastir.

Merlet, J.-P. &. (2010). A portable, modular parallel wire crane for rescue operations. In Proceedings of the IEEE International Conference on Robotics and Automation . *In Proceedings of the IEEE International Conference on Robotics and Automation* , (pp. 2834–2839).

Merlet, J.-P. (2008). Kinematics of the wire-driven parallel robot MARIONET using linear actuators. *In Proceedings of the IEEE International Conference on Robotics and Automation.*

Mijangos, M. R. (2013). *CableBOT- Parallel Cable Robotics for Improving Maintenance and Logistics of Large-Scale Products*. Récupéré sur CableBOT.

Ming, A. &. (1994). Study on multiple degree-of-freedom positioning mechanism using wires (Part 1). *International Journal of the Japan Society for Precision Engineering*, pp. 131–138.

Miroslav Bjekić, A. M. (2015.). Prediction Of Pull-In And Pull-Out Torque Characteristics Of The Permanent Magnet Step Motor. *Techn. – Électrotechn. et Énerg., 60, 1,*, (pp. p. 29–38,). Bucarest,.

Mohamed Tazi, F. H. (2018). Modèle théorique pour estimer les incertitudes de positionnement de l'effecteur d'un robot parallèle à câble plan. *Conference: CNRIUT 2018At: AIX EN PROVENCE*.

Mohammad A. Khosravi, H. D. (2014). Robust PID control of fully-constrained cable driven parallel robots. *Mechatronics* , pp. 87–97.

Otis, M. J.-D. (2008). Hybrid control with multi-contact interactions for 6DOF haptic foot platform on a cable-driven locomotion interface. . *In Symposium on haptic interfaces for virtual environment and teleoperator systems (HAPTICS)* ., (pp. pp. 161–168).

Otis, M. J.-D. (2010). Human safety algorithms for a parallel cable-driven haptic interface. *Advances in Intelligent and Soft Computing*, pp. 187–200.

Otis, M. J.-D.-L. (2009). Determination and management of cable interferences between two 6-DOF foot platforms in a cable-driven locomotion interface. *Man and Cybernetics Systems,*, pp. 528–544.

Philipp TempelPhilipp Tempel, A. S. (2017). Application of the Rigid Finite Element Method to the Simulation of Cable-Driven Parallel Robots. *Conference: 7th IFToMM International Workshop on Computational Kinematics* . France.

Pott, A. (2008). Forward kinematics and workspace determination of a wire robot for industrial applications. *In Lenarˇ ciˇ c, J., & Wenger P. (Eds.), Advances in Robot Kinematics.* Berlin: Springer.

Pott, A. (2013). An improved force distribution algorithm for over-constrained cable-driven parallel robots. *In Computational Kinematics* (pp. pp. 139–146). Dordrecht: Springer.

Pott, A. (2018). *Cable-Driven Parallel Robots Theory and Application.* Germany: Springer Cham.

Pott, A. M. (2010). Large-scale assembly of solar power plants with parallel cable robots. *In 41st International Symposium on Robotics (ISR) and 6th German Conference on Robotics (ROBOTIK)* , (pp. pp. 999–1004).

Pott, A. M. (2012). IPAnema: A family of cable-driven parallel robots for industrial applications. *In Bruckmann, T., & Pott,A. (Eds.), Cable-Driven Parallel Robots. Mechanisms and Machine Science (vol. 12*, (pp. pp.119–134). Berlin: Springer.

R. Wang, Y. L. (2021). Analysis and multi-objective optimal design of a planar differentially driven cable parallel robot . *Robotica Vol. 39(12)*, pp. pp.1–17, 2021.

Rauter, G. Z.-W. (2010). A tendon based parallel robot applied to motor learning in sports. *In Proceedings of the 3rd IEEE RAS & EMBS* ., (pp. pp. 82–87).

Reza Babaghasabha, M. A. (2016). Adaptive robust control of fully constrained cable robots: singular perturbation approach. *Nonlinear Dyn (2016)* , pp. 607–620.

Reza Babaghasabha, M. A. (s.d.). Vision Based PID Control on A Planar Cable Robot. *The 22nd Iranian Conference on Electrical Engineering (ICEE2014), Shahid Beheshti University* (p. 2014). Shahid Beheshti University.

Rodnunsky, J. &. (1991). Aerial cableway and method for filming subjects in motion. . *U. S. Patent No. 5*, pp. 224, 426.

Rogelio Lozano, B. B. (1992). Adaptive Control of Robot Manipulators with Flexible Joints. *IEEE TRANSACTIONS ON AUTOMATIC CONTROL, , FEBRUARY* ., p. VOL. 37.

ROGER BOSTELMAN, J. A. (2015). RoboCrane Project: An Advanced Concept. *Intelligent Systems Division National Institute of Standards and Technology Gaithersburg, Maryland 20899.*

Rongrong Tang, Q. Y. (2022). Variable Impedance Control Based on Target Position and Tracking Error for Rehabilitation Robots During a Reaching Task. *Front. Neurorobot.,*.

Shoham, M. (2005). Twisting wire actuator. *ASME Journal of Mechanical Design*, pp. 441–445.

Shoham, M. (2006). Twisting wire actuator. *Patent, EP 1685452 A2, Oct. 27, 2003.*

Surdilovic, D. &. (2004). STRING-MAN: A new wire robot for gait rehabilitation. *In IEEE International Conference on Robotics and Automation.* pp. 2031–2036.

Surdilovic, D. Z. (2007). STRING-MAN: Wire-robot technology for safe, flexible and human-friendly gait rehabilitation. *In International Conference on Rehabilitation Robotics (ICORR).* pp. 446–453.

Tadokoro, S. V. (1999). A portable parallel manipulator for search and rescue at large-scale urban earthquakes and an identification algorithmfor the installation in unstructured environments. *In Proceedings of IEEE International Conference on Intelligent Robots and Systems IROS 1999.*

Tairen Sun, H. P. (2011). Neural network-based sliding mode adaptive control for robot manipulators. *Neurocomputing, Volume 74, Issues 14–15*, pp. Pages 2377-2384.

Tanaka, M. S. (1988). Kineto-statics of skycam-type wire transport. *In Proceedings USA-Japan Symposium on Flexible Automation*, (pp. pp. 689–694). Japan .

Technology, P. (2017). *Kalmar Unveils Automation-Ready Terminal Gantry Cran*. Récupéré sur Port Technology Team.

Thomas, F. O. (2002). Uncertainty model and singularities of 3-2-1 wire-based tracking systems. . *In Advances in Robot Kinematics (ARK).* Spain: Kluwer Academic Publishers.

Tom Erez, K. L. (2013.). An integrated system for real-time Model Predictive Control of humanoid robots. *2013 IEEE-RAS International Conference on Humanoid Robots.*

Tuan, L. M. (2013). Adaptive sliding mode control of overhead cranes with varying cable length. l . *J Mech Sci Techno*, pp. 885–893 .

twinkl. (2017). *Dysgraphia* . Récupéré sur https://www.twinkl.com/.

Uhlmann, E. K. (2008). Entwicklung von Werkzeugmaschinen mit Parallelkinematik unter Verwendung von Seilantrieben. . *Fertigungsmaschinen mit Parallelkine matik*, pp. pp. 37–62.

Vallery, H. L. (2013). Multidirectional transparent support for overground gait training. *In IEEE International Conference on Rehabilitation Robotics (ICORR)* ., (pp. pp. 1–7).

Verhoeven, R. (2004). Analysis of the workspace of tendon-based stewart platforms. *PhD thesis, Germany: University of Duisburg-Essen.* Germany.

Voss, K. H. (2012). Investigation of a cable-driven parallel mechanism for interaction with a variety of surfaces, applied to the cleaning of free-form buildings. *Advances in Robot Kinematics (ARK)* (pp. pp. 261–268). Dordrecht: Springer.

Voss, K. H. (2013). A cable-driven parallel mechanism for the interaction with hemispherical surfaces. *Mechanisms and Machine Science* (pp. pp. 409–417). Berlin: Springer.

W. Yuqi, C. J. (2022.). Study on the design and control method of a wire-driven waist rehabilitation. *training parallel robot‖, Robotica, Volume 40, Issue 10,* , pp. pp. 3499 – 3513.

W.M. Nunes, L. R. (2011). Cable-Based Parallel Manipulator for Rehabilitation of Shoulder and Elbow Movements . *2011 IEEE İnternational Conference on Rehabilitation Robotics,*, (pp. pp. 1–6).

Wang, H. (2016). Adaptive Control of Robot Manipulators With Uncertain Kinematics and Dynamics". *IEEE Transactions on Automatic Control* .

Wei Lv, L. T. (2017). Sliding Mode Control of Cable-Driven Redundancy Parallel Robot with 6 DOF Based on Cable-Length Sensor Feedback . *Mathematical Problems in Engineering*, , p. ID 1928673.

Woernle, C. (2012). Trajectory tracking for a three-cable suspension manipulator by nonlinearfeedforward and linear feedback control. *In Bruckmann, T., & Pott, A. (Eds.), Cable-Driven Parallel Robots. Mechanisms and Machine Science* (pp. pp. 371–386). Berlin:: Springer.

Y. Shtessel, C. E. (2015). Sliding Mode Control and Observation . *Control Engineering (eBook)*, pp. ISBN 978-0-8176-4893-0.

Y. Wang, K. W. (2022). Research on mechanical optimization methods of cable-driven lower limb. *rehabilitation robot,‖ Robotica, Vol.40(1)*, pp. pp.154-169.

Yongchun Fang, P. W. (2014). Dynamics Analysis and Nonlinear Control of an Offshore Boom Crane . *IEEE TRANSACTIONS ON INDUSTRIAL ELECTRONICS* , p. VOL. 61.

Zeng Q, E. K. (2014). Tri-pyramid Robot: Design and kinematic analysis of a 3-DOF translational parallel manipulator. *Robotics and Computer-Integrated Manufacturing* , pp. 648-657.

Zeng Q, E. K. (2016). Tri-pyramid Robot: Stiffness modeling of a 3-DOF translational parallel manipulator. *Robotica* , pp. 383-402.

Zi-Jiang Yang, Y. F. (2012). Decentralized Adaptive Robust Control of Robot Manipulators Using Disturbance Observers . *IEEE TRANSACTIONS ON CONTROL SYSTEMS TECHNOLOGY*, pp. VOL. 20, .

Zitzewitz, J. V. (2009). A versatile wire robot concept as a haptic interface for sport simulation. *In Proceedings of the 2009 IEEE International Conference on Robotics and Automation (ICRA).* pp. 313–318.

Zitzewitz, J. V. (2010). Forward kinemat ics of redundantly actuated, tendon-based robots. *In IEEE/RSJ International Conference on Intelligent Robots and Systems (IROS).*, (pp. pp. 2289–2294).

1. Description of software (LabView)

Graphical Programming Technique involves the use of VISUAL BLOCK Connections instead of traditional text-based coding, which greatly simplifies algorithm implementation for non-coders. LabView (Laboratory Virtual Instrument Engineering Workbench) stands as the pioneering and prevailing implementation of graphical programming to this day. It offers a robust and cohesive environment for creating various instrumental applications.

Figure 01 *symbol LabView.*

Efficient LabView applications are designed with minimal resource consumption, including code, data, block diagrams, front panels, and GUI updates. This approach minimizes human errors in data collection and process operations while reducing data transcription mistakes. As a result, more reliable data becomes available, leading to improved product quality control and facilitating new discoveries.

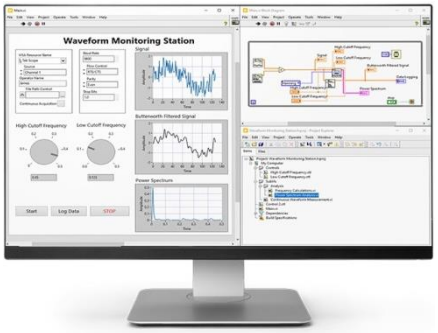

Figure 02 *interface LabView.*

LabView programs, also referred to as virtual instruments (VIs), mimic physical instruments in both appearance and operation. They are equipped with an extensive collection of VIs and functions, enabling tasks such as data acquisition, analysis, display, and storage. Additionally, LabView offers tools for troubleshooting code and features built-in capabilities for connecting user applications to the Web through the LabView Web Server.

LabView serves as an essential tool for managing large and professional applications. It incorporates integrated project management tools, graphical debugging tools, and standardized source code control integration, streamlining the development process. As an open development environment, LabView caters to various application needs, providing the necessary tools for most scenarios.

2. Stages of creation of the control interface

To create a professional control interface using LabView, follow these steps:

1. Launch the LabView program on your computer.
2. Once the LabView software is open, proceed to create a new file by selecting the "New" option from the menu or toolbar. This action will open a blank project or VI (Virtual Instrument) window, depending on your specific LabView version and configuration see fig 03 .

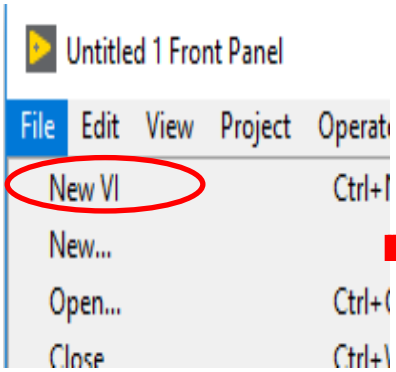

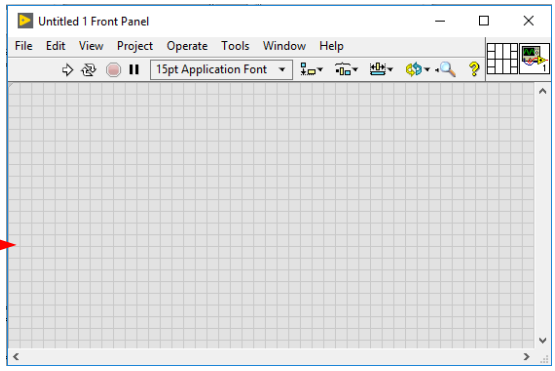

Figure 03 *create new file.*

Figure 04 *new interface to control.*

3. At this point, you can start designing your control interface by dragging and dropping various controls, indicators, and other elements onto the front panel of the VI. The front panel is the user interface of your LabView application (see fig 04), where users can interact with the controls and view the indicators.

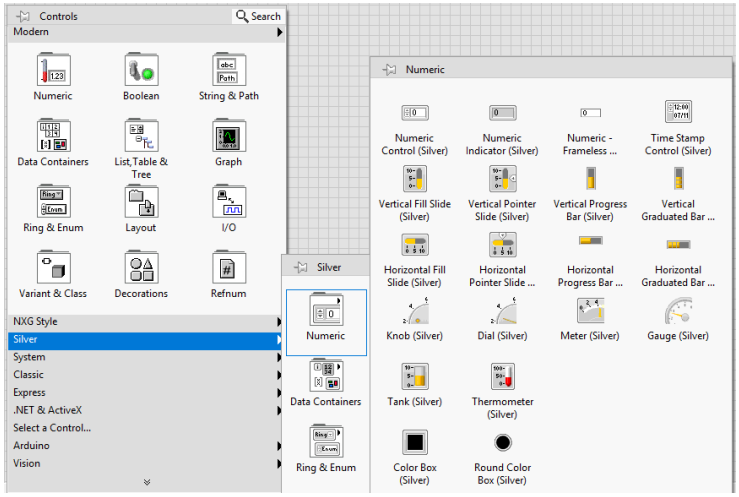

Figure 05 *elements onto the front panel of the VI.*

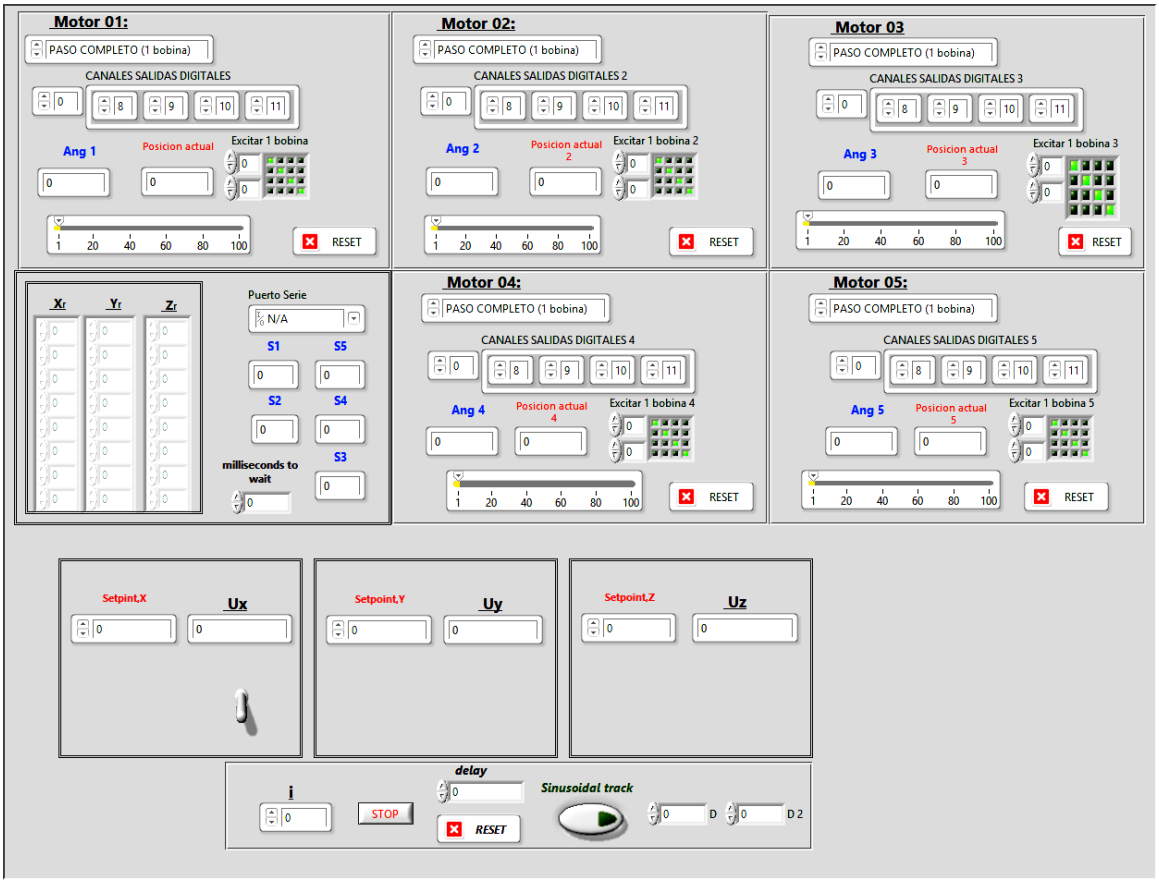

Figure 06 *final interface the control the system* .

4. Additionally, you can create the necessary back-end functionality by using graphical programming techniques, connecting the blocks or nodes together on the block diagram see fig 07 . The block diagram is where you implement the logic and functionality of your LabView program.

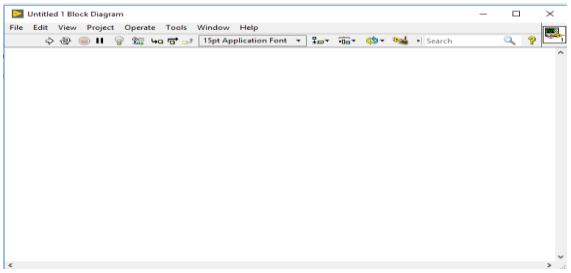

Figure 07 *The block diagram.*

5. Throughout the development process, it is essential to ensure that your interface aligns with professional standards, providing a user-friendly and intuitive experience for the end-users.

6. To verify the correctness and functionality of your control interface, you can execute the VI in the LabView environment or run it on the target hardware (if applicable).
7. Refer to Figures for a visual representation of the process, which may illustrate the LabView interface or specific steps involved in creating the control interface.

Not, creating a professional control interface with LabView requires attention to detail, thoughtful design, and testing to deliver a reliable and effective user experience.

To create a block diagram in LabView, follow these steps:

Click on the "Show Block Diagram" button at the bottom left of the LabView window, or select "Window" from the menu bar and click on "Show Block Diagram" to switch to the block diagram view see figure 08.

Add Blocks and Connect Them: In the block diagram view, you will see a white canvas where you can add and connect various blocks. Blocks in LabView are known as "nodes" and "functions." You can find them in the "Functions Palette" on the left-hand side of the window see figure 09.

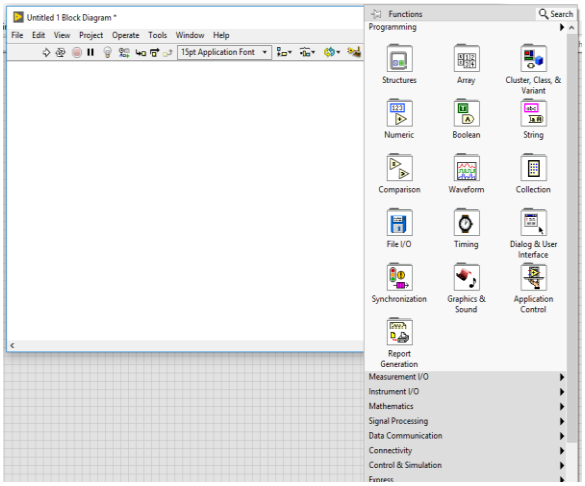

Figure 08 *Functions Palette.*

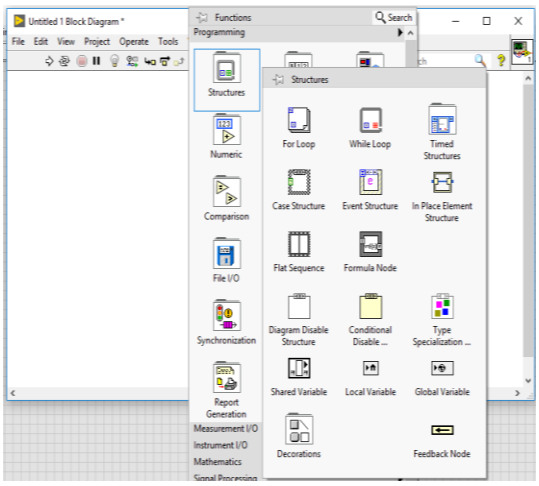

Figure 09 *various blocks.*

Use Wiring Tool: To connect blocks, use the Wiring tool, which is located on the toolbar or can be accessed by pressing the "W" key. Click and drag from an output terminal of one block to an input terminal of another block to create a wire connection.

Create Logic: Use various nodes and functions in the block diagram to create the desired logic for your application. LabView offers a wide range of functions for arithmetic, Boolean operations, data manipulation, and more see figure 10 and 11.

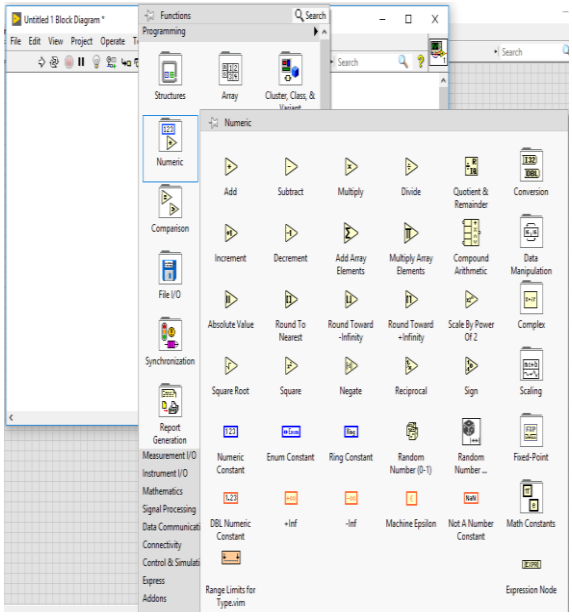

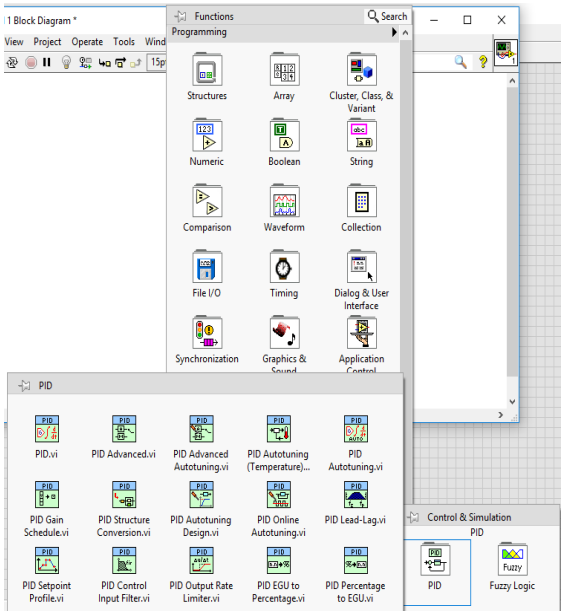

Figure 10 *blocks diagram to logic.* **Figure 11** *blocks diagram to PID.*

Finally, after extensive development efforts, we now possess an integrated algorithm capable of controlling our robot seamlessly. The algorithm's adaptability ensures its efficient operation across a wide range of applications, enabling versatile and effective robotic control as you can see in figure 12,13 and 14.

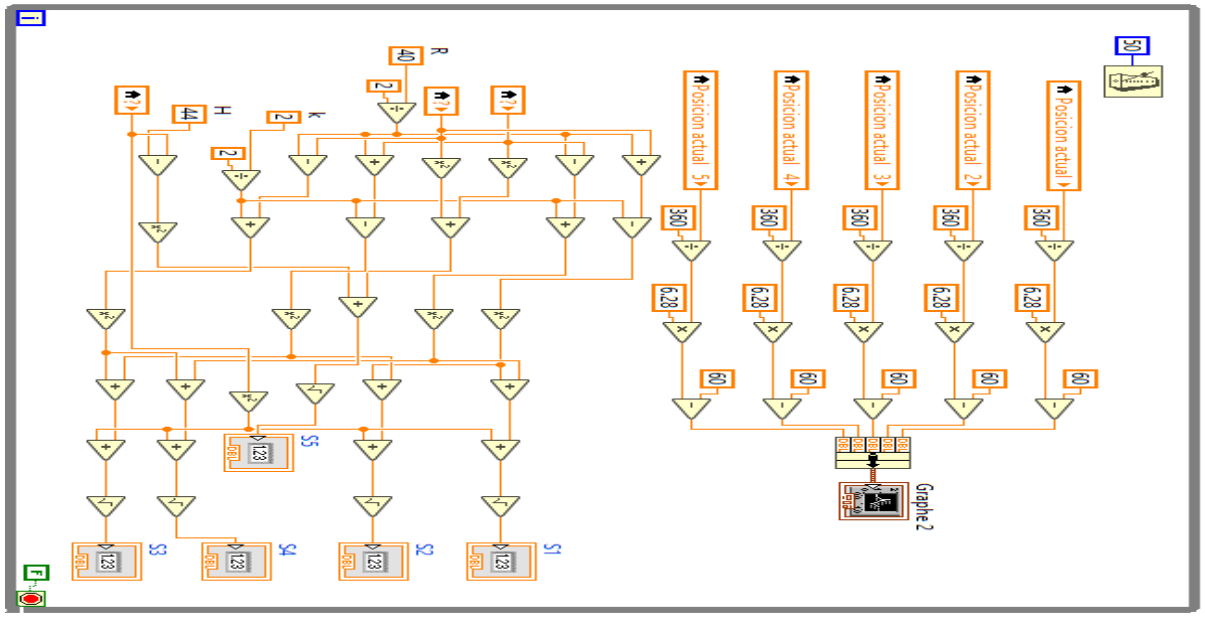

Figure 12 *blocks diagram to kinematic model.*

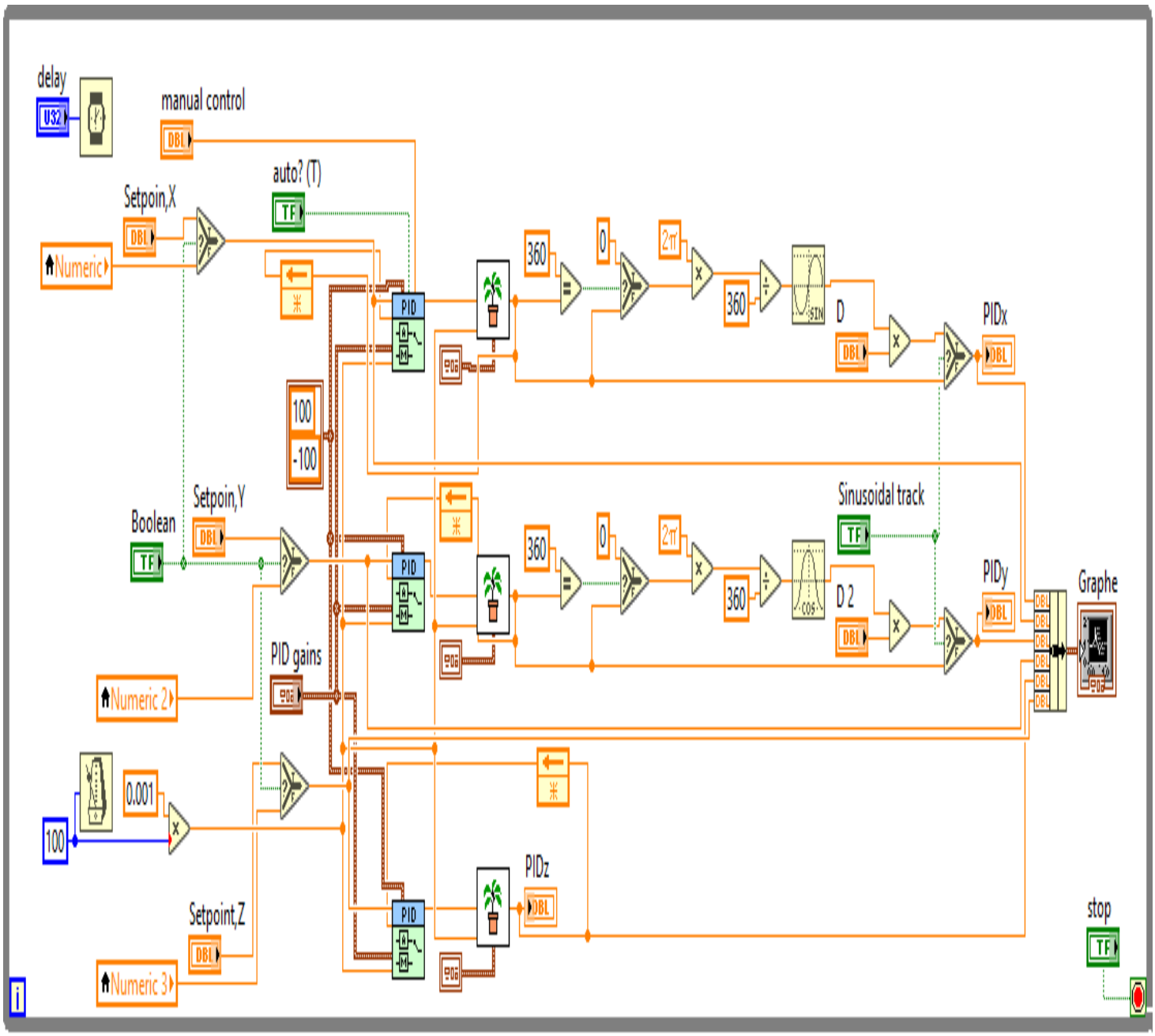

Figure 13 *blocks diagram to PID control .*

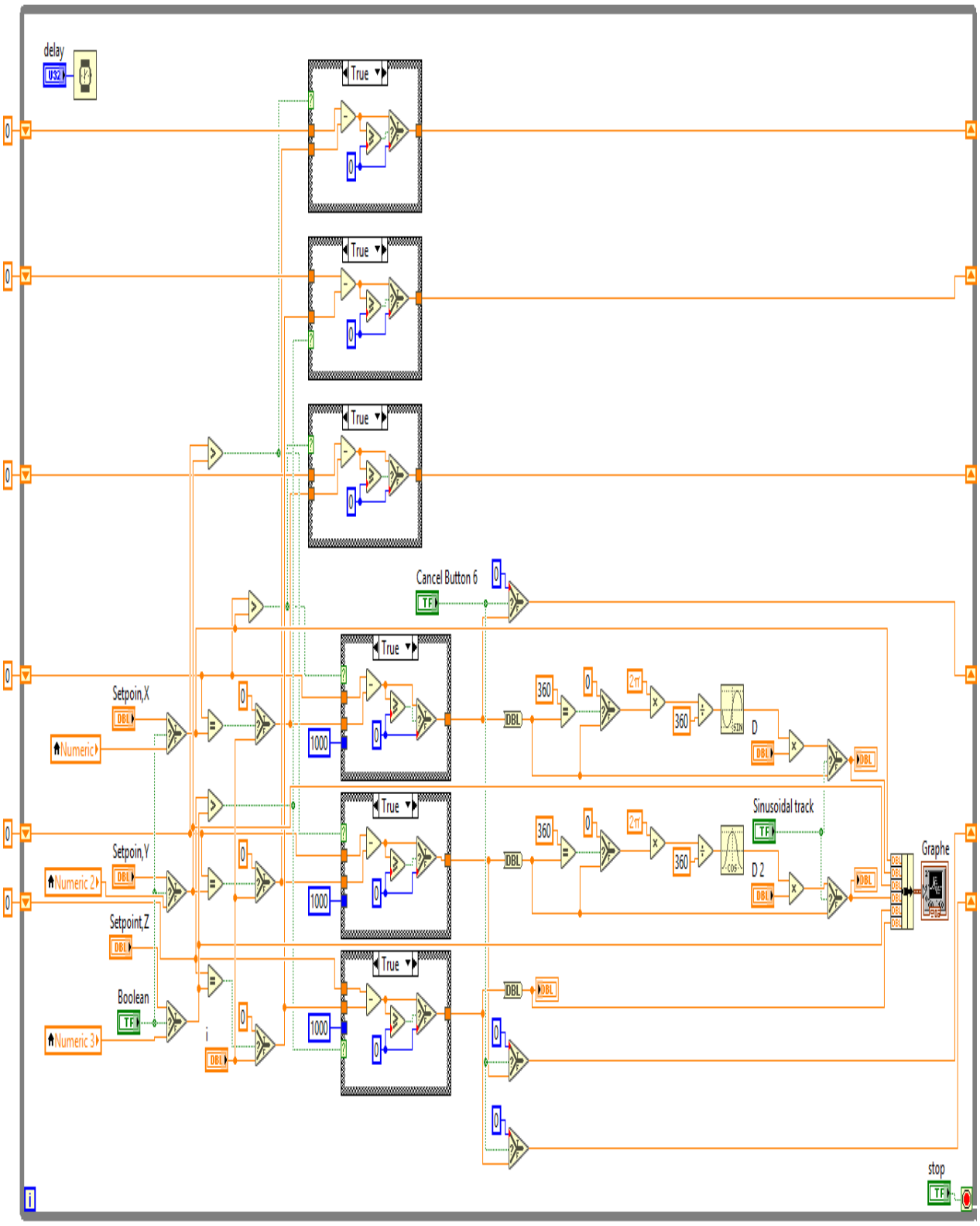

Figure 14 *blocks diagram to open loop control .*

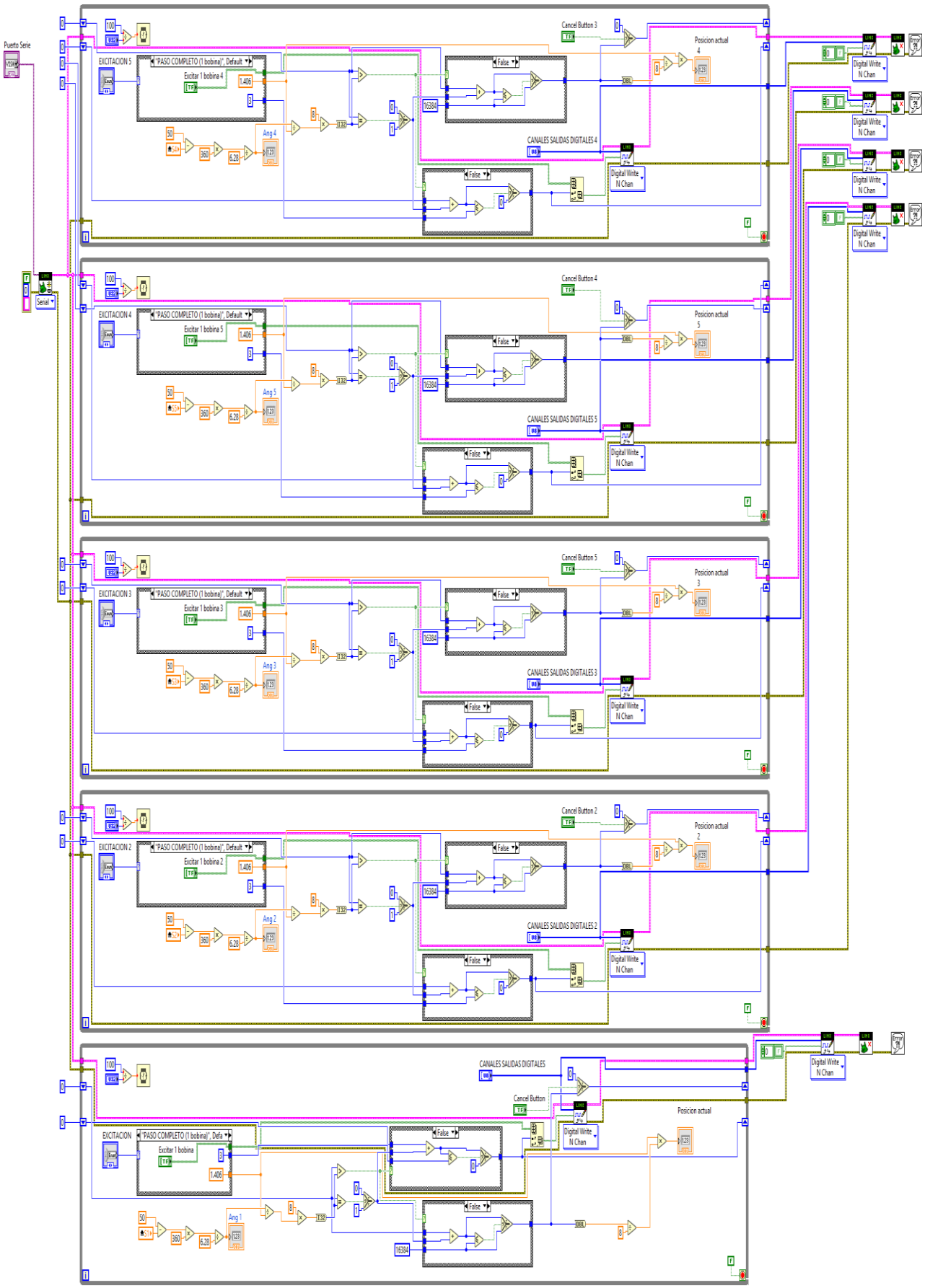

Figure 15 *blocks diagram to all stepper motor.*

Finely

Debug and Test: Once your block diagram is complete, you can test your program by clicking the "Run" button or pressing Ctrl+R (Cmd+R on Mac) to execute the VI. Monitor the front panel to observe the changes in controls and indicators as the program runs. After that save the VI by clicking "File" in the menu bar and selecting "Save" or "Save As."

That's it! You have now created a block diagram in LabView. The block diagram allows you to implement the functionality of your LabView application using graphical programming. Remember to save your work regularly and explore the various functionalities and features that LabView offers to enhance your program's capabilities.

1. Definition of App MIT Inventor:

The term "MIT App" typically refers to mobile applications developed using the MIT App Inventor framework. MIT App Inventor is a visual development environment that enables users to create mobile apps for Android devices without extensive coding knowledge. It was created by the Massachusetts Institute of Technology (MIT) to make app development accessible and user-friendly for individuals with little or no programming experience.

Using MIT App Inventor, users can build mobile apps by visually assembling blocks of code and linking them together, following a block-based programming approach. This approach allows users to create app functionality and interactions by selecting and configuring pre-defined blocks of instructions, eliminating the need to write traditional lines of code. The platform's simplicity and visual interface make it a popular choice for students, educators, hobbyists, and anyone interested in developing mobile apps without the complexities of conventional programming languages.

Figure 01 *– site de « App Inventer ».*

1.1 Creation an application android with arduino

To create an app using MIT App Inventor that communicates with Arduino, follow these steps:

1.1.1 Configuration the arduino:

Set up the Arduino: First, you'll need to set up your Arduino with the appropriate hardware and sensors you want to interact with through the app. Write the Arduino code to read sensor data and send/receive data to/from the app using serial communication (e.g., via USB or Bluetooth).

Connect the Arduino to the Computer: Connect your Arduino board to your computer via USB or Bluetooth, depending on the communication method you've chosen in your Arduino code.

1.1.2 Create an app MIT

- Set Up MIT App Inventor: Go to the MIT App Inventor website (https://appinventor.mit.edu) and log in to your account.
- Start a New Project: Click on "Start New Project" to create a new app.
- Designer Interface: In the Designer interface, design the user interface of your app. Add buttons, labels, sliders, and other components that you want to use to interact with your Arduino.

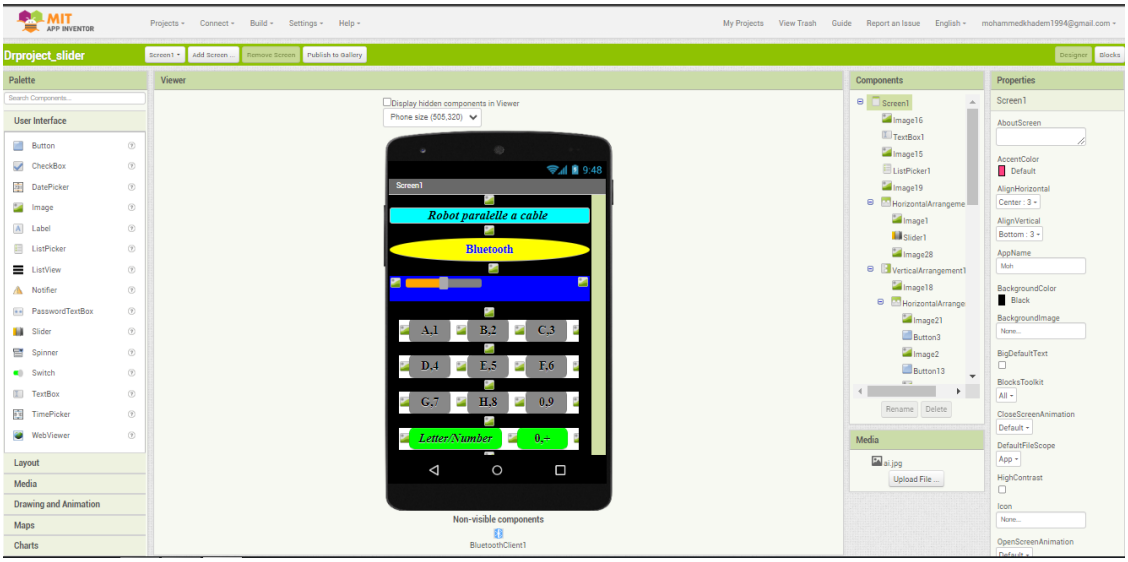

***Figure 02** – interface de site App inventer.*

- Blocks Editor: Switch to the Blocks Editor. Here, you'll write the code to handle the communication between the app and the Arduino. Go to "Connect" -> "Arduino" in the Blocks Editor and select the appropriate communication method (USB or Bluetooth).

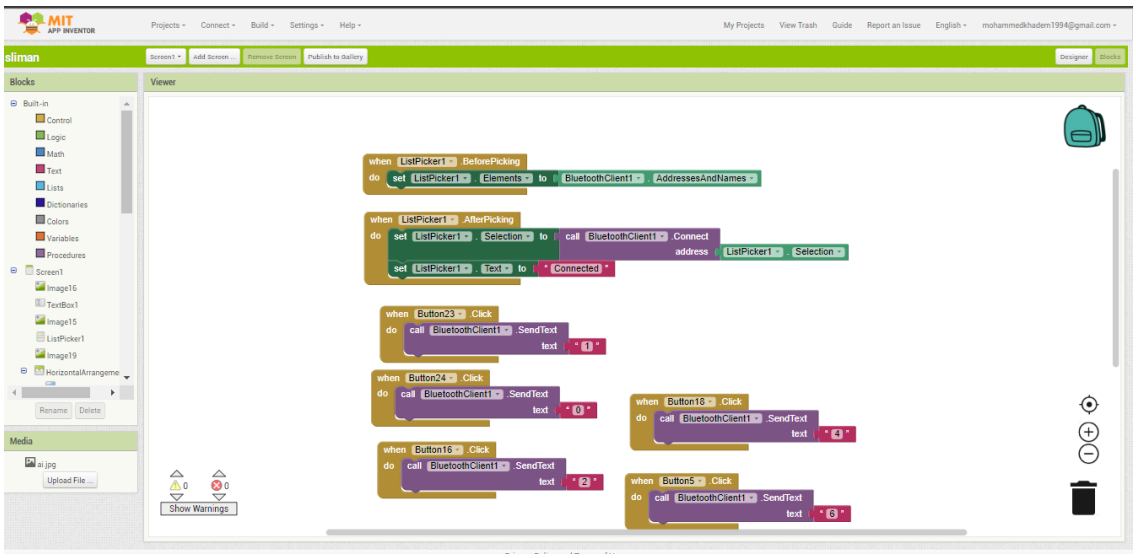

Figure 03 *– bloque de site App inventer.*

- Configure Communication: Set up the communication parameters in the Blocks Editor (e.g., baud rate for serial communication). Use blocks like "When Button Click" to send specific commands to the Arduino and blocks like "When Arduino. Ready" to read data from the Arduino.

1.1.3 Test application on arduino

- Test on a Device: To test your app, you'll need to install the MIT AI2 Companion app on your Android device from the Google Play Store. Connect your device to the same Wi-Fi network as your computer and click on "Connect" in the MIT App Inventor interface to pair your device.
- Upload Arduino Code: Upload the Arduino code to your Arduino board via the Arduino IDE.
- Live Testing: Now, you can use the "Live Testing" feature in MIT App Inventor to see your app running on your connected device in real-time as you interact with the components you added.
- Save and Package: Once you are satisfied with your app, save your project and download the APK file. This APK file is the installation package for your app.

1.1.4 Test final application on android

Install on Your Device: To distribute your app, you can either upload it to the Google Play Store or directly install it on other Android devices by allowing installations from unknown sources in the device settings.

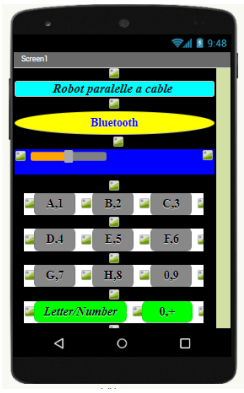

Figure 04 *– Application Final De L'interface De Contrôle.*

By following these steps, you'll be able to create an app with MIT App Inventor that communicates with Arduino and controls various sensors and actuators connected to the Arduino board.

2. Programming

2.1 Arduino IDE

The Arduino IDE (Integrated Development Environment) is a versatile software platform specifically designed for programming Arduino boards. This feature-rich environment empowers users to write, compile, and upload code to Arduino microcontrollers seamlessly. With its user-friendly interface, the Arduino IDE caters to both novices and seasoned developers, making programming accessible to everyone. The key components of the Arduino IDE include a comprehensive code editor, a compiler, and a firmware downloader. These elements work in tandem to facilitate the writing of code in the Arduino programming language, which can then be effortlessly uploaded to the connected Arduino board for execution. One of the notable strengths of the Arduino IDE lies in its provision of an array of libraries and examples. These resources are invaluable aids for project development, offering pre-written code snippets and fully functional sample projects that users can modify and build upon for their own applications.

By offering a unified environment that combines programming, compilation, and uploading functionalities, the Arduino IDE streamlines the development process, ensuring that even those new to programming can swiftly embark on their journey of creating innovative projects with Arduino boards.

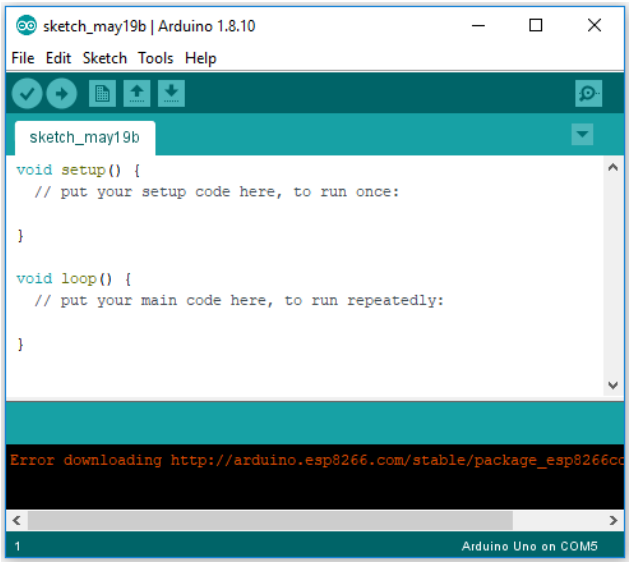

Figure 05 *– interface the arduino IDE.*

2.2 Configuration the arduino IDE

To begin programming and interacting with Arduino boards using the Arduino IDE, follow these steps:

a) Launch the Arduino IDE: After completing the installation, open the Arduino IDE on your computer.

b) Select the Arduino Board: In the Arduino IDE, navigate to the "Tools" menu, and then click on "Board". Choose the specific Arduino board you are using from the list of available options. If your board is not listed, you might need to install additional board definitions. To do this, go to "Tools", then "Board Manager", and select the appropriate board from the list of available options.

c) Choose the Serial Port: In the "Tools" menu, click on "Port" and choose the serial port to which your Arduino board is connected. The connected Arduino board should appear in the list as a serial port. If you are unsure about the correct port to choose, you can disconnect the Arduino board, check the available ports, reconnect the board, and observe the new port that appears. This will be the port

corresponding to your Arduino board. Verify Settings: Before proceeding further, double-check that the selected board and port settings are correct.

With these steps completed, your Arduino IDE is now fully configured and ready to be used for programming and interacting with Arduino boards. You can now start creating exciting projects and experimenting with your Arduino board!

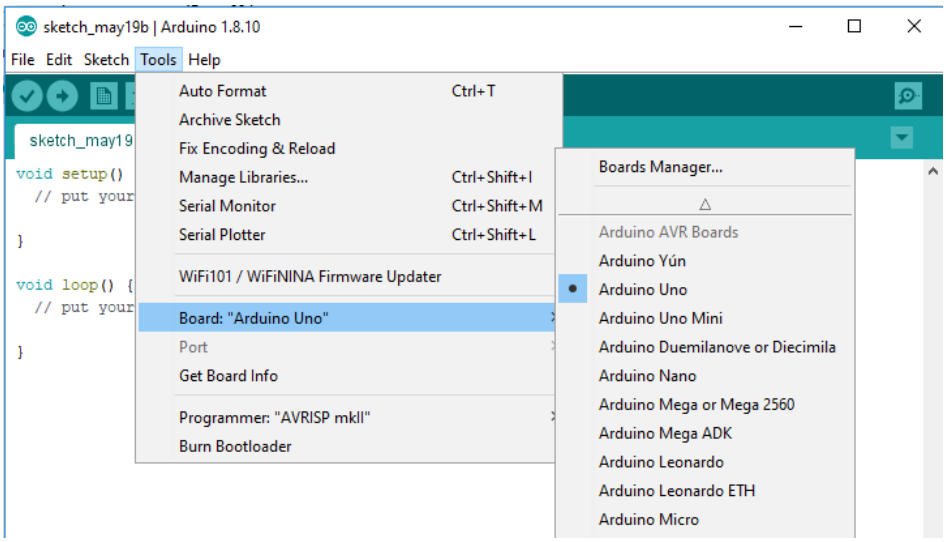

Figure 06 *– Configuration the Arduino IDE*

3. Test the robot Pyramidal CDPR with App android

3.1 Connect with Bluetooth

In this part, the control interface is connected (Smart phone) to a parallel robot with 5 stepper motor cable by Bluetooth module hc-05 to perform several movements forward, backward, left and right. LAW. And creation the letter Please look at the figure.16

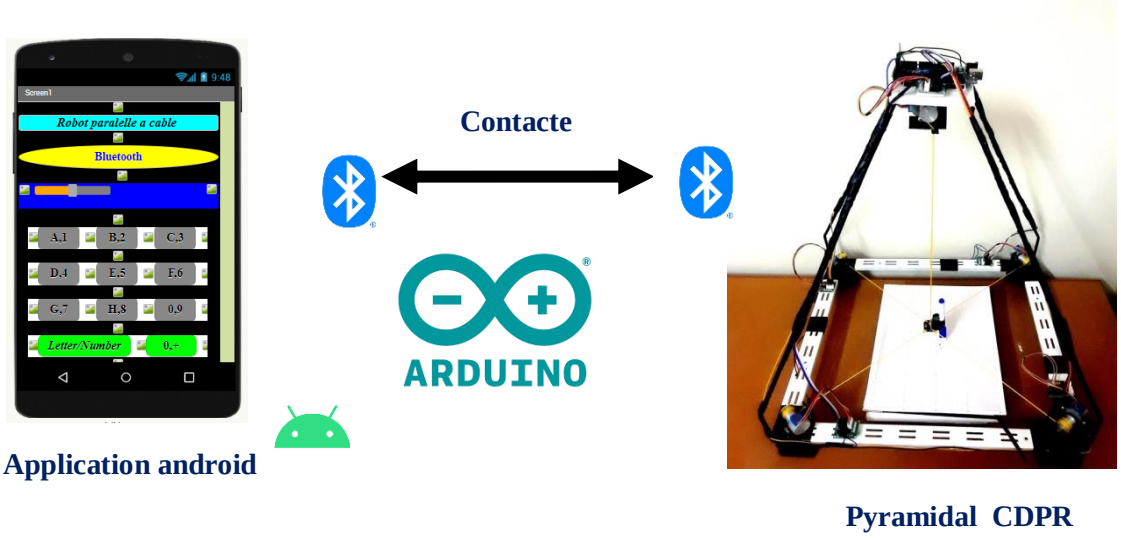

Figure 07 *– Un moyen de connecter l'application avec l'Androïde*

1. Definition The Solidworks/Software

SolidWorks is a powerful 3D CAD (computer-aided design) software that empowers users to create and model intricate parts and assemblies with exceptional precision. This versatile software finds extensive application across various industries, including mechanical design, aerospace, automotive, electronics, architecture, and many other engineering disciplines. With SolidWorks, users can seamlessly simulate real-world operating conditions, enabling them to test and validate their designs before fabrication. Additionally, it facilitates the generation of detailed 2D drawings directly from the 3D models, streamlining the documentation process and enhancing the overall efficiency of the design workflow.

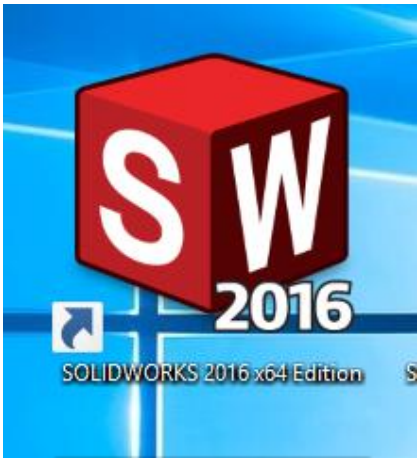

Figure 01 *elements onto the front panel of the VI.*

1.1 How To Creation Design 3d In Solidworks

In this section, we provide a comprehensive explanation of the design stages involved in creating the cable parallel robot. The design process entails meticulous attention to detail, as we address each individual piece separately. Moreover, during this undertaking, we take into careful consideration the fixed values that were previously determined in the analytical and mathematical part of the project. By integrating these established values into the design, we ensure a coherent and precise implementation of the robot's components.

The initial step is to launch the SolidWorks program. Subsequently, we proceed to open a new file (as illustrated in Figure 02), which triggers the appearance of a new window offering three options: Part, Assembly, or Drawing (as demonstrated in Figure 03).

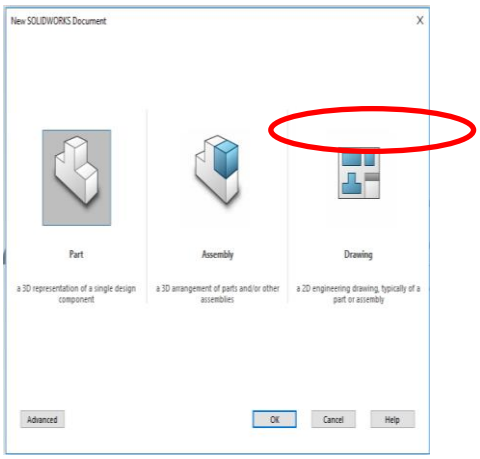

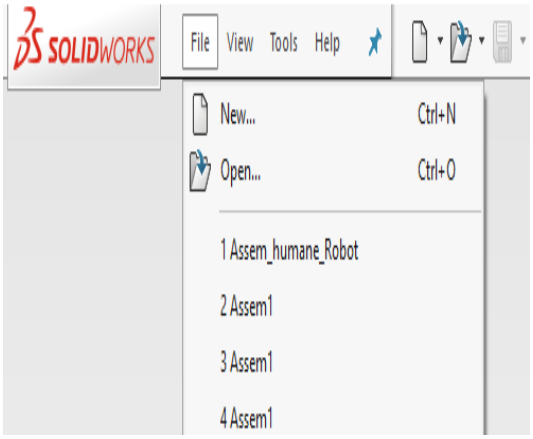

Figure 02 *elements onto the front panel of the VI.* **Figure 03** *elements onto the front panel of the VI.*

After opening a new file, the primary task is to select the plane on which we intend to create the part for our design (as exemplified in Figure 04). Once the plane is defined, we proceed to draw the parts based on their respective projections.

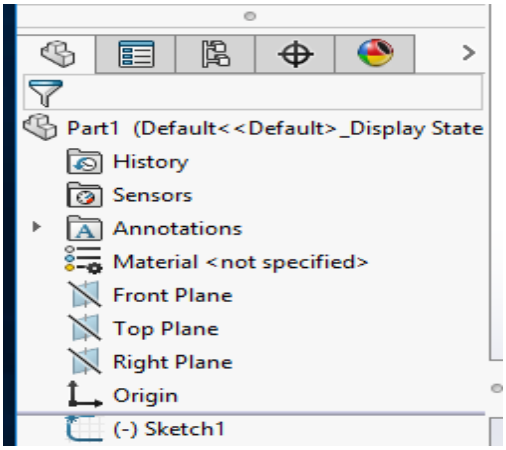

Figure 04 *elements onto the front panel of the VI.*

To streamline the drawing process, SolidWorks provides a variety of options representing geometric shapes (as illustrated in Figure 5), which prove immensely helpful in accurately constructing the parts.

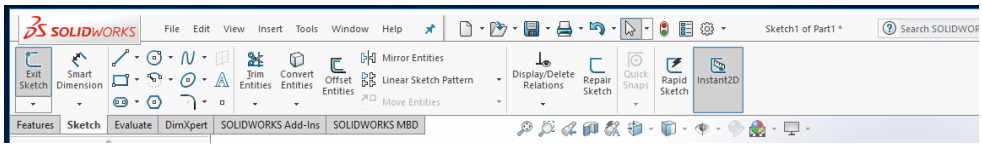

Figure 05 *elements onto the front panel of the VI.*

Furthermore, in Figure 6, we encounter a range of options for creating the 3D model, including features like cavity, cut, and fill, among others. These tools and functionalities enhance our ability to develop intricate and realistic 3D models for our design.

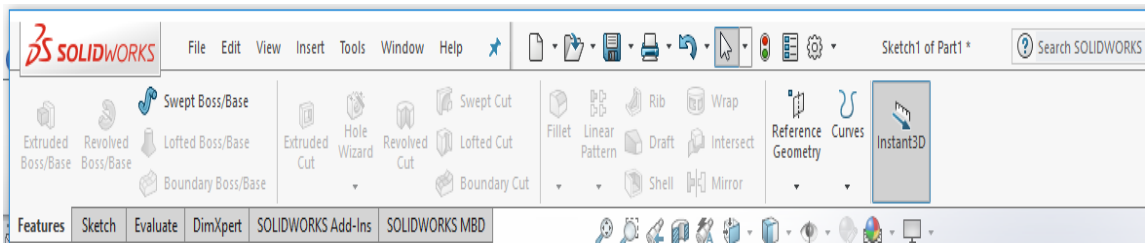

Figure 06 *elements onto the front panel of the VI.*

Regarding Figure 07, it depicts a series of supplementary options alongside specific objectives that necessitate activation when implementing additional procedures. For instance, when undertaking tasks like mechanical movement analysis or analyzing forces exerted on the structure, these specific options need to be enabled. An exemplification of this scenario is showcased in Figure 12, wherein a simulation demonstrates the analysis of forces applied to the structure. This feature empowers users to comprehensively assess the structural integrity and performance under various force scenarios, enhancing the overall design and engineering capabilities of the SolidWorks software.

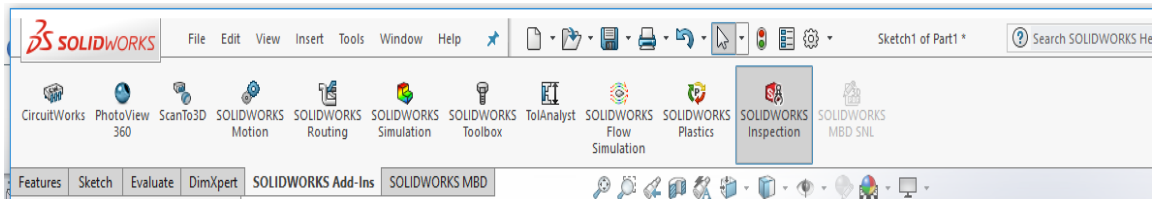

Figure 07 *elements onto the front panel of the VI.*

1.2 How To Assembly Parts in Solidworks

Figures 8 and 9 represent essential options within the assembly part, showcasing how to call and incorporate individual parts efficiently. In Figure 8, the process involves using the "extract button" to retrieve specific parts. Subsequently, in Figure 9, we proceed to gather and assemble these extracted pieces using the various available options. These options significantly streamline the assembly process, allowing users to build complex systems by

efficiently combining the individual components. With the aid of these features, SolidWorks empowers users to create intricate and well-structured assemblies with ease and precision.

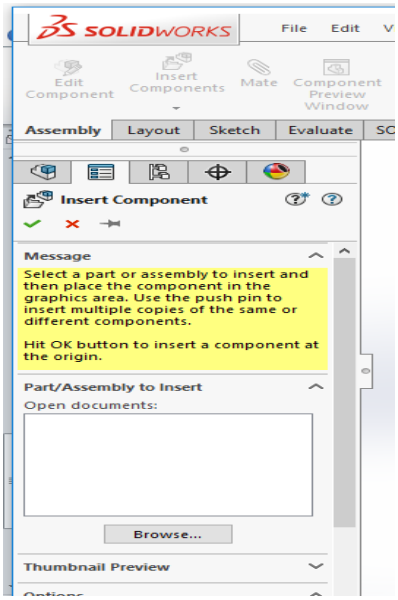

Figure 08 *elements onto the front panel of the VI.*

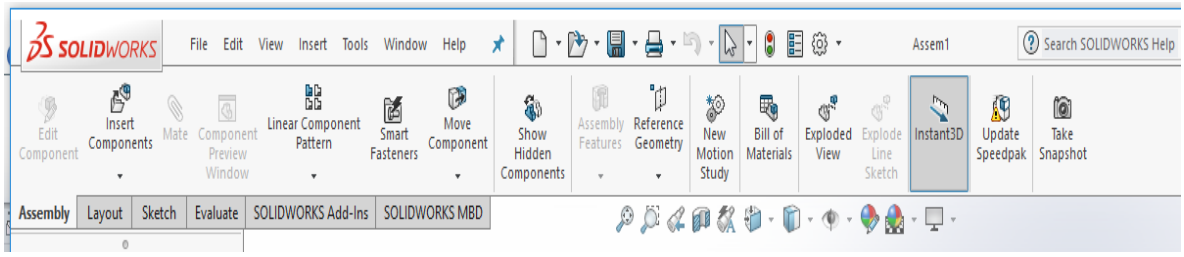

Figure 09 *elements onto the front panel of the VI.*

To begin the design process for individual components, we opt for the first option, "Part." After successfully completing the design of these parts (as depicted in Figure 10), we advance to the next phase. In this stage, we access the "Assembly" option to meticulously assemble the designed components into the overall system, resulting in a comprehensive representation (as evident in Figure 11).

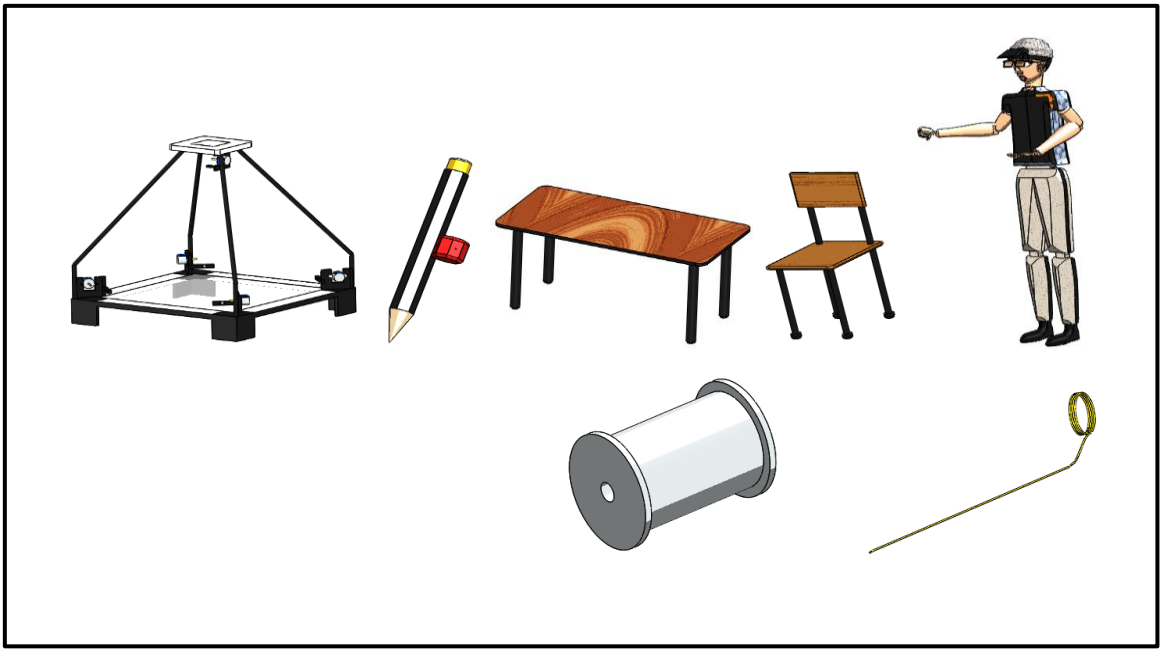

Figure 10 *elements onto the front panel of the VI.*

Figure 11 *elements onto the front panel of the VI.*

1.3 How To Create Simulation in Solidworks

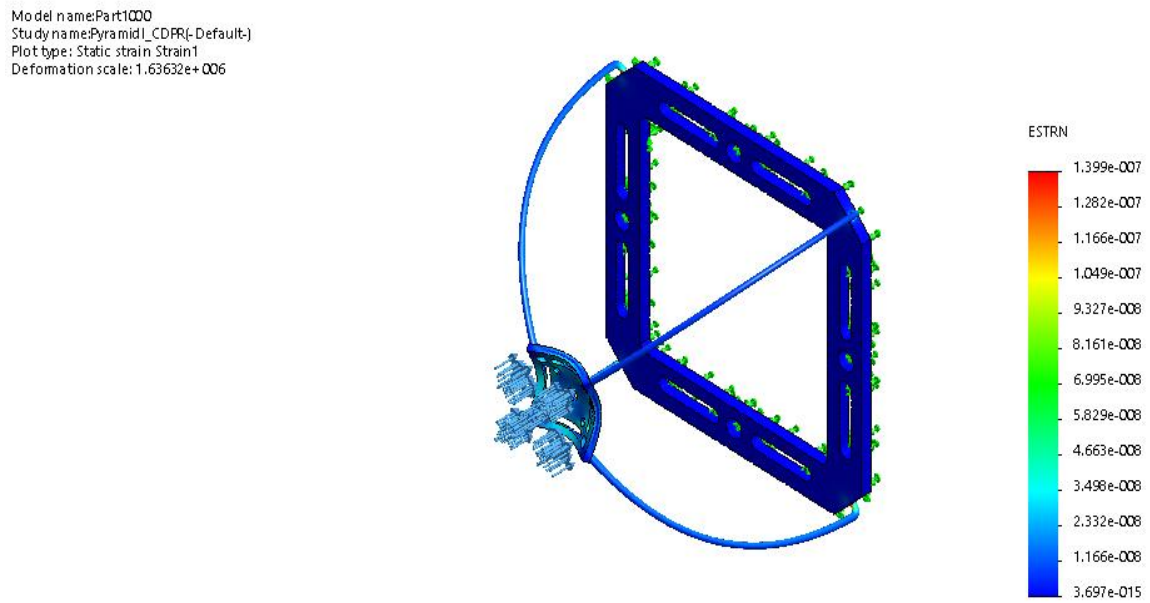

Figure 12 *elements onto the front panel of the VI.*

Figure 12 showcases a simulation analyzing the forces applied to the cable parallel robot's structure. To conduct this analysis in SolidWorks, one must select the Simulation option. Following that, additional procedures are specified, and values pertaining to the structure's specific stability are entered to arrive at the simulation depicted in Figure 12.

This intricate process of simulation and analysis necessitates a considerable amount of time for thorough study and examination. The meticulous evaluation of the forces acting on the robot's structure is crucial to ensure its stability, safety, and overall performance. The time invested in this rigorous examination is well-justified as it significantly contributes to enhancing the reliability and effectiveness of the cable parallel robot's design and functionality.

UNIVERSITÀ DELLA CALABRIA

Dipartimento Di Ingegneria Meccanica, Energetica E Gestionale

FINAL REPORT

Short-Term Training Abroad (Course Development).
2022-2023

Title of the thesis: ***Design and control of a cable parallel robot with the application to rehabilitation.***

The trainee:
Khadem Mohammed
m.khadem@univ-skikda.dz

The Supervisor:
Pr. Giuseppe Carbone
Giuseppe.carbone@unical.it

Department: Mechanical, Energy And Management Engineering
Faculty: Faculty of technology
University: University of Calabria.
From: 19/01/2023 to 16/02/2023

February 16, 2023, University of Calabria (Italy)

For one months from 19 January 2023 till 16 February 2023, I did an internship in the laboratory Mechanical, Energy And Management Engineering (University of Calabria) in Italy . This internship project is a part of my research Ph.D. program which I conduct at University 20 aout 1955, Skikda.

So I would like to thank the professor Giuseppe Carbone, director of the scientific laboratory (DIMGM) at the University of Calabria in Italy, for accepting our request and for the good reception we received. I would also like to thank the professor Francesco for supporting us with necessary information during our work, and I thank all the PhD students who shared information and advice with us during the training period.

The objective of this work is to research a new strategy for the development of pyramid cable-driven parallel robot. by consulting some researchers with experience in cable-driven parallel robots. In addition, some PhD students participated in expressing their opinions on how to develop this pattern and find new ways to improve the performance of this robot. This training was carried out in several stages, which are summarized in the following points:

Part One:

- **The first step** was to assemble and configure the prototype, where some components, such as cables, have been changed and the end-effector has been fabricated by 3D printing in order to be accurate.
- **The second step,** implementation of the kinematic model on the prototype, Where the cable length is calculated by a kinematic model, it aims to control the number of motor cycles.
- **Third step,** implementation of the PID control on the prototype in order to reduce the error and avoid sagging of the cables. But the process was not completed because the motors used are slow. So they were not relied upon to control this robot.

Part Tow:

- **The first step,** implementation algorithm open-loop control on the prototype in order to reduce the error and avoid sagging of the cables. This algorithm was used to test several different trajectories.
- **The second step,** created a control interface for a smart phone using the Mit Inventor site. This interface (Android application) was created in order to facilitate the use of this robot, as it contains some different paths for letters and numbers.

- **Third step,** validate several tests by Using the experimental prototype, some different continuous and sinusoidal paths were tested to verify the performance of this robot.

General conclusion

Through the results obtained from the successive experiments. We conclude that using an open-loop control algorithm, we can control the robot and improve its performance accuracy, but this accuracy has a direct impact on response speed. Nevertheless, with this performance, we get good results. Finally, we got a new control pattern for this robot based on an open-loop control algorithm through a smart phone for the purpose of rehabilitation applications in drawing and writing.

The Trainee **The Supervisor**

A. DEFINITION

The University of Calabria (Università della Calabria) is a public research university located in Rende, Calabria, Italy. It was founded in 1972 and offers a wide range of undergraduate, graduate, and doctoral programs across various fields of study. The university is known for its large campus and commitment to academic excellence and research.

B. LOCATION

The University of Calabria is located in Rende, a town in the province of Cosenza in the region of Calabria, Italy. It is situated at the foot of the Sila mountain range, which offers a picturesque backdrop to the campus. The university's sprawling campus covers an area of over 2000 acres, making it one of the largest university campuses in Europe.

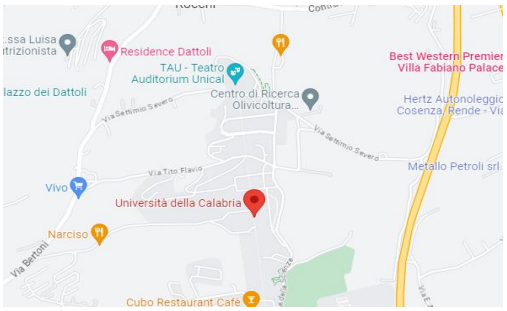

Article

M. Khadem, F. Inel, G. Carbone and A. Slimane Tich Tich, “A novel pyramidal cable-driven robot for exercising and rehabilitation of writing tasks”, Robotica. https://doi.org/10.1017/S026357472300111X

F. Inel, M. Khadem and A. Slimane Tich Tich, “Realization and Simulation a Novel Kind of Parallel Cables-Based Robot with Five Cables”, WSEAS TRANSACTIONS on CIRCUITS and SYSTEMS. http://dx.doi.org/10.37394/23201.2022.21.30

Inel, Foued, Mohammed Khadem, and Abdelghafour Slimane Tich Tich. "The Objective Oriented Design of a CUBE Cable-based Parallel Robot for Arm Rehabilitation Tasks." WSEAS Transactions on Systems 23 (2024): 1-7. http://dx.doi.org/10.37394/23202.2024.23.1

Conference paper

Khadem, M., Inel, F., Carbone, G. “Design and Validation of a Novel Pyramidal Cable-Driven Robot”. In: Niola, V., Gasparetto, A., Quaglia, G., Carbone, G. (eds) Advances in Italian Mechanism Science. IFToMM Italy 2022. Mechanisms and Machine Science, vol 122. Springer, Cham. https://doi.org/10.1007/978-3-031-10776-4_24

Khadem, M., Inel, F., Carbone, G. “Simulation of 2D paths using a Cable-Driven Parallel Robot”. Conference: The 4th International Conference on Electromechanical Engineering (ICEE2022) November 22-23, 2022, university of Skikda At: skikda, Algeria

Khadem, M., Inel, F., Carbone, G. “Simulation of Predefined Trajectories for a 3D Cable-Driven Parallel Robot”. Conference: The 4th International Conference on Electromechanical Engineering (ICEE2022) November 22-23, 2022, university of Skikda At: skikda, Algeria

Khadem, M., Inel, F., Carbone, G. “Design of a 3D Cable-Driven Robot for Material and Product Transmission in a Petrochemical Base” Conference: The International Conference on Petrochemistry and Energy Transition (ICPET23.), November 21-23 2023At: skikda, Algeria